ISSN 0003-2654
VOL. 122 NO. 3 MARCH 1997

The Analyst

An international analytical science journal

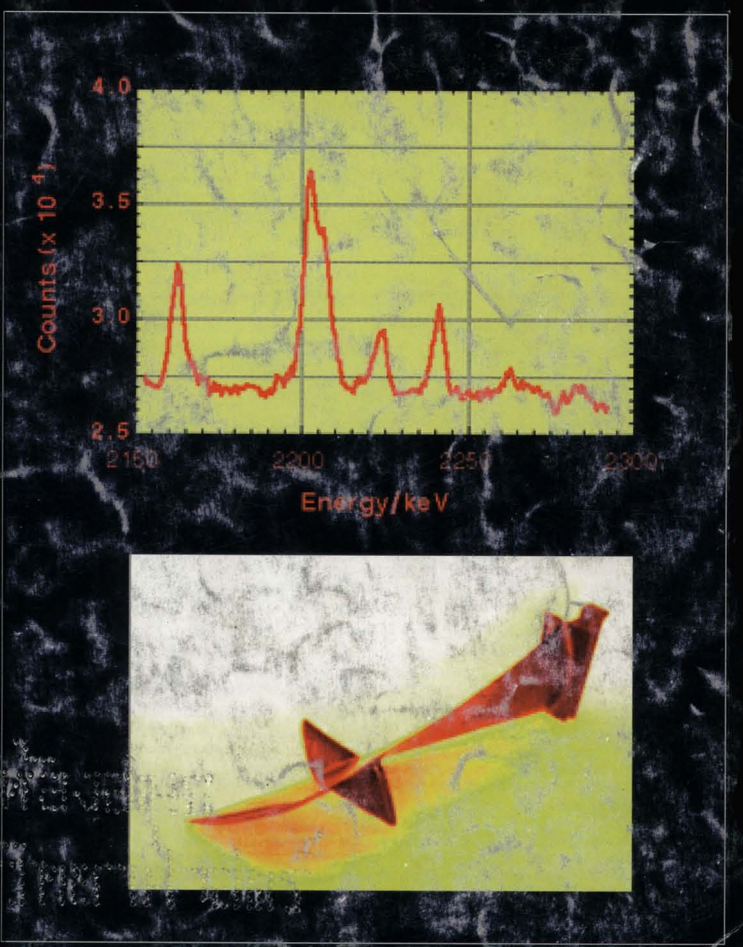

The Analyst

The Analytical Journal Of The Royal Society Of Chemistry

Publishing Division, Analytical

Managing Editor, **Harpal S. Minhas**

Deputy Editor, **Sarah J. R. Williams** Editorial Secretaries: **Claire Harris; Frances Thompson**

Telephone: +44(0)1223 420066; **Fax**: +44(0)1223 420247; **E-mail**: ANALYST@RSC.ORG

www:http://chemistry.rsc.org/rsc/

Production Division, Analytical

Production Manager, **Janice M. Gordon**

Production Editor, **Caroline Seeley** Technical Editors: **Judith Frazier, Ziva Whitelock, Roger A. Young** Secretary: **Ann Philips**

Telephone: +44(0) 1223 420066; **Fax**: +44(0) 1223 423429; **E-mail**: ANALPROD@RSC.ORG

For enquiries relating to manuscripts from receipt to acceptance, contact the **Publishing Division**, and for enquiries relating to manuscripts post-acceptance contact the **Production Division, Royal Society of Chemistry, Thomas Graham House, Science Park, Milton Road, Cambridge, UK CB4 4WF**

Information for Authors

Full details of how to submit material for publication in *The Analyst* are given in the Instructions to Authors in the January issue. Separate copies are available on request.

The Analyst publishes original research papers, critical reviews, tutorial reviews, perspectives, news articles, book reviews and a conference diary.

Original research papers. *The Analyst* publishes full papers on all aspects of the theory and practice of analytical chemistry, fundamental and applied, inorganic and organic, including chemical, physical, biochemical, clinical, pharmaceutical, biological, environmental, automatic and computer-based methods. Papers on new approaches to existing methods, new techniques and instrumentation, detectors and sensors, and new areas of application with due attention to overcoming limitations and to underlying principles are all equally welcome.

Full critical reviews. These must be a critical evaluation of the existing state of knowledge on a particular facet of analytical chemistry.

Tutorial reviews. These should be informally written although they should still be a critical evaluation of a *specific* topic area. Some history and possible future developments should be given. Potential authors should contact the Editor before writing reviews.

Perspectives. These articles should provide either a personal view or a philosophical look at a topic relevant to analytical science. Alternatively, they may be relevant historical articles. Perspectives are included at the discretion of the Editor.

Particular attention should be paid to the use of standard methods of literature citation, including the journal abbreviations defined in Chemical Abstracts Service Source Index. Wherever possible, the nomenclature employed should follow IUPAC recommendations, and units and symbols should be those associated with SI.

Every paper will be submitted to at least two referees, by whose advice the Editorial Board of *The Analyst* will be guided as to its acceptance or rejection. Papers that are accepted must not be published elsewhere except by permission. Submission of a manuscript will be regarded as an undertaking that the same material is not being considered for publication by another journal.

Associate Scientific Editors. For the benefit of all potential contributors wishing to discuss the scientific content of their paper(s) a Group of Associate Scientific Editors exists. Requests for help or advice on scientific matters can be directed to the appropriate member of the Group (according to discipline). Currently serving Associate Scientific Editors are listed in each issue of *The Analyst* (and *Analytical Communications*).

Manuscripts (four copies typed in double spacing) should be addressed to:

H. S. Minhas, Managing Editor, *or*
J. F. Tyson, US Associate Editor

All queries relating to the presentation and submission of papers, should be addressed to the Publishing Division and any correspondence regarding accepted papers and proofs, should be directed to the Production Division for *The Analyst*. Members of the Analytical Editorial Board (who may be contacted directly or *via* the Editorial Office) would also welcome comments, suggestions and advice on general policy matters concerning *The Analyst*.

There is no page charge.

Fifty reprints are supplied free of charge.

The Analyst (ISSN 0003–2654) is published monthly by The Royal Society of Chemistry, Thomas Graham House, Science Park, Milton Road, Cambridge, UK CB4 4WF. All orders, accompanied with payment by cheque in sterling, payable on a UK clearing bank or in US dollars payable on a US clearing bank, should be sent directly to The Royal Society of Chemistry, Turpin Distribution Services Ltd., Blackhorse Road, Letchworth, Herts, UK SG6 1HN. Turpin Distribution Services Ltd., is wholly owned by the Royal Society of Chemistry. 1997 Annual subscription rate (Sterling) £535.00: (US Dollars) $963.00. Purchased with *Analytical Abstracts* £1072.00: $1930.00. Purchased with *Analytical Abstracts* plus *Analytical Communications* £1260.00: $2268.00. Purchased with *Analytical Communications* £670.00: $1206.00. Customers in Canada will be charged the sterling price plus a surcharge to cover GST. Prices for electronic subscription are available upon application. Air freight and mailing in the USA by Publications Expediting Inc., 200 Meacham Avenue, Elmont, NY 11003.

USA Postmaster: Send address changes to: *The Analyst*, Publications Expediting Inc., 200 Meacham Avenue, Elmont, NY 11003. Periodicals postage paid at Jamaica, NY 11431. All other despatches outside the UK by Bulk Airmail within Europe, Accelerated Surface Post outside Europe. PRINTED IN THE UK.

RSC JOURNALS GRANTS FOR INTERNATIONAL AUTHORS

At its meeting in December 1996, the Council of The Royal Society of Chemistry (RSC) decided that some of the surplus from Journals publishing should be used specifically to support international authors who publish in RSC journals. In the first instance, funding would be made available for visits to other countries for one or more of the following objectives:-

- to collaborate in research;
- to exchange research ideas and results;
- to give or receive special expertise and training.

UK and Ireland residents are specifically excluded from applying for this funding. However, members of the RSC resident in the UK and Ireland may apply for Jones Travelling Fellowships which have similar objectives.

The RSC operates under a Royal Charter which requires it to advance chemical science. One way it has been doing this for over 150 years is by disseminating chemical knowledge through its chemistry journals. RSC publishing on chemistry and related topics has become a very significant activity, with the journals having a large worldwide circulation.

In an area of publishing which is now very commercial and competitive the RSC, as befits a not-for-profit organisation, has held firm to its long standing objectives of providing a service to its members and to chemistry. We provide high quality journals and other information services and maintain very high standards of refereeing and editing. The RSC journal prices are very much at the low end of the range charged by commercial publishers particularly when compared on the basis of price per paper and price per word.

The RSC publishing activities generate a cash surplus, some of which is used to develop and enhance the publishing services provided. What specifically distinguishes the RSC from commercial publishers, however, is that most of the surplus is used to promote and support chemistry, mainly in the UK. The funds are used in a wide variety of ways including subsidising chemistry conferences, providing student bursaries, providing training and updating courses for teachers, publishing general chemistry information for schools, carrying out studies and making contributions to reviews of UK and European science policy.

Now, in recognition that dissemination of chemical knowledge is a truly international activity for the RSC, knowing no boundaries in academic or industrial research, and because 80% of our authors and 90% of the journal revenue comes from outside the UK, the RSC Council has introduced the new policy of making some of the surplus from publishing available to international authors who support RSC journals by contributing to them.

Application Procedure

Applications are invited from those wishing funds from the RSC Journals Grants for International Authors.

There are no restrictions on the countries between which visits may be made but a significant proportion of grants will be for visits to the UK and other European Union countries. Applicants should have a recent record of publishing in the RSC journals. Each grant is unlikely to exceed £2,000 and there will be about 100 grants available each year.

Applications will be assessed by a panel chaired by the President of The Royal Society of Chemistry.

For further information and application form, contact: RSC Journals Grants for International Authors, The Royal Society of Chemistry, Thomas Graham House, Science Park, Milton Road, Cambridge CB4 4WF, UK. Fax +44 (0) 1223 420247. E-mail jnlsrev@rsc.org

UK and Ireland residents are <u>not</u> eligible to apply for the RSC Journals Grants for International Authors but are eligible to apply for the existing Jones Travelling Fellowships to make overseas laboratory study visits. For further information and application form, contact: Mr S Langer, The Royal Society of Chemistry, Burlington House, Piccadilly, London W1V 0BN. Fax +44 (0) 171 437 8656. E-mail LANGERS@rsc.org

T D Inch
Secretary General

The Analyst

Critical Review

Hydrogen Measurement by Prompt Gamma-ray Activation Analysis

A Review

Rick L. Paul

Analytical Chemistry Division, National Institute of Standards and Technology, Gaithersburg, MD 20899, USA

Summary of Contents

Keywords: *Hydrogen; prompt gamma rays; activation analysis; cold neutrons*

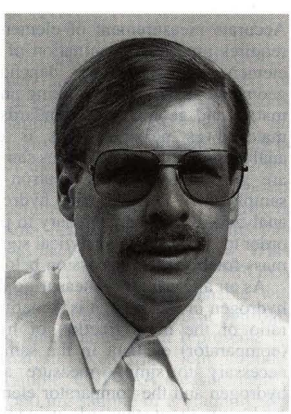

Rick L. Paul earned a B.S. in chemistry from Western Illinois University and a Ph.D. from Purdue University, where his research interests included neutron activation analysis of meteorites. He was a postdoctoral research associate at San Jose State University before coming to the National Institute of Standards and Technology in 1991. His current areas of research include cold neutron prompt gamma-ray activation analysis as well as radiochemical neutron activation analysis. He is an author of over 30 papers on PGAA.

Introduction

Hydrogen, the ninth most abundant element (by mass) in the Earth's atmosphere and crust, is present in virtually all materials. It has long been known that chemical properties of many substances are directly related to hydrogen content. The hydrogen content of organic compounds determines the degree of saturation and hence reactivity of carbon–carbon bonds. A major concern for several US industries today is the effect of trace hydrogen on materials properties. Hydrogen is known to cause embrittlement in steels at levels of 10 μg g^{-1} and to affect the cracking strength of titanium alloys at mass fractions below 50 μg g^{-1}.[1] In semiconductors, hydrogen causes bulk electrical effects at concentrations of 10 μg cm^{-3} or even lower.[2]

Prompt gamma-ray activation analysis (PGAA) is suitable for the detection of hydrogen, both at high levels (mass fractions > 1%) and at lower levels, in a wide variety of materials.[3–5] The technique is described in detail elsewhere.[6–11] The sample is irradiated by a beam of neutrons, inducing nuclei of many elements to undergo neutron capture. Upon de-excitation, these nuclei emit prompt gamma-rays, which are measured using a high resolution gamma-ray detector. Qualitative analysis is accomplished by identification of gamma-ray energies, while comparison of gamma-ray intensities with those emitted by standards yields quantitative analysis. Hydrogen absorbs neutrons *via* the $^{1}H(n,\gamma)^{2}H$ reaction, resulting in the emission of a 2223.3 keV gamma-ray. The analysis is nondestructive and, since both the neutron and gamma radiation are penetrating, the entire volume of sample irradiated by the neutron beam is analyzed. Because the analytical signal results from a nuclear and not a chemical reaction, the results are independent of the chemical form of the element. Finally, since the analysis is performed *in situ*, extraction of hydrogen from the sample is not required.

Two separate PGAA facilities are available at the National Institute of Standards and Technology Research Reactor. The University of Maryland–NIST thermal neutron† PGAA (TNPGAA) facility, in operation since 1978, has proven useful for the determination of > 1 mg of hydrogen (mass fraction > 0.1% for a 1 g sample) in materials. Because the presence of hydrogenous shielding materials gives rise to a hydrogen gamma-ray background of 1 mg, this instrument is not normally used to measure hydrogen at trace levels. A second PGAA spectrometer, constructed as part of the Cold Neutron Research Facility and in operation since late 1990, uses a beam of 'cold' neutrons (λ > 4 nm, energies < 0.005 eV) to irradiate samples. Because the hydrogen background of the cold neutron (CN)PGAA spectrometer is low (< 10 μg), due to its nearly hydrogen-free construction, this instrument has been useful for analysis of 10 μg to 1 mg of hydrogen in samples. In this paper

† Uranium atoms undergo fission to produce fast neutrons with energies 100 keV to 10 MeV. Moderation produces thermal neutrons with an average energy of 0.025 eV. Moderation at low temperature produces cold neutrons with energies < 0.25 eV.

we describe these two facilities and their capabilities for hydrogen measurement, outline a procedure for measuring hydrogen by PGAA, discuss sources of error in PGAA measurements and how to correct for these errors, and relate applications for analysis of hydrogen in materials.

Facilities

Both the thermal and cold neutron PGAA facilities at NIST are described in detail elsewhere.[7–11] The thermal neutron PGAA facility is located above the reactor core. Neutrons pass through a series of collimators in a 6 m long vertical aluminum beam tube. The 2.5 cm diameter unfiltered beam exits the top of the reactor, intercepting the target at 1 m above the exit. Targets are irradiated at a neutron flux of 3.3×10^8 cm^{-2} s^{-1} (at 20 MW reactor power). Prompt gamma-rays are measured by a germanium detector (27% efficiency relative to a 7.6 cm × 7.6 cm sodium iodide crystal), surrounded by a heavily-shielded, split annulus, thallium-doped sodium iodide detector, which gives the facility both anti-Compton and pair spectrometry capabilities. The analyzer consists of an Ethernet-based Canberra Nuclear Acquisition Interface Module‡ connected to a Digital VAXstation 2000, and routinely collects 16,384 channels of Compton-suppressed data over a gamma-ray energy range of 0 to 8 MeV.

The CNPGAA instrument is located on a straight guide in the Cold Neutron Research Facility. Reactor neutrons are moderated by passage through D_2O ice at 30 K and then pass down the guide and through a cold beryllium–bismuth filter on their way to the CNPGAA station. The neutron beam is free of reactor gamma-rays and fast neutrons. The neutron flux at the sample position is 1.5×10^8 cm^{-2} s^{-1} (thermal equivalent). Prompt gamma-rays are measured by a high purity germanium detector (26% relative efficiency, 1.9 keV resolution), which is surrounded by a bismuth germanate Compton shield (Fig. 1). Gamma-ray spectra up to 10 MeV are collected using Canberra Nuclear Data Software on a VAXstation 3100. The hydrogen sensitivity (counts s^{-1} mg^{-1}) for this instrument is a factor of three to four better than that measured for the TNPGAA instrument, and the hydrogen background is a factor of more than 100 lower.

Selection and Preparation of Samples

Although it is not always possible to choose the size and shape of a sample, as when analyzing an intact turbine blade or silicon disk, certain guidelines exist when a choice is possible. If analysis of the entire sample is desired, the sample must be smaller than the collimated neutron beam. For the CNPGAA instrument, sample diameter is also limited by presence of an upper neutron guide, which is 30 mm above the center of the CNPGAA neutron beam. Because of this, samples larger than 60 mm in diameter may be analyzed only on the outer edges. In order to avoid significant neutron self-shielding and gamma-ray attenuation during irradiation, the sample thickness should preferably not exceed 10 mm, and should be considerably less if the sample contains large amounts of elements which are strong neutron absorbers (such as B, Cd, Sm, Gd). The mass of the sample should be large enough to produce an observable signal for the element(s) of interest, but not so large that the total sample count rate saturates the detector. For the majority of materials analyzed, a relatively thin target with a diameter of 10 mm to 20 mm and a mass of 0.1 to 1 g represents the ideal sample size and geometry.

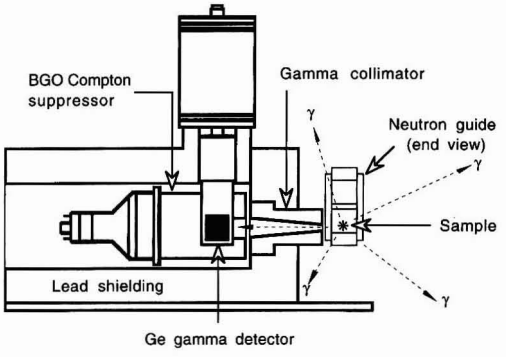

Fig. 1 Side view of the CNPGAA spectrometer in the NIST Cold Neutron Research Facility.

‡ The identification of certain commercial equipment, instruments, or materials does not imply recommendation or endorsement by the National Institute of Standards and Technology. These identifications are made only in order to specify the experimental procedures in adequate detail.

Although PGAA has occasionally been used for analysis of thin films, it should be remembered that the technique measures total hydrogen. Samples analyzed should be homogeneous whenever possible, in order to simplify corrections for neutron self-shielding, scattering and gamma-ray attenuation. If a thin layer on a substrate is analyzed for hydrogen, the substrate should preferably consist of a material which does not significantly absorb neutrons and does not contain hydrogen or any other element which emits a gamma-ray near 2223 keV.

Sample preparation is minimal. In order to avoid irregular sample geometries, powdered samples are usually made into cylindrical pellets using a hydraulic press and a 12 mm diameter die. Powders containing large quantities of elements which strongly absorb neutrons may be diluted with graphite if desired to avoid high gamma-ray count rates and large self-shielding corrections. If the surface of the sample contains grease or other contamination, it should be cleaned with ethanol or another suitable solvent prior to analysis. Small samples (those weighing < 2 g) are usually sealed into bags of FEP Teflon in a clean hood. Since the hydrogen content of this Teflon is negligible, this material is ideal for packaging samples for hydrogen analysis.

Preparation of Standards and Blanks

Accurate measurement of element mass fractions by PGAA requires precise determination of element sensitivities. Since element sensitivities are dependent upon the matrix and geometry of the material being analyzed, it is imperative that matrix and geometry of standards and samples be as closely matched as possible. This is especially important when analyzing highly hydrogenous samples, as element sensitivities are greatly affected by neutron scattering by hydrogen. If samples of widely differing hydrogen mass fraction are being analyzed, it may be necessary to prepare multiple standards in order to calibrate the analytical signal as a function of hydrogen mass fraction (see discussion below).

As an alternative to measuring the absolute mass fraction of hydrogen in a sample, it is sometimes sufficient to measure the ratio of the mass fraction of hydrogen to that of another (comparator) element in the sample. In this case it may be necessary to simply measure a standard containing both hydrogen and the comparator element, or even to perform the analysis without standards, using tabulated values of sensitivity ratios. The use of ratio measurements to eliminate measurement errors in PGAA is discussed below.

When determining hydrogen at trace levels, it is necessary to measure a blank. The blank should closely match the sample matrix and geometry, but should be free of hydrogen. Measurement of a blank allows correction for background generated from neutron capture by environmental hydrogen

(which often varies with sample matrix) and also for background due to spectral interferences.

Sample Irradiation and Gamma-ray Counting

Targets (*i.e.*, samples and standards) for irradiation are usually suspended in the neutron beam by means of Teflon strings at a 45° angle to both the detector and the neutron beam. For large and irregularly shaped samples, special sample holders and mounting procedures are employed. Samples for determination of trace hydrogen by CNPGAA are often irradiated inside an evacuated magnesium sample box in order to eliminate hydrogen background from neutron capture by water vapor in the air. Irradiation times are dependent upon the quantity of hydrogen in the target, the desired precision of the analysis, and the available beam time. Typical analysis times range from a few minutes to >48 h.

Target count rates are corrected for variations in the neutron flux over the course of an analysis. These variations are monitored by irradiating a Ti foil at regular intervals. For the TNPGAA instrument, the measured flux variation is small (generally <0.5% on a day-to-day basis). Larger variations have been measured for the CNPGAA instrument.

Data reduction and spectral manipulation are accomplished using Nuclear Data spectroscopy applications software, which includes a peak search and the SUM program written at NIST.[12] The SUM program allows peak and background channels to be entered manually and is useful for integration of small peaks on high backgrounds.

Evaluation and Minimization of Uncertainties

Experimental uncertainties are evaluated using guidelines set by the International Organization for Standardization (ISO).[13] Uncertainties from individual sources are added in quadrature to obtain the combined standard uncertainty for each measurement. The combined standard uncertainty is then multiplied by a coverage factor (usually 2) to obtain an expanded standard uncertainty corresponding to a confidence interval of approximately 95%. A discussion of sources of uncertainty and their relative contribution to the combined standard uncertainty of PGAA measurements is given below. Methods for minimizing each uncertainty are also described.

Counting Uncertainties

Counting uncertainties arise from the fact that radioactive decay is a random process, hence any measurement based on observing radiation emitted in nuclear decay is subject to some degree of statistical fluctuation. Because the statistics are straight forward, this uncertainty in any measurement may be accurately determined. Both the PEAK and SUM programs calculate the uncertainties associated with the integrated peaks. Uncertainties arising from gamma-ray counting can be lowered by increasing the counting time, hence long counting times are usually required when peak-to-background ratio is low. When measuring milligram amounts of hydrogen by CNPGAA, relative standard uncertainties of <1% are obtainable with reasonably short analysis times. For measurement of hydrogen at trace levels, the counting uncertainty often represents the major uncertainty in the analysis, even when long counting times are employed. For example, CNPGAA measurement of 60 mg kg^{-1} hydrogen in a 500 mg sample of a titanium alloy counted for 10 h yielded a relative standard counting uncertainty of 11%. The evaluation of counting uncertainties is discussed in detail by Knoll.[14]

Neutron Flux Variation and Sample Positioning

The standard uncertainty associated with variations in the flux of the neutron beam and positioning of the sample may be determined by repeated measurement of a titanium foil whose geometry is comparable to that of the sample. The relative standard uncertainty is approximately 1% for measurements by CNPGAA, and ≤0.5% for TNPGAA measurements.

Gamma-ray Background

Neutron capture by hydrogen in the shielding and in the atmosphere gives rise to hydrogen background gamma rays in both the TNPGAA and CNPGAA facilities. The magnitude of this background is dependent upon the matrix of the sample. If the sample contains nuclides which significantly scatter neutrons, additional neutrons may be scattered into the shielding and surrounding environment, thus enhancing the hydrogen gamma-ray background. Scattering-induced background enhancement has been observed with both the TNPGAA[15] and CNPGAA instruments. For this reason, the hydrogen gamma-ray background is determined from irradiation of a blank whenever possible. Although hydrogen itself has by far the largest scattering cross section (bound σ_s = 80 b) of any element,[§] significant enhancement of background H, Al, and Pb gamma-rays has been observed with neutron scattering by other elements. Irradiation of graphite and beryllium targets by CNPGAA yielded up to a factor of 10 enhancement in the hydrogen background. Measurement errors arising from background enhancement may be minimized by calibrating background count rates as a function of target total neutron scattering cross-section.[15] In the future, background enhancement in CNPGAA may be minimized by lining the inside of the sample chamber with neutron absorbing ^{6}Li-glass.

Subtraction of a hydrogen background count rate from the sample count rate does not introduce significant additional measurement uncertainty unless the background count rate is a significant fraction of the total hydrogen count rate. For the CNPGAA instrument, in the absence of significant background enhancement, a 12 h background determination yields a relative standard uncertainty in background hydrogen count rate of ~10%. If the sample count rate is ≤5 times the background count rate, *i.e.*, if the sample contains less than 50 μg of hydrogen, the relative standard uncertainty of the measurement arising from background subtraction is >1%.

Neutron Self-shielding and Scattering

Perhaps the greatest potential source of error in PGAA measurements arises from the interaction of neutrons with the target matrix. If the target matrix contains large quantities of strongly absorbing nuclides, self-shielding occurs, resulting in a decrease in the average neutron flux within the sample, and a corresponding decrease in element sensitivities. If the target composition, density and appropriate absorption cross-sections are known, and if the sample size and shape are well defined (*e.g.*, a sphere, a slab, or a cylinder), this self-shielding effect may be corrected for using well known general absorption laws.[16] Corrections for neutron self-shielding are larger for CNPGAA than for TNPGAA because of larger neutron capture cross-sections. Shielding corrections may be significant even for very thin (<1 mm) targets if appreciable amounts of B, Cd, Gd or Sm are present. For a 0.8 mm thick geological sample containing mass fraction of ≈1% m/m of boron the calculated self-shielding correction factor is about 5% for TNPGAA and 13% for CNPGAA.

Neutron scattering is a significant source of error in PGAA when hydrogenous samples are measured. The effects of neutron scattering by hydrogen on element sensitivities in TNPGAA have been studied extensively.[17–20] Measurements of 2 mm thick, disk-shaped targets have shown that sensitivities

§ Average neutron scattering cross sections for most elements are < 10b.

for most elements increase by 1.8% per 1% increase in H mass fraction. For a series of hydrogenous disks approximately 12 mm in diameter, and ranging in thickness from 1 to 12 mm, sensitivities are enhanced relative to sensitivities for non-hydrogenous disks. These enhancements are largely the result of elastic scattering which changes the mean free path of the neutron within the target and therefore changes the probability for neutron absorption. Experiments have shown that the effects of elastic scattering are minimized when spherical targets are measured.

The effects of neutron scattering on CNPGAA sensitivities are different and more pronounced than those observed for TNPGAA.[21,22] Sensitivities for CNPGAA decrease markedly with both increasing H mass fraction and target thickness. Studies indicate that interaction of cold neutrons with a warm target results in an increase in the average energy of the neutron beam. The effect is observed for both cylindrical and spherical targets.

In TNPGAA, uncertainties arising from neutron scattering by hydrogen are minimized either by careful matching of geometry and matrix of the standards and samples or by calibrating element sensitivities as a function of H mass fraction. The latter procedure was used in the analysis of hydrogen and boron in 40 food and mineral supplements with hydrogen mass fractions ranging from 0.83 to 9.82%.[23] Mixtures of D_2O–H_2O–$B(OH)_3$ and pellets prepared from homogeneous mixtures of graphite, mannitol, and boron carbide were used to calibrate H and B sensitivities. Both H and B sensitivities showed good linear correlation with hydrogen mass fraction over the range of 0 to 11%. Relative standard uncertainties associated with calibration of TNPGAA sensitivities have been evaluated at $\leqslant$1%, based on calibration curve data.

Such procedures give less satisfactory results for CNPGAA. Because scattering effects are more pronounced for CNPGAA, even small differences in sample scattering power and geometry can result in significant changes in element sensitivities. For this reason, CNPGAA has not often been used to measure element mass fractions in highly hydrogenous samples. A more common approach in CNPGAA has been to use a method of internal standards by measuring ratios of element mass fractions. Recent studies indicate that measurement errors arising from the effects of neutron self-shielding and scattering are largely eliminated when ratios are measured.[24,25] This method has been used in the determination of hydrogen in titanium alloys.[5] The ratio of hydrogen mass fraction to titanium mass fraction is measured and, since the titanium content of the alloy is known, the hydrogen mass fraction is easily calculated.

A future approach to eliminating errors due to neutron scattering in CNPGAA may be to cool the target in order to bring it into thermal equilibrium with the neutron beam.[22] The effects of neutron scattering on CNPGAA sensitivities in the cold target would then be similar to those observed for targets in TNPGAA, and could be mitigated by the use of spherical targets.

Gamma-ray Attenuation

Attenuation of the gamma-ray signal prior to detection may result in significant measurement error. The degree of attenuation is proportional to the thickness, density, and mass number (Z) of the attenuating medium, and is inversely proportional to gamma-ray energy. If the signal is collimated, the collimator should be composed of a high Z, high density material (*e.g.*, lead or tungsten) in order to minimize the number of attenuated gamma-rays reaching the detector. Gamma rays emitted from a target are also subjected to a certain amount of attenuation by the emitting material. If the target is very thick, is of high density, or contains large quantities of high Z elements, this self-attenuation may be significant, particularly for gamma-rays of low energy ($\leqslant$ 500 keV). Errors arising from gamma-ray attenuation are not eliminated when element ratios are measured, especially when count rates given by gamma-rays of vastly different energies are compared.[25] As an example, consider the measurement of hydrogen in a 1 cm thick cylinder of titanium mounted 45° to the detector. Gamma-ray attenuation within the sample results not only in a 12% decrease in the 2223 keV hydrogen signal, but also in a 3% decrease in the ratio of the 1381 keV Ti to the 2223 keV hydrogen signal. Several approaches may be used to minimize measurement errors arising from gamma-ray attenuation. Errors due to gamma-ray self-attenuation may be minimized by matching matrix and geometry of samples and standards. Alternatively, if the geometry and composition of the sample are known, self-attenuation of gamma rays may be corrected using derived equations.[26] If one of the elements present in the sample matrix emits a spectrum of gamma-ray lines covering a range of energies, a third option is to calibrate gamma attenuation as a function of energy by comparing the relative intensities of these lines with those measured in a thin foil of the same material (where self-attenuation is minimal).

Sample Heterogeneity

Sample heterogeneity can introduce errors into PGAA measurements, regardless of whether absolute mass fractions or ratios are measured.[25] Element sensitivities may be dependent on the distribution of the elements in a target. Corrections for neutron self-shielding or gamma-ray attenuation are difficult, if not impossible, for heterogeneous targets, since equations derived for these corrections assume a homogeneous composition for the sample. One method of minimizing measurement errors due to sample heterogeneity is to analyze the sample in several different orientations, then report the average of the measurements.

Spectral Interferences

Because of the complexity of prompt gamma-ray spectra, spectral interferences often constitute a major source of error in PGAA measurements. Current tabulations of prompt gamma-rays list few interferences for the H 2223.3 keV gamma-ray. Lone *et al.*[27] list gamma-rays by Ba (2220.0 keV), Os (2223.3 keV), and Xe (2225.2 keV) in the H energy region, while Tuli's compilation[28] includes Gd (2220.3 keV), Ge (2223.0 keV), Nd (2223.5 keV), Ru (2223.8 keV), Sn (2224.7 keV), and Ba (2224.8 keV). However, these lists are incomplete and subject to error. Spectra of some elements have many small peaks which are not listed in these compilations. When measuring hydrogen at very low levels by CNPGAA, even tiny peaks in the hydrogen region can become major sources of error. For this reason, accurate determination of hydrogen at low levels in many materials is possible only after rigorous examination of spectra of samples and carefully prepared blanks.

Although materials are available that have been certified as hydrogen-free by another analytical technique, it is often necessary to prepare blanks by removal of hydrogen from these materials. Many metals (*e.g.*, Ti, Zr) readily lose hydrogen when heated in a vacuum. More volatile materials or those that decompose upon heating may require freeze-drying to remove residual moisture. It is desirable to prepare more than one blank in order to check the material for complete loss of hydrogen. If analysis of a blank reveals a peak in the hydrogen region, the relative intensity of this line to that of a known peak for an element present in the material should be calculated. If this ratio is the same for each blank analyzed, the peak is likely to be an interference and not due to residual hydrogen in the blank.

CNPGAA analyses of samples and blanks containing Co and Cu have revealed previously unlisted peaks for these elements

near 2223 keV. A small peak at 2219 keV interfered with measurement of hydrogen in titanium, however, this peak was reduced with the use of Compton suppression.[5] The magnitude of error introduced by spectral interferences in hydrogen measurements depends upon the mass fraction of the interfering element, the intensity of the interfering gamma-ray peak, and the mass fraction of hydrogen in the sample. For example, failure to correct for the titanium interference peak in the analysis of a 0.2 g sample of titanium containing hydrogen at 215 mg kg^{-1} yields a value for hydrogen that is 25 to 30% too high.

Other Sources of Uncertainty

Measurements by PGAA are affected by many of the same sources of uncertainty that affect measurements by delayed neutron activation analysis (NAA). These include uncertainties arising from pulse pileup correction and sample weighing, which are negligible for most PGAA measurements. For hygroscopic samples, absorption of water represents an additional source of error, which can generally be eliminated by storing samples in a desiccator prior to analysis. A discussion of sources of error in NAA is given elsewhere.[29]

Expanded Standard Uncertainties of Measurements

For determination of hydrogen at percentage levels in biological and geological samples by TNPGAA, expanded standard uncertainties are often less than 5% with counting times of < 24 h. Determination of large amounts of hydrogen by CNPGAA usually yields higher expanded uncertainties than TNPGAA, except where it is possible to measure the ratio of hydrogen to another element. Higher expanded uncertainties are often obtained when neutron self-shielding, gamma-ray attenuation, or sample heterogeneity are significant, or when measuring hydrogen at very low levels. Measurement of 50 to 200 mg kg^{-1} in titanium alloys resulted in expanded uncertainties of 10 to 30% with analysis times of 5 h or longer.[5] Future improvements to the CNPGAA instrument are expected to result in smaller uncertainties for measurement of trace hydrogen.

Limits of Detection of Hydrogen

Limits of detection (LOD) for hydrogen in selected matrices by thermal and cold neutron PGAA are given in Table 1. The LOD for a 1 g sample counted for 24 h is calculated as described by Currie,[30] using the equation

$$\mathrm{LOD} = 4.65\,(R_b/t)^{1/2}/S$$

where R_b is the background counting rate (counts s^{-1}), t is the duration of the count (s), and S is the hydrogen sensitivity in counts s^{-1} mg^{-1}. The hydrogen signals from coal fly ash, bovine liver, and quartz are presumed to be free of spectral interferences. Because of the presence of a Ti interference peak at 2219 keV, the CNPGAA LOD for hydrogen in Ti-6Al-4V is higher than in the other three matrices.

Table 1 LOD for hydrogen in selected matrices for thermal and cold neutron PGAA

	Limit of detection/mg kg^{-1}			
	Coal Fly Ash (SRM 1633)	Bovine Liver (SRM 1577)	Quartz	Ti-6Al-4V*
Thermal	27	46	nd†	nd
Cold	8.5	nd	5.0	15

* An alloy of titanium containing ≈6% aluminum and 4% vanadium by mass. † nd, not determined.

Applications

CNPGAA has been used to measure hydrogen in a wide variety of materials (see Tables 2 and 3). Considerable emphasis has been placed upon the ability of the technique to measure hydrogen in metals. Hydrogen mass fractions of 50 to 750 mg kg^{-1} have been measured in titanium alloy jet engine compressor blades in order to determine whether hydrogen embrittlement may be responsible for blade failure.[5,31] The technique has also been used to analyze a series of titanium alloy standards containing 100 to 20000 mg kg^{-1} hydrogen,[5] and to measure < 100 mg kg^{-1} hydrogen in samples of nanocrystalline Fe, Pd, and Cu. Attempts to measure hydrogen in semiconductor materials have met with limited success. Less than 10 mg kg^{-1} hydrogen has been measured in hydrothermal quartz, while hydrogen mass fractions of 50 to 80 mg kg^{-1} have been measured in crystals of semiconductor grade germanium.[4,32] Other industrially important materials analyzed for H by CNPGAA have included pure and substituted fullerenes (as little as 0.02% m/m H measured),[33] solid proton conductors,[34] hydrofluorocarbons and solid acid catalysts,[35] zeolite catalysts, and samples of substituted lithium niobate. Hydrogen has also been measured in geological materials, including the Allende meteorite,[10,36] United States Geological Survey (USGS) rock standards and terrestrial basalts.

TNPGAA has proven valuable for the determination of hydrogen (at mass fractions of 0.83 to 12%) and up to 22 other elements in foods and mineral supplements.[23,37–39] Analysis of 22 USGS reference standards yielded hydrogen mass fractions from 0.02 to 3.1%.[40] TNPGAA has also measured 580 to 920 mg kg^{-1} hydrogen in ground ash from Mt. St. Helens,[41] 3.7 to 4% m/m hydrogen in bituminous coal standard reference materials,[42] and 0.09 to 0.61% m/m hydrogen in construction materials (sand, cement and concrete).[43]

Future Developments

Future developments in the CNPGAA instrument, such as the addition of improved neutron and gamma-ray shielding to the system and continued fine tuning of Compton suppression electronics are expected to result in lower gamma-ray background, higher signal to noise ratio and better H LOD. Such improvements should also result in smaller uncertainties in hydrogen measurements and also shorter analysis times. The replacement of the D_2O cold source with a liquid hydrogen source will result in a 5–10 fold increase in the neutron capture rate, reducing the sample size required for measurement. The installation of a neutron focusing lens will make it possible to analyze samples less than a millimeter in diameter without loss in sensitivity as well as to probe larger samples for compositional mapping. The lens, which has been tested at the CNPGAA station, focuses the neutron beam to 0.5 mm, resulting in an increase by a factor of 80 in neutron current density over the unfocused beam.[48] Future plans also call for the development of a lens which will bend the neutron beam as well as focus it. The new lens will lower the sample position by more than 40 mm, removing samples from the immediate vicinity of the upper neutron guide.

Much work still remains in order to ensure accurate measurement of hydrogen in materials by CNPGAA. Reliable blanks need to be prepared for many materials in order to minimize errors due to spectral interferences. Further studies are also needed with cryogenic samples in order to develop a method for minimizing the effects of neutron scattering on CNPGAA measurements of highly hydrogenous samples.

The potential of PGAA for measurement of hydrogen in materials is great and has yet to be fully realized. Research areas which should be more fully exploited in the future include the use of PGAA to study hydrogen embrittlement in a variety of metals, to accurately measure the degree of deuteration of

Table 2 Some materials analyzed for hydrogen by CNPGAA*

Material	Hydrogen content: CNPGAA	Hydrogen content: Other methods
Titanium (alloyed and pure):		
SRM 354 (unalloyed)	224 ± 22 mg kg^{-1} [a]	215 ± 6 mg kg^{-1} [b]
SRM 352c (unalloyed)	58 ± 20 mg kg^{-1} [a]	49 ± 0.9 mg kg^{-1} [b]
Ti-6Al-4V standards	117 ± 39 mg kg^{-1} [c]	114 ± 60 mg kg^{-1} [d]
	164 ± 138 mg kg^{-1} [c]	175 ± 115 mg kg^{-1} [d]
Nanocrystalline metals:		
Fe	0.250 ± 0.078% m/m [a]	
	0.214 ± 0.040% m/m [a]	
Pd	0.0080 ± 0.0086% m/m [a]	
Cu	0.0031 ± 0.013% m/m [a]	
Quartz:	6 ± 12 mg kg^{-1} [e]	5.4 mg kg^{-1} [f]
	10 ± 12 mg kg^{-1} [e]	12 mg kg^{-1} [f]
	≤5 mg kg^{-1} [e]	4.9 mg kg^{-1} [f]
	≤6 mg kg^{-1} [e]	4.6 mg kg^{-1} [f]
Semiconductor-grade germanium:	80 ± 55 mg kg^{-1} [e]	
	75 ± 50 mg kg^{-1} [e]	
	50 ± 40 mg kg^{-1} [e]	
Pure and substituted fullerenes:		
C_{60}	C:H (atom ratio) = 180 ± 30 [g]	
K_3C_{60}	C:H (atom ratio) = 114 ± 11 [g]	
$Rb_{2.6}K_{0.4}C_{60}$	C:H (atom ratio) = 68 ± 6 [g]	
Na_2RbC_{60}	C:H (atom ratio) = 180 ± 35 [g]	
Solid proton conductors:		
Yb doped $SrCeO_3$	3.1 ± 0.8 mol% [h]	2.5 mol% [i]
Undoped $SrCeO_3$	0.7 ± 0.1 mol% [h]	0.5 mol% [i]
Allende meteorite:	160 ± 10 mg kg^{-1} [j]	190 mg kg^{-1}, 180 mg kg^{-1} [k]; 110 mg kg^{-1}, 150 mg kg^{-1} [l]

* All stated uncertainties are expanded standard uncertainties as defined in the text. [a] Previously unpublished results. [b] NIST certified values determined by hot extraction of hydrogen at 1400 °C and vacuum fusion of the sample at 1950 °C. [c] Ref. 5. [d] Determined using a LECO inert gas fusion analyzer, ref. 5. [e] Ref. 4. [f] Determined by IR, ref. 4. [g] Ref. 33. [h] Ref. 34. [i] Determined by thermal gravimetry, ref. 34. [j] Ref. 36. [k] Ref. 44. [l] Ref. 45.

Table 3 Some materials analyzed for hydrogen by TNPGAA*

Material	Hydrogen content: TNPGAA	Hydrogen content: Other methods
Biological materials:		
SRM 1549 (Milk powder)	5.9 ± 0.8% m/m [a]	
SRM 1570 (Spinach)	5.45 ± 0.08% m/m [b]	5.57% m/m [d]
SRM 1571 (Orchard Leaves)	5.84 ± 0.08% m/m [b]	5.84 ± 0.26% m/m [d]
SRM 1577 (Bovine Liver)	6.83 ± 0.08% m/m [c]	6.97 ± 0.16% m/m [d]
Ground beef	9.89 ± 0.12% m/m [a]	
Whole milk (fluid)	10.77 ± 0.09% m/m [a]	
Potato chips	7.32 ± 0.11% m/m [a]	
Corn flakes	6.14 ± 0.07% m/m [a]	
USGS reference standards:		
GSP-1	785 ± 40 mg k^{-1} [e]	680 ± 170 mg kg^{-1} [f]
STM-1	0.18 ± 0.02% m/m [e]	0.19% m/m [f]
AGV-1	0.18 ± 0.02% m/m [e]	0.20 ± 0.04% m/m [f]
PCC-1	0.58 ± 0.01% m/m [e]	0.57 ± 0.03% m/m [f]
Volcanic ash (Mt. St. Helens):		
	580 ± 90 mg kg^{-1} [g]	
	900 ± 100 mg kg^{-1} [g]	
	920 ± 70 mg kg^{-1} [g]	
	870 ± 40 mg kg^{-1} [g]	
Construction materials:		
Sand	0.28 ± 0.01% m/m [e]	
Cement	0.088 ± 0.014% m/m [e]	
Concrete	0.61 ± 0.01% m/m [e]	

* All stated uncertainties are expanded standard uncertainties as defined in the text. [a] Ref. 37. [b] Ref. 38. [c] Ref. 23. [d] Ref. 46. [e] Ref. 40. [f] Ref. 47. [g] Ref. 41. [h] Ref. 43.

materials, and to measure absorption of hydrogen by materials to determine their potential for use in hydrogen fuel cells.

The cooperation of the NIST reactor staff during the PGAA measurements is gratefully acknowledged. R. Lindstrom, E. Mackey and D. Anderson are thanked for their advice and interest in this work.

References

1 Meyn, D. A., *Metall. Trans.*, 1974, **5**, 2405.
2 Chevallier, J., and Aucouturier, M., *Ann. Rev. Mater. Sci.*, 1988, **18**, 219.
3 Lindstrom, R. M., Paul, R. L., Vincent, D. H., and Greenberg, R. R., *J. Radioanal. Nucl. Chem.*, 1994, **180**, 271.
4 Paul, R. L., and Lindstrom, R. M., *Diagnostic Techniques for Semiconductor Processing*, MRS Symposium Proceedings Volume 324, ed. Glembocki, O. J., Pang, S. W., Pollak, F. H., Crean, G. M., and Larrabee, G., Materials Research Society, Pittsburgh, PA, 1994, pp. 403–408.
5 Paul, R. L., Privett III, H. M., Lindstrom, R. M., Richards, W. J., and Greenberg, R. R., *Metall. Mater. Trans. A*, 1996, **27A**, 3682.
6 Lindstrom, R. M., *J. Res. Nat. Inst. Stand.*, Techn 1993, **98**, 127.
7 Failey, M. P., Anderson, D. L., Zoller, W. H., Gordon, G. E., and Lindstrom, R. M., *Anal. Chem.*, 1979, **51**, 2209.
8 Anderson, D. L., Failey, M. P., Zoller, W. H., Walters, W. B., Gordon, G. E., and Lindstrom, R. M., *J. Radioanal. Chem.*, 1981, **63**, 97.
9 Lindstrom, R. M., Zeisler, R., Vincent, D. H., Greenberg, R. R., Stone, C. A., Mackey, E. A. Anderson, D. L., and Clark, D. D., *J. Radioanal. Nucl. Chem.*, 1993, **167**, 121.
10 Paul, R. L., Lindstrom, R. M., and Vincent, D. H., *J. Radioanal. Nucl. Chem.*, 1994, **180**, 263.
11 Mackey, E. A., Anderson, D. L., Chen, H., Downing, R. G., Greenberg, R. R., Lamaze, G. P., Lindstrom, R. M., Mildner, D. F. R., and Paul, R. L., *J. Radioanal. Nucl. Chem.*, 1996, **203**(2), 411.
12 Lindstrom, R. M., *Biol. Trace Elem. Res.*, 1994, **43–45**, 597.
13 International Standards Organisation, *Guide to the Expression of Uncertainty in Measurement*, 1st edn. ISO, Geneva, 1993.
14 Knoll, G. F., *Radiation Detection and Measurement*, Wiley, New York, 1989, pp. 65–99.
15 Anderson, D. L., and Mackey, E. A., *J. Radioanal. Nucl. Chem.*, 1993, **167**, 145.
16 Fleming, R. F., *Int. Appl. Radiat. Isot.*, 1982, **33**, 1263.
17 Copley, J. R. D., and Stone, C. A., *Nucl. Instrum. Meth.*, 1989, **A281**, 593.
18 Mackey, E. A., Gordon, G. E., Lindstrom, R. M., and Anderson, D. L., *Anal. Chem.*, 1991, **63**, 288.
19 Mackey, E. A., Gordon, G. E., Lindstrom, R. M., and Anderson, D. L., *Anal. Chem.*, 1992, **64**, 2366.
20 Mackey, E. A., and Copley, J. R. D., *J. Radioanal. Nucl. Chem.*, 1993, **167**, 127.
21 Paul, R. L., and Mackey, E. A., *J. Radioanal. Nucl. Chem.*, 1994, **181**, 321.
22 Mackey, E. A., *Biol. Trace Element Res.*, 1994, **43–45**, 103.
23 Anderson, D. L., Cunningham, W. C., and Mackey, E. A., *Biological Trace Element Research*, 1990, **27**, 616.
24 Lindstrom, R. M., Fleming, R. F., Paul, R. L., and Mackey, E. A., *Proceedings of the International k_0 Users Workshop*, Gent, 1992, pp. 121–124.
25 Paul, R. L., *J. Radioanal. Nucl. Chem.*, 1995, **191**, 245.
26 Debertin, K., and Helmer, R. G., *Gamma- and X-Ray Spectrometry with Semiconductor Detectors*, Elsevier, Amsterdam, 1988.
27 Lone, M. A., Leavitt, R. A., and Harrison, D. A., *Atomic Data and Nuclear Data Tables*, 1981, **26**, 511.
28 Tuli, J. K., in *Prompt Gamma Neutron Activation Analysis*, ed. Alfassi, Z. B., and Chung, C., CRC Press, Boca Raton, FL, 1995, pp. 177–223.
29 Blaauw, M., Ammerlaan, M. J. J., and Bode, P., *Appl. Radiat. Isotop.*, 1993, **44**, 547.
30 Currie, L. A., *Anal. Chem.*, 1968, **40**, 586.
31 Paul, R. L., and Lindstrom, R. M., *Review of Progress in Quantitative Nondestructive Evaluation*, vol. 13, ed. Thompson, D. O., and Chimenti, D. E., Plenum Press, New York, 1994, pp. 1619–1624.
32 Paul, R. L., and Lindstrom, R. M., *International Workshop on Semiconductor Characterization: Present Status and Future Needs*, ed. Bullis, W. M., Seiler, D. G., and Diebold, A. C., AIP Press, Woodbury, NY, 1996, pp. 342–345.
33 Neumann, D. A., Copley, J. R. D., Reznik, D., Kamitakahara, W. A., Rush, J. J., Paul, R. L., and Lindstrom, R. M., *J. Phys. Chem. Solids*, 1993, **54**, 1699.
34 Krug, F., Schober, T., Paul, R., and Springer, T., *Solid State Ionics*, 1995, **77**, 185.
35 Crawford, M. K., Corbin, D. R., and Vernooy, P. D., *Trans. Am. Nucl. Soc.*, 1994, **71**, 168.
36 Paul, R. L., Lindstrom, R. M., and Vincent, D. H., *J. Radioanal. Nucl. Chem.*, 1995, **190**, 181.
37 Anderson, D. L., Cunningham, W. C., and Lindstrom, T. R., *J. Food Comp. Anal.*, 1994, **7**, 59.
38 Anderson, D. L., Cunningham, W. C., and Alvarez, G. H., *J. Radioanal. Nucl. Chem.*, 1993, **167**, 139.
39 Anderson, D. L., and Cunningham, W. C., *Trans. Am. Nucl. Soc.*, 1994, **71**, 21.
40 Anderson, D. L., Sun, Y., Failey, M. P., and Zoller, W. H., *Geostand. News.*, 1985, **9**, 219.
41 Anderson, D. L., Phelan, J. M., Vossler, T., and Zoller, W. H., *J. Radioanal. Chem.*, 1982, **71**, 47.
42 Germani, M. S., Gokmen, I., Sigleo, A. C., Kowalczyk, G. S., Ohmez, I., Small, A., Anderson, D. L., Failey, M. P., Gulovali, M. C., Choquette, C. E., Lepel, E. A., Gordon, G. E., and Zoller, W. H., *Anal. Chem.*, 1980, **52**, 240.
43 Anderson, D. L., Gordon, G. E., and Lepel, E. A., *Can. J. Chem.*, 1983, **61**, 724.
44 Scoon, J. H., in *The Allende Meteorite Reference Sample*, ed. Jarosewich, E., Clarke, Jr. R. S., and Barrows, J. N., *Smithsonian Contrib. Earth Sci.*, 1987, **27**, 39.
45 Willis, J. P., in: *The Allende Meteorite Reference Sample*, ed. Jarosewich, E., Clarke, Jr. R. S., and Barrows, J. N., *Smithsonian Contrib. Earth Sci.*, 1987, **27**, 39.
46 Gladney, E. S., O'Malley, B. T., Roelandts, I., and Gills, T. E., *National Bureau of Standards Special Publication NBS SP 260-111*, 1987.
47 Gladney, E. S., Burns, C. E., and Roelandts, I., *Geostand. News.*, 1983, **7**, 3.
48 Chen, H., Sharov, V. A., Mildner, D. F. R., Downing, R. G., Paul, R. L., Lindstrom, R. M., Zeissler, C. J., and Xiao, Q.-F., *Nucl. Instrum. Meth. B*, 1995, **95**, 107.

Paper 6/06419A
Received September 17, 1996
Accepted December 4, 1996

Ozone Degradation of Residual Carbon in Biological Samples Using Microwave Irradiation

Wenchun Jiang†, Stuart J. Chalk‡, H. M. 'Skip' Kingston*

Department of Chemistry and Biochemistry, Duquesne University, Pittsburgh, PA 15282, USA

In an attempt to produce complete oxidation of a biological matrix, bovine liver, ozone was investigated as an additional, potentially non-contaminating, oxidizing reagent after nitric acid digestion. Experiments were carried out to determine the decomposition efficiency of residual carbon species, primarily *o*-, *m*- and *p*-nitrobenzoic acids (NBAs), using ozone. The NBAs were degraded by purging sample digests with ozone, while heating the solutions with microwave energy at atmospheric pressure. The effects of the degradation temperature and solution pH on the ozonation of NBAs were determined. Solid phase extraction (C_{18}) was used to extract NBAs from the acid digestate solutions prior to HPLC analysis. Reversed phase HPLC was used to determine NBA concentrations in digest solutions. After 2.5 h of purging ozone at 80 °C, 33.65 ± 3.80% *o*-NBA degradation, 19.39 ± 1.74% *m*-NBA degradation, and 26.47 ± 3.36% *p*-NBA degradation were obtained.

Keywords: *Ozone; biological samples; microwave digestion; residual carbon; nitrobenzoic acids*

Today, microwave energy has been widely applied to sample digestion for the analysis of biological, geological, and environmental materials. Microwave enhanced sample preparation techniques dramatically speed up sample dissolution and decomposition, but do not eliminate organic carbon residues due to the incomplete oxidation of organic compounds. Research on microwave sample decomposition has been based on comparison and optimization of conventional acid digestion procedures using microwave energy in open or closed vessels. The completeness of these techniques can be evaluated by considering the residual carbon content, recovery of analytes, and digestion time. Since organic carbon residues interfere with detection by some instrumental techniques, the completeness of decomposition can be a crucial factor for accurate analysis.

Nitric acid, the most commonly used mineral acid, oxidizes the majority of organic matrix components with the primary exception of aromatic ring structures, particularly nitrobenzoic acids (NBAs).[1–7] Pratt *et al.*[1] identified *o*-, *m*- and *p*-NBAs as the major residual organic compounds after nitric acid digestion of bovine liver in sealed perfluoroalkoxy (PFA) vessels at a maximum temperature of 180 °C and a sustained maximum pressure of 8 atm (1 atm = 101.325 kPa). A number of researchers have identified that residues from incomplete nitric acid oxidation act as interferences with some analytical techniques such as polarography, voltammetry, and ETAAS.[1,4,5,8,9] In spectroscopic techniques with high energy interfaces, such as ICP-OES, ICP-MS, and FAAS, small amounts of residual carbon is not a significant limitation.

To take account of residual carbon Pratt *et al.* also successfully demonstrated that refluxing with perchloric acid ($HClO_4$) can decompose the residual organic products remaining after nitric acid digestion.[1] However, a drawback of using perchloric acid is the possible formation of explosive products if safety precautions are not taken.[10] Thus, an alternative oxidizing reagent is desirable to completely and safely decompose organic carbon residues. The goal is the evaluation of ozone as an alternative decomposition reagent for analytical sample preparation, especially coupled to microwave decompositions.

This work extends the studies of Pratt *et al.*[1] and Würfels *et al.*[4,5] who identified that the major residual organic species in nitric acid digests of bovine liver are *o*-, *m*- and *p*-NBAs, arising from the nitration of aromatic amino acid constituents of original sample protein. This research focuses on the addition of ozone to aqueous acidic solutions to aid the microwave degradation of NBAs. The application of ozone to decompose *o*-, *m*- and *p*-NBAs also allows an investigation into the oxidation processes needed to efficiently destroy or minimize organic carbon residues.

Experimental

Reagents and Standards

NIST SRM 1577a, bovine liver, was used as the biological matrix in this study. Samples were vacuum-dried at room temperature for 24 h in accordance with the instructions on the certificate of analysis.

Compressed air (reagent grade) was used as the source of oxygen to produce ozone. Ozone concentrations were measured by the decolorization of potassium indigo trisulfonate (Aldrich, Milwaukee, WI, USA) solution. Doubly distilled 18 MΩ NanoPure water (Barnstead, Dubuque, IA, USA) was used to prepare all solutions. 2-Nitrobenzoic acid (*o*-NBA) (96%, Aldrich), 3-nitrobenzoic acid (*m*-NBA) (99%, Aldrich) and 4-nitrobenzoic acid (*p*-NBA) (99%, Eastman Kodak, Rochester, NY, USA) were used to prepare aqueous samples for the NBA degradation studies. All other reagents were certified ACS reagent grade.

The HPLC eluent used was 5% methanol (HPLC grade)–15% acetonitrile (HPLC grade)–80% H_2O (18 MΩ) (by volume before mixing), to which 0.05% trifluoroacetic acid was added to acidify the solution to a pH of 2–2.3.

Apparatus

The ozonator used for ozone production in this work was a Model ss-150 (Pillar Technologies, Hartland, WI, USA). It was purchased from Radiation Disposal Systems (Charlotte, NC, USA) and was redesigned to a Model ss-300 (Select Industrial Systems, Waukesha, WI, USA) to double the ozone production rate.

Fig. 1 shows a schematic representation of the ozonation apparatus set-up. The reaction vessel was a Teflon microwave vessel, 28 cm tall with an id of 3.8 cm (Prolabo, Paris, France). The total volume was approximately 320 ml. The gas stream was introduced into the reaction vessel *via* a 25 μm pore size

† Present address: Caelum research Corporation, 7505 Standish Place, Rockville, MD 20855, USA.

‡ Present address: Department of Natural Sciences, University of North Florida, Jacksonville, FL 32224, USA.

Teflon gas sparger (Omnifit, Toms River, NJ, USA) located close to the bottom of the vessel.

Ultraviolet and visible spectra were obtained using a Cary 1E UV/VIS spectrophotometer (Varian Australia, Springvale Victoria, Australia). The instrument was interfaced to a Grid 3861S-25 PC computer (Varian Australia) running Varian Cary 13E software Version 2. The pH of the solutions was calculated or measured using a Model 710A pH meter (Orion, Boston, MA, USA) equipped with a pH combination electrode (Orion, part No. 91–56).

The atmospheric pressure microwave unit used in this research was a Maxidigest MX350 (Prolabo). A gas bulb thermometer (Prolabo) and a PC computer (Dell 450/MX, Austin, TX, USA) running MEGAL 500 software (Prolabo) were used to control microwave power based on the measurement of the temperature. The closed vessel microwave unit used for the dissolution of bovine liver was an MLS 1200 MEGA (Milestone, Sorisole, Italy). High pressure vessels were used for these digestions (Milestone).

HPLC analysis was performed using a Model M-6000A (Waters Associates, Milford, MA) coupled to a Model 440 absorbance detector (Waters Associates) and an HP 3396A integrator (Hewlett-Packard, Avondale, PA). The reversed phase column used was a Vydac Equivalent C_{18} column (non-endcapped, 25 cm × 4.6 mm, 5 μm particle size) (Whatman, Clifton, NJ, USA). Solid phase extraction was performed on a Mega Bond Elut octadecylsilyl (C_{18}) cartridge (endcapped) (ChromTech, Apple Valley, MN, USA). A Bond Elut adapter (ChromTech) and poly(propylene)polyethylene syringe (Aldrich) were used to push solvents through the cartridge.

Procedures

The ozone transfer rate into water and the ozone decomposition rate in water were initially evaluated. Ozonated air was purged through 50 ml of doubly distilled water in the Teflon vessel for a certain period of time with different flow rates (110, 190 and 328 ml min^{-1}). The concentration of the ozone solutions were determined immediately using the Indigo Blue method.[11] The ozone decomposition rate was determined by measuring the decrease of the ozone absorbance at 260 nm over a period of 1 h.

In order to study the degradation of *o*-, *m*- and *p*-NBAs at different pHs, solutions of the NBAs were made up in different concentration nitric acid solutions and water. Ozone was then purged through these solutions for 90 min at 80 or 115 °C, the solutions were cooled, made up to volume in 100 ml calibrated flasks and analyzed using solid phase extraction (SPE) and HPLC.

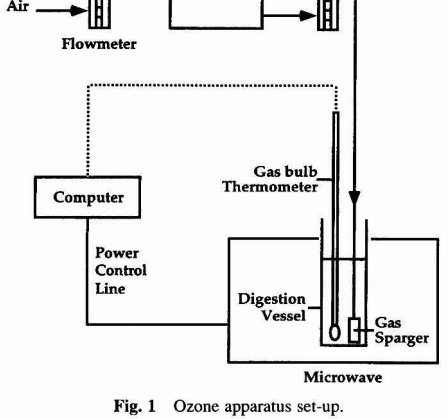

Fig. 1 Ozone apparatus set-up.

Bovine liver samples were digested using a closed vessel high pressure microwave system. Each batch contained four samples of bovine liver (~ 0.25 g each) and two blanks in 10 ml of concentrated nitric acid using the high pressure vessels. Three of the samples were put in regular sample vessels and the remaining one was put in the monitor vessel to measure the pressure and temperature change during the digestion. The microwave energy was programmed to heat at 600 W until reaching 180 °C (in about 2 min), and the temperature was kept at 180 °C for about 8–9 min. The samples and rinses were transferred to calibrated flasks, diluted to 50 ml, and were directly used for the atmospheric microwave vessel ozonation study. *o*-, *m*- and *p*-NBA solutions were also prepared using a flow rate of 328 ml min^{-1} to study the mechanism of the ozonation. After purging ozone (1–2 h) at a temperature of 80 °C or higher, the solutions were transferred and diluted to 100 ml calibrated flasks before SPE and HPLC analysis.

The C_{18} cartridges used for SPE were conditioned by passing 5 ml of methanol through them, followed by at least 10 ml of doubly distilled water prior to extraction of an aqueous sample. An aliquot of 0.5 ml of the sample solution was passed through the cartridge, followed by a wash with 5 ml of pH 2 aqueous *o*-phosphoric acid and finally eluted with 2 ml of methanol.

Results and Discussion

Ozone Transfer Rate and Decomposition Rate in Solution

By varying the ozone gas flow rate, it was shown that higher gas flow rates produced greater ozone transfer rates into water. Therefore, a 328 ml min^{-1} gas flow rate was chosen as the ozone purging flow rate for subsequent experiments. At this flow rate, the ozone generator produced 445 mg of ozone per hour. This ensured a fast ozone mass transfer and a high ozone concentration without violent bubbling of the samples, minimizing any loss of solution. The saturated ozone solution that was produced decomposed by 50% in 1 h once the gas flow was turned off. At the flow rate of 328 ml min^{-1}, pure water can be saturated with ozone in less than 10 min, which indicated that the dissolution rate of ozone was much faster than the decomposition rate of ozone under the experimental conditions; therefore, a saturated ozone solution could be maintained.

SPE Sample Clean-up

The efficiency of the extraction of NBAs by the C_{18} solid phase cartridges was investigated at the level of NBAs expected in the digests. Table 1 shows the SPE cartridge extraction efficiency for a 1 ml aliquot of 66.7 ppm of each of *o*-, *m*-, *p*-NBA solution (200 μg total). The efficiency of extraction for each NBA was excellent (99–103%). Replicate extractions on the same column and on different columns were statistically indistinguishable. Owing to the levels of NBAs being well below the capacity of the cartidges (50 mg), it was anticipated that this efficiency would also be acheivable on real sample digests even though other organic species may be present.

HPLC of Nitrobenzoic Acid

An interesting observation in the HPLC chromatograms was the changing retention time of the compounds. Continuous injections of bovine liver digestate solution onto the HPLC column caused the retention time of the compounds to increase significantly. This was attributed to the retention of some large organic species extracted by the C_{18} cartridge which changed the surface of the column packing and thus the chromatography.

Pumping acetonitrile through the column for approximately 30 min washed out the retained organics and the retention times returned to their original values. The use of a guard column could alleviate this problem.

o-, m- *and* p-*NBA Degradation*

Table 2 shows the effects of pH and temperature on the degradation. Since this research focuses on the application of ozone with nitric acid to improve the oxidation of organic residues, in these experiments nitric acid was used to adjust the pH of the NBA solutions. The mechanism of ozonation of NBAs in acidic solution was expected to be an electrophilic reaction.[12,13] However, the presence of nitrosyl ($-NO_2$) and carboxylic acid (–COOH) groups (both electron-withdrawing) on the aromatic ring makes it electron deficient, so it is difficult for ozone to electrophilically attack the ring structure at low pH. The reaction rate observed should therefore be relatively slow in 25% nitric acid[13] and concentrated nitric acid solutions as was observed.

The pK_a values of *o*-, *m*- and *p*-NBA in water at 25 °C are 2.17, 3.49 and 3.77 respectively.[14] Increasing the solution pH increases the concentration of deprotonated forms of NBAs. When the NBAs are deprotonated (NBA^-), carboxylate ($-COO^-$), an electron-donating group, replaces –COOH and electrophilic attack by ozone is favored. Thus, the increase from pH − < 0.1 to 3.2 results in very different oxidation rates. Even at a pH of 0.8, most of the NBA molecules are protonated, but the existence of a small concentration of the deprotonated species provides partial oxidation. At a pH of 3.2, about 85% degradation of NBAs can be achieved in 90 min at 80 °C, suggesting that it would be better to neutralize the digestate solution, with a non-contaminating reagent, such as ammonia, prior to ozonation to enhance the destruction of NBAs. Both of these reagents could be introduced as high purity gases.

Temperature also helps the oxidation process. The higher the temperature, the faster the degradation rate. As these experiments were designed for the purging of ozone through solution in an atmospheric pressure microwave system, the temperature of the reaction was limited by the boiling point of the reagent used (118 °C for nitric acid). At this temperature the experimental conditions are rather violent and thus, for safety reasons, a lower temperature (80–90 °C) was used and is recommended. Hydrogen peroxide has been shown to increase the rate of decomposition of nitrogenzoic acids in aqueous solution. The addition of hydrogen peroxide to the reaction mixture was also tested while bubbling ozone through the solution. No additional decomposition was seen when compared to ozone alone.

Table 1 Extraction efficiency of *o*-, *m*- and *p*-nitrobenzoic acids on the same and different C_{18} columns

		Extraction*		
Cartridge I—		A	B	C
	o-NBA	100 ± 0.9	100 ± 0.7	100 ± 0.6
	m-NBA	99 ± 1.4	99 ± 1.5	99 ± 1.2
	p-NBA	100 ± 0.7	100 ± 0.8	100 ± 0.8
Cartridge II—		A	B	C
	o-NBA	102 ± 1.7	100 ± 1.6	100 ± 1.5
	m-NBA	102 ± 1.7	100 ± 1.3	100 ± 1.5
	p-NBA	103 ± 1.8	100 ± 1.1	101 ± 0.8
Cartridge III—		A	B	C
	o-NBA	100 ± 1.3	100 ± 0.7	100 ± 1.1
	m-NBA	100 ± 1.4	99 ± 1.2	99 ± 1.3
	p-NBA	100 ± 0.8	100 ± 0.7	99 ± 0.7

* Mean ± % RSD of three replicate injections. Extractions A, B, and C were consecutive on each column.

Table 2 Degradation of *o*-, *m*- and *p*-nitrobenzoic acids in acid solutions

Solution	pH	Temperature/ °C	Time/ min	Degradation (% ± %RSD*) *o*-NBA	*m*-NBA	*p*-NBA
18 MΩ water	~ 3.2	80	90	84 ± 3.8	85 ± 3.2	88 ± 3.4
1% HNO_3	0.8	80	90	58 ± 0.5	63 ± 3.2	69 ± 0.1
25% HNO_3	< 0.1	80	90	23 ± 1.4	15 ± 2.4	19 ± 0.7
Conc. HNO_3	< 0.1	80	90	27 ± 1.7	17 ± 1.7	21 ± 0.5
Conc. HNO_3	< 0.1	115	90	42 ± 0.4	27 ± 1.6	28 ± 0.4

* %RSDs were calculated from three replicate digestions.

Degradation of Bovine Liver Digestate

The estimated total organics in the original SRM 1577a bovine liver sample was ~ 97.4% of the sample dry mass (calculated from ref. 15). After closed vessel nitric acid digestion at 180 °C, HPLC analysis of the digestate solution was performed and is shown in Fig. 2. The major organic residues are *o*-, *m*-, *p*-NBA and an unidentified peak at a retention time of ~ 10 min. The concentrations of the three NBA isomers were calculated and are summarized in Table 3. The average total NBA residue was 2.70% (m/m). Not taking into account the amount of the unidentified compound, the closed vessel nitric acid digestion decomposed ~ 94.7% (m/m) of the organics in the original

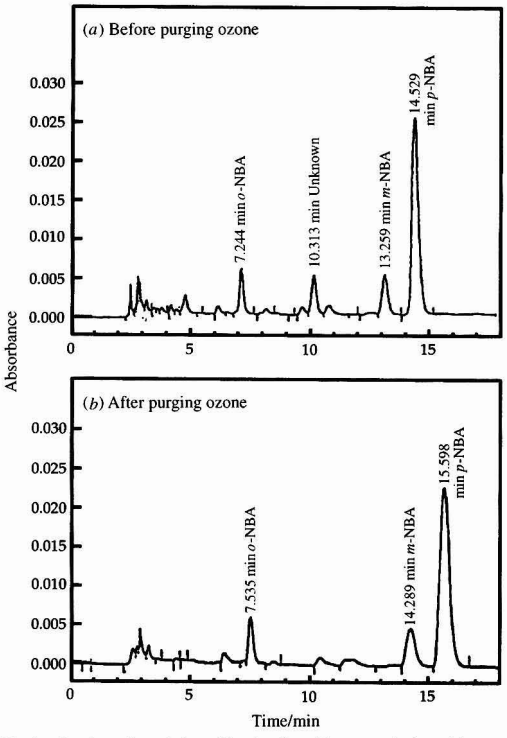

Fig. 2 One hour degradation of bovine liver digestate solution with ozone purging at 80 °C using an atmospheric pressure microwave system, (*a*) before and (*b*) after.

bovine liver sample. In comparison to the 3.01% (m/m) NBA residues found in the Pratt *et al.*[1] work, the amount of total NBA residues in our experiments was 0.31% lower. However, in the work by Pratt *et al.*, the major organic residues were *o*-, *m*- and *p*-NBA; and no unknown peak such as that appearing at ~ 10 min was reported. The decomposition of *o*-, *m*- and *p*-NBA in the digestate solutions was not as much as the decomposition of *o*-, *m*- and *p*-NBA in aqueous solution. The presence of the other residual carbon species that are more easily oxidized and react with ozone preferentially may be one reason for this, but is likely not to be the only contributing factor.

Table 3 Concentrations of *o*-, *m*- and *p*-nitrobenzoic acids after closed vessel digestion of bovine liver

Sample	Mass/g	*o*-NBA (%)	*m*-NBA (%)	*p*-NBA (%)	Total NBA (%)
1	0.2178	0.61	0.45	1.59	2.66
2	0.2181	0.59	0.42	1.58	2.59
3	0.2069	0.70	0.50	1.65	2.85
	Mean	0.63	0.46	1.61	2.70
	s	0.06	0.04	0.04	0.13
	%RSD	9.52	8.70	2.48	4.81

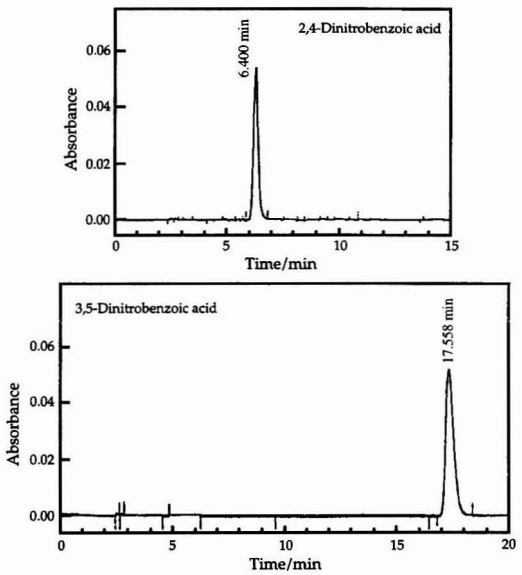

Fig. 3 HPLC analysis of 2, 4- and 3, 5-dinitrobenzoic acid under the same conditions as nitrobenzoic acid analysis.

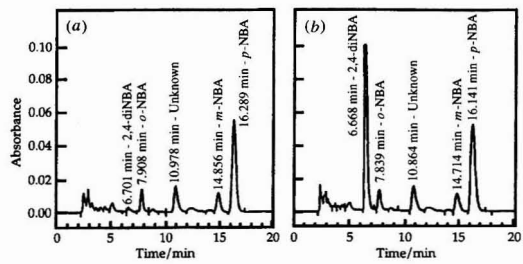

Fig. 4 HPLC analysis of (*a*) bovine liver digestate and (*b*) a 2,4-dinitrobenzoic acid spike of the same solution.

Bovine liver biological tissue has significant protein content. Many biological tissues with proteins containing an aromatic side chain will also have significant quantities of *o*-, *m*- and *p*-NBA remaining after digestion. These digestion products are typical of protein containing tissues.[1]

Since dinitrobenzoic acid has been reportedly found in biological sample digestate solutions as one of the major organic residues,[4] experiments were performed to identify whether or not the unknown peak was dinitrobenzoic acid. Fig. 3 shows the HPLC analysis of 2,4-dinitrobenzoic acid (top) and 3,5-dinitrobenzoic acid (bottom). Based on the retention times, neither seemed to be the unidentified peak. However, 2,4-dinitrobenzoic acid had a retention time of 6.4 min, which is close to a small peak (retention time 6.7 min) shown in Fig. 4. Spiking of the digestate solution by adding ~ 20 ppm of 2,4-dinitrobenzoic acid to the solution indicated that this peak is most likely to be 2,4-dinitrobenzoic acid [see Fig. 4 (*b*)]. The estimated concentration is ~ 0.01% (m/m) of the dry bovine liver sample.

In the Würfels *et al.* paper,[4] 5% 2,4-dinitrobenzoic acid was reported to be one of the organic residues after nitric acid digestion of bovine liver sample. However, in the Pratt *et al.* work, dinitrobenzoic acid was not reported.[1] This possibly indicates that the difference of the temperature and pressure during digestion can lead to a shift in the distribution of digestion products. However, it should be noted that in the Pratt *et al.* experiments, isobutyl methyl ketone (IBMK) was used to extract the NBAs from the digestion solution before HPLC analysis. In our experiment, the NBAs were extracted from the digestate solution by using SPE. It is possible that the extraction method used in these experiments is more efficient, allowing the recovery of the additional unknown peak.

The degradation could be improved by the addition of other reagents with the ozone such as peroxide for instance. However the goal of this study was to evaluate the degradation of ozone alone and not to add any other additional reagents to the ozone decomposition. Ozone is produced just prior to its addition in the decomposition system from filtered air or oxygen. It is not a classical reagent and may not contribute significantly to the analytical blank.

After an hour of purging ozone at 80 °C through bovine liver digestate solution, 17.08 ± 2.69% *o*-NBA degradation, 4.78 ± 3.21% *m*-NBA degradation, and 6.88 ± 2.95% *p*-NBA degradation result (see Fig. 2). Most of the unknown peaks were degraded by ozone in the first hour of purging. After 2.5 h of purging ozone at 80 °C, 33.65 ± 3.80% *o*-NBA degradation, 19.39 ± 1.74% *m*-NBA degradation, and 26.47 ± 3.36% *p*-NBA degradation were obtained.

Conclusions

It has been shown in this research that ozone can oxidize *o*-, *m*- and *p*-NBA, and has the potential to be used as an additional decomposition and/or finishing reagent. Deprotonated NBAs react faster with ozone than protonated NBAs, strongly suggesting an electrophilic attack of the benzene ring. Thus, increasing the pH of the solution to increase the concentration of the deprotonated NBA significantly improves the ozonation rate. When ozone was applied to closed vessel bovine liver digestate solution, the decomposition of residual *o*-, *m*- and *p*-NBA and other residual carbon was shown.

A better understanding of the chemistry of the ozonation of biological sample digestate solutions is an important goal for further research. Since the pH of the solution is essential for the degradation of NBAs, the reaction efficiency could be increased if an appropriate reagent can be found to neutralize the digestate solution (*i.e.*, ammonia) without introducing contamination. This research demonstrates the feasibility of ozone as an

alternative decomposition method. Additional studies to optimize its use seem appropriate.

References

1 Pratt, K. W., Kingston, H. M., MacCrehan, W. A., and Koch, W. F., *Anal. Chem.*, 1988, **60**, 2024.
2 Kingston, H. M., and Jassie, L. B., *J. Res. Nat. Bur. Stand.*, 1988, **93**, 269.
3 Krushevska, A., Barnes, R. M., Amarasiriwaradena, C. J., Foner, H. A., and Martines, L., *J. Anal. At. Spectrom.*, 1992, **7**, 845.
4 Würfels, M., Jackwerth, E., and Stöppler, M., *Anal. Chim. Acta*, 1989, **226**, 17.
5 Würfels, M., Jackwerth, E., and Stöppler, M., *Anal. Chim. Acta*, 1989, **226**, 1.
6 Kingston, H. M., Walter, P. J., Chalk, S. J., Lorentzen, E., and Link, D. D., in *Microwave Enhanced Chemistry*, ed. Kingston, H. M., and Haswell, S., American Chemical Society, Washington, DC, 1997, ch. 3.
7 Walter, P. J., Chalk, S. J., Kingston, H. M., and Lorentzen, E. M. L., in *Microwave Enhanced Chemistry*, ed. Kingston, H. M., and Haswell, S., American Chemical Society, Washington, DC, 1997, ch. 2.
8 Jackwerth, E., and Gomiscek, S., *Pure Appl. Chem.*, 1984, **56**, 479.
9 Kotz, L., Henze, G., Kaiser, G., Pahlke, S., Veber, M., and Tolg, G., *Talanta*, 1979, **26**, 681.
10 Hertz, J., and Pani, R., *Fresenius' Z. Anal. Chem.*, 1987, **328**, 487.
11 Langlais, B., Reckhow, D. A., and Brink, D. R., *Ozone in Water Treatment: Application and Engineering*, Lewis Publishers, Chelsea, MI, 1991, p. 103.
12 Langlais, B., Reckhow, D. A., and Brink, D. R., *Ozone in Water Treatment: Application and Engineering*, Lewis Publishers, Chelsea, MI, 1991.
13 Jiang, W., Masters Thesis Duquesne University, 1996.
14 *Lange's Handbook of Chemistry*, ed. Dean, J. A., McGraw Hill, New York, NY, 1979, 5.
15 *Certificate of Analysis: Standard Reference Material 1577a—Bovine Liver*, US Department of Commerce, The National Bureau of Standards, Gaithersburg, MD, 1982.

Paper 6/05282G
Received July 29, 1996
Accepted November 15, 1996

The Analyst

Determination of Organophosphorus Pesticides in Foods Using an Accelerated Solvent Extraction System

Hirotaka Obana*[a], Kosuke Kikuchi[b], Masahiro Okihashi[a] and Shinjiro Hori[a]

[a] *Osaka Prefectural Institute of Public Health, 1-3-69, Nakamichi, Higashinarik-ku, Osaka, 537, Japan. E-mail: obana@iph.pref.osaka.jp*

[b] *Japanese Consumers' Co-operative Union, 1-17-18, Nishiki-cho, Warabi, 335, Japan*

Residual organophosphorus pesticides in foods were determined by accelerated solvent extraction (ASE), gel permeation chromatography and GC–FPD. Pesticides were extracted at 100 °C under 1500 psi pressure in less than 20 min. Wet samples were extracted after mixing with Extrelut drying agent. Four foods were spiked with 19 pesticides at 0.1 ppm or less. The average recoveries of these pesticides were 80–90% and the precision was < 10%. Both methamidophos and acephate gave 37–50% recoveries and 6–40% precision. These results suggested that ASE can be used to extract residues of organophosphorus pesticides in foods.

Keywords: *Organophosphorus pesticides; foods; accelerated solvent extraction; gas chromatography–flame photometric detection*

Laboratories that monitor pesticides have developed various means of measuring residual levels in foods. Multiresidue methods are usually applied in pesticide monitoring because several compounds can be targeted simultaneously, which reduces labor and material costs. Extraction is one of the most important steps in the analysis. Conventional manual liquid–liquid partition consumes time and it is labor intensive. Moreover, it sometime results in an emulsion that can lower the reproducibility of the analysis. Japanese laboratories cannot freely drain waste containing dichloromethane owing to legal restrictions (< 10 μg ml^{-1}).[1] Dichloromethane is a frequently used solvent in multiresidue methods,[2,3] so an alternative method is required that incorporates non-halogenated solvents.

The latest automated extraction methods use less solvent and give improved analytical precision. Supercritical fluid extraction (SFE) is an example that has been adapted to residual pesticides analysis.[4–8] Pesticides have also been analyzed after microwave-assisted extraction.[9,10] On the other hand, Richter *et al.*[11] reported that environmental contaminants such as PCBs and PAHs were rapidly and effectively extracted at temperatures above 100 °C with pressurized solvents. They showed that solvents solubilize pesticides and penetrate sample matrices better under these conditions. Both accelerated solvent extraction (ASE) and microwave extraction operate under the same principle of automated solvent extraction at high temperature.

In this study, we extracted organophosphorus pesticides from foods using ASE.

Experimental

Pesticide Standards

Organophosphorus pesticides were purchased from Wako (Osaka, Japan): acephate, chlorpyrifos, chlorpyrifos-methyl, diazinon, dichlorvos, dimethoate, dioxabenzofos, edifenphos, EPN, ethion, ethoprophos, fenthion, fenitrothion, malathion, methamidophos, methidathion, phosalone, pirimiphos-methyl and prothiofos. Each compound was dissolved in hexane to make a 1000 μg ml^{-1} stock standard solution. The stock standard solution was diluted with acetone and used in the recovery tests at 1 μg ml^{-1}. Organophosphorus pesticides cause matrix effects that result in over-estimation of the recoveries in GC analysis.[6,7] To prevent this, standard mixtures were diluted with the respective cleaned-up extract from pesticide-free samples.

Reagents

Acetone, hexane, ethyl acetate and anhydrous Na_2SO_4 were of pesticide analysis grade and cyclohexane was of HPLC grade. All reagents were purchased from Wako.

Diatomaceous Earth

Particles of diatomaceous earth (Extrelut for refilling; particle size 160–800 μm) (Merck, Darmstadt, Germany) were heated at 550 °C for 15 h to exclude interferences in the GC analysis.

Food Preparation

Samples were purchased at a local market in Osaka and before use we confirmed that organophosphorus pesticide residues were below detectable levels. Pesticide residues were analyzed using a liquid–liquid extraction described by Yoshida *et al.*[12] About 500 g of broccoli or grapefruit were chopped in a conventional food processor (MK-K3, Matsushita, Osaka, Japan) for 5 min to obtain thoroughly mixed homogenates. The operating manual recommended that wet samples should be mixed with a drying agent to facilitate solvent penetration into sample matrices.[13] An aliquot of 5 g of sample homogenate and 6 g of Extrelut particles was ground in a mortar (12 cm id) with a pestle until the mixture became homogeneous. In the fortification study, 0.5 ml of pesticide mixture at 1 μg ml^{-1} was added to the sample homogenate to a final concentration of 0.1 ppm on a sample mass basis and the mixture was left for 30 min before adding Extrelut. Pesticides were added to flour at a final concentration of 0.05 ppm, then extracted without extra Extrelut. The procedure was performed twice for each sample because of GC separation preferences. One group consisted of methamidophos, acephate and dimethoate and the other of the remaining 16 pesticides. Mixtures of samples and Extrelut were placed in stainless-steel cells (33 ml; 11 cm × 1.9 cm id).

ASE

Accelerated solvent extraction was performed with a Dionex AS 200 system (Dionex, Sunnyvale, CA, USA). The pre-set default conditions were as follows: extraction temperature, 100 °C; extraction pressure, 1500 psi (10.5 kPa); pre-heating period, 5 min; static extraction period, 5 min; solvent flash, 19.8 ml; nitrogen purge, 60 s; and collection, in 60 ml glass vials with Teflon coated rubber caps (I-CHEM, New Castle, DE, USA). The extraction cell was heated and pressurized immediately after introducing it into the heating port. The pressure valve was

sometimes opened to maintained the pre-set pressure, and the extracted solvent was collected from pre-heating. After extraction, the cell was purged with fresh extraction solvent and additional nitrogen to collect the remaining extract in the cell. The extraction process was automated according to the assigned extraction method. The extracts were usually suspended and the water layer which lay separated in the bottom of vial because it was also co-extracted with solvent. The extract was transferred into a separating funnel. The collecting vial was washed with 10 ml of hexane twice, then hexane was added to the extract. As the suspension of the extract became heavier with hexane, the organic layer was left for about 2 h to form water droplets from the organic layer. After the water portion had been discarded, the extract was dried by adding anhydrous Na_2SO_4. The extract was carefully evaporated almost to dryness with warming at <40 °C and the residue was dissolved in ethyl acetate–cyclohexane (1 + 1) for gel permeation chromatography (GPC) and diluted to 7 ml.

GPC[14]

Extracts were injected into an AS-2000 system (abc Laboratories, Columbia, MO, USA) equipped with an Environsep-ABC column (300 × 21.2 mm id). The mobile phase was ethyl acetate–cyclohexane (1 + 1) at a flow rate of 5 ml min^{-1}. Food extract (5 ml) was loaded into the GPC system. The first 70 ml were discarded and the following 80 ml were collected as the pesticide fraction. A further 50 ml were eluted for the GPC wash. The pesticide fraction was concentrated to 3.5 ml with an evaporator for GC determination.

GC–FPD Determination

Pesticides were determined using a GC 17A instrument (Shimadzu, Kyoto, Japan) equipped with a flame photometric detector. A DB-210 column (5 m × 0.25 mm id, 0.25 μm thickness) (J & W Scientific, Folsom, CA, USA) was used for methamidophos, acephate, and dimethoate determinations. The temperature program was initial temperature 80 °C (held for 1 min), increased at 10 °C min^{-1} to 260 °C (held for 4 min). A DB-5 column (30 m × 0.25 mm id, 0.25 μm thickness) (J & W) was used for the other pesticides. The temperature program was initial temperature 80 °C (held for 1 min), increased at 20 °C min^{-1} to 120 °C (no hold), then at 4 °C min^{-1} to 280 °C (held for 5 min). Carrier gas was helium. A 2μl volume was injected in the splitless mode at 250 °C. The detector temperature was set at 300 °C. The chromatogram was recorded using a CR7A integrator (Shimadzu).

Results and Discussion

Extraction From Flour

First, a recovery test was performed with flour with a low water content, so that no drying agent needed to be added to the sample during extraction. Flour (10 g) spiked with 0.05 ppm of

Table 2 ASE extraction of 19 organophosphorus pesticides from grapefruit and orange juice by ASE using cyclohexane–acetone (1 + 1)

	Grapefruit		Orange juice	
Pesticide	Mean recovery (%)*	RSD (%)	Mean recovery (%)*	RSD (%)
Dichlorvos	82.8	15.3	87.1	10.5
Methamidophos	8.7	20.1	9.3	48.5
Ethoprophos	99.6	13.9	61.1	13.5
Dioxabenzofos	100.0	19.6	51.6	16.8
Acephate	10.2	19.4	10.6	45.3
Dimethoate	97.9	14.1	74.7	8.0
Diazinon	102.0	12.6	73.4	7.5
Chlorpyrifos-methyl	105.1	17.6	75.7	6.0
Fenitrothion	99.7	8.2	76.5	10.9
Pirimiphos-methyl	101.7	14.0	88.4	4.5
Malathion	98.2	9.1	76.3	6.3
Chlorpyrifos	105.1	10.4	79.2	7.5
Fenthion	105.6	10.2	80.9	5.9
Methidathion	100.5	4.4	73.7	9.0
Prothiofos	103.1	9.6	75.2	9.7
Ethion	97.5	21.8	110.5	19.1
Edifenphos	100.9	14.9	74.1	13.6
EPN	107.1	13.4	87.6	15.3
Phosalone	90.3	13.8	70.3	14.3

* Means of three experiments.

Table 1 ASE extraction of 17 organophosphorus pesticides in flour using three solvent mixtures

	Cyclohexane–acetone (1 + 1)		Dichloromethane–acetone (1 + 1)		Ethyl acetate–acetone (1 + 1)	
Pesticide	Mean recovery (%)*	RSD (%)	Mean recovery (%)*	RSD (%)	Mean recovery (%)*	RSD (%)
Dichlorvos	36.6	12.1	42.9	37.0	46.6	30.3
Ethoprophos	100.7	2.5	95.1	3.8	141.4	24.1
Dioxabenzofos	100.8	3.6	83.2	18.1	95.5	27.7
Dimethoate	49.1	1.8	86.0	16.1	199.2	34.4
Diazinon	99.2	2.4	93.5	1.6	134.3	26.7
Chlorpyrifos-methyl	100.7	5.1	92.9	13.6	104.6	28.4
Fenitrothion	111.7	5.3	90.7	12.8	105.9	29.0
Pirimiphos-methyl	96.4	4.8	106.0	0.8	155.4	24.3
Malathion	106.3	4.6	93.4	5.4	137.8	19.1
Chlorpyrifos	94.9	3.4	93.8	7.0	125.3	25.2
Fenthion	90.1	4.8	88.3	0.1	146.1	24.4
Methidathion	113.6	14.1	88.5	13.9	106.9	32.1
Prothiofos	89.2	5.5	92.6	5.8	128.6	26.0
Ethion	85.5	7.3	96.3	5.2	142.3	25.6
Edifenphos	115.8	11.7	91.2	6.6	141.3	28.6
EPN	87.1	10.5	93.5	11.3	128.6	31.5
Phosalone	106.5	10.9	93.4	7.3	140.6	33.2

* Means of three experiments.

each pesticide was extracted with three solvent mixtures each containing 50% acetone. As shown in Table 1, extraction with cyclohexane–acetone (1 + 1) and dichloromethane–acetone (1 + 1) resulted in good recoveries. The recoveries of most of the pesticides was 83–115%. The RSDs were acceptable, usually < 10%, using cyclohexane–acetone (1 + 1). With ethyl acetate–acetone (1 + 1) the RSD varied from 19 to 34%. The recovery of dichlorvos was around 40% with all three mixtures and the precision was also poor. One explanation is that the compound was lost during sample preparation because dichlorvos is volatile with a vapor pressure of 290 mPa at 20 °C.[15]

Extraction From Wet Samples

Since one aim of this study was to develop a dichloromethane-free extraction procedure, we extracted pesticides from grapefruit and orange juice with cyclohexane–acetone (1 + 1) (Table 2). In this study methamidophos and acephate were added in addition to the 17 pesticides in Table 1. The recoveries of the 17 pesticides except methamidophos and acephate varied from 82 to 105% in grapefruit and from 51 to 110% in orange juice. Little methamidophos or acephate was extracted under the conditions tested. The extraction precision of these pesticides was poor in orange juice.

Extraction Conditions

We studied the effects of static extraction time, temperature and pressure to improve the extraction rates of methamidophos and acephate in orange juice (Table 3). Other conditions were the same as those described above. Since two of the pesticides were water soluble,[16] orange juice seemed to be one of the most difficult foods from which to obtain satisfactory recoveries. The appropriate conditions for orange juice should also be sufficient for drier samples. Time and temperature did not improve the recoveries under the conditions tested. Only a higher extraction pressure slightly improved the recovery. Further improvement by increasing the pressure was unlikely since the mechanical pressure limit of the ASE system is 3000 psi.

Table 3 Effects of extraction time, temperature and pressure on recoveries of methamidophos and acephate*

	Recovery (%)	
Variable	Methamidophos	Acephate
Time/min—		
5	15.4	9.3
10	11.9	9.6
15	11.7	7.7
Temperature/°C—		
50	5.8	4.5
100	8.1	8.0
150	6.4	4.2
Pressure/psi—		
1500	9.5	16.0
2000	13.3	20.0
2500	15.0	22.2

* The extraction solvent was cyclohexane–acetone (1 + 1) and other conditions were the default values as described in the text. Values are means of two experiments.

Table 4 ASE extraction of methamidophos and acephate from orange juice using various solvents

	Recovery (%)*	
Solvent	Methamidophos	Acephate
Cyclohexane–acetone (1 + 1)	9.3	10.6
Toluene–acetone (1 + 1)	46.6	45.3
Dichloromethane–acetone (1 + 1)	36.0	36.5
Ethyl acetate–acetone (1 + 1)	16.1	30.5
Acetonitrile	28.2	30.6
Ethyl acetate	56.1	47.8

* Means of two experiments.

Table 5 ASE extraction of 19 organophosphorus pesticides in foods using ethyl acetate

	Orange juice (0.1 ppm)		Grapefruit (0.1 ppm)		Broccoli (0.1 ppm)		Flour (0.05 ppm)	
Pesticide	Mean recovery (%)*	RSD (%)	Mean recovery (%)*	RSD (%)	Mean recovery (%)*	RSD (%)	Mean recovery (%)*	RSD (%)
Dichlorvos	91.5	4.6	102.8	10.0	87.4	3.9	92.7	9.9
Methamidophos	56.6	7.9	60.3	17.0	53.7	6.2	37.3	41.5
Ethoprophos	68.9	6.5	91.4	4.7	114.0	4.8	90.1	9.8
Dioxabenzofos	67.0	4.9	88.6	6.8	97.0	4.8	60.3	7.9
Acephate	54.8	9.0	59.1	20.9	50.8	6.1	55.7	10.1
Dimethoate	91.8	5.0	109.3	9.9	103.2	3.0	83.5	9.2
Diazinon	81.9	4.3	86.6	5.2	88.0	4.6	90.9	2.2
Chlorpyrifos-methyl	76.9	2.9	87.0	5.6	87.8	4.6	72.3	3.1
Fenitrothion	97.6	7.3	89.0	6.0	102.8	5.5	91.4	4.3
Pirimiphos-methyl	85.3	2.2	85.5	7.0	88.0	5.4	105.7	1.7
Malathion	81.9	4.1	89.5	5.9	99.5	5.1	77.5	0.4
Chlorpyrifos	74.1	2.7	87.3	6.2	81.4	5.1	95.2	2.7
Fenthion	79.6	4.8	90.3	4.2	91.4	7.7	92.3	2.3
Methidathion	80.9	11.3	91.4	5.2	110.9	6.7	73.5	4.7
Prothiofos	68.9	4.4	90.1	3.7	88.5	6.2	96.1	2.3
Ethion	78.1	5.8	90.1	4.1	87.5	9.0	98.1	2.1
Edifenphos	90.9	7.4	90.9	5.4	101.5	7.2	67.9	5.1
EPN	83.1	9.1	85.7	3.5	91.9	5.7	98.4	2.0
Phosalone	97.5	9.5	84.0	6.2	93.4	6.4	96.8	1.5
Average	79.3		87.4		90.4		82.9	

* Means of three experiments.

We studied the effects of extraction solvents on the recoveries of methamidophos and acephate in orange juice under the default extraction conditions (Table 4). Ethyl acetate recovered 56 and 47% of spiked methamidophos and acephate, respectively. Toluene–acetone (1 + 1) gave a secondary recovery of around 45%. The recovery with cyclohexane–acetone (1 + 1) was the lowest among the six solvent systems tested.

Since ethyl acetate gave the best results, it was used to extract 19 pesticides from four spiked foods. As shown in Table 5, the average recoveries of the 19 pesticides in the four samples were considerably better: 79.3% in orange juice, 87.4% in grapefruit, 90.4% in broccoli and 82.9% in flour. The recovery of methamidophos and acephate ranged from 50 to 60% except for methamidophos in flour (37%). Most RSDs were < 10%. Although methamidophos and acephate tend to show poor precision, the poor reproducibility of these pesticide peaks on the chromatograms in GC–FPD might have caused the fluctuating recoveries. These results suggested that ethyl acetate is a useful solvent in ASE with which to determine residual organophosphorus pesticides.

ASE extraction was compared with hexane extraction in pesticide-containing samples (Table 6). These samples were found in our routine surveillance and stored at −20 °C until analysis. Whereas the ASE extraction seemed to give slightly lower recoveries for the samples tested, the precision of ASE is better than that of hexane extraction.The colours of the hexane extracts were deeper than those in ASE extracts.

The advantages of ASE over liquid–liquid extraction were as follows. The extraction procedure is simple, requiring only mixing of the samples with drying agent and transferring the mixture to an extraction cell. One sample can be extracted within 20 min, including washing the solvent line for the next extraction. The solvent volume with a 33 ml cell is 50–60 ml, which depends on the sample volume. Even though the volume is not large, the ratio of solvent (50 ml) to sample (5 g) is 10, whereas it is 2–5 in conventional procedures.[2,14,17,18] Hence ASE should combine good recovery and precision with rapid extraction. Another advantage over the conventional method is continuous separation of the extract from sample residues during extraction. The disadvantage of ASE in this study is the 2 h waiting to remove water from the extract after adding hexane. Without hexane, small water droplets appeared after evaporation even when the extract was dried with anhydrous Na_2SO_4. Ethyl acetate at elevated temperature solubilized water to a greater extent during extraction than by conventional means at room temperature. Water remaining in the extract decreased the precision of the recovery tests (data not shown). Although thermal degradation of the target compounds is a potential concern because of elevated temperature during extraction, Richter *et al.*[11] reported that the thermal degradation of DDT to DDE or DDD and of endrin to endrin aldehyde or endrin ketone did not occur during ASE at 150 °C.

This study demonstrated that ASE automatically and rapidly extracted organophosphorus pesticides from foods with good accuracy and precision. ASE could be introduced as a means of determining residual levels of organophosphorus pesticides in foods. We are studying its applicability to multiresidue analyses of agrochemicals other than organophosphorus pesticides.

Table 6 Comparison between ASE and hexane extraction in pesticide-containing samples

		ASE		Hexane	
Food	Pesticide	Mean (ppm)*	RSD (%)	Mean (ppm)*	RSD (%)
Banana	Chlorpyrifos	0.03	9.7	0.05	13.4
Okra	Phosalone	0.05	4.0	0.08	27.5
Sweetie	Chlorpyrifos	0.22	2.7	0.27	13.2
	Malathion	0.03	20.9	0.03	35.9

* Means of three experiments.

References

1 Prime Minister's Office of Japan, *Bulletin 54*, December 27, 1993 (in Japanese).
2 Cairns, T., Luke, M. A., Chiu, K. S., Navarro, D., and Siegmund, E. G., *Rapid Commun. Mass Spectrom.*, 1993, **7**, 1070.
3 Luke, M. A., Froberg, J. E., Doose, G. M., and Masumoto, H. T., *J. Assoc. Off. Anal. Chem.*, 1981, **64**, 1187.
4 Skopec, Z. V., Clark, R., Harvey, P. M. A., and Wells, R. J., *J. Chromatogr. Sci.*, 1993, **31**, 445.
5 Hopper, M. L., and King, J. W., *J. Assoc. Off. Anal. Chem.*, 1991, **74**, 661.
6 Lehotay, S. J., Aharonson, N., Pfeil, E., and Ibrahim, M. A., *J. AOAC Int.*, 1995, **78**, 831.
7 Lehotay, S. J., and Eller, K. I., *J. AOAC Int.*, 1995, **78**, 821.
8 Stuart, I. A., MacLachlan, J., and McNaughtan, A., *Analyst* 1996, **121**, 11R.
9 Lopezavila, V. L., Young, R., Benedicto, J., Ho, P., Kim, R., and Beckert, W. F., *Anal. Chem.*, 1995, **67**, 2096.
10 Lopezavila, V., Young, R., Kim, R., and Beckert, W. F., *J. Chromatogr. Sci.*, 1995, **33**, 481.
11 Richter, B. E., Jones, B. A., Ezzell, J. L., Porter, N. L., Avdalovic, N., and Pohl, C., *Anal. Chem.*, 1996, **68**, 1033.
12 Yoshida, S., Konaka, H., and Nishimune, T., *J. Food Hyg. Soc. Japn.*, 1991, **32**, 267.
13 *ASE 200 Accelerated Solvent Extractor Operator's Manual*, Document No. 031149, Revision 01, Dionex, Sunnyvale, CA, 1995, Sect. 3–5.
14 Committee on Analytical Methods for Pesticide Residues, *Food Sanit. Res.*, 1995, **45**, 31 (in Japanese).
15 *The Agrochemical Handbook*, Royal Society of Chemistry, Cambridge, 3rd edn., 1991, p. A0141.
16 *The Agrochemical Handbook*, Royal Society of Chemistry, Cambridge, 3rd edn., 1991, pp. A0001 and A0265.
17 *Pesticide Analytical Manual*, ed. McMahon, B. M., and Hardin, N. F., Food and Drug Administration, Washington, DC, 3rd edn., 1994, vol. 1, pp. 302–305.
18 Fillion, J., Hindle, R., Lacroix, M., and Selwyn, J., *J. AOAC Int.*, 1995, **78**, 1252.

Paper 6/06063C
Received September 3, 1996
Accepted October 28, 1996

Simultaneous Spectrofluorimetric Determination of Selenium(IV) and (VI) by Flow Injection Analysis

M. J. Ahmed†, C. D. Stalikas, P. G. Veltsistas, S. M. Tzouwara-Karayanni and M. I. Karayannis*

Laboratory of Analytical Chemistry, Department of Chemistry, University of Ioannina, Ioannina 451 10, Greece

A simple, sensitive, highly selective, automatic spectrofluorimetric method for the simultaneous determination of selenium(IV) and (VI) as selenite–selenate by flow injection analysis (FIA) has been developed. The method is based on the selective oxidation of the non-fluorescent reagent 2-(α-pyridyl)thioquinaldinamide (PTQA) in acidic solution (1.5–3.0 M H_2SO_4) by Se^{IV} to give an intensely fluorescent oxidation product (λ_{ex} = 350 nm; λ_{em} = 500 nm). Selenium(VI) is reduced on-line to Se^{IV}, in a reduction coil installed in a photo-reactor, which is then treated with PTQA and the fluorescence due to the sum of Se^{IV} and Se^{VI} is measured; Se^{VI} is determined from the difference in fluorescence values. Various analytical parameters, such as effect of acidity, flow rate, sample size, dispersion coefficient, temperature, reagent concentration and interfering species were studied. The photo-reduction conditions were optimized, with an FIA procedure, for Se^{VI} on the basis of its reduction efficiency. The calibration graphs were rectilinear for 0.1–2.4 μg ml^{-1} of Se^{VI} and 10 ng ml^{-1}–2.2 μg ml^{-1} of Se^{IV}, respectively. The method was applied to the determination of Se in several Standard Reference Materials (alloy, sediments and tea), as well as in some environmental waters (tap and surface water), food samples (flour and egg), a biological sample (human hair), soil sample and in synthetic mixtures. Up to 25 samples per hour can be analysed with an RSD ≈ 0.1–2%.

Keywords: *Flow injection; spectrofluorimetry; selenium speciation; 2-(α-pyridyl)thioquinaldinamide; on-line photo-reduction; environmental; biological; soil samples*

Recently, there has been increasing interest in trace determination of selenium because of its dual role, as an essential nutrient at low concentrations (10–40 μg ml^{-1} in serum), or a highly toxic compound (selenosis) at an intake of 5 mg kg^{-1} of Se (in the mammals of a seleniferous region).[1] It is contained in the enzyme glutathione peroxidase (GSHPx), which affords cells protection against oxidative damage.[2] A selenium deficiency in man may also result in cardiomyopathy.[2] The narrow concentration range between the two opposite effects (0.1–4.0 mg kg^{-1} in plants), requires accurate and precise knowledge of the selenium species present in the environment.[3] In the environment, Se levels generally fall in the ranges 0.1–400 ng ml^{-1} in natural waters,[4] 1 ng ml^{-1} in the atmosphere[3] and 0–80 μg g^{-1} in soils.[5] Selenium finds its way into the environment through its widespread use in the glass and electronics industries, as well as from the combustion of fossil fuels and uses in agriculture. Detailed information about the availability and mobility of Se in the environment and its biogeochemical cycle, however, requires the additional knowledge of the different chemical forms and oxidation states in which this element can exist. The inorganic Se species most frequently found in water and soils are selenite (SeO_3^{2-}) and selenate (SeO_4^{2-}).[3] In this regard, a method for speciation is needed because its availability for plant uptake, mobility in soil, and toxicity in biota depends on the oxidation state of the Se.[6] Therefore, its accurate determination at trace levels using simple and rapid methods is of paramount importance.

Analytical techniques for Se speciation have recently been reviewed.[7–9] Automatic flow techniques have hardly been applied to the determination of Se. Until now, only few methods have been described that use flow injection analysis (FIA) and these methods either use FIA combined with HG–AAS[8,10] or FIA with spectrophotometric detection.[11] But these methods suffer from several limitations: (*i*) indirect determination of Se^{VI} because it does not give hydrides, and (*ii*) the matrix affects both hydride generation and reduction yields of Se^{VI} to Se^{IV}. The spectrophotometric methods suffer from sensitivity and selectivity due to various or many interferences. In this respect, interlaboratory comparisons of inorganic Se in biological and environmental samples showed unacceptable differences using these techniques.[12] Recent developments in the automation of instrumentation leads to an improved precision.[13] Recently, photochemical reactions have been applied to the on-line reduction and oxidation of inorganic and organic substances in flow injection methods.[14,15] Measures and Burton[16] studied the photochemical oxidation of an organometallic form of selenium(Se^{2-}) into inorganic Se^{IV} with a high pressure mercury lamp. All of these systems have been used for on-line photochemical oxidation or reduction to enhance the detection of a variety of inorganic and organic compounds with AAS[17] and spectrophotometric techniques.[15]

The aim of the present study was to develop a more simple FIA system for the simultaneous determination of Se^{IV} and Se^{VI} with 2-(α-pyridyl)thioquinaldinamide (PTQA) using a reduction coil installed in a photo-reactor in the reaction manifold. PTQA has been reported as a spectrofluorimetric reagent,[18] but has not previously been used for the simultaneous determination of Se^{IV} and Se^{VI} in a flow injection system. This paper reports its use in a very sensitive, highly specific automatic spectrofluorimetric method for the simultaneous determination of Se^{IV} and Se^{VI}. The method is based on the selective oxidation of the non-fluorescent reagent, PTQA, in an acidic medium (1.5–3.0 M H_2SO_4) by Se^{IV} to produce an intensely fluorescent product followed by the direct measurement of the fluorescence intensity in aqueous solution at room temperature. Oxidation is very rapid and no extraction is required. With suitable masking the reaction can be made highly selective. The reaction mechanism of the present method is as reported earlier.[18]

Experimental

Apparatus

The manifold for simultaneous determination of Se^{IV} and Se^{VI} was of Teflon tubing (0.8 mm id) and linear dual connectors were used (Fig. 1). It consisted of a four-way pneumatically

† Present address: Department of Chemistry, University of Chittagong, Chittagong-4331, Bangladesh.

actuated injection valve (Rheodyne, Type 50 Teflon, Cotati, CA, USA), an eight-channel peristaltic pump (Ismatec, Glattburg-Zurich, Switzerland) and a spectrofluorimeter (RF-551, Shimadzu, Japan), equipped with a 12 μl flow-through cell for measurement.

Data processing and collection was performed with an IBM-compatible Personal Computer (PC) by means of software written in Microsoft Q-Basic. The interface unit was an RTL 800/815 multifunction Input/Output board. A Varian AA-300 Atomic Absorption Spectrophotometer equipped with a hydride system at 196.1 nm using an air–acetylene flame was used for comparison of the results. A digital pH-meter (Model-PHM83 AUTOCAL, Radiometer, Copenhagen, Denmark) was used to measure the pH of the solutions.

Photoreduction-reactor

The photoreduction-reactor comprised a high pressure mercury light source (2 cm od, 25 cm long, 125 W, DESAGA) and a quartz coil (40 cm long × 0.8 mm id). The source emits short wavelength light at λ_{max} = 254 nm. The effective irradiation length was 6 cm. The unit is covered with aluminium foil or thick paper in order to increase the light intensity reaching the coil by reflectance and to prevent eye exposure to ultraviolet radiation.

Reagents

All chemicals used were of analytical-reagent grade or the highest purity available. Doubly distilled water and HPLC-grade propan-2-ol, which is non-fluorescent under ultraviolet radiation, were used throughout.

Se^{IV} standard solutions. A 100 ml amount of stock Se^{IV} solution (1 mg ml^{-1}) was prepared by dissolving 333.1 mg of general-reagent grade sodium selenite (Merck, Darmastadt, Germany) in doubly distilled water. The solution was kept in a refrigerator in a polyethylene container for preservation. Working standard solutions were prepared daily by appropriate dilution in 2 M H_2SO_4.

Se^{VI} standard solutions. A 100 ml amount of stock Se^{VI} solution (1 mg ml^{-1}) was prepared by dissolving 467.4 mg of ACS-grade sodium selenate (99%, Aldrich, Steinheim, Germany) in doubly distilled water. The solution was kept in a refrigerator in a polyethylene container. Working standard solutions were prepared daily by appropriate dilution in 2 M H_2SO_4.

Carrier solution. 2.0 M H_2SO_4 (Merck) was used as the carrier solution.

2-(α-Pyridyl)thioquinaldinamide (PTQA), solution (10^{-3} M). The reagent was synthesized according to the method of Porter.[19] The contents, containing 2-aminopyridine (2 mol), quinaldine (1 ml) and sulfur powder (1.5 mol), were mixed and refluxed for 6 h in a 250 ml round bottomed flask fitted with bulb condenser under controlled temperature (140–150 °C) at 1 atm pressure over a sand bath. The reaction mixture was kept overnight. The thio-compound was filtered and crystallized using petroleum ether to give a bright yellow crystalline (needle) solid. The compound recrystallized from ethanol was dried under vacuum (0.1 mg of Hg) for 24 h. The melting point of this synthesized compound (PTQA) was 155 ± 2 °C and the elemental analysis data (C = 72.25, N = 13.35 and H = 4.25%) were very close to the literature values,[19] *e.g.*, melting point (155 ± 1 °C); C (=72.43); N (=13.55) and H (=4.55%). The reagent solution (10^{-3} M) was prepared by dissolving the requisite amount (0.0266 g in 100 ml) of PTQA in HPLC-grade propan-2-ol. A freshly prepared reagent solution (10^{-4} M) was used whenever required.

Other solutions. Solutions of a large number of inorganic ions and complexing agents were prepared from their AnalaR grade or equivalent grade water soluble salts. In the case of insoluble substances, special dissolution methods were adopted.[20]

Stock solutions and environmental samples were kept in a refrigerator in poly(propylene) bottles.

Preparation of the Samples

Food samples (rice flour and egg) were purchased from a local supermarket. These samples were homogenized thoroughly. Soil samples was collected from local agricultural field sites and homogenized in a mortar. Human hair (3–5 cm long from male) was cut from the occipitonuchal region of the head. They were cleaned by stirring with acetone, rinsing with tap water, stirring in a detergent solution (which had no detectable Se), rinsing with tap water, doubly distilled water and finally with acetone. They were then dried at 45 °C and cut into small pieces for analyses (sampled person did not use Se-containing shampoo).

Procedure

The standards (0.01–2.2 μg ml^{-1} Se^{IV} or 0.1–2.4 μg ml^{-1} Se^{VI}) and samples were injected into a carrier stream by means of the peristaltic pump, P (Fig. 1). Then the sample was measured by different ways using a selector valve. The sample stream was firstly directed through path 1, treated with a 10–30-fold molar excess of the PTQA reagent solution and passed directly into the measuring cell of a spectrofluorimeter where the fluorescence intensity due to Se^{IV} was measured at 500 nm with excitation at 350 nm. Then the sample stream was passed through path 2 to photo-reduction coil (R_1) by using a second selector valve where Se^{VI} was reduced to Se^{IV}. The sample stream was then treated with the PTQA reagent at the end of the coil and the overall mixture was passed to the same cell of the spectrofluorimeter where the fluorescence intensity due to total Se was measured; Se^{VI} was determined from the difference in fluorescence intensity values. The reaction is very rapid and the fluorescence intensity remains stable for 24 h. The PTQA reagent does not show any fluorescence in the absence of Se^{IV}.

The concentrations of Se^{IV} and Se^{VI} were evaluated from the peak heights of the signal by using the calibration curves prepared with standard solutions.

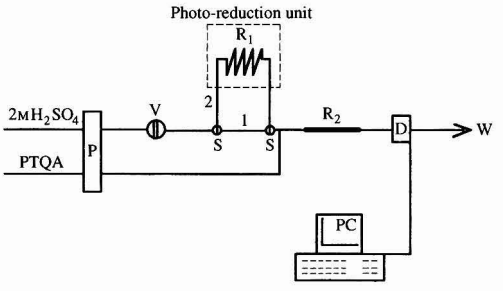

Fig. 1 Schematic representation of FI manifold employed for the simultaneous determination of Se^{IV} and Se^{VI}. P, Pump; V, valve; S, selector valve; R_1, photoreduction coil; R_2, single bead string reactor (SBSR); D, detector; W, waste; and PC, personal computer.

Results and Discussion

Optimization of the Flow Injection System

Preliminary tests were carried out with the aid of different flow assemblies to select the optimal manifold configuration. The assembly in Fig. 1 was selected as the one producing the best compromise between peak height and the shape of the peak.

In order to optimize the proposed flow injection manifold, the influence of the hydrodynamic and chemical parameters on the magnitude of the peak height, the shape of the peak and reproducibility of the results were studied. The univariate method was adopted for the optimization of the system. Table 1 shows results of optimization of working conditions for 0.5 μg ml^{-1} of Se^{IV} and 1.0 μg ml^{-1} of Se^{VI}.

The optimum length of the photo-reduction coil (R_1) was established by using a 1.0 μg ml^{-1} Se^{VI} solution, the single bead string reactor (SBSR) (R_2), for better mixing and lower dispersion, being of length 100 cm and having an acidity of 1.5–3.0 M H_2SO_4. Photo-reduction coil (R_1) lengths of 15, 30, 40, 60 and 80 cm were tested, keeping the power of the lamp and its distance from reaction coil constant. For any combination of the above parameters the efficiency of the reduction was determined by comparison of the plateau achieved with that corresponding to a 1.0 μg ml^{-1} Se^{IV} solution processed in the same way. A coil length of 40 cm was chosen, because the reduction was almost complete, reproducibility was good and back-pressure relatively low. Different wavelengths of the UV radiation were also tested. For each wavelength, the efficiency of the reduction was determined. The effective wavelength of photo-reduction of the Se^{VI} was λ_{max} = 254 nm. Different lamp powers were also tested but no significant effect on reduction was observed. Different distances of the reaction coil from the lamp were tested keeping the length of the coil and wavelength constant. A length of 6 cm was selected because maximum conversion efficiency was achieved.

A length 100 cm for the SBSR reactor (R_2), a sample size of 100 μl, an overall flow rate of 0.4 ml min^{-1} and a reagent flow rate of 0.3 ml min^{-1} were selected, these being a compromise between the sampling rate and the height of the peak.

Of the various acids (sulfuric, hydrochloric, nitric and phosphoric) studied, sulfuric acid was found to be best acid for the system. Different concentrations of sulfuric acid were tested in the range shown in Table 1. The fluorescence intensity was at maximum and constant when the solution (1.0 μg ml^{-1}) contained 1.5–3.0 M H_2SO_4 (Fig. 2) at room temperature, which was the optimum acidity range. The photoreduction efficiency for 1.0 μg ml^{-1} of Se^{VI} in this acidity range was also tested. More than 97% of the Se^{VI} can be reduced to Se^{IV} in this acidity range. For all subsequent measurements 2.0 M H_2SO_4 was used as carrier for this manifold.

The effect of propan-2-ol on the fluorescence was studied and no adverse effect was observed over a wide range of propan-2-ol concentrations. A 10^{-4} M solution of PTQA in propan-2-ol was sufficient to prevent any precipitation or turbidity or bubbling and to allow accurate measurements for this manifold. Other common organic solvents, *e.g.*, chloroform, benzene, tetrachloromethane and ethanol, were also tried but no fluorescence was observed in the organic phase, with the exception of ethanol.

The reaction is rapid. A constant maximum fluorescence intensity was obtained just after the dilution to volume and remained strictly unaltered for 24 h. Different concentrations of PTQA solution were tested in the ranges shown in Table 1. A reagent concentration of 2×10^{-4} M was selected as optimum for this manifold. The fluorescence intensity of the Se^{IV}–PTQA system within the prescribed acidity range was maximum and constant for Se^{IV} to reagent molar ratios in the range 1 : 10–1 : 30 when the Se concentration was 1.0 μg ml^{-1} (Fig. 3). At different Se^{IV} concentrations (0.1 and 0.5 μg ml^{-1}), the effect of varying the reagent concentration was similar.

Table 1 Selected chemical and FIA parameters obtained with the optimization experiments

Parameter	Studied range	Selected value
Size of sample loop/μl	30–180	100
Overall flow rate/ml min^{-1}	0.20–1.0	0.40
Reagent flow rate/ml min^{-1}	0.05–0.60	0.30
Length of the photo-reaction coil, R_1/cm	15–80	40
Length of the SBSR reactor, R_2/cm	20–180	100
pH	0.1–1.3	0.40–0.75 (preferably 0.6)
Concentration of reagent (M)—		
H_2SO_4	0.50–4.5	1.50–3.0 (preferably 2.0)
PTQA	3×10^{-5}–6×10^{-4}	2×10^{-4}

Evaluation of the Method

The reproducibility of the proposed procedure and sample throughput were determined by repeated injection of a sample containing 0.5 μg ml^{-1} Se^{IV} and 1.0 μg ml^{-1} Se^{VI}. The RSD (n = 5) was 0.1–2% for 0.01–2.2 μg ml^{-1} Se^{IV} and 0.1–2.4 μg ml^{-1} Se^{VI} indicating that this method is highly precise and reproducible. The calibration graphs obtained from the peak heights were rectilinear for 10 ng ml^{-1} to 2.2 μg ml^{-1} of Se^{IV} and 0.1–2.4 μg ml^{-1} of Se^{VI}, respectively. The detection limits, defined as three times the baseline noise, were 1 ng ml^{-1} for Se^{IV} and 10 ng ml^{-1} for Se^{VI}. The sample throughput was 25 measurements per hour. The dispersion coefficients were estimated with a 0.5 μg ml^{-1} Se^{IV} and 1.0 μg ml^{-1} Se^{VI} standard solutions as described earlier.[21] Important features of the proposed method for simultaneous determination of Se^{IV} and Se^{VI} are summarised in Table 2.

The performance and reproducibility of the proposed method are also shown in Tables 3–6. The reliability of the proposed procedure was also assessed by analysing Certified Reference Materials. The results for total Se were in good agreement with certified values (Table 3). The method was also tested by analysing several synthetic mixtures containing standard Se^{IV} and Se^{VI} (Table 4). The reliability of the proposed procedure was also tested by performing recovery studies. The average

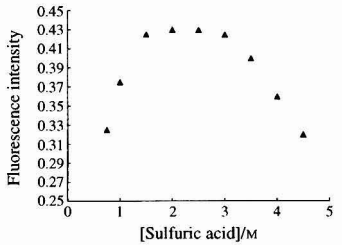

Fig. 2 Effect of acidity on the fluorescence intensity of the Se^{IV}–PTQA system.

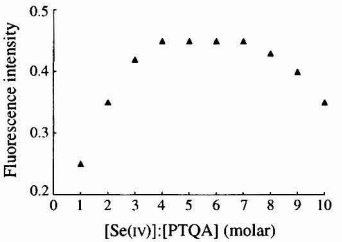

Fig. 3 Effect of reagent on the fluorescence intensity of the Se^{IV}–PTQA system.

percentage recovery obtained for the addition of Se^{IV} and Se^{VI} spikes to some environmental water and flour samples was quantitative as shown in Table 5. The results of food, hair and soil analyses by the present method was in excellent agreement with those obtained by HG-AAS (Table 6). The precision and accuracy of the method are satisfactory.

Table 2 Analytical features of the proposed method

Parameter	Se^{IV}	Se^{VI}
Acidity/M	1.50–3.0	1.50–3.0
Fluorescence stability/h	24	24
Temperature/°C	25	25
Reagent (fold molar excess)	1 : 10–1 : 30	1 : 10–1 : 30
Linear range/μg ml^{-1}	0.01–2.2	0.1–2.4
Detection limit/ng ml^{-1}	1	10
Dispersion coefficient	1.65	1.70
Reproducibility (% RSD)	0.1–2	0.1–2
Sample throughput/samples h^{-1}	28	22

Table 3 Recoveries of total Se for Certified Reference Materials

	Se/μg g^{-1}	
Type	Certified value	Found ± s*
Marine Sediment (NRC-PACS 1)	1.09 ± 0.11	1.06 ± 0.08
Estuarine Sediment (CEC-CRM 277)	2.04 ± 0.18	1.95 ± 0.10
Tea (NRC-CRM C85-05)	0.041 ± 0.004	0.043 ± 0.004
Selenium eutectic alloy (%)	2.60 ± 0.10	2.58 ± 0.15

* n = 5.

Table 4 Simultaneous determination of Se^{IV} and Se^{VI} in synthetic mixtures of standard Se^{IV} and Se^{VI}

Added/μg ml^{-1}			Found*/μg ml^{-1}			Relative error (%)		
Se^{IV}	Se^{VI}	Total†	Se^{IV}	Total†	Se^{VI}‡	Se^{IV}	Total†	Se^{VI}
0.20	0.20	0.40	0.20	0.40	0.20	+1.0	+1.3	+1.5
0.20	0.50	0.70	0.20	0.70	0.50	−0.50	−0.20	−0.20
0.50	0.20	0.70	0.50	0.70	0.20	−0.20	+0.30	+1.5
0.40	0.60	1.0	0.40	1.0	0.60	0.0	0.0	0.0
0.50	1.0	1.5	0.50	1.5	1.0	0.0	+1.0	+1.0
1.0	0.50	1.5	1.0	1.5	0.50	0.0	−0.20	−0.40
0.0	1.0	1.0	0.01	1.0	1.0	+1.0	0.0	−1.0
1.0	0.0	1.0	1.0	1.0	0.0	0.0	0.0	0.0

* n = 5. † Se^{IV} + Se^{VI}. ‡ Calculated by subtraction of Se^{IV} from total Se.

The interference of several ions which may occur in environmental samples was studied by using a solution containing a mixture of Se^{IV} and Se^{VI} at concentrations of 0.5 μg ml^{-1} and 1.0 μg ml^{-1}, respectively, adding various concentrations of interfering ions up to the amounts where the relative error reached a value of about 5%. The errors were calculated by comparing the peak height to that obtained after the injection of an aqueous solution of Se^{IV} and Se^{VI} containing no interfering ions, as a reference. The results are summarized in Table 7. During the interference studies, if a precipitate was formed, it was removed by centrifugation. Positive interference from permanganate or hydrogen peroxide was eliminated by boiling the solution with sodium azide, a reducing agent which had no reducing effect on either Se^{IV} or Se^{VI}.

Applications

The proposed method was used to determine the total selenium content in a number of certified reference materials (sediments, tea and alloy) (Table 3). The method was also successfully applied to the simultaneous determination of the Se^{IV} and Se^{VI} content in a number of synthetic mixtures of Se^{IV} and Se^{VI} (Table 4). The method was also extended to the simultaneous determination of Se^{IV} and Se^{VI} in a number of environmental waters. The samples were spiked with one of the two concentrations of Se^{IV} and Se^{VI} and recoveries determined (Table 5). The results of the analyses of real samples (soil, human hair and food) by our procedure were in excellent agreement with those obtained by HG-AAS (Table 6).

Determination of Total Selenium in Certified Reference Materials

Sediment (1–2 g) or tea (2–5 g) or alloy (0.05–0.1 g) was placed in a 50 ml beaker and digested using a procedure described by Cutter.[22] The beaker with the testing material and concentrated nitric acid was covered with a watch glass and heated gently for 3 h. Perchloric acid was added and the mixture was heated until

Table 6 Determination of total Se in real samples

	Total Se/μg g^{-1}		
Sample	AAS	Proposed method*	Relative error (%)
Soil (surface)	0.375	0.380	+1.3
Hair (human)	nd†	nd	—
Egg (yolk)	0.170	0.167	−1.7
Flour (rice)	nd	nd	—

* n = 5. † nd: not detected.

Table 5 Analysis of spiked environmental water and flour samples

Sample	Se^{IV} added/ ng ml^{-1}	Se^{VI} added/ ng ml^{-1}	Reduced through photo-reactor	Total Se added*/ ng ml^{-1}	Total Se found*/ ng ml^{-1}	Se^{VI} found†/ ng ml^{-1}	Recovery ± s (%)
Tap water	100	100	No	200	100	—	100 ± 0.3
	100	100	Yes	200	199	99	99.5 ± 0.5
Lake water—							
Sample 1	200	80	No	280	201	—	100.5 ± 0.4
	200	80	Yes	280	278	79	99.5 ± 0.6
Sample 2	500	50	No	550	499	—	99.8 ± 0.2
	500	50	Yes	550	545	45	99.0 ± 0.8
Flour (rice)	300	60	No	360	301.5	—	100.5 ± 0.5
	300	60	Yes	360	358.0	58	99.5 ± 0.6

* Determined as Se^{IV}. † Calculated by subtracting the Se^{VI} from the total Se.

only a slight amount of moisture remained. A third 3 h nitric acid heating was performed and the sample was again carefully evaporated. Concentrated HCl was added under heating to ensure that all the Se was present as Se^{IV}. The contents of the beaker were filtered through a Whatman No. 40 filter paper into a 25 ml calibrated flask. The solution was then diluted up to the mark with 2.0 M H_2SO_4. The total Se content was determined as described under Procedure using tartrate as masking agent. In the case of the tea sample, interference from permanganate was removed by adding sodium azide and boiling the solution before measurement. The results for total Se were in good agreement with certified values. The results of total Se by on-line photo-reduction were also in excellent agreement with those obtained by HCl reduction. The results are shown in Table 3.

Simultaneous Determination of Se^{IV} and Se^{VI} in Synthetic Mixtures

Synthetic mixtures of standard Se^{IV} and Se^{VI} of different concentrations were prepared with 2.0 M H_2SO_4. The Se^{IV} and Se^{VI} contents were determined spectrofluorimetrically as described under Procedure. The precision for the determination of Se^{IV} and Se^{VI} was measured by analysing (n = 5) the samples listed in Table 4. The relative errors for all samples were < 2%.

Table 7 Effect of interfering ions on the determination of 0.5 μg ml^{-1} Se^{IV} and 1.0 μg ml^{-1} Se^{VI}, respectively

Interfering ion	Maximum permissible concentration*/ μg ml^{-1} Se^{IV}	Se^{VI}
Ammonium	100	100
Bromide	100	100
EDTA	100	100
Fluoride	100	100
Persulfate	100	100
Silicate	100	100
Tartrate	5000	5000
Aluminium	100	100
Antimony(V)	50	50
Arsenic(III)	50	50
Beryllium	50	50
Calcium	50	50
Cerium(III, IV)	50	50
Chromium(III)	100	100
Cobalt(II)	100	100
Copper(II)	100	100
Iron(II, III)	50	50
Lanthanum	100	100
Magnesium	50	50
Manganese(II)	100	100
Mercury(II)	50	50
Molybdenium(VI)	100	100
Nickel(II)	100	100
Potassium	2000	2000
Silver(I)	50	50
Tin(II, IV)	50	50
Tungsten(VI)	50	50
Uranium(VI)	50	50
Vanadium(V)	50	50
Zinc+	100	100

* For acetate, alkali metals, sodium azide, carbonate, citrate, chloride, dichromate, fluoride, iodide, nitrate, oxalate, perchlorate, phosphate and sulfate the maximum permissible concentration is 1000 μg ml^{-1}. A 5% error criterion is adopted for all the interferents.

Analysis of Spiked Environmental Water and Flour Samples

The proposed method was applied to the determination of Se^{IV} and Se^{VI} added to some environmental water and flour samples. A preliminary study showed Se^{IV} and Se^{VI} to be below the limits of detection in the samples. The samples were spiked with one of two concentrations of Se^{IV} and Se^{VI} with 2.0 M H_2SO_4 and the recoveries determined (the standard additions technique was used and in the case of the flour sample, the standard was added before digestion). The recoveries in all cases were high (between 99.0 and 100.5%) and are shown in Table 5.

Determination of Total Selenium in Real Samples

An air-dried homogenised soil sample (5–10 g) was weighed accurately and placed in a 100 ml beaker. The sample was digested and reduced following the method recommended by Cutter.[22] The content of the beaker was filtered through a Whatman No. 40 filter paper into a 25 ml calibrated flask. It was then diluted up to the mark with 2.0 M H_2SO_4.

Human hair (2–5 g) or egg yolk (5–10 g) or rice flour (5–10g) was placed in a 100 ml beaker. Following the procedure recommended by Bratakos *et al.*,[23] the sample was digested with a mixture of nitric and perchloric acids and the Se^{VI} species were reduced with HCl. The contents of the flask were filtered through a Whatman No. 40 filter paper into a 25 ml calibrated flask. The solution was then diluted up to the mark with 2.0 M H_2SO_4.

Suitable aliquots of the above samples were transferred into a 10 ml calibrated flask and the total Se contents were determined as described under Procedure using tartrate as masking agent. The results of soil, hair, egg and flour analyses by the FIA method were found to be in good agreement with those obtained by HG-AAS. The results are shown in Table 6.

The very low value of total selenium for the hair sample is probably due to the type, quality and quantity of the foods consumed by Greeks.[24] The low value of total selenium for the rice flour sample is probably due to low selenium in soils. Bratakos *et al.*[23] also reported such low selenium contents in foods produced in Greece. Occurrence of such low selenium contents have been reported in the soils of some countries.[5,25]

Conclusions

The use of a photo-reduction-reactor with an FIA system has been shown to be effective in the speciation of selenium. Automation of the system has resulted in much shorter analysis times, with greater reduction efficiency than using conventional heated digestion methods. The proposed FIA method using PTQA is not only one of the most sensitive methods for the simultaneous determination of Se^{IV} and Se^{VI} but is also excellent in terms of selectivity and simplicity. It offers also a very efficient procedure for speciation analysis. Therefore, this method will be successfully applied to the monitoring trace amounts of selenium species in environmental, biological and soil samples.

M.J.A. thanks the State Scholarship Foundation of Republic of Greece (I.K.Y.) for the award of a postdoctoral fellowship.

References

1 Shamberger, R. J., *Biochemistry of Selenium*, Plenum, New York, 1983.
2 Levander, O. A., *Trace Elements in Human and Animal Nutrition*, Academic Press, New York, 1986, pp. 209–279.
3 Masscheleyen, P. H., and Patrick, W. H., Jr., *Environ. Toxicol. Chem.*, 1993, **12**, 2235.
4 Fishbein, L., *Int. J. Environ. Anal. Chem.*, 1984, **17**, 113.

5 Iyengar, G. V., Kollmer, W. E., and Bowen, H. J. M., in *The Elemental Composition of Human Tissues and Body Fluids*, Verlag Chemie, Weinheim, 1978.
6 Masscheleyen, P. H., DeLaune, R. D., and Patrick, W. H., Jr., *J. Environ. Health*, 1991, **26**, 555.
7 Robberecht, H., and Van Grieken, R., *Talanta*, 1982, **29**, 823.
8 Olivas, R. M., Donard, O. F. X., Camara, C., and Quevauviller, Ph., *Anal. Chim. Acta*, 1994, **286**, 357.
9 Sanz Alaejos, M., and Diaz Romero, C., *Chem. Rev.*, 1995, **95**, 227.
10 Welz, B., and Schubert-Jacobs, M., *At. Spectrosc.*, 1991, **12**, 91.
11 Linares, P., Luque de Castro, M. D., and Valcarcel, M., *Analyst*, 1986, **111**, 1405.
12 Cai, Y., Cabanas, M., Fernandez-Turiel, J. L., Abalos, M., and Bayona, J. M., *Anal. Chim. Acta*, 1995, **314**, 183.
13 Pitts, L., Worsfold, P. J., and Hill, S. J., *Analyst*, 1994, **119**, 2785.
14 Liu, Ren-Min, Liu, Dao-Jie, and Sun, Ai-Ling, *Analyst*, 1992, **117**, 1767.
15 Motomizu, S., and Sanada, M., *Anal. Chim. Acta*, 1995, **308**, 406.
16 Measures, C. I., and Burton, J. D., *Anal. Chim. Acta*, 1980, **120**, 177.
17 Atallah, R. H., and Kalman, D. A., *Talanta*, 1991, **38**, 167.
18 Pal, B. K., Chakrabarti, A. K., and Ahmed, M. J., *Anal. Chim. Acta*, 1988, **206**, 345.
19 Porter, H. D., *J. Am. Chem. Soc.*, 1954, **76**, 127.
20 Pal, B. K., and Chowdhury, B., *Mikrochim. Acta*, 1984, **II**, 121.
21 Ruzicka, J., and Hansen, E. H., *Anal. Chim. Acta*, 1978, **99**, 37.
22 Cutter, G. A., *Anal. Chem.*, 1985, **57**, 2951.
23 Bratakos, M. S., Zafiropoulos, T. F., Siskos, P. A., and Ioannou, P. V., *J. Food Sci.*, 1987, **52**, 817.
24 Bratakos, M. S., Zafiropoulos, T. F., Siskos, P. A., and Ioannou, P. V., *Int. J. Food Sci. Technol.*, 1988, **23**, 585.
25 Forbes, S., Bound, G. P., and West, T. S., *Talanta*, 1979, **26**, 473.

Paper 6/06357H
Received September 16, 1996
Accepted November 11, 1996

The Analyst

Concentration of Platinum(IV) From Acidic Chloride and Sulfate–Chloride Aqueous Media With Reversed Micellar Solutions of Oxyethylated Surfactant

Alexander I. Bulavchenko*, Tat'yana Yu. Podlipskaya, Elena K. Batishcheva and Vladislav G. Torgov

Institute of Inorganic Chemistry, Russian Academy of Sciences, Siberian Branch, 630090 Novosibirsk, Russia

The possibility of employing reversed micelles of oxyethylated surfactants to concentrate platinum from acidic aqueous media was investigated. A procedure for reversed micellar concentration is described. Platinum concentration was effected by means of desolubilization in a non-traditional back-extraction stage by dilution of the reversed micellar solution with chloroform or a mixture of chloroform with hexane. In acidic sulfate–chloride media the distribution ratio of Pt^{IV} increased to about 10^2–5×10^3 in the presence of Br^- and I^- as complexing agents. In chloride media the distribution ratio could be increased to about 2×10^3 by using $SnCl_2$. The maximum recovery of platinum from the extract did not exceed 85%. With I^- as a complexing agent, no back-extraction could be performed. With this back-extraction procedure, the Pt^{IV} concentration factor varied from about 10^2 to 10^3 depending on the aqueous feed composition. It was shown spectrophotometrically that Pt^{IV} complex species were the same in the feed, extract and desolubilized aqueous solution. The possibility of the spectrophotometric determination of platinum with $SnCl_2$ directly in the reversed micellar solution is demonstrated.

Keywords: *Reversed micellar extraction; oxyethylated oil-soluble surfactant; platinum(IV); chloride and sulfate–chloride aqueous media*

Surfactants and reversed micellar solutions are widely used in many analytical procedures as auxiliary agents to increase analytical sensitivity and selectivity.[1–3] In recent years there has been a trend to develop procedures with surfactants playing the main role. The use of reversed micellar surfactant solutions for the separation and concentration of metals has attracted considerable attention. Vijayalakshmi and co-workers[4,5] studied the equilibrium extraction and concentration of polyvalent metal ions with water-in-oil (w/o) microemulsions and showed the possibility of separating trivalent from divalent metal ions. Apanasenko *et al.*[6] performed the reversed micellar concentration of Al and Ga with a fivefold concentration factor. Earlier, a threefold concentration of Ni^{II} was achieved with the help of w/o microemulsions of ionic surfactants.[7] The solubilization and complexation of metals in reversed micelles has been studied.[8,9]

Water-in-oil microemulsion formation and the extraction of metals with mixed micelles of surfactants and various types of extractants has been investigated.[10] Neuman and co-workers[11,12] considered the role of reversed micelles in extraction with the well known extractant di(2-ethylhexyl)phosphoric acid. Leodidis and Hatton[13] studied the selective solubilization of alkali and alkaline earth metal ions with reversed micelles. The possibility of separating metals having similar properties with the help of reversed micelles in liquid membrane processes has been demonstrated for the pair Ni^{II}–Co^{II}.[14]

This brief survey indicates that this area of research is still in its infancy. The unique properties of reversed micellar solutions are very under-utilized and at present there is no serious competition with traditional extraction techniques.

We have developed a procedure for the reversed micellar concentration of metals[15] differing from solvent extraction concentration[16] in having a non-traditional back-extraction stage. In this stage the reversed micelles are broken by heating or by the the addition of chloroform[17] and the solubilized metal-enriched aqueous solution separates as an aqueous phase (Fig. 1). The non-use of an aqueous stripping agent solution and the low solubilizing capacity of reversed micelles have resulted in a considerably higher concentration of chloride metal complexes (Fe^{III}, Pt^{IV} and Pd^{II})[18] compared with solvent extraction concentration.

The aim of this work was to develop further the reversed micellar concentration procedure to determine low Pt^{IV} concentrations in aqueous acidic media. The effects of various complexing agents (Br^- and I^-) and $SnCl_2$ on the distribution ratio, recovery and concentration factor in the extraction and back-extraction stages were studied. The method was applied to the determination of low concentrations of Pt^{IV} in the presence of Fe^{III}.

Experimental

Reagents

Oxyethylated isononylphenol with an average degree of oxyethylation of 4, manufactured by Diagnosticum (Belgorod, Russia) as Neonol APh_9-4 (an analogue of Triton N-42), was used as the oil-soluble micellation surfactant. The hydrophilic–lipophilic balance (HLB) was 9.1 ± 0.3 and the mass fraction of the main substance (the sum of the oxyethylated homologues) was 99.8%. The distribution functions of the homologues had a Poisson shape. The contribution of the homologue with a degree of oxyethylation of 4 was 30%. The surfactant was used as

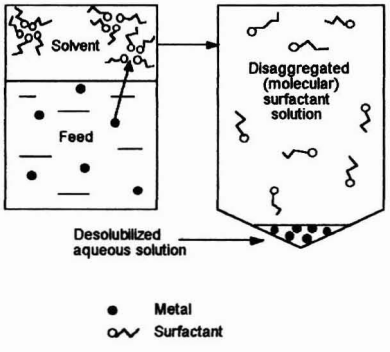

Fig. 1 Scheme for reversed micellar concentration of metals.

received. The solvent (reversed micellar solution) contained 10% v/v Neonol APh_9-4 in decane. Analytical-reagent grade organic diluents (decane, hexane and chloroform) were used without further purification. All other reagents were chemically pure. Distilled water was used to prepare aqueous solutions.

Solutions of Pt^{IV} were prepared by diluting a solution of chloroplatinic acid. The acid was obtained by dissolving 99.9% pure metallic platinum in HNO_3–HCl (1+3). The stock solution contained 0.2 mol l^{-1} Pt^{IV} in 2.4 mol l^{-1} HCl. A solution of Fe^{III} (2.5 mol l^{-1} + 1.5 mol l^{-1} HCl) was obtained by dissolving $FeCl_3 \cdot 6H_2O$ in hydrochloric acid. Sulfate–chloride and chloride solutions had the compositions saturated Na_2SO_4 + 3 mol l^{-1} H_2SO_4 + 0.05 mol l^{-1} HCl, 4 mol l^{-1} NaCl + 1.2 mol l^{-1} HCl and 1 mol l^{-1} HCl. The complexing agents (HBr and NaI) and $SnCl_2$ were added to the feed as aliquot portions of the solutions: 7.1 mol l^{-1} HBr, 0.5 mol l^{-1} NaI and 0.5 mol l^{-1} $SnCl_2$ + 2 mol l^{-1} HCl.

Apparatus

Spectrophotometric measurements were performed on a Specord M-40 UV/VIS spectrophotometer (Carl Zeiss, Jena, Germany). Colorimetric determinations of Fe^{III} and Pt^{IV} were performed on a KFK-2MP photoelectric colorimeter (ZOMZ, Zagorsk, Russia).

Determination of Pt^{IV} and Fe^{III} in Aqueous Media

Concentrations of Pt^{IV} and Fe^{III} in stock and working standard solutions were determined colorimetrically using published procedures with $SnCl_2$[19] and sulfosalicylic acid,[20] respectively.

Concentration With Reversed Micellar Solutions (Extraction and Back-extraction Stages)

The procedure for the reversed micellar concentration of metals is shown schematically in Fig. 2. The solvent extraction stage was performed in a glass separating funnel with a volume of 100–1500 ml. A water-to-oil ratio of 5 : 1 was used in most instances. The feed served as the continuous phase. The phases were contacted for not more than 30 min under mild stirring with a propeller mixer. After extraction, the raffinate was analysed for Pt^{IV} and/or Fe^{III} content. The extract was transferred into a conical-bottomed flask (Fig. 1) with polyethylene-coated walls and diluted with chloroform or chloroform–hexane [route (1), Fig. 2]. After the addition of chloroform, the solution became turbid and the solubilized aqueous solution of the metal coagulated into a separate transparent phase. This took 1–2 h for most of the systems. The separated aqueous solution was removed with a glass measuring pipette, measured and analysed for the metal content.

Spectrophotometric Determination of Pt^{IV} Directly in Reversed Micellar Phase

As an alternative procedure, the metal concentration can be determined directly in the reversed micellar phase without micelle breaking and separation of the solubilized aqueous solution [route (2), Fig. 2]. In this approach, the determination

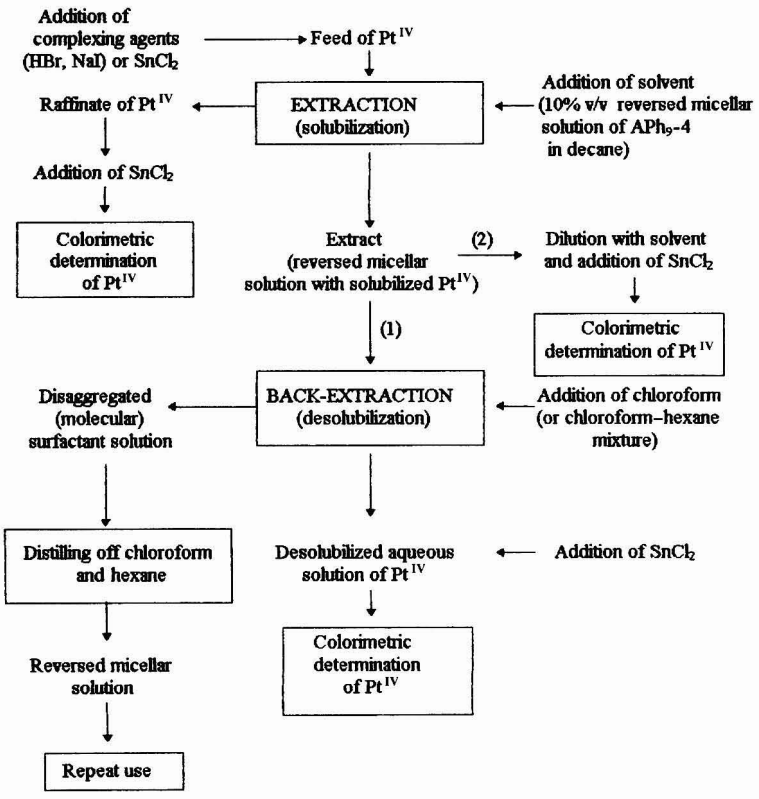

Fig. 2 Analytical procedure for reversed micellar concentration of platinum.

of Pt^{IV} is effected colorimetrically by a procedure developed for aqueous media. This 'water' procedure is applicable here since the interaction of analytical reagents with platinum takes place in the water cores of the micelles. To prepare a standard reversed micellar solution of Pt^{IV}, an aliquot of an aqueous solution of Pt^{IV} was solubilized by the injection method into the solvent. An aliquot (0.5–3.0 ml) of this standard solution of Pt^{IV} or of its extract was then transferred into a 25 ml calibrated flask and diluted with the solvent to about 20 ml [route (2) Fig. 2], then 0.21 ml of an aqueous solution of $SnCl_2$ (2.66 mol l^{-1} $SnCl_2$ + 3 mol l^{-1} HCl) was solubilized into the solution by the injection method. The resulting solution was diluted to volume with the solvent, allowed to stand for 40 min and then scanned photometrically against a reagent blank in a cell with a pathlength of 5 cm at a wavelength of 400 nm. A blank solution was prepared in the same way with the same composition except that it did not contain platinum. The calibration graph was linear for platinum concentrations in the range 10^{-6}–10^{-5} mol l^{-1}. Determination of platinum directly in the reversed micellar solution was employed to calculate the extraction parameters in a number of systems.

Results and Discussion

Results for the reversed micellar concentration of Pt^{IV} in the extraction stage are given in Table 1.

Extraction Stage

Extraction of chloride complexes of Pt^{IV}

The distribution isotherms of Pt^{IV} from acidic chloride and sulfate–chloride solutions are shown in Fig. 3. The dependences are linear for low metal concentrations and the distribution ratio of Pt^{IV} in the presence of Cl^- did not exceed 12.9 ± 0.7. To determine the Pt^{IV} complex species in the media under study, the corresponding absorption spectra were measured. The absorption maximum of Pt^{IV} in the visible region was at 453 nm, corresponding to the chloride complex ($PtCl_6^{2-}$).[21] The electronic absorption spectra of Pt^{IV} measured in all stages of reversed micellar concentration (Fig. 4) indicated that the Pt^{IV} complex species was the same as that in the feed, extract and desolubilized aqueous solution. The bathochromic shift of the absorption maximum by 11 nm for the chloride complex of platinum in reversed micelles may be due to its interaction with protonated oxyethylate groups of the surfactant molecules.

Effect of Br^- *and* I^- *on extraction of* Pt^{IV} *from acidic sulfate–chloride media*

Spectrophotometric studies indicated that in acidic sulfate–chloride solutions of Pt^{IV} in the presence of Br^-, the bromide complex of platinum ($PtBr_6^{2-}$) is formed. The equilibrium in the solutions at room temperature is established within 2 d. In the presence of Br^-, the distribution ratio of Pt^{IV} increases by an

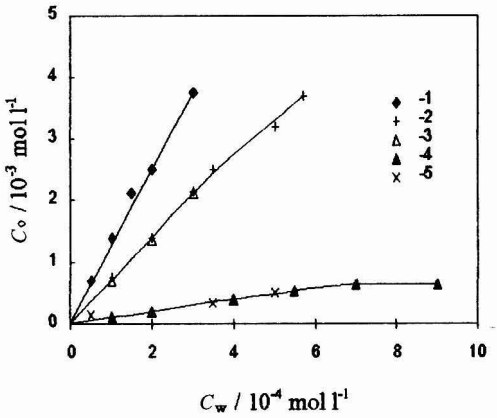

Fig. 3 Distribution isotherms of Pt^{IV} and Fe^{III} from acidic aqueous media: 1, saturated Na_2SO_4 + 3 mol l^{-1} H_2SO_4 + 0.05 mol l^{-1} HCl; 2–5, 4 mol l^{-1} NaCl + 1.2 mol l^{-1} HCl, with 1 and 4, Pt^{IV}, 2, Fe^{III} 3, Fe^{III} in the presence of Pt^{IV} [$C_{f(Fe)} = C_{f(Pt)}$] and 5, Pt^{IV} in the presence of Fe^{III} [$C_{f(Pt)} = C_{f(Fe)}$].

Table 1 Results for reversed micellar concentration of Pt^{IV} in the extraction stage (95% confidence level). For abbreviations, see text [eqn. (1)]

Model system No.	Feed: Supporting electrolyte and complexing agent	Feed: Metal	Feed: $C_f/10^{-4}$ mol l^{-1}	V_w/V_o	D	R_e (%)	K_e
1	Saturated Na_2SO_4 + 3 mol l^{-1} H_2SO_4 + 0.05 mol l^{-1} HCl	Pt	1.72 ± 0.03	5	12.9 ± 0.7	72.1 ± 1.1	3.6 ± 0.2
2	Saturated Na_2SO_4 + 3 mol l^{-1} H_2SO_4 + 0.001 mol l^{-1} HCl + 0.05 mol l^{-1} HBr	Pt	1.37 ± 0.03	5	88.7 ± 3.5	94.7 ± 1.4	4.7 ± 0.2
3	Saturated Na_2SO_4 + 3 mol l^{-1} H_2SO_4 + 0.002 mol l^{-1} HCl + 0.002 mol l^{-1} NaI	Pt	1.82 ± 0.04	50	(4.74 ± 0.16) × 10^3	99.0 ± 1.5	49.5 ± 2.1
4	1 mol l^{-1} HCl + 0.02 mol l^{-1} $SnCl_2$	Pt	5.00 ± 0.09	5	(1.78 ± 0.07) × 10^3	99.7 ± 1.5	5.0 ± 0.2
5	1 mol l^{-1} HCl + 0.05 mol l^{-1} $SnCl_2$	Pt	(5.0 ± 0.1) × 10^{-2}	50	(2.00 ± 0.08) × 10^3	97.6 ± 1.5	48.8 ± 2.0
6	Saturated Na_2SO_4 + 3 mol l^{-1} H_2SO_4 + 0.05 mol l^{-1} HCl	Pt	1.81 ± 0.03	5	12.9 ± 0.7	72.0 ± 1.1	3.6 ± 0.2
		Fe	(1.10 ± 0.02) × 10^2	5	≤0.05	1.00 ± 0.02	0.050 ± 0.002
7	4 mol l^{-1} NaCl + 1.2 mol l^{-1} HCl	Pt	3.92 ± 0.07	5	0.95 ± 0.05	16.1 ± 0.2	0.80 ± 0.03
		Fe	4.34 ± 0.09	5	6.4 ± 0.4	56.2 ± 0.8	2.8 ± 0.1

order of magnitude and shows a maximum (Fig. 5, curve 1) at a 500-fold excess of HBr relative to Pt^{IV}. A greater increase in the distribution ratio (to about 5000) was obtained with I^- as the complexing agent. The dependence shows a broad maximum at a tenfold excess of I^- (Fig. 5, curve 2).

Effect of $SnCl_2$ *on extraction of* Pt^{IV} *from dilute hydrochloric acid media*

The logarithmic dependence of the distribution ratio of Pt^{IV} when concentrated from 1 mol l^{-1} HCl is linear over a wide range of $SnCl_2$ concentrations (Fig. 5, curve 3). The addition of a 40-fold molar excess of $SnCl_2$ relative to Pt^{IV} increases the distribution ratio by four orders of magnitude.

Extraction of chloride complex of Pt^{IV} *in the presence of* Fe^{III}

The extraction of these two metals, which frequently accompany each other, is considered for the case of the collective extraction of Pt^{IV} and Fe^{III} from acidic chloride and sulfate–chloride media in the absence of complexing agents. The distribution ratio of Pt^{IV} from chloride media at low concentrations does not change even at a 50-fold molar excess of Fe^{III}. It was also found that in the extraction of metals with equal concentrations in the systems being studied, the distribution isotherms of Fe^{III} and Pt^{IV} (Fig. 3) do not change in the region of constancy of the distribution ratios. Hence in the systems studied the metals are extracted into reversed micelles independently of each other.

The results for the extraction of Pt^{IV} with oxyethylated surfactants in decane from acidic chloride and sulfate–chloride media follow the general regularities found for the extraction of platinum with oxygen-containing extractants (alcohols, ethers, etc.).[22] The increase in recovery when using complexing agents results from the increased stability of the complexes formed. In this study we did not investigate in detail the chemical interaction between platinum and surfactants, but it seems most probable that there is an interaction between anionic platinum complexes and protonated oxyethylate groups of the surfactant molecules.

From the point of view of methodology, the extraction with oxyethylated surfactants should be carried out with great care because of a high probability of the formation of w/o emulsions owing to the low interfacial tension.

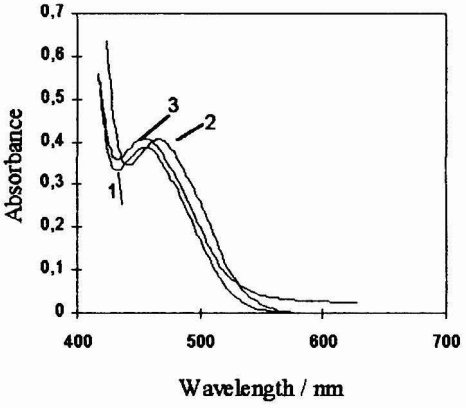

Fig. 4 Absorption spectra of Pt^{IV} (against a reagent blank) in all stages of reversed micellar concentration. 1, Feed: saturated Na_2SO_4 + 3 mol l^{-1} H_2SO_4 + 0.05 mol l^{-1} HCl; $C_{f(Pt)} = 7.5 \times 10^{-3}$ mol l^{-1}, using a 1.0 cm cell. 2, Extract: $C_{o(Pt)} = 7.5 \times 10^{-3}$ mol l^{-1}, using a 1.0 cm cell. 3, Desolubilized aqueous solution (back-extraction by chloroform addition up to 30% v/v); $C_{s(Pt)} = 7.5 \times 10^{-2}$ mol l^{-1}, using a 0.1 cm cell.

Back-extraction Stage

Reversed micellar back-extraction (desolubilization) with polar organic diluents has rarely been studied in the past. Deso-

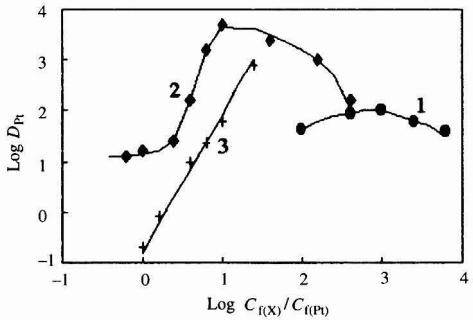

Fig. 5 Distribution ratio of Pt^{IV} *versus* concentration of X (HBr, NaI or $SnCl_2$). 1, Saturated Na_2SO_4 + 3 mol l^{-1} H_2SO_4 + 0.001 mol l^{-1} HCl; $C_{f(Pt)} = 1.0 \times 10^{-4}$ mol l^{-1}, X = HBr; 2, saturated Na_2SO_4 + 3 mol l^{-1} H_2SO_4 + 0.002 mol l^{-1} HCl; $C_{f(Pt)} = 2.0 \times 10^{-4}$ mol l^{-1}, X = NaI; and 3, 1 mol l^{-1} HCl; $C_{f(Pt)} = 5 \times 10^{-4}$ mol l^{-1}, X = $SnCl_2$.

Table 2 Results for reversed micellar concentration of Pt^{IV} in the back-extraction stage and combined data (95% confidence level). For abbreviations, see text (eqn. (1))]

Model system No.*	Metal	$C_s/10^{-2}$ mol l^{-1}	V_o/V_s	R_{be} (%)	K_{be}	R (%)	K
1	Pt	5.89 ± 0.15	110	86.4 ± 4.4	95.0 ± 3.7	62.3 ± 3.4	342 ± 11
2	Pt	5.52 ± 0.14	120	70.9 ± 3.6	89.0 ± 3.5	67.2 ± 3.7	403 ± 14
3	Pt†	—	—	—	—	—	—
4	Pt	6.08 ± 0.14	30	81.3 ± 4.1	24.4 ± 1.0	81.1 ± 4.4	122 ± 4
5	Pt	0.823 ± 0.019	42	80.4 ± 4.1	33.8 ± 0.3	78.4 ± 4.3	(1.64 ± 0.53) × 10^3
6	Pt	6.54 ± 0.15	120	83.6 ± 4.2	100 ± 4	60.2 ± 3.3	361 ± 12
	Fe	0.107 ± 0.002	120	1.62 ± 0.08	1.95 ± 0.07	1.62 ± 0.08	0.097 ± 0.003
7	Pt	1.00 ± 0.02	33	96.2 ± 4.9	31.8 ± 1.2	15.5 ± 0.8	25.5 ± 0.8
	Fe	1.46 ± 0.03	33	36.3 ± 1.8	12.0 ± 0.5	20.4 ± 1.1	33.6 ± 1.0

* Numbering of model systems as in Table 1. † Back-extraction conditions were not found.

lubilization results for the systems studied are given in Table 2. In most cases, the desolubilization of the aqueous solution was carried out by the addition of one volume of chloroform to two volumes of reversed micellar solution. For systems with I^- as complexing agent, no desolubilization could be performed. As an example, consider in more detail finding the optimum back-extraction conditions for a reversed micellar solution obtained by extraction from the feed phase of composition 5×10^{-6} mol l^{-1} Pt^{IV} + 0.05 mol l^{-1} $SnCl_2$ + 1 mol l^{-1} HCl (system No. 5 in Tables 1 and 2). For this model system, the dilution of the reversed micellar solution to separate the solubilized aqueous solution was perfomed with chloroform or chloroform–hexane. Back-extraction data are shown as a schematic phase diagram in Fig. 6. Plotted on the abscissa is the concentration of chloroform (%v/v) in the decane–chloroform–hexane mixture formed after dilution of the reversed micellar solution, and on the ordinate the surfactant concentration (%v/v) in this mixture. The line connecting the axes of rectangular coordinates corresponds to the dilution of the reversed micellar solution with chloroform. The area inside the triangle corresponds to the dilution of the reversed micellar solution with the chloroform–hexane mixture. For example, point A in Fig. 6 corresponds to the dilution of one volume of reversed micellar solution with one volume of chloroform (after dilution the solution contains 5% v/v of the surfactant, 50% v/v of chloroform and 45% v/v of decane). Point B in Fig. 6 corresponds to the dilution of one volume of reversed micellar solution with four volumes of chloroform–hexane (5 + 3) (after dilution the solution contains 2% v/v of the surfactant, 50% v/v of chloroform, 30% v/v of hexane and 18% v/v of decane). It follows from the diagram that it is not always possible to separate the solubilized solution. Thus, no separation takes place at low chloroform concentrations and small dilutions of the reversed micellar solutions and also at high chloroform concentrations and large dilutions (single-phase regions in Fig. 6). Between these regions lie the region of back-extraction and a three-phase region. In the region of back-extraction the platinum recovery from the organic phase is not uniform. In the shaded portion it exceeds 50%. The best results given in Table 2 were obtained at the dilution of one volume of reversed micellar solution with 20 volumes of the chloroform–hexane (4 + 15).

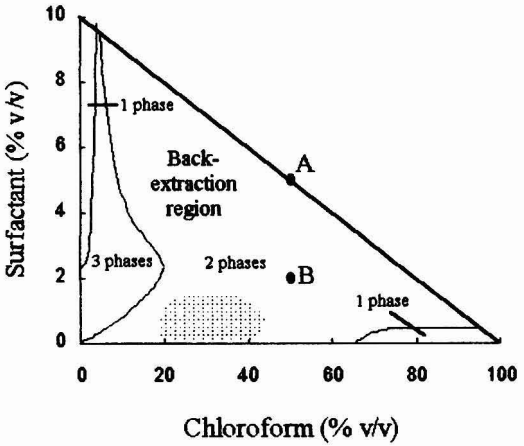

Fig. 6 Schematic phase diagram of the back-extraction of Pt^{IV} from the reversed micellar solution by addition of chloroform or chloroform–hexane. The region with back-extraction exceeding 50% is shaded.

Results for Reversed Micellar Concentration

The total reversed micellar concentration factor for platinum is determined as the overall concentration in the stages of extraction (K_e) and back-extraction (K_{be}):

$$K = K_e K_{be} = R_e \times \frac{V_w}{V_o} \times R_{be} \times \frac{V_o}{V_s} \quad (1)$$

where $K = C_s/C_f$ = total concentration factor, $K_e = C_o/C_f$ = concentration factor in the extraction stage, $K_{be} = C_s/C_o$ = concentration factor in the back-extraction stage, C = metal concentration, R_e = extraction (%), R_{be} = back-extraction (%), $R = R_e R_{be}/100$ = total recovery (%), V = volume and subscripts f, o, w and s represent the feed, extract, raffinate and solubilized aqueous solution, respectively. It can be seen from eqn. (1) that the main difference between reversed micellar concentration and conventional concentration by solvent extraction is that in the back-extraction stage the volume ratio of phases is determined by the solubilizing capacity of the reversed micellar solution. The increase in the concentration factor is limited by the recovery in both the back-extraction and extraction stages. An increase in the recovery in the extraction stage can be achieved either by increasing the distribution ratio ($D = C_o/C_w$) or by decreasing the w/o ratio:

$$R_e = \left(1 + \frac{V_w}{V_o} \times \frac{1}{D}\right)^{-1} \quad (2)$$

One of the ways of increasing the concentration in the back-extraction stage is to decrease the solubilizing capacity of the reversed micellar solution. This reasoning is illustrated by the experimental results in Tables 1 and 2. The highest contribution to the concentration factor is made by the back-extraction stage. In sulfate–chloride media the back-extraction contribution was the determining factor (approximately 10^2). For chloride media this contribution was approximately 25, the difference being determined by the solubilizing capacity of the reversed micellar solution, which in turn depends on the type and concentration of the background electrolyte in the feed (a more detailed investigation of this problem will be performed in future studies). For the system 1 mol l^{-1} HCl + 0.05 mol l^{-1} $SnCl_2$, the possibility of increasing the Pt^{IV} concentration in the extraction stage was demonstrated: a tenfold increase in the w/o ratio led to the same increase in the concentration factor (the total recovery was not decreased). Unfortunately, we failed to find a system for which high distribution ratios (approximately 10^3) would combine with a low solubilizing capacity of the reversed micellar solution ($V_o/V_s \approx 10^2$). In the most promising system (containing I^-), the solubilized aqueous solution could not be separated at all. Possibly here we have a situation often encountered in the concentration by solvent extraction when high recoveries values in the extraction stage lead to considerable worsening of the back-extraction.

In Tables 1 and 2 are also presented data on the collective extraction of the Pt^{IV}–Fe^{III} pair of metals, showing the possibility of a fairly good relative concentration of Pt^{IV} from acidic sulfate–chloride media in the presence of a large excess of Fe^{III}.

Conclusion

The results of this study indicate that reversed micellar concentration with oxyethylated surfactants has some promise for the determination of platinum in dilute acidic chloride and sulfate–chloride aqueous media. The possibility of increasing the concentration factor in both the extraction and back-extraction stages has been demonstrated. At the present stage of

development, the problem remaining is the incomplete recovery of platinum in the back-extraction stage, which may result, in the best case, in an approximately 20% underestimation of the platinum content in the feed determined using reversed micellar concentration. Further research efforts should therefore be concentrated on the elucidation of the mechanism of the desolubilization process and on looking for new ways of separating the solubilized aqueous solutions (*e.g.*, with the help of an electric field). From the point of view of methodology, ways of by-passing the problems are possible, such as repeated treatment of the raffinate with a reduced reversed micellar solution (*i.e.*, after distilling off chloroform and hexane) and repeated desolubilization. However, this will complicate the analytical procedure considerably. The use of large volumes of organic diluents and working with small volumes of desolubilized aqueous solution are further drawbacks to desolubilization by dilution.

The determination of platinum directly in the reversed micellar solution is inferior to desolubilization with regard to absolute concentration, since the concentration of platinum is determined per unit volume of the whole reversed micellar solution and the reversed micellar concentration factor will be determined only by the concentration in the extraction stage. Nevertheless, attempts to determine the metal directly in the reversed micellar phase appear to be promising, the task consisting in finding a procedure which would determine the metal concentration only in the water cores of the micelles. The use of ion-selective electrodes with a hydrophilic membrane may turn out to be the simplest approach.

References

1 Savvin, S. V., Chernova, R. K., and Shtykov, S. N., *Surface-active Substances*, Nauka, Moscow, 1991.
2 Issopoulos, P. B., and Economou, P. T., *Fresenius' J. Anal. Chem.*, 1992, **342**, 439.
3 Pavon, J. L. P., and Cordero, B. M., *Analyst*, 1992, **117**, 215.
4 Vijayalakshmi, Ch. S., Annapragala, L. V., and Gulary, E., *Sep. Sci. Technol.*, 1990, **25**, 711.
5 Vijayalakshmi, Ch. S., and Gulary, E., *Sep. Sci. Technol.*, 1992, **27**, 173.
6 Apanasenko, B. B., Reznic, A. I., and Sokolova, A. N., *Dokl. Akad. Nauk SSSR*, 1990, **315**, 106.
7 Ovejero-Ecudero, F. J., Angelino, H., and Casamatta, G., *J. Dispers. Sci. Technol.*, 1987, **8**, 89.
8 Osseo-Asare, K., *Sep. Sci. Technol.*, 1988, **23**, 1269.
9 Robinson, B. H., Steytler, D. C., and Tack, R. D., *J. Chem. Soc., Faraday Trans. 1*, 1979, **75**, 481.
10 Paatero, E., Sjoblom, J., and Datla, S. K., *J. Colloid Interface Sci.*, 1990, **138**, 88.
11 Neuman, R. D., Zhou, N.-F., Wu, J., Jones, M. A., Gaonkar, A. G., Park, S. J., and Agrawal, M. L., *Sep. Sci. Technol.*, 1990, **25**, 1655.
12 Neuman, R. D., Jones, M. A., and Zhou N.-F., *Colloids Surf.*, 1990, **46**, 45.
13 Leodidis, E. B., and Hatton, T. A., *Langmuir*, 1989, **5**, 741.
14 Moutaoukel, J., and Christian, T., *Langmuir*, 1992, **8**, 1039.
15 Bulavchenko, A. I., Batishcheva, E. K., and Torgov, V. G., *Russ. Pat.*, 1 805 990, 1990.
16 Zolotov, Yu. A., and Kuzmin, N. M., *Extractional Concentration*, Khimiya, Moscow, 1971.
17 Bulavchenko, A. I., and Torgov, V. G., *Abstracts of International Organic Substances Solvent Extraction Conference (ISECOS'92), Voronezh, Russia*, 1992, Vol. 2, p. 201.
18 Bulavchenko, A. I., Batishcheva, E. K., and Torgov, V. G., *Sep. Sci. Technol.*, 1995, **30**, 239.
19 Milner, O. I., and Shipman, G. F., *Anal. Chem.*, 1955, **27**, 1476.
20 Cheng, K. L., Bray, R. H., and Kurtz, T., *Anal. Chem.*, 1953, **25**, 347.
21 Babaeva, A. B., *Dokl. Akad. Nauk SSSR*, 1938, **20**, 365.
22 Zolotov, Yu. A., Iofa, B. Z., and Chuchalin, L. K., *Extraction of Halide Complexes of Metals*, Nauka, Moscow, 1973.

Paper 6/05773J
Received August 19, 1996
Accepted October 14, 1996

Determination of Trace Amounts of Zinc in Water Samples by Flow Injection Isotope Dilution Inductively Coupled Plasma Mass Spectrometry

Tarn-Jiun Hwang and Shiuh-Jen Jiang*

Department of Chemistry, National Sun Yat-Sen University, Kaohsiung, 80424, Taiwan

Flow injection isotope dilution ICP-MS was applied to the determination of zinc in several water samples. A matrix separation and preconcentration system was used for the separation of Mg, Ca, S and Cl matrix and preconcentration of trace amounts of zinc in high salt content samples. A complete preconcentration cycle was accomplished in 4 min. The isotope ratio for each injection was calculated from the peak areas of the flow injection peaks. The precision for the isotope ratio determination was better than 1.7%. A detection limit of 0.014 ng ml^{-1} was obtained for zinc with this method. The method was successfully applied to the determination of trace levels of zinc in SLRS-2 riverine water, SLEW-2 estuarine water, NASS-3 open ocean sea-water and CASS-3 nearshore sea-water reference samples.

Keywords: *Flow injection; isotope dilution; inductively coupled plasma mass spectrometry; zinc; matrix separation; water samples*

ICP-MS is a powerful technique for trace multielement and isotopic analysis.[1–3] This technique combines the characteristics of the ICP for atomizing and ionizing injected material with the sensitivity of MS. It has been satisfactorily applied to the analysis of diverse samples. However, highly saline solutions can cause both spectroscopic and non-spectroscopic interferences.[4–13] Spectral overlaps are seen from polyatomic ions derived from matrix elements such as Na, Ca and Cl. Changes in analyte count rates are observed with high levels of salts or heavy matrix ions. Orifice plugging is also a problem for samples of high solid content.

Several calibration methods have been adapted to ICP-MS to help deal with matrix effects.[10,14–19] The matrix interference problems can also be dealt with by separating the analytes from the matrix. Several matrix–analyte separation and preconcentration techniques have been adapted to ICP-MS analysis.[20–30] We describe here the implementation of an on-line matrix–analyte separation and preconcentration technique with ICP-MS to determine Zn, using a miniature column packed with SO_3–quinolin-8-ol carboxymethyl-cellulose.[28–31]

Isotope dilution (ID) techniques have been applied in several previous ICP-MS applications.[14,17,27,29,32–34] Isotope dilution is well recognized as a definitive analytical technique for the determination of the trace elements. Since another isotope of the same element represents the ideal internal standard for that element, ID results are expected to be highly accurate even when the sample contains high concentrations of concomitant elements and/or there is sample loss during the preparation or pretreatment process.

In this work, flow injection (FI)–ID–ICP-MS was used to determine the concentrations of zinc in water samples. Matrix separation and preconcentration were used for separation of interfering ions. The influence of instrumental operating conditions, preconcentration system conditions and non-spectroscopic and spectroscopic interferences due to the matrix on the precision and accuracy of isotope ratio determination was also investigated. The method was applied to the determination of zinc in SLRS-2 riverine water, SLEW-2 estuarine water, NASS-3 open ocean sea-water and CASS-3 nearshore sea-water reference samples.

Experimental

ICP-MS Device and Conditions

An ELAN 5000 ICP-MS instrument (Perkin-Elmer SCIEX, Thornhill, ON, Canada) was used. It was equipped with an ultrasonic nebulizer (U-5000 AT+ Cetac, Omaha, NE, USA). The gas flow rates were controlled by a four channel mass flow controller.

The ICP and ultrasonic nebulizer operating conditions were selected to maximize the sensitivity of zinc using a simple flow injection system. A 100 μl volume of 10 ng ml^{-1} Zn solution was injected into a 0.5 mol l^{-1} HNO_3 carrier solution and analyzed by ICP-MS. The operating conditions used throughout this work are summarized in Table 1.

Data acquisition parameters used for isotope ratio measurement are listed in Table 1. The isotopes monitored were ^{66}Zn and ^{67}Zn. Version 2.2 of the ELAN 5000 software was used. Under the combinations of dwell time and sweeps/reading, a data point could be obtained in < 1 s for each isotope. The isotope ratio was calculated from the peak areas of the flow injection peaks. The mean isotope ratio and RSD were calculated from isotope ratios measured from several repeated injections.

Table 1 Equipment and operating conditions*

ICP-MS	PE SCIEX ELAN 5000
Plasma conditions—	
Outer gas flow rate	16 l min^{-1}
Auxiliary gas flow rate	0.9 l min^{-1}
Nebulizer gas flow rate	1.1 l min^{-1}
Rf power	1.1 kW
*Mass spectrometer settings**—	
Photon stop (S2)	−10.05 V
Bessel box barrel	+15.34 V
Einzel lenses 1 and 3 (E1)	−0.04 V
Bessel box end lens (P)	−79.10 V
Resolution	Normal
Dwell time	40 ms
Sweeps/reading	5
Readings/replicate	135
Number of replicates	1
Points/spectral peak	1
Isotopes monitored	^{66}Zn and ^{67}Zn
Ultrasonic nebulizer—	
Desolvation tube temperature	135 °C
Condenser temperature	0 °C

* Definitions and descriptions of these terms are given in user manuals.

Flow Injection

In order to investigate the effect of the sample matrix on the precision and accuracy of isotope ratio determinations, a simple FI system was built. The system was composed of a Rheodyne (Cotati, CA, USA) Model 5041 rotary sample injection valve and a Gilson (Middleton, WI, USA) Minipuls-3 peristaltic pump. A 100 μl portion of the test mixture solution was injected into a 0.5 mol l^{-1} nitric acid carrier solution and analyzed by ICP-MS.

Preconcentration System

A laboratory-made sample pretreatment system was used to separate trace amounts of zinc from matrix elements. A schematic diagram of the matrix separation and preconcentration system is shown in Fig. 1. This system was composed of three Gilson Minipuls-3 peristaltic pumps and two Rheodyne Model 5041 PTFE six-port four-way rotary valves whose switching was actuated by Rheodyne Model 5701 pneumatic actuators and Rheodyne Model 7163 solenoid valve kits. The automation of the flow injection system was controlled by a personal computer through a laboratory-made I/O card and switching circuit.

The operating procedure for the preconcentration system is described below. The first rotary valve was used as a selection valve between buffer and sample. At the start of a preconcentration cycle, sample was pumped to wash the system while buffer solution was pumped to condition the column. After a suitable period, valve 1 was switched to load the sample and pump 2 was stopped. After 10.0 ml of sample had been loaded, pump 1 was stopped and valve 1 was rotated back to buffer solution to wash the column. Then valve 2 was switched to let 0.5 mol l^{-1} HNO_3 to pass through the column to elute the retained metal ion into the ultrasonic nebulizer. After elution, both valves were switched back and pump 2 was turned on to let the buffer solution condition the column for the next analysis.

An Omnifit (Cambridge, UK) high performance column (50 mm × 10 mm id) was used. It was equipped with a moveable end piece to allow for adjustment of the amount of ion-exchange material. During this study, the column was packed with about 150 mg of SO_3–quinolin-8-ol carboxymethylcellulose (Knapp Logistic Automation, Graz, Austria). At a suitable pH, commonly encountered matrix components such as alkali and alkaline earth elements are not strongly retained on the ion-exchange materials and are separated from the elements of interest. The operating parameters of the preconcentration system used in this experiment are shown in Table 2. The preconcentration system was connected to the nebulizer with PTFE tubing (20 cm × 0.8 mm id).

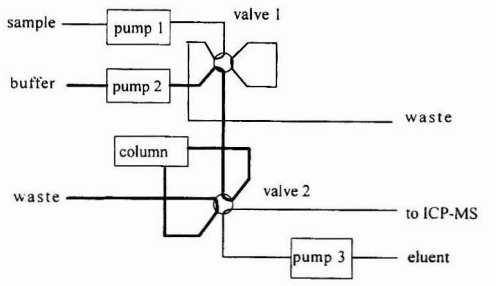

Fig. 1 Schematic diagram of matrix–analyte separation and preconcentration system. This figure shows the flow path of the system in column wash step.

Reagents

$Mg(NO_3)_2$, $Ca(NO_3)_2$, $(NH_4)_2SO_4$ and NaCl were obtained from Fisher (Fair Lawn, NJ, USA). A zinc stock standard solution (1.0 × 10^6 ng ml^{-1}) was obtained from Fisher.

Enriched isotope (^{67}Zn) was purchased from Cambridge Isotope Laboratories (Andover, MA, USA). This stable isotope was received as an oxide. A stock standard solution of zinc of approximately 100 mg l^{-1} was prepared by dissolution of an accurately weighed amount of the material in nitric acid and dilution to volume. The concentration of the spiked solution was verified by reverse spike isotope ID–ICP.

All buffers and eluents were prepared using high purity deionized water (Milli-Q reagent water system, Millipore, Bedford, MA, USA). The ammonium acetate buffer solutions were adjusted with ammonia solution and acetic acid in the pH range 2–8. All the buffers were purified by triple filtration on an SO_3–quinolin-8-ol carboxymethyl-cellulose column. After the uptake step, the absorbed analyte was eluted with 0.5 mol l^{-1} HNO_3 (Fisher, trace metal grade).

Evaluation of Retention

The effect of the pH of the loading solution on the chelation of zinc was studied with the preconcentration system in an off-line mode. Solutions of 100 ng ml^{-1} zinc were buffered to suitable pH values, then 10 ml of these solutions were 'loaded' on to the SO_3–quinolin-8-ol carboxymethylcellulose column at a flow rate of 2.3 ml min^{-1}. Finally, any retained metal was eluted with 5 ml of 1.0 mol l^{-1} HNO_3 into a 10 ml calibrated flask and the collected eluate was diluted to volume with distilled, deionized water. The amounts of metals were then determined by ICP-MS. Recoveries were calculated against the theoretical concentrations.

The tolerance of the matrix separation system for co-existing matrix ions was examined by adding relatively high concentrations of Mg^{2+}, Ca^{2+}, SO_4^{2-} and Cl^- to 1 ng ml^{-1} of zinc metal solutions (for simple FI analysis 5 ng ml^{-1} Zn solution was used). Each solution was injected into FI–ICP-MS and matrix separation–ICP-MS systems successively and the isotope ratio of Zn was determined for comparison.

Sample Preparation

SLRS-2 riverine water reference material for trace metals, SLEW-2 estuarine water reference material for trace metals,

Table 2 Preconcentration system and operating conditions

Column	SO_3–quinolin-8-ol carboxymethyl-cellulose
Buffer solution	pH 4; 0.1 mol l^{-1} ammonium acetate
Eluent	0.5 mol l^{-1} HNO_3
Pump 1 (sample) flow rate	10.0 ml min^{-1}
Pump 2 (buffer) flow rate	4.5 ml min^{-1}
Pump 3 (eluent) flow rate	3.0 ml min^{-1}

Preconcentration method—

Step	Pump in operation	Valve position	Duration/s
System wash	1, 2, 3	1 load 2 load	20
Sample loading	1, 3	1 inject 2 load	60
Column wash	2, 3	1 load 2 load	40
Elution	3	1 load 2 inject	60
Column wash	2, 3	1 load 2 load	60

NASS-3 open ocean sea-water reference material for trace metals and CASS-3 nearshore sea-water reference material for trace metals (National Research Council of Canada, Ottawa, Canada) were obtained to demonstrate the applicability of the method to real samples. A 25 ml aliquot of these acidified reference materials was adjusted to pH 4 with 5 ml of 1.0 mol l^{-1} purified ammonium acetate buffer solution. After a suitable amount of enriched isotope has been added, this solution was diluted to 50 ml with distilled, deionized water.

The analyte concentration in the sample was calculated using the equation given in a previous paper.[27] Owing to a mass bias effect, the intensities obtained during isotope ratio determinations were used to calculate the isotopic abundance of zinc. Since the mass bias effect could be factored out during ID calculation, in this study the measured isotope ratio did not correct the mass bias effect.

Results and Discussion

Effect of pH *on Retention*

The amount of zinc chelated with SO_3–quinolin-8-ol carboxymethylcellulose is related to the pH of the solution, and this effect was examined for Zn in the pH range 2–8. The results are shown in Fig. 2. Zinc was chelated quantitatively in the pH range 4–8. For the analysis of the sea-water sample, a solution with pH between 3.5 to 4 should be chosen; at this pH, Zn was complexed by SO_3–quinolin-8-ol carboxymethylcellulose and was retained on the column relatively completely. Meanwhile, as shown in Fig. 2, the interfering ions Mg^{2+} and Ca^{2+} chelated with the resin only when the pH value was >4. Most of the Mg and Ca wash through the column at pH < 4, which can be used to reduce the interferences of Mg and Ca in the ICP-MS analysis. In subsequent experiments, all the loading sample solutions were adjusted to pH 4.

Relationship Between Sample Loading Flow Rate and Recovery

The sample uptake rate did not affect the recovery significantly in the range 3–13 ml min^{-1}. For the purposes of trace Zn concentration, a much faster sample flow rate should be used to save experimental time, and a 10 ml min^{-1} sample loading flow rate was used in the following experiments.

Selection of Eluent and Flow Rate

Owing to the formation of extra molecular ion interferences when HCl and $HClO_4$ were used as eluents, in order to avoid any possible interferences and reduce the background, these acids were not used in this study. The elution of Zn^{2+} from the column was examined with HNO_3 at various concentrations. The recovery of Zn was complete if the concentration of HNO_3 was $\geq$0.5 mol l^{-1}, since it was difficult to nebulize a concentrated acid solution owing to the viscosity and density and, when a high concentration of acid was nebulized, matrix effects were observed. To avoid matrix effects and signal suppression by high acid levels, the lowest possible acid concentration for elution which yielded 100% recovery was used. In subsequent experiments, 0.5 mol l^{-1} HNO_3 was used as the eluent to obtain best recovery and elution peaks for Zn. The recovery of Zn at pH 4 for replicate measurements (n = 7), using 10 ml of 1 ng ml^{-1} standard solution, was 100.2 ± 0.4%.

Fig. 3 shows the effect of the eluent flow rate on the ion signal. An increase in the eluent flow rate decreased the width of the elution peak and saved analysis time. However, an increased eluent flow rate also decreased the nebulization efficiency, causing the ion signal to decrease significantly. The effect of eluent flow rate on the peak shape of the elution curve was similar to that in previous work.[28] Hence an eluent flow rate of 3.0 ml min^{-1} was selected to increase the ion signals in the following experiments, although a slightly greater duration of analysis was required. Under the selected preconcentration conditions, a complete preconcentration cycle was accomplished in 4 min. A typical elution curve for a solution containing 1 ng ml^{-1} of Zn is shown in Fig. 4. Under the operating conditions of the preconcentration system, the peak half-width for the flow injection peak was about 12 s, which is equivalent to 0.6 ml; this means that with an injection volume of 10 ml a preconcentration factor of about 17 could be obtained for Zn.

Detection Limit and Reproducibility

The calibration plot based on peak area for ^{66}Zn was linear with a correlation coefficient better than 0.9995 at levels near the detection limit up to at least 50 ng ml^{-1}. The detection limit calculated from the calibration plot was 0.014 ng ml^{-1}. It was based on the conventional definition of the concentration of the analyte yielding a signal equivalent to three times the standard deviation of the blank. The detection limit obtained by this method is comparable or superior to previous results obtained with ICP-MS detection.[35–38] The reagent blank was 0.13 ng ml^{-1} for Zn. A possible explanation is that the system is contaminated with Zn. Zinc is a common contaminant in the

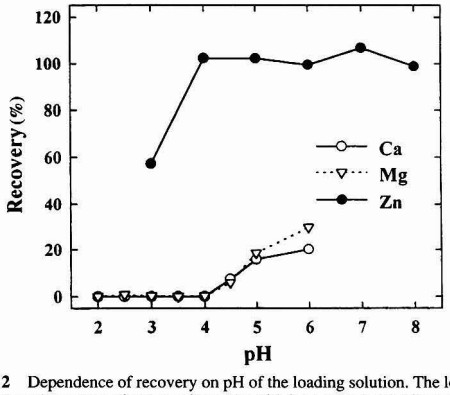

Fig. 2 Dependence of recovery on pH of the loading solution. The loaded sample volume was 10 ml at a flow rate of 2.3 ml min^{-1}. The flow rate of the eluent (1.0 mol l^{-1} HNO_3) was 2.0 ml min^{-1}.

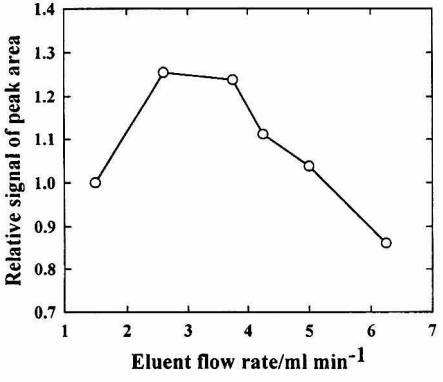

Fig. 3 Dependence of ion signal on eluent flow rate. The eluent was 0.5 mol l^{-1} HNO_3 solution. The loaded sample volume was 10 ml at a flow rate of 10 ml min^{-1}. All data are relative to the first point.

reagent and solutions; a better detection limit is to be expected with much more purified reagents.

The repeatability was determined by seven injections of a 1 ng ml^{-1} Zn solution. The repeatability of the peak areas of these seven injections was 1.4%.

Non-spectroscopic and Spectroscopic Interferences

As described earlier, the retentions of matrix elements on the ion-exchange material are usually different from that of zinc, hence zinc can be separated from the matrix and collected on the cellulose. The effectiveness of matrix elimination with this separation system is demonstrated by the following experiments. Solutions containing zinc and matrix elements were analyzed by matrix separation–ICP-MS and the results were compared with those obtained using a simple FI–ICP-MS system. Table 3 shows the results of adding various concentrations of S, Cl, Mg and Ca ions to a test solution containing 5 ng ml^{-1} Zn. As shown, the $^{66}Zn/^{67}Zn$ ratio was increased when 500 μg ml^{-1} S was added, which indicated an interference at *m/z* 66 from $^{34}S^{16}O^{16}O^{+}$ and/or $^{32}S^{34}S^{+}$.[39] Moreover, the $^{66}Zn/^{67}Zn$ ratio increased significantly when 1000 μg ml^{-1} of Mg was added, which indicated an interference at *m/z* 66 from $^{40}Ar^{26}Mg^{+}$, although the $^{66}Zn/^{67}Zn$ ratio did not change significantly when 250 mg ml^{-1} of Ca and 15000 mg ml^{-1} of Cl were added. The precision of the isotope ratio determination was poor when simple FI sample introduction was used. This could be due to the suppression of the ion signal by the high concentration matrix elements. Finally, a solution containing 500 μg ml^{-1} S, 250 μg ml^{-1} Ca, 1000 μg ml^{-1} Mg and 15000 μg ml^{-1} Cl was spiked to 5 ng ml^{-1} Zn standard solution. The concentrations of the matrix ions were about half of the concentrations of these ions in the sea-water matrix. As shown in Table 3, the $^{66}Zn/^{67}Zn$ ratio increased to 16.34 when this matrix solution was added.

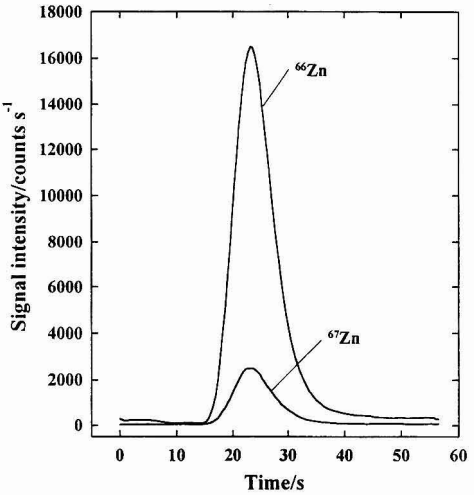

Fig. 4 Typical elution curve for 1 ng ml^{-1} Zn solution. The loaded sample volume was 10 ml at a flow rate of 10 ml min^{-1}. The eluent (0.5 mol l^{-1} HNO_3) flow rate was 3.0 ml min^{-1}. Time zero represents the start of elution.

Table 3 Isotope ratios of Zn in various matrices with different methods of analysis*

	$^{66}Zn/^{67}Zn$†	
Sample composition	FI‡	Matrix separation§
Zn standard	6.41 ± 0.07	6.47 ± 0.05
Zn standard + S 500 μg ml^{-1}	7.59 ± 0.53	6.35 ± 0.11
Zn standard + Ca 250 μg ml^{-1}	6.60 ± 1.07	6.45 ± 0.08
Zn standard + Mg 1000 μg ml^{-1}	11.81 ± 0.71	6.59 ± 0.09
Zn standard + Cl 15000 μg ml^{-1}	6.64 ± 1.56	6.53 ± 0.08
Zn standard + S 500 μg ml^{-1} + Ca 250 μg ml^{-1} + Mg 1000 μg ml^{-1} + Cl 15000 μg ml^{-1}	16.34 ± 8.55	6.49 ± 0.06

* The expected value of $^{66}Zn/^{67}Zn$ is 6.77. † Mean of three measurements ± standard deviation. ‡ FI carrier (0.5 mol l^{-1} HNO_3) flow rate = 3.0 ml min^{-1}; 100 μl sample loop. Concentration of Zn standard solution used in FI, 5 ng ml^{-1}. § The operating conditions for the matrix–analyte separation and preconcentration system are given in Table 2. Concentration of Zn standard solution used in matrix separation, 1 ng ml^{-1}.

Table 3 also shows that a stable $^{66}Zn/^{67}Zn$ ratio could be obtained when S, Cl, Mg and Ca were separated from the analyte with the matrix separation system. Hence, for the analysis of highly saline samples, the interfering ions must be separated before Zn is determined. In general, in order to achieve accurate, reliable and sensitive results, preconcentration and separation are needed when the concentrations of analyte elements in the original material or the prepared solution are too small to be determined directly by MS or when matrix elements interfere with the determination.

The precision (RSD 0.7–1.7%), shown in Table 3, was slightly worse than that obtained for isotope ratio measurements during continuous introduction of aqueous solutions. Moreover, the precision for the measured isotope ratio was slightly worse than that calculated by the counting statistics (RSD 0.5–0.6%).[40] A poorer precision in isotope ratio measurements is to be expected when transient sample introduction techniques are used because the ions of interest are observed for a shorter time and averaging of nebulizer fluctuations, *etc.*, is less efficient. The slight but reproducible differences between the found and expected values are similar to those commonly seen in isotope ratio measurements with ICP-MS and were probably caused by some mass discrimination in ion extraction, focusing, mass analysis and detection.[38]

Determination of Zinc in Water Samples

In order to demonstrate that the system is effective for practical analysis, four water reference samples (NRCC SLRS-2, SLEW-2, NASS-3 and CASS-3) were analyzed. The amount of Zn in each sample was determined by ID–ICP-MS after on-line sample pretreatment using the matrix separation and preconcentration method. In order to decrease the retention of alkaline earth ions when analyzing sea-water samples, a low pH buffer solution (pH 4) and careful washing of the column with buffer solution were used. The results of the analysis of standard reference materials are given in Table 4. Good agreement

Table 4 Concentrations of Zn in reference materials as measured by ID–on-line preconcentration–ICP-MS (n = 3)

	Concentration*/ng ml^{-1}	
Sample	Found	Certified
SLRS-2 riverine water	3.35 ± 0.06	3.33 ± 0.15
SLEW-2 estuarine water	1.12 ± 0.05	1.10 ± 0.14
CASS-3 nearshore sea-water	1.30 ± 0.17	1.24 ± 0.25
NASS-3 open ocean sea-water	0.208 ± 0.035	0.178 ± 0.025

* Mean ± 95% confidence limit.

between the experimental results and certified values show the applicability of this system to real sample analysis.

Conclusion

The use of ICP-MS and an SO_3–quinolin-8-ol carboxymethylcellulose miniature column flow system provide a simple, rapid and accurate technique to determine routinely trace amounts of Zn in water samples. This preconcentration method yielded an enrichment factor of 17 and sample consumption was thus reduced.

This research was supported by a grant from the National Science Council of the Republic of China under contract NSC 85-2621-M- 110-009.

References

1 Houk, R. S., Fassel, V. A., Flesch, G. D., Svec, H. J., Gray, A. L., and Taylor, C. E., *Anal. Chem.*, 1980, **52**, 2283.
2 Jarvis, K. E., Gray, A. L., and Houk, R. S., *Handbook of Inductively Coupled Plasma Mass Spectrometry*, Blackie, Glasgow, 1992.
3 Houk, R. S., *Anal. Chem.*, 1986, **58**, 97A.
4 Boomer, D. W., and Powell, M. J., *Anal. Chem.*, 1987, **59**, 2810.
5 Olivares, J. A., and Houk, R. S., *Anal. Chem.*, 1986, **58**, 20.
6 Vaughan, M. A., and Horlick, G., *Appl. Spectrosc.*, 1986, **40**, 434.
7 Tan, S. H., and Horlock, G., *Appl. Spectrosc.*, 1986, **40**, 445.
8 McLaren, J. W., Beauchemin, D., and Berman, S. S., *Anal. Chem.*, 1987, **59**, 610.
9 Vaughan, M. A., and Horlick, G., *Appl. Spectrosc.*, 1987, **41**, 523.
10 Thompson, J. J., and Houk, R. S., *Appl. Spectrosc.*, 1987, **41**, 801.
11 Gregoire, D. C., *Appl. Spectrosc.*, 1987, **41**, 897.
12 Gray, A. L., and Williams, J. G., *J. Anal. At. Spectrom.*, 1987, **2**, 599.
13 Tan, S. H., and Horlick, G., *J. Anal. At. Spectrom.*, 1987, **2**, 745.
14 Dean, J. D., Ebdon, L., and Massey, R., *J. Anal. At. Spectrom.*, 1987, **2**, 369.
15 Beauchemin, D., McLaren, J. W., Mykytiuk, A. P., and Berman, S. S., *Anal. Chem.*, 1987, **59**, 778.
16 Beauchemin, D., McLaren, J. W., and Berman, S. S., *Spectrochim. Acta, Part B*, 1987, **42**, 467.
17 Beauchemin, D., McLaren, J. W., Mykytiuk, A. P., and Berman, S. S., *J. Anal. At. Spectrom.*, 1988, **3**, 305.
18 Date, A. R., Cheung, Y. Y., and Stuart, M. E., *Spectrochim. Acta, Part B*, 1987, **42**, 3.
19 Lichte, F. A., Meier, A. L., and Crock, J. G., *Anal. Chem.*, 1987, **59**, 1150.
20 Heithmar, E. M., Hinners, T. A., Rowan, J. T., and Riviello, J. M., *Anal. Chem.*, 1990, **62**, 857.
21 Porta, V., Sarzanini, C., and Abolino, O., *Anal. Chim. Acta*, 1992, **258**, 237.
22 Vaughan, M. A., and Templeton, D. M., *Appl. Spectrosc.*, 1990, **44**, 1685.
23 Beauchemin, D., and Berman, S. S., *Anal. Chem.*, 1989, **61**, 1857.
24 Yang, H.-J., Huang, K.-S., Jiang, S.-J., Wu, C.-C., and Chou, C.-H., *Anal. Chim. Acta*, 1993, **282**, 437.
25 Orians, K. J., and Boyle, E. A., *Anal. Chim. Acta*, 1993, **282**, 63.
26 Bloxham, M. J., Hill, S. J., and Worsfold, P. J., *J. Anal. At. Spectrom.*, 1994, **9**, 935.
27 Hwang, T.-J., and Jiang, S.-J., *J. Anal. At. Spectrom.*, 1996, **11**, 353.
28 Yang, K.-L., Jiang, S.-J., and Hwang, T.-J., *J. Anal. At. Spectrom.*, 1996, **11**, 139.
29 Lu, P.-L., Huang, K.-S., and Jiang, S.-J., *Anal. Chim. Acta*, 1993, **284**, 181.
30 Huang, K.-S., and Jiang, S.-J., *Fresenius' J. Anal. Chem.*, 1993, **347**, 238.
31 Schramel, P., Xu, L. Q., Knapp, G., and Michaelis, M., *Mikrochim. Acta*, 1992, **106**, 191.
32 Gregoire, D. C., and Lee, J., *J. Anal. At. Spectrom.*, 1994, **9**, 393.
33 Bowins, R. J., and McNutt, R. H., *J. Anal. At. Spectrom.*, 1994, **9**, 1233.
34 Liaw, M.-J., and Jiang, S.-J., *J. Anal. At. Spectrom.*, 1996, **11**, 555.
35 Ebdon, L., Ford, M. J., Hutton, R. C., and Hill, S. J., *Appl. Spectrosc.*, 1994, **48**, 507.
36 Haraldsson, C., Lyven, B., Pollak, M., and Skoog, A., *Anal. Chim. Acta*, 1993, **284**, 327.
37 Ebdon, L., Fisher, A. S., Worsfold, P. J., Crews, H., and Baxter, M., *J. Anal. At. Spectrom.*, 1993, **8**, 691.
38 Jiang, S.-J., Palmieri, M. D., Fritz, J. S., and Houk, R. S., *Anal. Chim. Acta*, 1987, **200**, 559.
39 Reed, N. M., Cairns, R. O., Hutton, R. C., and Takaku, Y., *J. Anal. At. Spectrom.*, 1994, **9**, 881.
40 Warren, A. R., Allen, L. A., Pang, H.-M., Houk, R. S., and Janghorbani, M., *Appl. Spectrosc.*, 1994, **48**, 1360.

Paper 6/06577E
Received September 24, 1996
Accepted December 3, 1996

Determination of Gold in Geological Samples and Anode Slimes by Atomic Absorption Spectrometry After Preconcentration Wth Amberlite XAD-16 Resin

A. Tunçeli and A. R. Türker
Gazi Üniversitesi, Fen-Edebiyat Fakültesi, Teknikokullar, TR-06500 Ankara, Turkey

A method was developed for the determination of trace levels of gold in geological materials and anode slimes involving the adsorption of gold on Amberlite XAD-16 resin followed by FAAS determination after elution. The adsorption behaviour of the chloro complex of gold from hydrochloric acid solution was also investigated and the recovery of gold was found to be 95.48 ± 0.04% at the 95% confidence level. The degree of preconcentration ranges from 10- to 75-fold for different sample volumes. The detection limit of gold was 0.046 mg l^{-1}. The adsorption isotherm and adsorption capacity of XAD-16 resin were investigated for gold. The adsorption isotherm was found to be of the Langmuir type and the adsorption capacity of the resin was 0.55 mmol g^{-1} (108 mg g^{-1}). The influence of geological matrix elements on the adsorption of gold was also evaluated. The gold contents of anode slime and a reference standard ore were determined by applying the proposed method.

Keywords: *Resin preconcentration; separation; gold; geological samples; anodic slime; flame atomic absorption spectrometry*

Because of the low abundance of gold and high salt concentrations in geological samples and anode slimes, the direct determination of gold by FAAS in solutions obtained by wet decomposition of samples is often difficult or even impossible. For this reason, separation of gold from the sample matrix and increases in analyte concentrations are useful steps in the analysis. In trace element analysis, preconcentration and separation methods also enhance the sensitivity and precision of the determination.[1] For sub-μg g^{-1} levels in geological samples, ETAAS, ICP-AES and neutron activation analysis have been the dominant and preferred methods either with or without separation and preconcentration steps.[2–6] However, FAAS has been widely used after a preconcentration step for trace analysis because it is a relatively simple method and requires less expensive instrumentation.[7,8]

The analysis of geological samples and anode slimes for gold is very difficult owing to the high concentrations of widely varying matrix elements such as Fe and Cu. Therefore, before the determination, the gold must be separated from the sample matrix and enriched. For this purpose, several separation and preconcentration techniques for gold, such as solvent extraction,[9–12] coprecipitation[4] and ion-exchange or adsorption,[13–15] have been developed.

Among these techniques, sorption is one of the most widely used. For this purpose, XAD resins[16–18] and various polymers[19,20] have been used. Because of the purity and good adsorption properties, the commercially available Amberlite XAD copolymers (XAD-2, -4, -7 and -8) have been widely used as adsorbents.[16–18] However, Amberlite XAD-16 has not been widely used for the preconcentration of trace elements.[21]

This paper describes the determination of gold in geological samples and anode slimes after preconcentration on a column packed with Amberlite XAD-16 resin, which has the largest surface area in the XAD series. The optimum conditions for adsorption and determination procedures are also discussed. The influence of interfering elements such as iron on the determination of gold was evaluated.

Experimental

Apparatus

A Philips (Eindhoven, The Netherlands) PU 9285 flame atomic absorption spectrometer equipped with an air–acetylene burner and gold hollow cathode lamp operated at 11.2 mA was used for the determination of gold. The operating conditions were wavelength 242.8 nm, bandpass 0.5 nm and fuel flow rate 0.9 l min^{-1}. Deuterium lamp background correction was used. All pH measurements were made with a Consort (Turnhout, Belgium) digital pH meter and a combined glass electrode.

Column Preparation

The column diameter and amount of resin were chosen taking into account the information obtained from our previous studies.[21] For subsequent experiments, a glass column (30 mm × 10 mm id) with a glass-wool plug over its stopcock was used. A 0.2 g amount of resin was rested on the glass-wool and compressed in order to avoid channel formation. Another plug of glass-wool was placed on top, so that the resin was not disturbed during sample passage. Before use, 1 mol l^{-1} hydrochloric acid was passed through the column for cleaning and preconditioning.

Reagents and Standard Solutions

Amberlite XAD-16 resin (Rohm and Haas, Philadelphia, PA, USA; surface area 800 m^2 g^{-1}; wet mesh size 20–60) was used after washing with methanol, 1 mol l^{-1} hydrochloric acid and triply distilled water and dried at 60 °C.

Analytical-reagent grade chemicals were used without further purification. Triply distilled water was used in all experiments. A stock standard solution of gold (1000 mg l^{-1}) was prepared by dissolving the appropriate amount of tetrachloroauric(III)acid trihydrate ($HAuCl_4 \cdot 3H_2O$) in water. Working standard solutions were prepared by dilution.

General Procedure for Optimization of the Preconcentration Step

Volumes of 100 ml of spiked solutions containing 25 μg of gold (0.25 mg l^{-1}) were used. The pH of the solution was adjusted to the desired value with hydrochloric acid and potassium hydroxide solutions. The resulting solution was passed through the column at an optimum flow rate of 5 ml min^{-1}. After the sample solution had been passed through the column, the retained metal ions were eluted from the resin by using 5 ml of 0.3 mol l^{-1} potassium iodide solution in methanol and 5 ml of pure methanol.

The eluate in a 10 ml calibrated flask was aspirated into an air–acetylene flame and the gold was determined by FAAS. The resin was used repeatedly after washing with 1 mol l^{-1} hydrochloric acid and water.

Using the procedure described above, the recovery of gold was calculated from the ratio of the concentration found by FAAS to that calculated theoretically.

Sample Preparation

Samples were dissolved by a commonly used method.[9,13,15] An anode slime sample and a geological standard reference material (Gold Ore MA-3 certified by the Canada Center For Mineral and Energy Technology) were dried at 110 °C for 2 h, then approximately 1 g of gold ore and 0.1 g of anode slime were weighed accurately into a beaker separately. In order to decompose the sample, about 20 ml of aqua regia were added to the beaker and the solution was evaporated to dryness. This decomposition procedure was repeated and 10 ml of water were added. The suspension formed was filtered through a fine filter-paper. The insoluble part retained on the filter-paper was washed with 1 mol l^{-1} hydrochloric acid and water. The filtrate and washings were collected in a 100 ml calibrated flask. Potassium hydroxide was used to adjust the pH of the solution to 2. Gold was preconcentrated from this solution with the column procedure described above and determined by FAAS.

Results and Discussion

Effect of Hydronium Ion Concentration

The retention of gold on the resin was studied as a function of pH and/or the concentration of hydrochloric acid. The results are shown in Fig.1. As can be seen, a quantitative recovery (≥95%) of gold was obtained at pH 2, and this pH was chosen as the optimum for subsequent experiments.

Effect of Elution Solutions

Elution studies were performed with halide solutions (potassium iodide and potassium bromide) in water and methanol and acidic solutions (hydriodic and hydrochloric acid) at various concentrations. The results are shown in Table 1. The best elution (>95% recovery) was obtained by using 5 ml of 0.3 mol l^{-1} potassium iodide solution in methanol. Gold was quantitatively eluted with this eluent. The use of potassium iodide in methanol as the eluent was very convenient because the stability constant for the iodide complex of gold was high. In addition, methanol improved the nebulization efficiency by decreasing the viscosity of the sample solution. A 5 ml volume of 0.3 mol l^{-1} KI solution and 5 ml of pure methanol were used as eluents in all subsequent experiments.

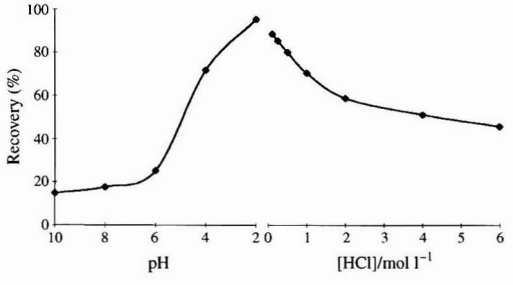

Fig. 1 Effect of hydronium ion concentration on the recovery of gold.

Effect of Sample Volume and Analyte Concentration

In order to deal with real samples containing very low concentrations of gold, the maximum applicable sample volume must be determined. Therefore, the effect of changes in the volume of sample solution passed through the column on the sorption of Au was investigated. Volumes of 100, 250, 500, 750 and 1000 ml of sample solutions containing 0.25, 0.10, 0.05, 0.033 and 0.025 mg l^{-1} of Au were passed through the column. The recovery of gold was approximately quantitative (about 95%) up to a sample volume of 750 ml. At higher sample volumes, the gold recovery decreased gradually with increasing volume of sample. In this work, the elution volume was 10 ml and the highest concentration factor was 75 for a 750 ml sample volume. These results also indicate the effect of analyte concentration on the retention of Au. Normally FAAS is unable to determine gold at levels below 0.1 mg l^{-1},[22] but the proposed technique allowed gold to be determined in the range 0.033–0.25 mg l^{-1}.

Effect of Sample and Eluent Flow Rate on Sorption

Since the retention of elements on an adsorbent depends on the flow rate of the metal solution, the effect of the flow rate was examined under the optimum conditions (pH, eluent type, *etc.*). The flow rate varied from 1 to 5 ml min^{-1}. It was found that the retention of gold was not affected by flow rate up to 5 ml min^{-1}. Since either suction or pressure is needed for flow rates higher than 5 ml min^{-1}, no test was carried out for such flow rates. The effect of eluent flow rate on the recovery was also examined. Three flow rates (1, 2.5 and 5 ml min^{-1}) were studied and recoveries of 95, 88 and 60%, respectively, at 5 ml min^{-1} were obtained. Since the recovery increases with decreasing flow rate of the eluent, 1 ml min^{-1} was adopted in all experiments.

Precision of Method

The precision of the method was investigated at the optimum pH of 2 for the spiked solution (0.25 mg l^{-1} Au) described above. For this purpose, the general procedure was performed successively and gold was determined in the solution by FAAS. The mean recovery for eight determinations at the 95% confidence level was 95.48 ± 0.04%. As can be seen, the recovery is quantitative and it is sufficient for preconcentration purposes. The precision of the method is very good, the RSD being about 2.1%.

Adsorption Isotherm and Adsorption Mechanisms

For the determination of the adsorption behaviour of the resin, the amount of adsorbed gold was studied as a function of gold

Table 1 Effect of elution solutions on the recovery of gold

Solution	Recovery (%)
5 ml of 0.1 mol l^{-1} KI in methanol and 5 ml of pure methanol	91.5
5 ml of 0.1 mol l^{-1} KBr in methanol and 5 ml of pure methanol	9.0
5 ml of 0.3 mol l^{-1} KI in methanol and 5 ml of pure methanol	95.0
5 ml of 1 mol l^{-1} KI in methanol and 5 ml of pure methanol	95.0
5 ml of 1 mol l^{-1} HCl	0.5
5 ml of 0.1 mol l^{-1} HI in water	1.0
5 ml of 0.1 mol l^{-1} HI in methanol and 5 ml of pure methanol	69.3
5 ml of 0.3 mol l^{-1} KI in methanol	59.6
5 ml of pure methanol	2.6

concentration (Fig. 2). The adsorption isotherm of gold conforms to the Langmuir equation.[23] Graphical treatment of the data yielded Langmuir parameters of capacity of the resin for gold 0.55 mmol g^{-1} (108 mg g^{-1}) and equilibrium binding constant, K, about 6×10^3 l mol^{-1}. The Langmuir treatment demonstrated that the surface is nearly fully covered with a monomolecular layer of gold at high concentrations. Therefore, at high concentrations adsorption does not increase linearly.

In addition to the adsorption isotherm of the resin, another important parameter, the adsorption mechanism was studied. Amberlite XAD-16 is a styrene–divinylbenzene copolymer. The metal is probably adsorbed as a chloro complex such as $HAuCl_4$. The adsorption might result in the formation of a complex compound such as that shown below:[24]

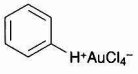

Effect of Matrix Elements

The determination of gold in naturally occurring ores is difficult owing to the high concentrations of other (accompanying) elements such as Na, Fe, Ni and Cu. For this reason, a fixed amount of gold was taken with various combined amounts of matrix elements such as Fe, Cu, Ni, Na, K, Mg, Ca and the recommended procedure was applied. The results are summarized in Table 2.

The recovery of gold decreased by in the presence of a large excess of matrix elements, because of the insufficient resin capacity. Especially iron, generally present in the ore matrix, decreased the gold adsorption.[25] Gjerde and Fritz[25] found that a 1000-fold excess of iron over gold decreased the gold recovery from 98% to 80%. For this reason, the effect of iron on the adsorbance and recovery of gold was specially investigated. The results are given in Table 3. As can be seen, by using the proposed method an approximately 5000-fold excess of iron over gold did not interfere; the recovery of gold was almost constant.

In order to explain which element(s) cause the large decreases in recovery shown in Table 2, the effect of each individual matrix element on the recovery of gold was investigated. For this purpose, only the effect of 250 mg l^{-1} of each matrix element on 0.25 mg l^{-1} of gold was studied. The results are given in Table 4. The recovery of gold did not decrease when the matrix elements were studied individually, but when they were used all together the recovery of gold decreased by about 22.5% (Table 2). The reason for this result might be attributed to the insufficient column capacity. The retention of Cu and Ni on XAD-16 resin at pH 2 is less,[21] but the retention of Fe is high (about 40%). Hence, it can be said that the capacity of resin has been fully utilized when the matrix elements were used all together at a high concentration (250 mg l^{-1}).

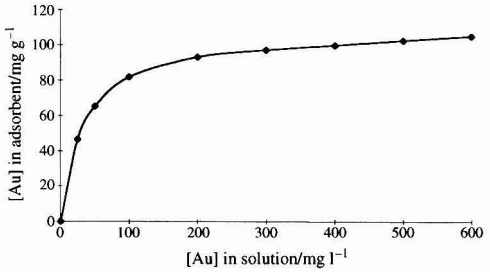

Fig. 2 Adsorption isotherm of XAD-16 for gold.

Application

The proposed method was applied to the determination of gold in an anode slime and a geological sample. As the geological

Table 2 Effect of combined matrix elements on the recovery of gold

Foreign metal (Fe, Cu, Ni, Na, K, Ca, Mg) concentration/ mg l^{-1}	Au		
	Added/ mg l^{-1}	Found/ mg l^{-1}	Recovery (%)
0	0.25	0.24	95.0
25	0.25	0.22	86.4
125	0.25	0.12	46.2
250	0.25	0.06	22.5

Table 3 Effect of iron concentration on the recovery of gold

Fe/ mg l^{-1}	Au/ mg l^{-1}	Recovery (%)
100	0.25	94.0
500	0.25	93.5
1000	0.25	94.6
1250	0.25	93.8

Table 4 Effect of individual matrix elements at a concentration of 250 mg l^{-1} on the recovery of gold

Element	Recovery of gold (%)
None	95.0
Cu	92.0
Ni	94.0
Na	99.5
K	97.6
Mg	96.0
Ca	104.0

Table 5 Determination of gold in real samples

Sample*	Au concentration		Recovery (%)	LOD‡ (mg l^{-1})
	Certified	Found†		
Gold Ore MA-3	7.49 ± 0.19 μg g^{-1}	7.23 ± 0.12 μg g^{-1}	96	0.046
Anode slime	0.076% m/m§	0.071 ± 0.003% m/m	93	0.046

* The composition of Gold Ore MA-3 (only gold was certified) was Si 25, Al 7.22, Fe 3.85, Ca 3.31, K 3.05, Na 2.42, C 0.76 and S 0.56% m/m, Ag 1.5 mg g^{-1} and Au 7.49 μg g^{-1}. The composition of the anode slime was Cu 18.86, Pb 7.67, Sn 1.36, Ag 2.29, Au 0.076, Fe 0.10 and SiO_2 1.69% m/m. † Average of five determinations at the 95% confidence level. ‡ Limit of detection based on 99.7% (3σ) confidence level (n = 10). § Determined spectrophotometrically by Makina ve Kimya Endüstrisi Kurumu.

sample a Certified Gold Reference Ore and as an anode slime the product from the brass plant of Makina ve Kimya Endüstrisi Kurumu were analysed. The results are shown in Table 5. The limit of detection was calculated on the basis of three times the standard deviation of the absorbance using a series of measurements of blank solutions prepared according to the procedure given under Sample Preparation without taking the sample. As can be seen, the preconcentration, separation and determination of trace amounts of gold by the proposed method in a geological material and anode slime in the presence of high concentrations of foreign cations and anions including iron (in MA-3 about a 5000-fold excess) could be performed successfully. The relative error was 3.5%, for gold ore and 6.6% for anode slime.

Conclusion

The proposed column preconcentration method provides a simple, sensitive and accurate method for the preconcentration of gold in geological materials and anode slimes and is also successful in the presence of iron. Gold can be retained on the column by adjusting the sample solution to pH 2 and then be eluted from the column using potassium iodide. Most of the metals including iron do not influence the gold determination. The precision and recovery were satisfactory. Further work is in progress to evaluate the use of XAD-16.

References

1 Mizuike, A., *Enrichment Techniques for Trace Analysis*, Springer, Berlin, 1983.
2 McHugh, J. B., *At. Spectrosc.*, 1983, **4**(2), 66.
3 Kontas, E., *At. Spectrosc.*, 1981, **2**(2), 59.
4 Chung, Y. S., and Barnes, R. M., *J. Anal. At. Spectrom.*, 1988, **3**, 1079.
5 Elson, C. M., and Chatt, A., *Anal. Chim. Acta*, 1983, **155**, 305.
6 *Inductively Coupled Plasma Emission Spectroscopy*, ed. Boumans, P. W. J. M., Wiley, New York, 1987, pt. 2, ch. 3, pp. 27–47.
7 Xu, S., Sun, L., and Fang, Z., *Anal. Chim. Acta*, 1991, **245**, 7.
8 Elçi, L., *Anal. Lett.*, 1993, **26**, 1025.
9 Brooks, R. R., Holzbecher, J., Ryan, D. E., and Zhang, H. F., *At. Spectrosc.*, 1981, **2**(5), **151.**
10 Tsukahara, I., *Talanta*, 1977, **24**, 633.
11 Marczenko, Z., and Kowalski, T., *Anal. Chim. Acta.*, 1984, **156**, 193.
12 McBryde, W. A. E., and Yoe, J. H., *Anal. Chem.*, 1948, **20**, 1094.
13 Elçi, L., Işıldar, S., and Doğan, M., *Anal. Chim. Acta*, 1994, **293**, 319.
14 Koshima, H., and Onishi, H., *Anal. Sci.*, 1988, **4**, 611.
15 Rivoldini, A., and Haile, T., *At. Spectrosc.*, 1989, **10**(3), 89.
16 Yang, X. G., and Jackwerth, E., *Fresenius' Z. Anal. Chem.*, 1989, **335**, 712.
17 Yang, X. G., and Jackwerth, E., *Fresenius' Z. Anal. Chem.*, 1989, **335**, 483.
18 Yang, X. G., and Jackwerth, E., *Fresenius' Z. Anal. Chem.*, 1990, **336**, 588.
19 Hoshi, S., Tanaka, Y., Inoue, S., and Matsubara, M., *Anal. Sci.*, 1989, **5**, 471.
20 Arık, N., and Türker, A. R., *Fresenius' J. Anal. Chem.*, 1991, **339**, 874.
21 Türker, A. R., and Tunçeli, A., *Fresenius' J. Anal. Chem.*, 1993, **345**, 755.
22 Taylor, M. J. C., Barnes, D. E., and Marshall, G. D., *Anal. Chim. Acta*, 1992, **265**, 71.
23 Adamson, A. W., *Physical Chemistry of Surfaces*, Wiley-Interscience, New York, 4th edn., 1982, p. 521.
24 Koshima, H., *Anal. Sci.*, 1986, **2**, 255.
25 Gjerde, D. T., and Fritz, J. S., *J. Chromatogr.*, 1980, **188**,. 391.

Paper 6/05008E
Received July 17, 1996
Accepted November 27,1996

Sorption of Arsenic, Bismuth, Mercury, Antimony, Selenium and Tin on Dithiocarbamate Loaded Polyurethane Foam as a Preconcentration Method for Their Determination in Water Samples by Simultaneous Inductively Coupled Plasma Atomic Emission Spectrometry and Electrothermal Atomic Absorption Spectrometry

Sonja Arpadjan, Lili Vuchkova and Elena Kostadinova
University of Sofia, Faculty of Chemistry, 1126 Sofia, Bulgaria

Column solid-phase extraction using dithiocarbamate loaded polyurethane foam was applied to the preconcentration of trace amounts of As, Bi, Hg, Sb, Se and Sn from water samples prior to their measurement by simultaneous ICP-AES and ETAAS. The sorption recoveries of all the analytes were higher than 97% for 150 ml water sample solutions passed through the column with pH ≈ 4.5 and sodium chloride concentration up to 3%. For As, Bi, Hg, Sb and Se, quantitative solid-phase extraction can be achieved over a wide pH range, from 0.5 to pH 5. The combination of the proposed preconcentration method with subsequent simultaneous analyte determination in the methanol eluates by ICP-AES permits the detection of 3 μg l^{-1} As and Se, 8 μg l^{-1} Bi, 0.12 μg l^{-1} Hg, 2 μg l^{-1} Sb and 6 μg l^{-1} Sn in water samples. ETAAS measurement after dissolution of the sorbed analytes in isobutyl methyl ketone allows the detection of 0.06 μg l^{-1} As and Sb, 0.1 μg l^{-1} Bi and Sn, 0.08 μg l^{-1} Se and 0.3 μg l^{-1} Hg.

Keywords: *Column solid-phase extraction; trace element preconcentration water samples; inductively coupled plasma atomic emission spectrometry; electrothermal atomic absorption spectrometry*

In routine laboratory measurements, As, Bi, Sb, Se and Sn are determined in their covalent hydride form and Hg in its atomic form in the vapour phase using atomic spectroscopic methods. However, for extremely low analyte concentrations a preliminary preconcentration is required. In comparison with the most commonly used solvent extraction enrichment procedure, column solid-phase extraction allows preconcentration from a larger sample volume, establishing higher concentration factors, simple storage and transportation of the pre-treated samples.[1–12] In a previous study a method was developed for the preconcentration of trace amounts of Cd, Co, Cu, Fe, Hg, Mn, Ni and Pb from analytical reagent-grade sodium salts and oxalic acid on polyurethane foam (PU) immobilized with ammonium hexamethylenedithiocarbamate (HMDC) or with a mixture of HMDC and methyltrioctylammonium chloride (MTOAC) prior to their measurement by AAS or ICP-AES.[13,14] Elution with 4 mol l^{-1} HNO_3 for subsequent ICP-AES determinations was found to be inappropriate for Hg determination. Quantitative elution of all the sorbed complexes can be achieved only by their total dissolution in organic solvents.[13–15]

The aim of this work was (i) to optimize the conditions for the quantitative column solid-phase extraction preconcentration of As^{III}, Bi^{III}, Hg^{II} Sb^{III}, Se^{IV} and Sn^{IV} on PU–HMDC from various water samples, (ii) to investigate the analytical potential of the subsequent simultaneous analyte determination in methanol eluates by ICP-AES and (iii) to investigate the analytical potential of the subsequent analyte determination in isobutyl methyl ketone (IBMK) eluates by ETAAS.

Experimental

Apparatus

ICP-AES measurements were performed with a simultaneous ICP spectrometer (Spectroflame ICP; SPECTRO, Kleve, Germany, holographic grating with 3600 lines mm^{-1}, plasma generator frequency 27.12 MHz). The plasma was run at 1750 W power with 21 l min^{-1} plasma, 0.99 l min^{-1} auxiliary and 0.66 l min^{-1} nebulizer argon flow rates. The spectra were measured at an observation height of 14 mm. The integration time was 10 s. A Meinhard-type nebulizer was used throughout. The wavelengths used, *viz.*, As 184.04, Bi 230.0, Hg 184.95, Se 196.09, Sb 206.8 and Sn 189.98 nm, offer the optimum signal-to-background ratio for the analytes.

ETAAS measurements were performed on a Perkin-Elmer (Norwalk, CT, USA) Zeeman 3030 atomic absorption spectrometer with an HGA-600 atomiser. The light sources used were electrodeless discharge lamps for As, Hg, Se, Sb and Sn and a hollow-cathode lamp for Bi. The spectral bandpass and the wavelength used were as recommended by Perkin-Elmer. Uncoated graphite tubes with pyrolytic graphite platforms were used as atomizers. The injection of the eluates (10 μl) into the tube and injection of the calibration standards (10 μl) and of the chemical modifier solution (10 μl) were carried out manually. The graphite furnace operating parameters are presented in Table 1. In all instances only peak areas (integrated absorbance) were used for quantification.

Reagents

All reagents were of analytical-reagent grade. Doubly distilled water was used throughout. Methanol and chloroform were used after additional purification by distillation. The organic solvent IBMK and the ligand HMDC (Fluka, Buchs, Switzerland) were used as received. The long-chain quaternary ammonium salt MTOAC was used as a 2% solution in IBMK.

Preparation of Standard Solutions for ICP-AES

A multi-element aqueous standard solution (100 μg ml^{-1} As, Sb, Se and Sn, 200 μg ml^{-1} Bi and 20 μg ml^{-1} Hg) was prepared from atomic absorption standard solutions (BDH,

Poole, Dorset, UK). Calibration standard solutions were prepared daily by appropriate dilution with 65% v/v aqueous methanol of HMDC (0.5% m/v HMDC).

Preparation of Standard Solutions for ETAAS

A multi-element aqueous standard solution containing 200 μg l^{-1} As^{III}, Sb^{III}, Se^{IV} and Sn^{IV}, 400 μg l^{-1} Se^{IV} and 800 μg l^{-1} Hg^{II} was prepared from atomic absorption standard solutions (BDH). The organic calibration standards were prepared daily in the following way: appropriate volumes from the multi-element aqueous standard solution were diluted to 10 ml with water in extraction tubes, then 2 ml of acetic acid buffer (pH 4.66) and 5.0 ml of a 1% solution of HMDC in IBMK were added. Extraction was performed for 1 min. Aliquots (10 μl) from the organic layer were used as calibration standards.

Preparation of Palladium Chemical Modifier Soluble in IBMK

A 1 ml volume of aqueous standard solution containing 30 μg l^{-1} Pd^{II} was diluted with 10 ml of 6 mol l^{-1} HCl in an extraction tube, then 3.0 ml of MTOAC solution in IBMK were added and extracted for 5 min. Using these conditions, Pd was extracted into IBMK as the ion association complex $PdCl_4(MTOA)_2$. A definite volume (10 μl) from this organic layer was injected into the platform of the graphite tube for ETAAS determination of As, Se and Sn.

Sorbent Preparation

Cubical foam pieces 5 mm long were cut from commercially available polyurethane foam (polyether type). The cleaned and dried foam pieces were soaked in a chloroform solution of HMDC (1.5 g of HMDC for 1 g of PU) and then squeezed occasionally until all the solution was retained in the PU cubes.

Table 1 Temperature programme for the determination of analytes in sorbent extraction eluates (10 μl IBMK solution) using a pyrolytic graphite platform and uncoated graphite tube

		Step			
Element	Parameter	I	II	III	IV
	Temperature/°C	120	Variable	Variable	Variable
	Ramp time/s	10	Variable	Variable	2
	Hold time/s	15	Variable	Variable	3
	Read	—	—	On	—
	Gas flow rate/ml min^{-1}	300	300	0	300
As*	Temperature/°C		1200	2200	2500
	Ramp/s		12	0	
	Hold/s		15	3	
Bi	Temperature/°C		700	1100	1500
	Ramp/s		10	0	
	Hold/s		20	5	
Hg	Temperature/°C		250	900	1600
	Ramp/s		5	1	
	Hold/s		10	14	
Sb	Temperature/°C		1100	1600	2200
	Ramp/s		12	0	
	Hold/s		15	5	
Se*	Temperature/°C		1100	2100	2400
	Ramp/s		12	0	
	Hold/s		15	3	
Sn*	Temperature/°C		1300	2300	2500
	Ramp/s		13	0	
	Hold/s		10	4	

* Addition of 10 μl of modifier solution [10 μg ml^{-1} Pd as $PdCl_4(MTOA)_2$ in IBMK].

Finally, the organic solvent was evaporated by drying the foam in air. The dithiocarbamate-loaded PU foam pieces were stored in a dark borosilicate glass container.

Column Preparation

The HMDC-loaded PU foam pieces (approximately 0.3 g) were transferred into a disposable syringe after packing a small wad of cotton-wool in the end of the column and covering it with a disc of filter-paper. The sample solution was passed through the sorbent column using a peristaltic pump as described previously.[13]

General Procedure for ICP-AES Measurements

Aqueous test solutions containing 2 μg of As, 5 μg of Bi, 2 μg of Sb, 3 μg of Se and 2 μg of Sn were pumped through the sorbent column at a flow rate of 2 ml min^{-1}. Dilute NH_3 solution (1 + 1) and HCl (1 + 1) were used for adjusting of the pH. The physically immobilized organic chelating ligand, HMDC, together with the analyte–dithiocarbamate complexes formed were completely dissolved in methanol. For this purpose, 3.0 ml of pure methanol were placed in a small, dry quartz beaker and was passed five consecutive times through the sorbent with the aid of the syringe plunger. The methanol solution was then diluted with 3.0 ml of doubly distilled water and nebulized into the argon plasma of the ICP-AES system. The emission intensity signals of the elements in this solution were measured against calibration standard solutions in order to evaluate the sorption efficiency. For each sample a new sorption column was applied.

General Procedure for ETAAS Measurements

Aqueous test solutions containing 50 ng of As, Bi, Sb and Sn, 100 ng of Se and 400 ng of Hg were pumped through the sorbent column at a flow rate of 2 ml min^{-1} after adjusting of the pH with dilute NH_3 and HCl. Elution was performed with 1.0 ml of IBMK as described for the ICP-AES technique. The atomic absorption signals of the elements in this IBMK solution were measured against organic calibration standard solutions. For each experiment a new column was prepared.

Results and Discussion

Influence of pH

The results for the influence of the pH of the water sample solution on the solid-phase extraction preconcentration with PU–HMDC sorbent are presented in Table 2. As^{III}, Bi^{III}, Hg^{II}, Sb^{III} and Se^{IV} form stable dithiocarbamate complexes with HMDC in the solid state in the pH range 1–5 and Sn^{IV} in the pH range 4–5. However, As^{V}, Sb^{V} and Se^{VI} do not form a complex

Table 2 Effect of pH on the recovery of trace elements in the analysis of water samples after solid-phase extraction preconcentration on polyurethane–HMDC (n = 3 parallel determinations)

	Recovery ± σ (%)					
pH	As^{III}	Bi^{III}	Hg^{II}	Sb^{III}	Se^{IV}	Sn^{IV}
1	97 ± 2	98 ± 1	99 ± 2	98 ± 2	98 ± 2	17 ± 3
2	94 ± 4	99 ± 2	99 ± 2	95 ± 3	94 ± 2	28 ± 6
3	95 ± 3	99 ± 2	99 ± 2	97 ± 2	96 ± 2	62 ± 5
4	99 ± 2	100 ± 2	100 ± 2	99 ± 2	99 ± 2	94 ± 3
5	95 ± 2	100 ± 2	100 ± 2	99 ± 2	97 ± 2	97 ± 3
6	62 ± 5	99 ± 2	100 ± 2	99 ± 2	70 ± 6	58 ± 4
7	< 5	99 ± 2	99 ± 2	99 ± 2	< 5	15 ± 5

with HMDC under any conditions. A reduction step must therefore precede the passage through the sorbent column. For As^{III}, Bi^{III}, Hg^{II}, Sb^{III} and Se^{IV}, sorption recoveries > 98% can also be achieved for water samples acidified with HCl (0.1–0.7 mol l^{-1} HCl in the solution). Hence when the determination of tin is not required, the water sample can simply be acidified with HCl before preconcentration instead of adjusting the pH to 4.5 ± 0.5 with dilute ammonia solution (1 + 1) or HCl (1 + 1).

Influence of Volume of Water Sample Solution

Water sample solution volumes up to 150 ml permit the achievement of quantitative solid-phase extraction preconcentration of all the analytes studied on PU–HMDC sorbent. Some decrease in the recovery for As, Sb, Se and Sn was observed when the sample volume was increased from 150 to 200 ml. The sorption for Bi and Hg is quantitative for a 200 ml sample volume. Hence the enrichment factor achieved for the proposed sorbent preconcentration ETAAS method is 150 (elution of the sorbed analyte–dithiocarbamate complexes with 1.0 ml of IBMK). The necessity to perform the ICP-AES measurements in at least 5.0 ml of methanol eluates leads to an enrichment factor of only 30.

Influence of Sodium Chloride Concentration

The influence of the concentration of NaCl on the efficiency of sorption on PU–HMDC was investigated in order to elucidate the possibilities of determining the studied analytes in sea-water samples using the proposed preconcentration procedure. The results obtained are presented in Table 3. The retention of Bi and Hg on the PU–HMDC sorbent is quantitative for all water sample volumes and sodium chloride concentrations studied. For the simultaneous quantitative preconcentration of all the analytes studied from a 150 ml water sample, the concentration of NaCl in the solution pumped through the PU–HMDC sorbent column must not exceed 3.5%.

Analysis of Water Samples

For the determination of trace amounts of As, Bi, Hg, Sb, Se and Sn in water samples, 3 g of KI were dissolved in 150.0 ml of sample solution and the pH was adjusted to 4.5 ± 0.5 with dilute ammonia solution (1 + 1) or HCl (1 + 1). When the determination of Sn is not required, the sample (150.0 ml) after addition of 3 g of KI is acidified with 1.5 ml of concentrated HCl. The sample is heated gently at 60 °C for 1 h to ensure the reduction of arsenic, antimony and selenium to their lower oxidation state. After cooling to room temperature, the sample is pumped through the sorption column at a flow rate of 2 ml min^{-1}, then the column is washed with 5 ml of doubly distilled water. In this state, prior to elution, the sorbent columns are suitable for conservation and transportation.

The elution and the measurements by ICP-AES and ETAAS were performed as described in the general procedure.

Absolute blanks of the proposed procedure are presented in Table 4. The largest part of the blank signal, especially for Bi and Sn, is due to the KI, and also to the ligand HMDC.

The limits of detection of each element, expressed as the blank value ± three times the standard deviation of the blank, are reported in Table 5. With the exception of Hg, the solid-phase extraction preconcentration ETAAS method ensures lower detection limits owing to the higher enrichment factor and the higher sensitivity of the graphite furnace measurement technique. The method using ICP does not offer any advantage over hydride generation ICP-AES. The 30-fold analyte preconcentration does not compensate for the poorer detection limit of the

Table 3 Effect of the water sample volume and NaCl concentration (synthetic mixtures) on the solid-phase extraction recovery (pH 4.3)

Volume*/ ml	NaCl (%)	Recovery ± σ (%)					
		As^{III}	Bi^{III}	Hg^{II}	Sb^{III}	Se^{IV}	Sn^{IV}
100 (n = 5)	3.5	99 ± 2	100 ± 2	100 ± 2	99 ± 2	99 ± 2	95 ± 6
100 (n = 5)	5	97 ± 2	98 ± 1	99 ± 2	98 ± 2	98 ± 2	93 ± 3
150 (n = 4)	3.5	99 ± 2	99 ± 2	99 ± 2	99 ± 2	99 ± 2	95 ± 4
150 (n = 4)	5	87 ± 6	98 ± 2	99 ± 2	90 ± 5	91 ± 5	90 ± 7

* n = Number of parallel determinations.

Table 4 Reagent blanks for preconcentration procedure. Doubly distilled water (150 ml) + 3 g of dissolved KI was pumped though 0.30 g of sorbent containing 0.15 g of HMDC; n = 5

Element	Blank ± σ/ng
As	4.5 ± 0.5
Bi	12.9 ± 0.6
Hg	6.8 ± 0.4
Sb	4.7 ± 0.4
Se	< detection limit
Sn	10.8 ± 1.2

Table 5 Detection limits (3σ) of polyurethane-HMDC preconcentration procedure for trace determination in waters by ICP-AES and ETAAS

Element	ICP-AES*/μg l^{-1}	ETAAS*/μg l^{-1}
As	3.2	0.06
Bi	8	0.1
Hg	0.12	0.3
Sb	2	0.06
Se	3	0.08
Sn	6	0.1

* Elution of the retained on the sorbent analytes (150 ml water sample pumped though the sorbent column) in 2.5 ml of methanol + 2.5 ml doubly distilled water for ICP-AES and in 1 ml IBMK for ETAAS measurements.

Table 6 Recovery of analytes added to sea-water (n = 4)

Element	Solid-phase extraction–ICP-AES			Solid-phase extraction		
	Added/ μg l^{-1}	Found ±σ/ μg l^{-1}	Recovery ±σ (%)	Added/ μg l^{-1}	Found ±σ/ μg l^{-1}	Recovery ±σ (%)
As	62.5	61.4 ± 2.8	98.2 ± 4.5	0.666	0.648 ± 0.042	97.3 ± 6.3
Bi	62.5	64.0 ± 3.5	102.4 ± 5.6	0.666	0.668 ± 0.026	100.3 ± 3.9
Hg	25.0	25.8 ± 1.6	103.2 ± 6.4	2.67	2.74 ± 0.07	102.6 ± 2.6
Sb	62.5	60.8 ± 3.2	97.3 ± 5.1	0.666	0.644 ± 0.028	96.7 ± 4.2
Se	125.0	122 ± 5	97.6 ± 4.0	1.33	1.26 ± 0.08	94 ± 6
Sn	125.0	127 ± 8	101.6 ± 6.4	0.666	0.687 ± 0.034	103.2 ± 5.1

direct simultaneous ICP-AES measurement technique additionally owing to the lower analytical potential of the ICP method in methanol solutions than in aqueous solutions. However, the combination of the described preconcentration procedure with hydride generation in methanol solutions of the analyte–dithiocarbamate complexes and subsequent simultaneous ICP-AES determination of As, Bi, Hg, Sb, Se and Sn leads to a substantial improvement in sensitivity.[16]

The accuracy of the procedure was investigated by determining the analyte content in spiked sea-water (Black Sea-water with analyte concentrations lower than the detection limit of the method). The results (Table 6) show sufficiently high recoveries and a precision (RSD) of 3–7%. The precision is very good despite working close to the detection limit. In addition, the accuracy and precision of the described methods were evaluated by comparing the results for waste waters with those obtained by direct ICP-AES measurements after hydride generation (Table 7). No significant differences in the results obtained were observed.

Conclusion

Solid-phase extraction on a PU–HMDC sorbent column is an effective preconcentration procedure for simple storage, transportation and measurement of trace levels of As, Bi, Hg, Sb, Se and Sn in various kinds of water samples using ICP-AES or ETAAS. The combination of the preconcentration procedure with the ETAAS measurement technique offers higher enrichment factors and higher sensitivity.

Table 7 Results ($\mu g\ l^{-1} \pm \sigma$) for the analysis of waste water ($n = 4$)

	PU–HMDC		HG-ICP in aqueous solution
Element	ETAAS	ICP-AES	
As	4.3 ± 0.2	4.5 ± 0.3	4.3 ± 0.2
Bi	6.7 ± 0.4	< 8	6.9 ± 0.4
Hg	< 0.4	0.28 ± 0.03	0.28 ± 0.02
Se	5.8 ± 0.4	5.6 ± 0.4	5.9 ± 0.3
Sb	8.2 ± 0.4	8.3 ± 0.5	8.1 ± 0.4
Sn	9.4 ± 0.5	9.2 ± 0.6	9.5 ± 0.5

The authors thank the Bulgarian Foundation of Sciences, Project X-519.

References

1 Braun, T., *Fresenius' Z. Anal. Chem.*, 1983, **314**, 652.
2 Burba, P., Rocha, J. C., and Schulte, A., *Fresenius' J. Anal. Chem.*, 1993, **346**, 414.
3 Jambor, J., and Javorek, T., *Collect. Czech. Chem. Commun.*, 1993, **58**, 1821.
4 Prakash, N., Csanady, G. J., Michaelis, M., and Knapp, G., *Mikrochim. Acta*, 1989, **3**, 257.
5 Maloney, M. P., Moody, G. J., and Thomas, J. D. R., *Analyst*, 1980, **105**, 1087.
6 Horvath, Z., Lasztity, A., Szakacs, O., and Bozsai, G., *Anal. Chim. Acta*, 1985, **173**, 273.
7 Terada, K., Matsumoto, K., and Nanao, Y., *Anal. Sci.*, 1985, **1**, 145.
8 Tong, A., and Akama, Y., *Anal. Chim. Acta*, 1990, **230**, 175.
9 Tong, A., Akama, Y., and Tanaka, S., *Analyst*, 1990, **115**, 947.
10 Yebra-Biurrun, M. C., Bermejo-Barrera, A., and Bermejo-Barrera, P., *Mikrochim. Acta*, 1992, **109**, 243.
11 Schilling, T., Schramel, P., Michalke, B., and Knapp, G., *Mikrochim. Acta*, 1994, **116**, 83.
12 Kantipuly, C., Katragadda, S., Chow, A., and Gesser, H., *Talanta*, 1990, **37**, 491.
13 Alexandrova, A., and Arpadjan, S., *Analyst*, 1993, **118**, 1309.
14 Alexandrova, A., and Arpadjan, S., *Anal. Chim. Acta*, 1995, **307**, 71.
15 Sperling, M., Yin, X., and Welz, B., *Analyst*, 1992, **117**, 629.
16 Vuchkova, L., and Arpadjan, S., *Talanta*, 1996, **43**, 479.

Paper 6/06917G
Received October 9, 1996
Accepted December 3, 1996

Direct Determination of Amiloride in Urine Using Isopotential Fluorimetry

José A. Murillo Pulgarín*, Aurelia Alañón Molina and Pablo Fernández López

Department of Analytical Chemistry and Foods Technology, University of Castilla La Mancha, 13071 Ciudad Real, Spain

A method for the determination of amiloride at concentrations between 15 and 152 ng ml^{-1} by means of matrix isopotential synchronous fluorescence spectrometry and derivative techniques is proposed. This method is useful for the determination of compounds in samples with unknown background fluorescence without the need for tedious pre-separation. As amiloride is widely used as a doping substance in sport, the method was successfully applied to the determination of amiloride in urine. To obtain maximum sensitivity and adequate selectivity, factors affecting fluorescence intensity were studied in the amiloride band centered at λ_{ex} = 362 nm and λ_{em} = 415 nm. As a result, the determination was performed in an ethanol–water (1 + 1, v/v) medium at pH 6.3, adjusted by using sodium citrate–citric acid (0.1 M) as buffer solution. The concentration of amiloride in urine samples can be calculated by recording its total luminescence spectrum and applying the isopotential trajectory of the urine that cuts the selected band of amiloride. The unknown analytical signal of urine is eliminated in the MISF spectrum obtained, by means of its first derivative. A calibration graph was constructed by measuring first derivative values at λ_{ex} = 357 nm and λ_{em} = 392 nm. Analytical parameters of the proposed method were calculated according to the error propagation theory. The sensitivity, repeatability, reproducibility and limit of determination achieved with the proposed method are adequate for the determination of amiloride in urine.

Keywords: *Amiloride; urine; spectrofluorimetry, diuretics*

Diuretics are defined as substances that produce an increase in the urinary elimination of sodium bound to an anion and water, leading to a reduction in extracellular liquids. Amiloride (*N*-amidino-3,5-diamino-6-chloropyrazine-2-carboxamide) is a weak diuretic, thrifty of potassium, since it inhibits the sodium–potassium interchange in kidneys by waterproofing the distal membrane to promote sodium excretion and potassium re-absorption.

This natriuretic agent is widely used in the treatment of several diseases. It can also be applied as a doping substance. In sports, diuretics are abused mainly for two reasons. The first is to obtain a rapid diminution of corporal weight, which is important in sports that are divided into different weight categories. The second is to reduce the concentration of medical drugs in urine by diluting the latter by means of the rapid production of an elevated volume of urine, leading to a smaller possibility of detecting other doping substances. An advantage in the use of amiloride is that low doses lead to high-volume urine excretion, obstructing its determination and therefore highly sensitive methods are required. Further, amiloride is potassium-sparing that is essential for energy production. It is known that potassium is lost by the muscles during ischaemia. This loss reduces the rate of glucolysis owing to the dependence of quinases on potassium to reach maximum activity. Nevertheless, no medical reason can justify a rapid decrease of weight in any sport. Additionally, this abuse causes grave dangers to health because of possible serious secondary effects.

Owing to the uncontrollable use of amiloride, the International Olympics Committee, since 1990 has included it in the list of forbidden substances.[1] Consequently, there is a need for the development of effective methods for determining this doping substance. Here we propose a fast, simple, and sensitive fluorimetric method for determining amiloride in urine samples, reaching the same sensitivity as direct determination but without the need for prior separation and concentration or derivatization procedures.

The therapeutic and doping dose of amiloride varies from 5 to 20 mg daily (one administration only). It is incompletely absorbed and it does not appear to be metabolized. The half-life in plasma varies from 6 to 10 h. About 50% of an oral dose is excreted in the unchanged form in urine and 40% is eliminated in the faeces within 72 h.[2] Consequently, the determination of amiloride in urine demands highly sensitive methods. Amiloride is a pale yellow to greenish yellow powder that exhibits violet fluorescence in solution.

There have been only a few reports on the determination of amiloride in tablets[3–6] or in biological fluids.[7,8] Normally the determination of amiloride at therapeutic levels by liquid chromatography requires various tedious preliminary procedures, such as extraction and preconcentration in an organic solvent. This causes many disadvantages (such as low recoveries), since all these procedures are based on equilibrium reactions.

We have previously reported a fluorimetric synchronous technique called matrix isopotential synchronous fluorescence spectrometry (MISF),[9] which is particularly useful for removing fluorescence matrix background effects and allows the determination of individual compounds in complex samples. It is essential that the matrix has an almost invariable composition. It is possible to maintain a constant background signal, even though its fluorescence intensity may vary, if a cut is made in the total fluorescence spectrum following one of the trajectories that joins points of equal intensity (isopotential trajectory) from an initial point to final excitation and emission wavelengths. This trajectory is obtained by means of a program developed in BASIC.[10] It is always possible to find the matrix trajectory that passes through the maximum fluorescence excitation and emission wavelengths of the component to be determined. Therefore, the same sensitivity is achieved as in direct determinations in the absence of background fluorescence. This technique can be improved by applying derivative methods.

Human urine is composed of numerous organic substances, most of which give a high absorbance in the ultraviolet region. A small number of these organic substances present fluorescence.[11] Owing to the high absorbance values in the ultraviolet region, the fluorescence intensity of the substance of interest (amiloride) does not vary linearly with concentration ($A < 0.05$). Consequently, it is recommended to measure fluorescence intensity at the maxima of the higher excitation wavelength and also to make an appropriate dilution of the urine. Additionally, as some of the urine components are

fluorescent, they provide high background fluorescence and, as a result, interfere with the direct determination of amiloride. Recent work in our laboratory has concerned the application of this fluorimetric technique to the determination of different drugs in biological fluids with excellent results.[9,12–17]

Experimental

Apparatus

All fluorimetric measurements were performed on an Aminco Bowman Series 2 instrument equipped with a continuous 150 W xenon lamp, connected to software which runs on the OS2 operating system. Quartz glass cuvettes with a pathlength of 1.0 × 1.0 cm were used.

Thermostatic equipment and a Crison Model 2001 pH meter with a glass–saturated calomel combination electrode and a Selecta Mixtaxel centrifuge were also used.

Software

A program was developed which enabled us to obtain the values of λ_{ex} and λ_{em} for any constant value of the fluorescence intensity from a three-dimensional spectrum. As the values obtained for a particular curve were not equidistant, the Lagrange interpolation method was applied to all points, which were placed in order, using emission wavelengths at 0.4 nm intervals. Once the trajectory had been defined, the spectrum was obtained by means of the Ftotal program.[10] The spectra obtained from it displayed the same format as those obtained directly with the Aminco Bowman Series 2 spectrofluorimeter.

The Ftotal program not only generates information on a fluorescent compound through the isometric representation of the three-dimensional spectrum as a level curve, but also processes the spectral data to obtain any type of spectrum of so-called new fluorimetric techniques.

The statistical analysis is totally covered by means of a program developed by us. This program has a menu that includes procedures such as least median of squares regression (detection of outlier and leverage points), least squares regression with replicates or not, weighted least squares regression, tests of regression and correlation, detection and determination limits, ellipse graph for the 95% confidence region for the true slope and intercept on the ordinate estimated from the regression method, dispersion and confidence bands for the calibration graph and ANOVA test for linearity and for comparison of several regression lines.[18–22]

Reagents

All experiments were performed with analytical reagent grade chemicals, pure solvent and Milli-Q-purified water. A stock standard solution of amiloride (Aldrich, Milwaukee, WI, USA) (250 mg dissolved in 1 l of water) was diluted to prepare suitable working standard solutions. The stock standard solution of amiloride was stored protected from light and maintained below 5 °C. Under these conditions, it was stable for 2 months. The working standard solutions of amiloride were stable for at least 2 h at room temperature.

A 1.0 M buffer solution of pH 6.3 was prepared by mixing appropriate amounts of citric acid with sodium hydroxide.

Urine samples were obtained from fasting, healthy people in the morning.

Procedure

Centrifuge urine for 15 min at 3800 rpm, transfer 10 ml of the clear supernatant solution into a 100 ml calibrated flask and dilute to volume with water. Store and maintain below 5 °C.

For the preparation of the calibration graph, place an aliquot of amiloride equivalent to 500–5000 ng in a 25 ml calibrated flask, add 2.5 ml of buffer solution (pH 6.3), 12.5 ml of ethanol and 5 ml of a solution of urine free from amiloride and dilute to volume with water.

Record 61 emission spectra of 192 nm width in steps of 0.4 nm, varying the excitation wavelength in 3.2 nm steps. Obtain the total luminescence spectra. Select a suitable trajectory which passes through the excitation and emission maxima of amiloride and obtain matrix isopotential synchronous spectra by means of Ftotal.[10] Calculate the first derivative according to the Savitzky and Golay algorithm.[23,24] Finally, determine the amiloride content by measuring the derivative signal at the emission wavelength of 392.0 nm and using the appropriate calibration graph.

Results and Discussion

Factors Affecting Fluorescence Intensity

Chemical variables were studied to obtain the best measurement conditions and maximum fluorescence sensitivity.

The influence of pH on the fluorescence intensity was studied by adding different amounts of HCl and NaOH to a urine solution and an amiloride solution. As can be seen in Fig. 1(*a*), the fluorescence intensity of amiloride is nearly constant at pH values between 2 and 7, whereas that due to urine decreases slowly from pH 4 to 8. A pH 6.3 was selected; this is approximately the pH value of urine of healthy people. The pH selected was adjusted by adding sodium citrate–citric acid buffer solution. The fluorescence intensity of amiloride and urine was not affected by the buffer and its concentration. A 0.1 M concentration of the buffer was therefore selected to obtain an adequate buffering capacity.

Amiloride is highly soluble in water, so it was not necessary to use an organic solvent. Nevertheless, it was desirable to study the variation of amiloride and urine fluorescence with changes in the dielectric constant of the medium. Owing to the physical and chemical properties of ethanol, it is suitable for such a study. Hence the effect of ethanol content in the medium was investigated by preparing samples of amiloride and urine with ethanol concentrations between 0 and 100% v/v for the amiloride solutions and between 0 and 80% v/v for the urine solutions (when the ethanol content is more than 80% some of the urine components are precipitated). The fluorescence intensity due to amiloride increases when the ethanol content in the medium increases whereas that due to urine increases slowly [Fig. 1(*b*)]. For these reasons, it is preferred to use a high ethanol

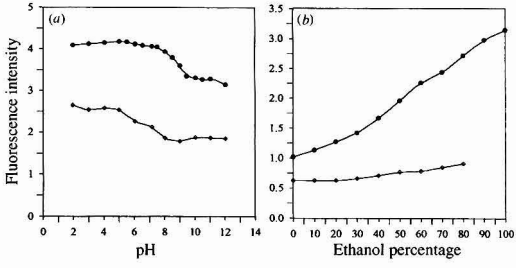

Fig. 1 (*a*) Influence of the pH on fluorescence intensity of urine (◇) and amiloride (●), measuring emission at 414.8 nm after excitation at 362 nm. Urine diluted 1 : 50; concentration of amiloride, 380 ng ml^{-1}; detector voltage, 500 V. (*b*) Influence of ethanol concentration on fluorescence intensity of urine and amiloride, measuring emission at 414.8 nm after excitation at 362 nm. Urine diluted 1 : 50; concentration of amiloride, 380 ng ml^{-1}; detector voltage, 450 V.

percentage but with the precaution that precipitation does not occur. Therefore, 50% of ethanol was selected.

Another factor that affects the fluorescence intensity is temperature. In both cases, fluorescence intensity decreased when the temperature was increased from 7 to 84 °C. Under the experimental conditions selected above, the temperature coefficients are about 0.99% $°C^{-1}$ for amiloride and about 0.59% $°C^{-1}$ for urine. This effect can be explained by a higher internal conversion as temperature increases, simplifying non-radiative deactivation of the excited singlet state.[25] Therefore, the use of a thermostat is recommended and a measurement temperature of 20 °C was chosen.

The influence of amiloride concentration on the fluorescence intensity was studied under the above conditions. The best range of pure amiloride concentration for the relationship between fluorescence intensity and concentration was found to be up to 152 ng ml^{-1}.

Determination of Amiloride in Urine

Previous experiments[9,11–17] have shown that the qualitative composition of the fluorescent metabolites of urine from healthy people of both sexes and different diets, aged between 25 and 35 years, which is the usual age of people taking doping substances, is almost constant, a necessary condition for the application of the proposed technique. Different samples of urine display the same type of fluorescence, with hardly any variation in the form of the spectrum and the location of the fluorescence maxima, although it is possible to observe some variations in their intensity.

All fluorimetric three-dimensional spectra were obtained by varying the emission wavelength from 310.0 to 502.0 nm and the excitation wavelength from 220.8 to 412.8 nm. Both excitation and emission bandpasses were 8 nm and the scan rate was 50 nm s^{-1}. Under these conditions, the time taken to determine contour spectra was 292 s.

Matrix isopotential synchronous fluorescence was applied to the determination of amiloride in urine, a very fluorescent matrix, under the optimum conditions established above.

As Fig. 2 shows, the fluorescence maxima characteristic of amiloride (solid line) are located in the UV region. As can readily be observed in this region, urine (broken line) shows two bands that prevent the determination of this compound without prior separation. Amiloride shows two broad peaks that are located at λ_{ex} = 284.8 nm, λ_{em} = 412.8 nm and λ_{ex} = 364.8 nm, λ_{em} = 412.8 nm. As at an excitation wavelength of 284.8 nm urine gives high absorbance values and there are more interferences, it is preferable to determine amiloride in urine samples with an excitation wavelength of 364.8 nm where urine needs only minor dilution and adequate selectivity is obtained. The isopotential trajectory for the urine spectrum also shown in Fig. 2 and, as can be observed, the trajectory A passes through the excitation and emission maxima of amiloride (λ_{ex} = 364.8 nm, λ_{em} = 412.8 nm).

Trajectory A was obtained from the spectrum corresponding to the arithmetic mean of 10 total fluorescence spectra of the different urine samples by means of the Ftotal program.[10]

Urine sample solutions containing amiloride gave signals smaller than those obtained with aqueous standard solutions, owing to some type of binding with other components of the urine.

Total luminescence spectra of amiloride were obtained in different urine samples to construct calibration graphs and to carry out recovery experiments.

Fig. 3 shows the effect of background fluorescence intensity (urine) on amiloride MISF and derivative spectra. It can be seen that the spectra are identical in form although their intensities are different by constant terms. They correspond to the values of the fluorescence intensity due to the three urines in the isopotential trajectory applied. It is easy to observe that derivatization totally removes the background effect.

The first derivative of MISF spectra was applied to all samples. The number of points through which the derivative was obtained was optimized, with the conclusion that derivative spectra with a suitable signal-to-noise ratio were obtained with 25 points.

In the same way we obtained the total luminescence spectra of amiloride in aqueous solution at the same concentrations. The MISF spectra were obtained by applying the isopotential trajectory (Fig. 2). We also obtained their first derivatives, as with the urine samples.

As can be readily seen in Fig. 4(*a*), which shows the MISF spectra of amiloride obtained in urine, it is not possible to determine this drug by measuring the maximum fluorescence

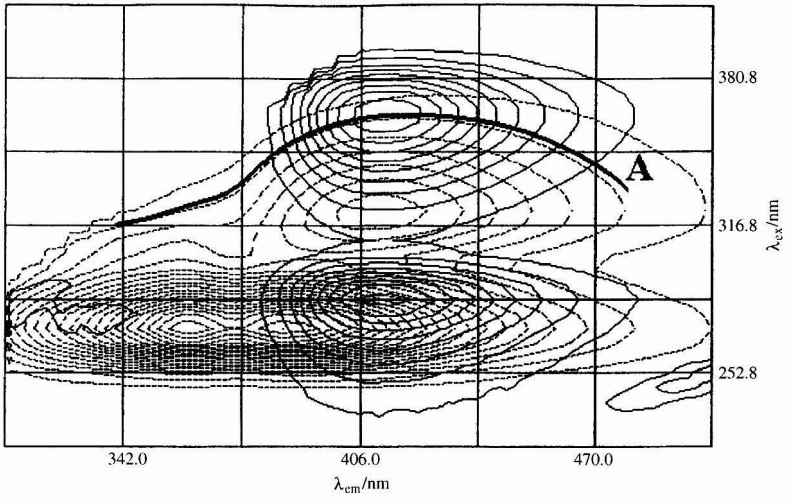

Fig. 2 Total fluorescence spectra of 152 ng ml^{-1} of amiloride (solid line) and diluted urine (1 : 50) (broken line). The line labelled A is the isopotential trajectory for the urine.

intensity (which is located at λ_{em} = 412.8 nm) with regard to the initial or final extremes (λ_{em} = 340.0 nm and λ_{em} = 480.0 nm) of the selected trajectory, since the fluorescence intensity does not reach a constant value. The first derivative technique was therefore applied. Calibration graphs were constructed by measuring the first derivative at λ_{ex} = 357.0 nm λ_{em} = 392.0 nm, where maximum sensitivity is achieved. Fig. 4(*b*) shows the spectra derived from the calibration of amiloride in urine.

In order to test the independence of the analytical signal of amiloride, *i.e.*, to show that the signal measured is independent of the urine, three calibration graphs from the first derivative signals were constructed with different urine samples.

The proposed method was evaluated by a statistical analysis of experimental data by fitting the least squares line according to $y = a + bx$, after discarding outliers with help of the least median of squares regression (LMS).[21] As LMS is a robust regression method, it is able to detect outlier points. These outliers cause errors in the true line when experimental data are fitted according to the least squares regression. Although the LMS method considers outliers to the points that give an absolute value of standardized residual above 2.5, owing to the robustness of the LMS fit, we only reject points that give an absolute value of standardized residual higher than 10. No outliers were detected. Table 1 shows the results of the statistical analysis.

To verify if the intercepts on the ordinate were negligible, significances were studied by applying Student's *t*-test at the 95% confidence level and suitable degrees of freedom.[19,20] If the intercepts on the ordinate for the lines calculated by the least

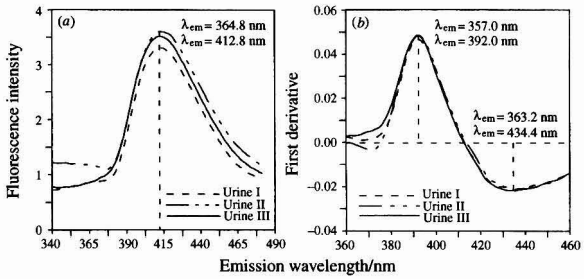

Fig. 3 (*a*) Set of MISF spectra of 122 ng ml^{-1} of amiloride in different urine samples. (*b*) Corresponding first derivative spectra.

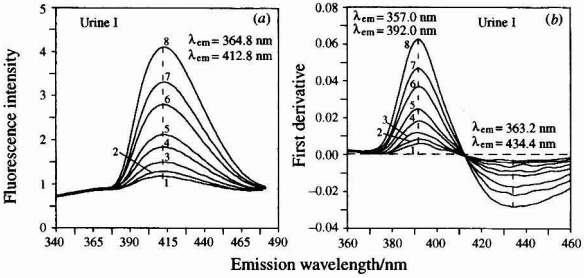

Fig. 4 (*a*) Set of MISF spectra of amiloride in urine. Amiloride concentrations: (1) 20; (2) 30; (3) 40; (4) 60; (5) 80; (6) 120; (7) 160; and (8) 200 ng ml^{-1}. (*b*) Corresponding first derivative spectra.

Table 1 Statistical data for the determination of amiloride in urine by means of first derivative matrix isopotential synchronous fluorescence

Fitting used*	Sample	Determination coefficient	Intercept on ordinate, *a*	Slope, *b*	Confidence interval for intercept	Confidence interval for slope	Exp. *t*-test	SD of estimation	Slope without intercept, *b'*
1	Urine I	0.9997	-1.750×10^{-4}	4.056×10^{-4}	—	—	—	7.2×10^{-4}	4.040×10^{-4}
	Urine II	0.9997	2.037×10^{-3}	3.733×10^{-4}	—	—	—	5.1×10^{-4}	4.190×10^{-4}
	Urine III	0.9999	-1.610×10^{-3}	3.981×10^{-4}	—	—	—	1.4×10^{-4}	3.631×10^{-4}
2	Urine I	0.9967	-5.244×10^{-4}	4.070×10^{-4}	1.247×10^{-3} to -2.295×10^{-3}	4.286×10^{-4}– 3.854×10^{-4}	0.725	1.2×10^{-3}	4.018×10^{-4}
	Urine II	0.9974	1.233×10^{-3}	3.961×10^{-4}	2.764×10^{-3} to -2.985×10^{-4}	4.148×10^{-4}– 3.775×10^{-4}	1.970	1.0×10^{-3}	4.085×10^{-4}
	Urine III	0.9995	-2.134×10^{-3}	4.172×10^{-4}	-1.421×10^{-3} to -2.846×10^{-3}	4.259×10^{-4}– 4.086×10^{-4}	7.323[b]	4.7×10^{-4}	3.958×10^{-4}
3	Global	0.9958	-4.751×10^{-4}	4.068×10^{-4}	4.579×10^{-4} to -1.408×10^{-3}	4.182×10^{-4}– 3.954×10^{-2}	1.056	1.2×10^{-3}	4.020×10^{-4}

* 1 = Least median of squares regression line according to $y = a + bx$ and $y = b'x$. 2 = Least squares regression line according to $y = a + bx$ (theoretical t = 2.447) and $y = b'x$. 3 = Overall least squares regression line according to $y = a + bx$ (theoretical t = 2.074) and $y = b'x$. [b] Experimental t-value is greater than the theoretical t-value and therefore the slope calculated without an intercept is not reliable.

squares technique are negligible, it is necessary to perform the least squares regression again according to the function $y = b'x$ and then the new value of the slopes of calibration graphs (b') may be calculated. As Table 1 shows, the intercept on the ordinate is significantly different from zero for the true line of urine III and consequently the fit according to $y = b'x$ is not recommended; nevertheless, the value of the slope for this regression is also given in Table 1.

To obtain the most representative calibration graph, an overall least squares was developed. The regression line shows homoscedasticity[19,20] and consequently the residuals manifest a uniform variance (the errors of measurements are independent of the amiloride concentration), it being unnecessary to weight the first derivative values according to the mean standard deviation. When the 95% confidence region for true slope and intercept[19,20] estimated is represented, the zero intercept on the ordinate falls within the joint confidence region. This means that the intercept is not significantly different from zero. The confidence interval for the corresponding slope is 3.946×10^{-4}– 4.095×10^{-4}. Nevertheless, the intercept significance was tested by applying Student's *t*-test. The result was not significantly different from zero, and therefore it is possible to establish a proportional relationship between the analytical signal and amiloride concentration. Therefore, the overall least squares fit according to $y = b'x$ was performed.

When the first derivative of matrix isopotential synchronous spectrofluorimetry was used and the overall least squares regression line according to $y = a + bx$ was considered, a detection limit of 2.78 ng ml^{-1} and a determination limit of 9.26 ng ml^{-1} were obtained on applying the IUPAC[21,22] definition, in which only the standard deviation of the blank is assumed. The propagation of errors approach will give values of detection and determination limits consistent with the reliability of the blank measurements and the signal measurements of the standards.[21,22] In this case a detection limit of 4.45 ng ml^{-1} and a determination limit of 14.82 ng ml^{-1} were obtained.

Precision, Accuracy and Interference Studies

To study the precision of the method, a series of 10 solutions at three different concentrations were prepared containing 15, 61 and 152 ng ml^{-1} of amiloride in urine and they were measured 15 times on the same day (repeatability study) and once a day for 10 d (reproducibility study). The SEs, assuming the error propagation theory, and RSD of repeatability at each of these levels were 2.2, 2.1 and 2.4 ng ml^{-1} and 14.4, 3.5 and 1.6%, respectively. The SEs and RSDs of reproducibility at each of these levels were 2.0, 1.9, and 2.2 ng ml^{-1} and 12.5, 3.1 and 1.4%, respectively. It can be seen that the SEs are approximately constant with the concentration, which is in agreement with the homoscedasticity that the calibration line presents.

The accuracy of the method was established by testing the analytical signal corresponding to three replicates of three samples of 15, 61 and 152 ng ml^{-1} of amiloride in different urine samples. The recoveries obtained were 107.0, 100.1 and 101.6%, respectively.

A comparison study of six samples of amiloride in urine at therapeutic levels was performed by means of MISF and the currently accepted method for doping substances (HPLC screening and GC–MS confirmation). The concentrations calculated in reverse by both methods are given in Table 2. As both methods should give same concentrations for the same samples, if least squares pair regression is applied at these concentrations, zero intercept on the ordinate and a slope of unity must be obtained. In order to test whether these methods are significantly different, the confidence intervals for the parameters of the linear regression model must be studied together. If the intercept on the ordinate, *a*, is plotted against the slope, *b*, for repeated random samples the points will be found to fall elliptically about the true centre (α, β) and, conversely, any confidence interval for the true combination of α and β will take the form of an elliptical region about the best estimates (*a*, *b*) as the centre.[19] Fig. 5 shows the 95% confidence region for the true slope and estimated intercept. As can be observed, the point corresponding to the zero intercept and unit slope falls within the joint confidence region. This means that the accuracies of the proposed and currently accepted method are not significantly different.

The specificity was studied by adding some closely related drugs to urine and testing to see if they caused interference in the amiloride quantification. The amiloride concentration was 152 ng ml^{-1} and the concentration of the drugs added (atenolol, furosemide, dipyridamole, aspirin, bumetanide, hydrochlorothiazide, hydroflumethazide, caffeine, metoprolol, quinidine and quinine) was slightly higher than would be expected at therapeutic doses. Except with quinidine and quinine, no significant variation of the analytical signal was observed from the value expected when amiloride was present alone. Nevertheless, quinidine and quinine do not present interferences if the calibration is performed at the minimum of the first derivative from the matrix isopotential synchronous spectrum that is located at λ_{ex} = 363.2 nm and λ_{em} = 434.0 nm.

Conclusions

A method for the direct fluorimetric determination of amiloride in urine by matrix isopotential synchronous fluorescence, without the need for prior separation, has been described. The determination of this natriuretic drug in urine can be performed at λ_{ex} = 357.0 nm and λ_{em} = 392.0 nm in the first derivative of the matrix isopotential synchronous scan.

As can be readily observed from the detection limits, only a 63% of error is caused by the standard deviation of the blank.

Table 2 Concentrations (ng ml^{-1}) of amiloride in urine samples calculated in reverse using the currently accepted method and the proposed method

$X_{Accepted}$	$Y_{Proposed}$
14	15
28	30
58	61
98	91
122	122
158	152

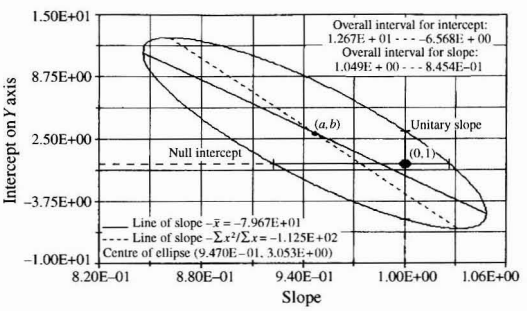

Fig. 5 The ellipse is the 95% confidence region for the true slope and intercept on the ordinate estimated from the overall least squares regression between the concentration calculated in reverse by the proposed MISF method and the currently accepted method for the determination of doping substances. The point (0,1) corresponds to zero intercept and unit slope. This point falls within the joint confidence region and consequently there are no significant differences in the accuracy of the two methods.

Therefore, the IUPAC definition with a standard deviation proportionality factor of three is inadequate.

An exhaustive statistical analysis was applied to all calibration graphs, including the least median squares robust regression and least squares. Owing to the homoscedasticity of the regression line, the weighted version is not recommended. The significance of the intercept on the ordinate was investigated through the ellipse method and Student's *t*-test at the 95% confidence level and was found not to be significantly different from zero.

To validate the method, precision, accuracy and interference studies were performed. As can be observed from the SEs and RSDs obtained from the repeatability and reproducibility experiments, excellent precision, better than in other spectrofluorimetric methods, is achieved without pre-separation procedures.[3–8] In a comparison of this method with the currently accepted method, their accuracies were not significantly different. The specificity of the proposed fluorimetric method is demonstrated by the few interferences from some closely related drugs to urine.

The authors gratefully acknowledge financial support from the Dirección General de Investigación Científica y Técnica (Project No. PB 94-0743). The authors gratefully thank the Laboratorio de Control del Dopaje del Consejo Superior de Deportes del Ministerio de Educación y Cultura for the determination of amiloride in urine samples by HPLC screening and GC–MS confirmation.

References

1 Rodríguez Bueno, C., *Dopaje*, Interamericana–McGraw-Hill, Madrid, 1992.
2 *Clarke's Isolation and Identification of Drugs*, ed. Moffat, A. C., Pharmaceutical Press, London, 1986, p. 339.
3 Kurani, S. P., Desai, D. K., and Seshadrinathan, A. G., *Indian Drugs*, 1986, **23**, 230.
4 Sastry, C. S. P., Suryanarayan, M. V., Tipirnani, A. S. R. P., and Satyanarayana, T., *Indian Drugs*, 1989, **26**, 651.
5 Wahbi, A. A. M., Bedair, M. M., Galal, S. M., and Gazy, A. A., *S. T. P. Pharm. Sci.*, 1933, **3**(2), 182.
6 García Sanchéz, F., Fernández Gutierrez, A., and Cruces Blanco, C., *Anal. Chim. Acta*, 1995, **306**, 313.
7 Karola, R., Knauf, H., and Ernst, M., *J. Chromatogr.*, 1982, **233**, 432.
8 Reewijk, H. J. E. M., Tjaden, U. R., and Van der Greef, J., *J. Chromatogr.*, 1992, **575**, 269.
9 Murillo, J. A., and Alañón, A., *Anal. Chim. Acta*, 1994, **296**, 87.
10 Murillo, J. A., and Alañón, A., *Comput. Chem.*, 1993, **17**, 34.
11 Leiner, M. J. P., Hubmann, M. R., and Wolfbeis, O. S., *Anal. Chim. Acta*, 1987, **198**, 13.
12 Murillo Pulgarín, J. A., and Alañón, A., *Analyst*, 1994, **119**, 1915.
13 Berzas Nevado, J. J., Murillo Pulgarín, J. A., and Gómez Laguna, M. A., *Analyst*, 1995, **120**, 171.
14 Murillo, J. A., Alañón, A., and Fernández, P., *Talanta*, 1996, **43**, 431.
15 Murillo, J. A., and Alañón, A., *Anal. Chim. Acta*, 1996, **317**, 359.
16 Murillo, J. A., Alañón, A., and Fernández, P., *Anal. Chim. Acta*, 1996, **326**, 117.
17 Murillo, J. A., and Alañón, A., *Microchem. J.*, 1995, **52**, 341.
18 Rousseeuw, P. J., and Leroy, A. M., *Robust Regression and Outlier Detection*, Wiley, New York, 1987.
19 Lark, P. D., Craven, B. R., and Bosworth, R. C. L., *The Handling of Chemical Data*, Pergamon Press, Oxford, 1968, ch. 4.
20 Massart, D. L., Vandeginste, B. G. M., Deming, S. N., and Kaufman, L., *Chemometrics: a Textbook*, Elsevier, Oxford, 1988.
21 Miller, J. N., *Analyst*, 1991, **116**, 3.
22 Gary, L., and Winefordner, J. D., *Anal. Chem.*, 1983, **55**, 712.
23 Savitzky, A., and Golay, M. J. E., *Anal. Chem.*, 1964, **36**, 1627.
24 Steinier, J., Termonia, Y., and Deltour, J., *Anal. Chem.*, 1972, **44**, 1906.
25 Seitz, W. R., in *Treatise on Analytical Chemistry*, ed. Elving, P. J., Meehan, E. J., and Kolthoff, I. M., Wiley, New York, 1981, pp. 194–196.

Paper 6/07219D
Received October 23, 1996
Accepted December 10, 1996

Phosphorimetric Determination of Dipyridamole in Pharmaceutical Preparations

José A. Murillo Pulgarín*, Aurelia Alañón Molina and Pablo Fernández López

Department of Analytical Chemistry and Foods Technology, University of Castilla La Mancha, 13071 Ciudad Real, Spain

Room temperature phosphorescence was applied to the determination of dipyridamole in pharmaceutical preparations. The response was linear in the concentration range 100–1600 ng ml^{-1}. The use of phosphorescence enhancers such as thallium(I) nitrate (external heavy atom), sodium dodecyl sulfate (microemulsion stabilizer) and sodium sulfite (deoxygenation agent) was studied and optimized to obtain maximum sensitivity and adequate selectivity. The determination was performed in 0.026 M sodium dodecyl sulfate, 0.0156 M thallium nitrate and 0.02 M sodium sulfite. The pH value was 11.5, adjusted by adding sodium hydroxide. The phosphorescence was totally developed in 15 min, after that the intensity was measured at λ_{ex} = 303 nm and λ_{em} = 616 nm. The recovery of the method was tested on commercial formulations containing dipyridamole. The recoveries obtained were 94.67 ± 0.58% for Persantin and 96.75 ± 1.37% for Asasantin. The overall least squares regression method was applied to find the most exact straight line that fits the experimental data. The detection limit according to the error propagation theory was 16.4 ng ml^{-1}. The repeatability and relative standard deviation were also determined according to this theory.

Keywords: *Dipyridamole; pharmaceuticals; phosphorimetry; room temperature phosphorescence*

Phosphorimetry is a selective method for measuring different organic compounds, such as pesticides,[1] PAHs[2,3] and some drugs.[4] Although room temperature fluorimetry is usually more sensitive than phosphorimetry, the broad band of spectra for different compounds limits the selectivity. Therefore, phosphorimetry is used because of its better selectivity over room temperature fluorescence and absorption spectrometry,[5–9] since not all molecules that fluoresce will phosphoresce, often completely eliminating the spectral interference, and the phosphorescence is shifted to a less crowded spectral region. However, the difficulties associated with low temperature phosphorescence (LTP) make this technique unpopular. Owing to these difficulties, LTP has not been used extensively for the identification and determination of many compounds. Since its discovery in 1967 by Roth,[10] room temperature phosphorimetry (RTP) has attracted great interest and has become a practical technique for the detection of many organic compounds.[10–18] As the sample must be adsorbed on an inert substrate such as filter-paper,[19,20] the technique has the disadvantages of cumbersome sample preparation, critical drying requirements and high phosphorescent background intensity from the filter-paper substrate.

RTP can also be observed from many organic compounds in liquid solutions incorporating the phosphors into organized media such as cyclodextrins, micellar systems and microcrystalline media or by using sensitized RTP. In 1980, Cline Love and co-workers[21,22] first investigated micelle-stabilized RTP and studied several PAHs. In a micellar solution the analytes included in the micellar assembly are apparently protected from the quenchers present in the solution. Observation of RTP in a micellar solution usually requires the presence of a heavy atom. It is placed as a counter ion outside the micelle, thus being in proximity to the hydrophobic molecules associated with the micelle. The high local concentration of the heavy atoms produces an efficient spin–orbit coupling that can diminish the fluorescence and increase the phosphorescence. Furthermore, the micelles can effectively screen molecules in the excited triplet state from the action of potential quenchers present in the bulk water phase. However, phosphorescence is not observed unless oxygen is removed, as it is a very efficient quencher that easily penetrates the micelles. Díaz García and Sanz-Medel[23] have proposed the substitution of the troublesome deoxygenation with nitrogen by chemical deoxygenation with sodium sulfite, thus avoiding foam formation and ensuring more permanent protection of the solution against contamination with oxygen. In the presence of sulfite, however, the phosphorescence is not immediately observed. The oxygen in the bulk water phase is removed first, followed by that in the micelle pseudophases as it diffuses out. Equilibrium is achieved in a few minutes.

In the spite of the interest in observing phosphorescence in micellar solutions, only a few analytical procedures have used this technique. In this work, the appropriate experimental conditions to obtain a reproducible and maximum phosphorescence signal, when sulfite is used to eliminate the oxygen from the micellar solutions, were studied.

Dipyridamole (2,2′,2″,2‴-{(4,8-dipiperidinopyrimino[5,4-*d*]pyrimidine-2,6-diyl)dinitrilo}tetraethanol) is shown in Fig. 1. It is an intensely yellow crystalline powder. Its solution gives a yellowish blue fluorescence. It is almost insoluble in water.

Dipyridamole is a vasodilator agent that is widely used in medicine. After oral administration, it stimulates a rise in the blood flow through the coronary circulation, providing more blood to the myocardium. This effect has been used in certain sports to increase energy production, such as *via* ATP molecules. Therefore, this vasodilator agent is classified, in doping terms, as a stimulant. Stimulants have been consumed in sports to increase efficiency and decrease tiredness. Stimulants include other substances that intensify the attention and could increase competitiveness and aggressiveness. Nevertheless, the uncontrolled use of such drugs could cause the loss of mental power and also have serious secondary effects that could cause grave danger to health.

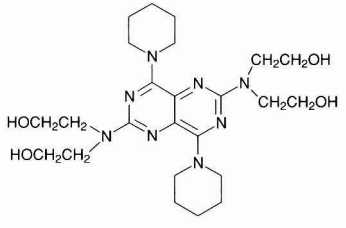

Fig. 1 Structure of dipyridamole.

There have been various reports describing the spectrophotometric determination of dipyridamole in pharmaceutical tablets.[24–34] In comparison with the method proposed here, these methods show low sensitivity and selectivity. The need for derivatization reactions[31–34] to increase the selectivity makes these methods tedious, low accuracy is achieved and the detection limits are higher than when direct spectrophotometry is used. Only three methods have utilized the highly fluorescent nature of this drug.[35–37] Although Shao *et al.*[35] developed a direct spectrofluorimetric determination, the method has low sensitivity. The methods of Wilczynska-Wojtulewicz[36] and Steyn[37] require various preliminary procedures such as extraction and separation by means of TLC. We propose the application of RTP to determine dipyridamole in pharmaceutical tablets. The main advantages of using RTP over spectrophotometric and fluorimetric methods for this purpose are the high selectivity and sensitivity achieved, together with a detection limit of < 20 ng ml^{-1} compared with approximately 2 μg ml^{-1} and 100 ng ml^{-1} for spectrophotometric and spectrofluorimetric methods, respectively.

Experimental

Apparatus

All phosphorimetric measurements were performed on an Aminco Bowman Series 2 luminescence spectrometer, connected to software which runs on the OS2 operating system. The instrument utilizes a 7 W integral pulsed xenon lamp for phosphorescence measurements. The gated photomultiplier tube detection includes a unique masking method for detection in < 200 μs after the initiation of the flash lamp. Quartz glass cuvettes with pathlengths of 1.0 × 1.0 cm were used. Thermostatic equipment and a Crison Model 2001 pH meter with a glass–saturated calomel combination electrode were also used.

Software

The AB2 program allows the operation of the instrument to obtain excitation and emission spectra, total phosphorescence spectra and time traces, such as decay curves and time resolved curves. The Ftotal program[38] was used to generate fluorescence and phosphorescence contour spectra. Statistical analysis was performed by means of a program developed by us, which has an option menu that includes all the procedures mentioned in this paper.

Reagents

All experiments were performed with analytical reagent grade chemicals, pure solvents and Milli-Q-purified water. Sodium dodecyl sulfate (SDS) was obtained from Sigma (St. Louis, MO, USA) and thallium(I) nitrate and sodium sulfite from Merck (Darmstadt, Germany).

A stock standard solution of dipyridamole (Aldrich, Milwaukee, WI, USA) (100.0 mg disolved 100 ml of 0.1 M SDS) was diluted to prepare working standard solutions. The stock standard solution of dipyridamole was stored and protected from the light and maintained below 5 °C. Under these conditions, it was stable for at least 2 weeks. The working standard solutions of dipyridamole were stable for at least 2 d at room temperature.

Stock standard solutions of 0.1 M SDS and 0.3 M thallium(I) nitrate were used. A 0.25 M sodium sulfite solution was prepared daily.

Procedure

For the preparation of the calibration graph, an aliquot of dipyridamole standard solution was pipetted into a 25 ml calibrated flask, then SDS as necessary to give a 0.026 M concentration, 2.5 ml of 0.025 M sodium hydroxide solution, 1.3 ml of 0.3 M thallium(I) nitrate solution and 2.0 ml of 0.25 M sodium sulfite were added. The solution was diluted to volume with water and shaken. After the flask had stood for 15 min in a thermostat at 20 °C, a portion of the solution was transferred into a phosphorescence cuvette and the RTP measured at an excitation wavelength of 303 nm and an emission wavelength of 616 nm.

For the analysis of Persantin (Boehringer Ingelheim, Barcelona, Spain), 10 tablets were weighed and for the analysis of Asasantin (Boehringer Ingelheim) ten capsules (which contained inside dipyridamole in the form of minute tablets) were weighed. In all instances, the solid was powdered, homogenized and about 0.1 g was taken for analysis. Suitable dilutions were made with 0.1 M SDS. In all instances, the excipients were not soluble in SDS, so after shaking and maintaining in an ultrasonic bath for 5 min the solutions had to be centrifuged.

Results and Discussion

Spectral Characteristics

Fig. 2 shows the total phosphorescence spectrum (solid line) and the total fluorescence spectrum (broken line) of dipyridamole. They are identical in form, varying only in the location of the emission wavelength of maximum intensity. In the Fig. 3(*a*) the phosphorescence (solid line) and fluorescence (broken line) excitation spectra at the emission wavelength of

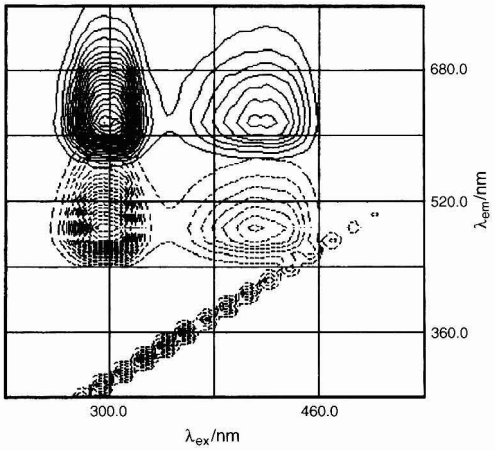

Fig. 2 Total phosphorescence spectrum (solid line) and total fluorescence spectrum (broken line) of dipyridamole.

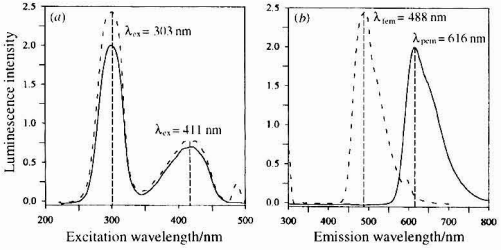

Fig. 3 Phosphorescence (solid line) and fluorescence (dashed line) spectra of dipyridamole. Photomultiplier voltage 800 V in phosphorescence and 410 V in fluorescence. (*a*) Excitation spectra; and (*b*) emission spectra.

maximum intensity are shown. Both excitation spectra are coincident, displaying two broad peaks at excitation wavelengths of 303 and 411 nm. The coincidence of the phosphorescence and fluorescence excitation spectra means an identical excitation process in both cases. This is justified in theory by the light absorption promoting an electron from the ground electronic state to the first and second excited singlets. The peak at 303 nm shows a higher luminescence intensity than that at 411 nm and the former excitation wavelength was therefore chosen for phosphorescence measurements.

Fig. 3(*b*) shows the phosphorescence (solid line) and fluorescence (broken line) emission spectra. The fluorescence spectrum gives a band with a characteristic emission wavelength of 488 nm, corresponding to the transition from the first excited singlet to the ground state. The phosphorescence spectrum presents a band at 616 nm corresponding to the transition from the excited triplet to the singlet ground state. The fluorescence and phosphorescence spectra show different characteristic emission wavelengths. This difference of 128 nm gives an idea of the non-radiant energy that is lost in the intersystem crossing and the subsequent vibrational relaxation to the lowest vibrational level of the excited triplet.

The phosphorescence lifetime of dipyridamole is approximately 1324 μs. This is the time required for the population of the excited triplet state to decrease to 1/e of its original value after the excitation source has been turned off. The lifetime is a means of considering the luminescence process in terms of rates. Fluorescence lifetimes are typically of the order of 1–20 ns. As phosphorescence is a spin forbidden process, phosphorescence lifetimes are considerably longer, generally ranging from milliseconds to seconds. Consequently, the phosphorescence lifetime is a measure of the forbiddenness of singlet–triplet transitions in a given molecule.

Factors Affecting Phosphorescence

Chemical variables were optimized to obtain maximum phosphorescence sensitivity and adequate selectivity.

Dipyridamole is almost insoluble in water, so it was necessary to use an organic solvent. Owing to the micellar properties of SDS it was used to dissolve dipyridamole; further, the semirigid structure of the solution favours the development of phosphorescence.

The extremely high sensitivity of the triplet state to quenching by oxygen requires deoxygenation of the sample. Owing to the high efficiency of this quenching process, it is necessary to eliminate totally the oxygen in the micellar solution. The method proposed for sample deoxygenation is based on the redox reaction of sulfite with molecular oxygen to product sulfate.[23] It was observed that a concentration of Na_2SO_3 of 0.02 M was required to eliminate oxygen completely from the solutions, which was evident from the intensity of the phosphorescence signal. This decreases at higher concentrations of Na_2SO_3. The decrease in the signal for higher concentrations of Na_2SO_3 has been interpreted as the displacement of thallium(I) from the micelle because of the high concentration of sodium in the solution.[23] An Na_2SO_3 concentration of 0.02 M was chosen.

The influence of pH on phosphorescence intensity was studied by adding different amounts of H_2SO_4 and NaOH to a dipyridamole solution. The phosphorescence is not significant at pH values up to 9.5. In Fig. 4 phosphorescence intensity is plotted *versus* the pH of the solution and, as can be readily observed, dipyridamole has maximum intensity at pH 11.5. Phosphate buffer was first used to adjust this pH value, but the phosphorescence intensity diminished. This is a quenching situation due to the formation of exciplexes. The explanation for this behaviour is that an excited dipyridamole molecule associates with the phosphate in the ground state. Consequently, the phosphorescence intensity of excited dipyridamole diminishes. This pH was subsequently adjusted by adding 2.5 ml of 0.025 M NaOH.

It was also necessary to establish how the phosphorescence intensity varies with changes in thallium concentration. Fig. 5(*a*) shows this relationship for thallium concentrations between 0.0024 and 0.0168 M. As can be readily observed, the phosphorescence intensity increases with increase in thallium concentration. For concentrations of thallium above 0.0168 M precipitation is observed. For lower concentrations of thallium, the heavy atom effect is very sensitive. When the thallium salt is not present the phosphorescence intensity disappears. A concentration of thallium of 0.0144 M gives high intensity without problems of precipitation.

The effect of SDS concentration was investigated by preparing samples with SDS concentrations between 0.014 and 0.074 M. As Fig. 5(*b*) shows, phosphorescence intensity of dipyridamole diminishes as the SDS concentration increases. For SDS concentrations lower than 0.014 M precipitation occurred. A 0.022 M concentration of SDS was therefore selected, giving good sensitivity while being sufficient to dissolve the dipyridamole.

From the above two experiments, the phosphorescence intensity is maximum with SDS and thallium concentrations in

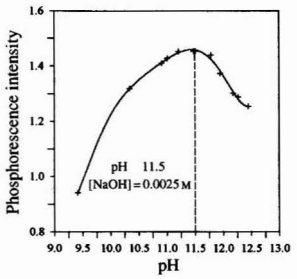

Fig. 4 Variation of phosphorescence intensity of dipyridamole with pH. The pH was varied from 9.5 to 12.5 by adding sodium hydroxide.

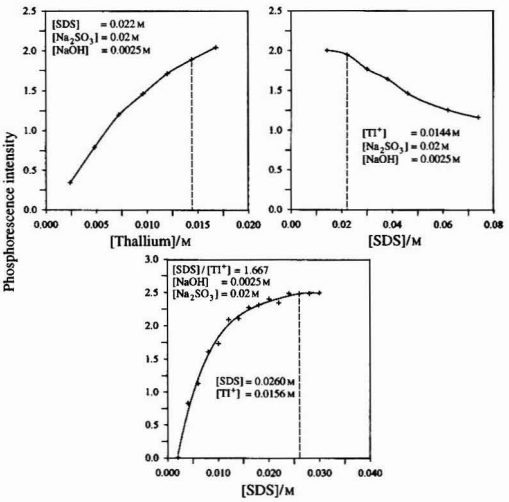

Fig. 5 (*a*) Effect of thallium(I) concentration on phosphorescence intensity at an SDS concentration of 0.022 M; (*b*) effect of SDS concentration on phosphorescence intensity at a thallium(I) concentration of 0.0144 M; and (*c*) effect of SDS and thallium(I) on phosphorescence intensity at an SDS to thallium(I) ratio of 1.667.

the proportion of 1.667, and Fig. 5(*c*) shows the phosphorescence intensity *versus* SDS concentration with this proportion maintained. As can be observed, the phosphorescence intensity increases as the concentration of SDS increases, reaching a constant value at SDS concentrations above 0.025 M. Concentrations of SDS of 0.026 M and of thallium(I) 0.0156 M were selected as adequate. At concentrations of SDS above 0.032 M precipitation occurred.

Another factor that affects the phosphorescence intensity is temperature, the phosphorescence intensity decreasing when the temperature increased from 15 to 79 °C. This decrease is measured by plotting the relative signal increment *versus* temperature, *i.e.*, the intensity at each temperature minus the intensity at the lowest temperature, divided by the intensity of the higher temperature and multiplied by 100. This relationship shows a linear behavior, the slope (which is the temperature coefficient of dipyridamole) being 1.36% $°C^{-1}$, the intercept on the ordinate 104.4% and the coefficient of the determination $r^2 = 0.995$.

The influence of dipyridamole concentration on the phosphorescence intensity was studied under the above conditions. The phosphorescence intensity reaches a constant value at dipyridamole concentrations above 20 μg ml^{-1}. The dipyridamole concentration range for a linear relationship between phosphorescence intensity and concentration was found to be up to 1600 ng ml^{-1}. The inner filtering effect is significant for concentrations of dipyridamole above 1600 ng ml^{-1}, and increases as the dipyridamole concentration increases. Consequently, calibration was performed for dipiridamole concentrations up to 1600 ng ml^{-1} with three replicates per point.

Determination of Dipyridamole

Under the operating conditions outlined above, we propose a method to determine dipyridamole by direct measurement of phosphorescence intensity with an emission wavelength of 616 nm and an excitation wavelength of 303 nm in the concentration range 100–1600 ng ml^{-1}. The delay time required was 120 μs with the photomultiplier tube masked. The gate time appropriate for this delay time was 800 μs and the detector voltage was 740 V. Both excitation and emission bandpasses were 16 nm and the scan rate was 5 nm s^{-1}.

A calibration graph was constructed with three replicates per point. Fig. 6 shows the average emission spectra of the calibration concentrations.

The proposed method was evaluated by a statistical analysis of the experimental data by fitting the overall least squares line according to $y = a + bx$.[39,40] Table 1 gives the results from the statistical analysis.

The calibration line presents homoscedasticity (standard residuals have a uniform variance) and therefore it is not necessary to weight the phosphorescence intensity values according to the mean standard deviation. In order to test the linearity of the overall least squares regression, the ANOVA test was performed.[39] The results are given in Table 2. When the 95% confidence region for true slope and intercept[40] estimated is represented, the zero intercept on the ordinate falls within the joint confidence region. This means that the intercept on the ordinate is not significantly different from zero. Therefore, the relationship between phosphorescence intensity and dipyridamole concentration is proportional. The confidence interval for the corresponding slope is 1.257×10^{-3}–1.238×10^{-3}. Nevertheless, the significance of the intercept was tested by applying Student's *t*-test (Student's *t*-test is more restrictive than the confidence region of the true slope and intercept). The experimental *t*-value obtained was 0.324, which is less than theoretical value of 2.12.

If the theory of error propagation is considered, the values of the detection and determination limits are consistent with the reliability of the blank measurements and the signal measurements of the standards.[41,42] In this case a detection limit of 16.4 ng ml^{-1} and a determination limit of 54.6 ng ml^{-1} were obtained. The detection limit according to Clayton considers the probability of false positive and false negative values, the detection limit being 18.8 ng ml^{-1}.

In order to study the precision of the method, a series of 10 solutions of 800 ng ml^{-1} of dipyridamole were measured on the

Table 1 Results from statistical analysis of data; least squares regression with replicates

Intercept on ordinate (*a*)	-1.705×10^{-3}
SD of intercept on ordinate (s_a)	5.3×10^{-3}
Slope (*b*)	1.249×10^{-3}
SD of slope (s_b)	5.8×10^{-6}
SD of regression (s_{yx})	1.3×10^{-2}
Coefficient of determination (r^2)	0.9996
Confidence interval of intercept on ordinate	9.447×10^{-3}, -1.286×10^{-2}
Confidence interval of slope	1.262×10^{-3}, 1.237×10^{-3}
Slope without intercept on ordinate	1.248×10^{-3}

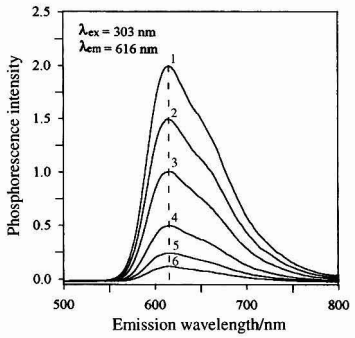

Fig. 6 Set of room temperature phosphorescence spectra. Dipyridamole concentration: 1, 1600; 2, 1200; 3, 800; 4, 400; 5, 200; and 6, 100 ng l^{-1}.

Table 2 ANOVA test: linearity test

Source of variation	SS*	DF*	MS*	$F_{exp.}$	$F_{theoretical}$
Due to regression	8.2804	1	8.2804		
Set means about the line (lack of fit)	2.6916×10^{-4}	4	6.7290×10^{-5}	0.31	3.26
Within line (pure error)	2.6363×10^{-3}	12	2.1969×10^{-4}		
Total	8.2833	17	0.4873		

* SS = Sum of squares of deviation; DF = degrees of freedom; MS = $\frac{SS}{DF.}$

same day. By applying the IUPAC definition, the mean standard deviation of replicates was 3.88 ng ml^{-1} and the relative error 1.1%, whereas if error propagation is assumed, the SE obtained was 2.59 ng ml^{-1} and the relative error 0.71% (95% confidence level). In this case the relative error for replicates is less on applying the SE of the regression line, owing to the classical hyperbolic shape of the confidence and dispersion bands of the true line which are closest at the mean concentration, this being very near to 800 ng ml^{-1}, where the standard deviation is reduced to the standard deviation of the mean, and therefore, the relative error is less. To estimate concentration values at greater distances from the mean concentration of the regression line, the error propagation method gives the greatest values for the relative error.

The accuracy of the method was established by testing the analytical signal corresponding to the concentrations of the calibration line. As can be seen from the RSDs in Table 3, the values obtained by applying the error propagation theory confirm that, to calculate the confidence interval of a measurement, the error propagation method may be used.

The determination of dipyridamole by RTP was compared with the currently accepted method.[37,43] In this, 1 ml of the problem solution is extracted at pH 10 with 8 ml of hexane–isoamyl alcohol (95 + 5) and the organic phase used directly for measurement of the fluorescence intensity (λ_{ex} = 405 and λ_{em} = 495 nm). A comparison study of 10 samples of dipyridamole was performed by applying least squared pair analysis[40] with the concentration calculated in reverse by means of the currently accepted method and the proposed method. As both methods should give the same concentrations for the same samples, a zero intercept on the ordinate and a slope of units must be obtained. Fig. 7 shows the 95% confidence region for the true slope and intercept estimated. As can be observed, the point corresponding to the zero intercept and unit slope falls within the joint confidence region. This means that the intercept is not significantly different from zero and the slope is not significant different from unity. Consequently, the accuracies of proposed and currently accepted method are not significantly different.

Table 3 RSDs obtained by applying error propagation theory

Xm_i	Ym_i	RSD (%)
100	0.1217	7.32
200	0.2441	3.58
400	0.5008	1.72
800	1.005	0.842
1200	1.495	0.591
1600	1.996	0.493

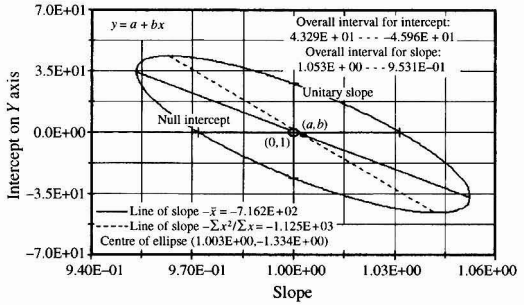

Fig. 7 Comparison between the proposed method and the currently accepted method. The ellipse is the 95% confidence region for the true slope and the intercept on the ordinate estimated from the overall least squares regression performed with the concentration calculated in reverse using both methods. The point (*a*, *b*) is the centre of the ellipse corresponding to the true intercept and estimated slope. The point (0, 1) means zero intercept and unit slope.

Applications and Interference Study

The recommended procedure was applied satisfactorily to the determination of dipyridamole in the Spanish pharmaceutical products that contain this vasodilator agent in different proportions (Persantin 100 mg and Asasantin 75 mg). The assay results expressed as a percentage of the nominal contents resulting from the average of three determinations of three different tablets were 94.67% for Persantin and 96.75% for Asasantin, the standard deviations being 0.58% and 1.37%, respectively. The recoveries agree well enough with the nominal content and the precision is quite satisfactory

The specificity of this determination was studied by adding related drugs to the pharmaceutical preparation of dipyridamole and other drugs with intrinsic fluorescence and testing to see if the added drugs cause interference in the dipyridamole quantification. In the first case, dipyridamole (1600 ng ml^{-1}) was spiked with saccharose, lactose and glucose (20 μg ml^{-1}). No interferences were found. In the second, the added drugs were aspirin, atenolol, spironolactone and canrenoic acid (1 μg ml^{-1}), amiloride, furosemide and triamterene (25 ng ml^{-1}), aspirin and nadolol (2 μg ml^{-1}), metoprolol (80 ng ml^{-1}) and caffeine, quinidine and quinine (1.6 μg ml^{-1}). Except for the furosemide, no significant variation of the analytical signal was observed from the value expected when dipyridamole is present alone. Nevertheless, interferences were observed if the concentrations of these drugs were increased.

Conclusions

A method for direct phosphorimetric determination of the vasodilator agent dipyridamole in pharmaceutical preparations has been developed. The determination can be performed by measuring phosphorescence intensity within an emission wavelength of 616 nm after excitation at 313 nm with excellent repeatability and sensitivity.

Owing to the high selectivity of the phosphorimetric methods, the determination of dipyridamole by RTP shows no significant interferences and is suitable for its determination in tablets. Other components of the tablets do not interfere in the phosphorescence spectra of dipyridamole.

An exhaustive statistical analysis was applied to the calibration graph, including least squares regression and ANOVA. The regression line shows homoscedasticity. The validity of the overall least squares regression is proved by the ANOVA test, the variation of group means about the line, which means the lack of fit, not being significantly different from the variation within groups (pure error). Therefore, the model chosen is an adequate description of the true relationship between phosphorescence intensity and dipyridamole concentration.

The proposed method was compared with the currently accepted method and the accuracies were not significantly different.

The authors gratefully acknowledge financial support from Dirección General de Investigación Científica y Técnica (Project No. PB 94-0743).

References

1 Moye, H. A., and Winefordner, J. D., *J. Agric. Food Chem.*, 1965, **13**, 516.
2 Inman, E. L., Jurgensen, A., Jr., and Winefordner, J. D., *Analyst*, 1982, **107**, 538.
3 McGlynn, S. P., Neely, B. T., and Neely, C., *Anal. Chim. Acta*, 1963, **28**, 472.

4 Winefordner, J. D., and Tin, M., *Anal. Chim. Acta*, 1964, **31**, 239.
5 Becker, R. S., *Theory and Interpretation of Fluorescence and Phosphorescence*, Wiley, New York, 1969.
6 Guilbault, G. G., *Practical Fluorescence: Theory , Methods and Techniques*, Marcel Dekker, New York, 1973.
7 Parker, C. A., *Photoluminescence of Solutions*, Elsevier, Amsterdam, 1968.
8 Schulman, E. G., *Fluorescence and Phosphorescence Spectroscopy: Physicochemical Principles and Practice*, Pergamon Press, Oxford, 1968.
9 Wehry, E. L., *Modern Fluorescence Spectroscopy*, Plenum Press, New York, 1976.
10 Roth, M., *J. Chromatogr.*, 1967, **30**, 276.
11 Schulman, E. M., and Walling, C., *J. Phys. Chem.*, 1973, **77**, 902.
12 Wellons, S. L., Paynter, R. A., and Winefordner, J. D., *Spectrochim. Acta, Part A*, 1974, **30**, 2133.
13 Vo-Dinh, T., *Room Temperature Phosphorimetry for Chemical Analysis*, Wiley, New York, 1984.
14 Hurtubise, R. J., *Solid Surface Luminescence Analysis: Theory, Instrumentation and Applications*, Marcel Dekker, New York, 1981.
15 Vo-Dinh, T., and Winefordner, J. D., *Appl. Spectrosc. Rev.*, 1977, **13**, 261.
16 Parker, R. T., Freedlander, R. S., and Dunlap, R. P., *Anal. Chim. Acta*, 1980, **119**, 189.
17 Su, S. Y., and Winefordner, J. D., *Talanta*, 1982, **28**, 713.
18 Dalterion, R. A., and Hurtubise, R. J., *Anal. Chem.*, 1983, **55**, 1084.
19 Wandruszka, R. M. A., and Hurtubise, R. J., *Anal. Chim. Acta*, 1977, **93**, 331.
20 Niday, G. J., and Seybold, P. G., *Anal. Chem.*,1978, **50**, 1577.
21 Cline Love, L. J., Skrilec, M., and Habarto, J. G., *Anal. Chem.*, 1980, **52**, 754.
22 Skrilec, M., and Cline Love, L. J., *Anal. Chem.*, 1980, **52**, 1559.
23 Díaz García, M. E., and Sanz-Medel, A., *Anal. Chem.*, 1986, **58**, 1436.
24 Babary, M., Elsayed, M. A. H., and Sabry, S. M., *Acta Pharm. Jugosl.*, 1990, **40**, 513.
25 Li, H., *Shenyang Yaoxueyuan Xuebao*, 1984, **1**, 239.
26 Shumeiko, V. A., *Farm. Zh.*, 1977, **3**, 88.
27 Hu, J., Sun, H., and Xu, Y., *Huasue Shijie*, 1987, **28**, 19.
28 Umapathi, P., Parimoo, P., and Thomas, S. K., *Indian Drugs*, 1994, **31**, 489.
29 Babary, M. H., Elsayed, M. A. H., Abdel-Hay, M. H., and Mohamed, S. M., *Anal. Lett.*, 1989, **22**, 1643.
30 Korany, M. A., and Haller, R., *Anal. Chem.*, 1982, **65**, 144.
31 Issa, A. S., Mahrous, M. S., Abdel Salam, M. A., and Soliman, N., *Talanta*, 1987, **34**, 670.
32 Ganescu, I., Preda, M., Papa, I., and Vladoianu, A., *Zentralbl. Pharm., Pharmakother. Laboratoriumsdiagn.*, 1988, **127**, 577.
33 Mahrous, M. S., Issa, A. S., Abdel Salam, M. A., and Soliman, N., *Anal. Lett.*, 1986, **19**, 901.
34 Sane, R. T., Nayak, V. G., Naik, N. R., and Gupte, D. D., *Indian Drugs*, 1983, **20**, 334.
35 Shao, Z., Pan, Z., and Gan, Z., *Zhongguo Yaoxue Zazhi*, 1991, **26**, 225.
36 Wilczynska-Wojtulewicz, I., *Chem. Anal. (Warsaw)*, 1977, **22**, 805.
37 Steyn, J. M., *J. Chromatogr.*, 1979, **164**, 487.
38 Murillo, J. A., and Alañón, A., *Comput. Chem.*, 1993, **17**, 34.
39 Massart, D. L, Vandeginste, B. G. M., Deming, S. N., and Kaufman, L., *Chemometrics: a Textbook*, Elsevier, Oxford, 1988.
40 Lark, P. D., Craven, B. R., and Bosworth, R. C. L., *The Handling of Chemical Data*, Pergamon Press, Oxford, 1968, ch. 4.
41 Miller, J. N., *Analyst*, 1991, **116**, 3.
42 Gary, L., and Winefordner, J. D., *Anal. Chem.*, 1983, **55**, 712.
43 *Clarke's Isolation and Identification of Drugs*, ed. Moffat, A. C., Pharmaceutical Press, London, 1986, pp. 562–563.

Paper 6/06511B
Received September 23, 1996
Accepted December 4, 1996

Enzymic Method for the Spectrophotometric Determination of Benzoic Acid in Soy Sauce and Pickles

Takashi Hamano*[a], Yukimasa Mitsuhashi[a], Nobumi Aoki[a], Masanori Semma[b] and Yoshio Ito[b]

[a] *Division of Food Chemistry, Public Health Research Institute of Kobe City, Minatojima-nakamachi 4–6, Chuo-ku, Kobe 650, Japan*
[b] *Faculty of Pharmaceutical Sciences, Mukogawa Women's University, Kyuban-cho 11–68, Koshien, Nishinomiya 663, Japan*

A simple spectrophotometric method for the determination of benzoic acid is described. Benzoic acid is measured enzymically through its reaction with benzoate 4-hydroxylase coupled with NADPH and O_2. The entire enzymic procedure required 20 min to complete. The method greatly simplifies the procedure for benzoic acid determination and permits the routine inspection of a number of samples with very little laboratory equipment. The method was compared with HPLC and satisfactory agreement was achieved.

Keywords: *Benzoic acid; benzoic acid hydroxylase; enzymic analysis; spectrophotometry; soy sauce; pickles*

Benzoic acid (BA) has low toxicity and is widely used as a preservative in various kinds of foods. It is also permitted for use in soy sauce, a typical seasoning in Japan and other oriental countries. Requests for the determination of BA in soy sauce are common in oriental laboratories.

To date, BA in foods has been determined chiefly by GC and HPLC procedures.[1–7] However, these methods require elaborate derivatization and/or clean-up procedures, especially when working with complex matrices such as soy sauce. Because of the steadily increasing number of samples of soy sauce requiring analysis for BA, the need for a faster assay method became evident.

In the oxidative metabolism of bacteria, specific hydroxylation plays an important role.[8] These steps are mediated by oxygenases. One such enzyme, benzoic acid hydroxylase (BAase),[9] converts BA into *p*-hydroxy-BA (PHBA) in the presence of NADPH as a hydrogen donor:

$$BA + NADPH + H^+ + O_2 \xrightarrow{BAase} PHBA + NADP^+ + H_2O$$

In this work, BA was hydroxylated by BA hydroxylase. Under specific conditions, the maximum rate of formation of $NADP^+$ was proportional to the initial BA concentration. Studies with soy sauce and pickles soaked in soy sauce were carried out to illustrate the feasibility of the proposed method.

Experimental

Apparatus

Spectrophotometer. Model UV-160 (Shimadzu, Kyoto, Japan).

Millipore filter. Millex-HA, 0.45 μm (Millipore, Bedford, MA, USA).

Micropipettes, 10–100 and 100–1000 mm^3. (Eppendorf, Westbury, NY, USA).

Microsyringe, 25 mm^3. (Hamilton, Reno, NV, USA).

Reagents

All reagents were of analytical-reagent grade unless specified otherwise.

BA stock standard solution, 1000 μg cm^{-3}. Prepared by dissolving 144.11 mg of sodium benzoate (Wako, Osaka, Japan) in 100 cm^3 of deionized water.

Working standard solutions. Appropriate volumes of stock standard solution were diluted with deionized water to obtain BA concentrations of 0.5–15 μg cm^{-3}.

Tris–maleate buffer, pH 6.2, 0.5 mol dm^{-3}. Prepared by dissolving 8.59 g of tris(hydroxymethyl)aminomethane (Sigma, St. Louis, MO, USA) and 49.65 g of maleic acid in about 800 cm^3 of deionized water. The solution was adjusted to pH 6.2 with 1 M HCl or 1 M NaOH and diluted to 1000 cm^3 with deionized water.

Pteridine co-factor, 4 mmol dm^{-3}. Prepared by dissolving 93.6 mg of 2-amino-6,7-dimethyl-5,6,7,8-tetrahydropteridine hydrochloride (Sigma) in 100 cm^3 of deionized water.

Iron(II) sulfate solution, 2 mmol dm^{-3}. Prepared by dissolving 55.6 mg of $FeSO_4 \cdot 7H_2O$ in 100 cm^3 of deionized water.

BA hydroxylase, 5000 nKat cm^{-3}. This was purified from a culture medium of *Aspergillus niger* (UBC 814) according to the procedure of Reddy and Vaidyanathan[10] and dissolved in Tris–maleate buffer. The enzyme solution can be stored for 2 d at 0–4 °C without any loss of activity. We define 1 nKat of the enzyme activity used as the amount of BA hydroxylase that catalyses the hydroxylation of 1 nmol of BA per second at 30 °C under our assay conditions.

Procedure

Assay of standard solution

A 1 cm^3 aliquot of a working standard solution of BA was introduced into a 10 cm^3 test-tube containing 3 cm^3 of Tris–maleate buffer, 100 mm^3 of pteridine and 100 mm^3 of iron(II) sulfate solution. A 20 mm^3 volume of BA hydroxylase solution was then injected to start the reaction. After incubating the mixture for 10 min at 30 °C, the decrease in absorbance (ΔA) at 340 nm was measured against a blank prepared as described above except that the enzyme solution was replaced with an equal volume of deionized water. This value was used to prepare the calibration graph.

Assay of the BA content in soy sauce and pickles

Liquid samples were used directly; samples with a high insoluble solid content were homogenized with four times their volume of deionized water and filtered through a Millipore filter to remove suspended matter. To prepare the sample solution, 10 cm^3 of pre-treated sample solution and 5 cm^3 of Tris–maleate buffer solution were mixed, adjusted to pH 6.2 with 1 M NaOH or 1 M HCl and diluted to volume in a 50 cm^3 calibrated flask.

A 1 cm^3 aliquot of the sample solution was assayed according to the procedure described under Assay of standard solution and its BA content was determined from the calibration graph.

Determination of BA by HPLC

For a comparison study, 10 mm^3 of the sample solution prepared as described above were analysed according to the method of Ikai *et al.*[11]

Results and Discussion

Optimization of the Enzyme Reaction

The proposed enzymic method was based on the hydroxylation of BA by NADPH to *p*-hydroxy-BA in the presence of a specific enzyme, benzoate hydroxylase. The amount of NADPH oxidized ($NADP^+$) during the enzymic reaction bears a stoichiometric relationship to the amount of BA. The decrease in NADPH concentration can be determined by measuring its absorbance at 334, 340 or 365 nm. The absorbance of NADPH was maximum at 340 nm and this value was chosen for maximum sensitivity. In order to obtain the maximum sensitivity for the proposed method, several experimental parameters, such as reaction pH, reaction temperature and the concentration of the enzyme, were optimized.

The effect of temperature (10–40 °C) on the sensitivity was studied first. As expected, the analytical signal (ΔA at 340 nm) increased with increase in temperature from 10 to 30 °C. However, the enzyme activity decreased drastically above 38 °C owing to instability of the enzyme at higher temperatures. Hence all experiments were performed at 30 °C.

The effect of pH on the sensitivity was examined next; using 50 nKat of the enzyme, the analytical signals at various pH values were measured. As shown in Fig. 1, the optimum pH for the assay of BA was found to be about 6.2. This value is in good agreement with previously reported results.[10] The reaction was also time dependent. The analytical signal increased with increase in reaction time from 2 to 5 min, then stayed constant up to 60 min (see Fig. 3). Considering the speed and the sensitivity of analysis, a reaction time of 10 min was chosen.

The optimum concentration of enzyme, *i.e.*, BA hydroxylase, was then determined. As shown in Fig. 2, the analytical signal increased significantly with increase in enzyme concentration from 5 to 25 nKat, at which point the reaction became nearly zero order with respect to the enzyme activity. Accordingly, 50 nKat of the enzyme were used in the routine inspection. Another feature of the enzyme used is the requirement for Fe^{2+} in its reactions. This ion appears to act as an activator of the enzyme.[10] Hence $FeSO_4$ was included in the reaction mixture in this work.

Interference Studies

Several common ingredients and/or additives of commercial soy sauce and pickles soaked in soy sauce were studied for their possible interfering effects in the determination of BA by the proposed method. The concentrations of interfering substances tested were limited to their possible ranges in normal soy sauce and pickles. Table 1 shows that none of the compounds studied interfered with the proposed method.

Calibration

A series of working standard solutions of BA were subjected to the assay. The relationship between the decrease in absorbance (ΔA) at 340 nm and the concentration (c) of BA was obtained by the least-squares method: $c = 18.75\ \Delta A + 0.02$.

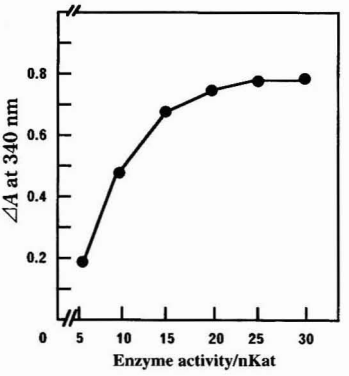

Fig. 2 Effect of BA hydroxylase activity on maximum reaction rate. Concentration of BA, 15 μg cm^{-3}; ΔA represent the decrease in absorbance at 340 nm.

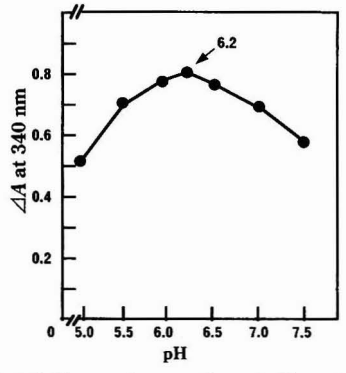

Fig. 1 Effect of pH on maximum reactions rate. Concentration of BA, 15 μg cm^{-3}; ΔA represents the decrease in absorbance at 340 nm.

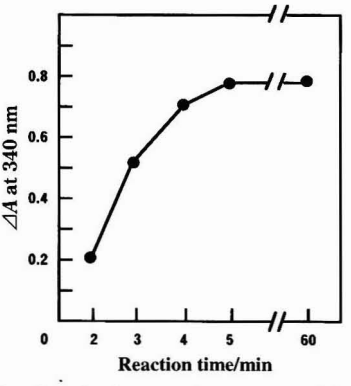

Fig. 3 Effect of reaction time on maximum enzyme activity. Concentration of BA, 15 μg cm^{-3}, ΔA represents the decrease in absorbance at 340 nm.

Recovery

Commercial soy sauce and pickles that had been verified to be free from BA were selected for the preparation of samples containing 30 and 300 μg g^{-1} of BA by adding the stock standard solution to the homogenized sample. The results are given in Table 2, and indicate that satisfactory recoveries were achieved for the samples examined.

Precision and Limit of Determination

The within-laboratory variability (inter-assay precision) was assessed by repetitive analyses of a standard BA solution added to a blank soy sauce sample; the results are being shown in Table 3. The RSD at the 5 and 15 μg cm^{-3} levels were 1.7 and 1.1%, respectively (five determinations).

The precision of the procedure for real samples was checked by repetitive analyses (n = 3) of five samples, which were positive for BA among the 20 samples of commercial soy sauce and pickles. The results in Table 4 indicate satisfactory precision for this determination. The proposed method has a limit of determination of 5 μg g^{-1}, calculated as the amount equal to ten times the standard deviation of the blank, when 5 g of sample were analysed.

Comparison With HPLC

The proposed method was compared with an HPLC method.[11] Five positive samples (two kinds of soy sauce, scallion, Japanese radish and cucumber soaked in soy sauce) analysed by the proposed method (see Table 4) were used for this comparison, and the results obtained by HPLC are also given in Table 4. The linear regression equation was obtained by the least-squares method and was found to be $y = 0.901x + 0.08$, where x and y represent the results given by HPLC and the proposed method, respectively. The correlation coefficient was 0.965. Hence there is close agreement between the results obtained by the two methods.

Conclusion

It has been demonstrated that the proposed method can be applied to the determination of BA in soy sauce and pickles with

Table 1 Effect of possible interfering substances

Substance*	Concentration/ μg cm^{-3}	Response (ΔA)†
None (control)	—	0.533
Ascorbic acid	10000	0.533
Sorbic acid	1000	0.534
p-Hydroxybenzoic acid	100	0.535
Salicylic acid	100	0.533
Nicotinic acid	200	0.532

* Each compound tested was mixed with BA standard solution (10 μg cm^{-3}), then subjected to analysis. † ΔA represents the decrease in absorbance at 340 nm.

Table 2 Recovery of BA from spiked soy sauce and pickles

Food	BA added/μg*	Recovery (%)†
Soy sauce (A)	30	96.2 ± 2.3
	300	99.1 ± 2.5
Soy sauce (B)	30	95.9 ± 3.1
	300	98.9 ± 2.7
Seaweed (soaked in soy sauce)	30	97.1 ± 2.9
	300	99.3 ± 3.3
Japanese radish (soaked in soy sauce)	30	98.6 ± 1.9
	300	99.7 ± 2.5
Scallion (soaked in soy sauce)	30	96.4 ± 2.3
	300	98.9 ± 2.4

* BA was added to 1 g of each sample at the level indicated. † Results are means of triplicate determinations ± RSD.

Table 3 Precision of the method in the determination of BA added to soy sauce. Standard BA solution was added to commercial soy sauce free from BA to give the concentration indicated

Replicate	Spiked value/ μg cm^{-3}	Analytical value/ μg cm^{-3}	Spiked value/ μg cm^{-3}	Analytical value/ μg cm^{-3}
1	5.0	5.1	15.0	14.8
2	5.0	4.9	15.0	15.2
3	5.0	5.0	15.0	14.9
4	5.0	5.1	15.0	15.0
5	5.0	5.0	15.0	15.1

Table 4 Determination of BA in soy sauce and pickles

	BA content*/μg g^{-1}					
	Proposed method			HPLC method†		
Food	Replicate values	Mean	s	Replicate values	Mean	s
Soy sauce (1)	305, 302 308	305	3.0	307, 301 304	304	3.0
Soy sauce (2)	435, 438 432	435	3.0	429, 423 431	428	4.2
Scallion, (soaked in soy sauce)	80, 81 78	79.6	1.5	78, 82 81	80.3	2.0
Japanese radish (soaked in soy sauce)	51, 49 50	50.3	1.0	48, 52 48	49.3	2.3
Cucumber (soaked in soy sauce)	116, 118 113	115.6	2.5	109, 116 108	111	4.4

* Triplicate analyses were performed on each sample. † Ref. 11.

acceptable precision, and the assay is faster (20 min per run) than HPLC (more than 60 min per run).

References

1 Chandan, R. C., Gordon, J. F., and Morrison, A., *Milchwissenschaft*, 1977, **32**, 534.
2 Larsson, B. K., *J. Assoc. Off. Anal. Chem.*, 1983, **66**, 775.
3 Leuenberger, U., Gauch, R., and Baumgartner, E., *J. Chromatogr.*, 1979, **173**, 343.
4 Archer, A. W., *Analyst*, 1980, **105**, 407.
5 Puttermans, M. L., Branders, C., Dryon, L., and Massart, D. L., *J. Assoc. Off. Anal. Chem.*, 1985, **68**, 80.
6 Ali, M. S., *J. Assoc. Off. Anal. Chem.*, 1985, **68**, 488.
7 Bui, L. V., and Copper, C., *J. Assoc. Off. Anal. Chem.*, 1987, **70**, 892.
8 Dagley, S., Evans, W. C., and Ribbons, D. W., *Nature (London)*, 1960, **188**, 560.
9 Byrde, R. J. W., Harris, J. F., and Woodcock, D., *Biochem. J.*, 1956, **64**, 154.
10 Reddy, C., and Vaidyanathan, C. S., *Biochim. Biophys. Acta*, 1975, **384**, 46.
11 Ikai, Y., Oka, H., Kawamura, M., and Yamada, M., *J. Chromatogr.*, 1988, **454**, 333.

Paper 6/06537F
Received September 23, 1996
Accepted November 25, 1996

Spectrophotometric Determination of Cobalt(II) Using the Chromogenic Reagent 4,4′-Diazobenzenediazoaminoazobenzene in a Micellar Surfactant Medium

Gu Jin, Yurui Zhu, Wanquan Jiang, Boping Xie and Bin Cheng

Department of Applied Chemistry, University of Science and Technology of China, Hefei, Anhui, 230026, China

A highly sensitive spectrophotometric method for the determination of cobalt(II) using the chromogenic reagent 4,4′-diazobenzenediazoaaminoazobenzene (BBDAB) was developed. The optimum conditions for the chromogenic reaction of cobalt(II) with BBDAB were studied in the presence of Triton X-100 and sodium tetraborate. The calibration graphs were rectilinear in the range 0–7 μg per 25 cm³ cobalt(II). The apparent molar absorptivity is 1.72×10^5 dm³ mol^{-1} cm^{-1} with a Sandell's sensitivity of 0.00035 μg cm^{-2}. The method was applied to the determination of cobalt in soil and vitamin B_{12} with satisfactory results.

Keywords: *4,4′-Diazobenzenediazoaminoazobenzene; cobalt determination; spectrophotometry; soil; vitamin B_{12}*

The spectrophotometry of micro amounts of cobalt has recently attracted much attention owing to environmental concerns. Various spectrophotometric methods for the determination of cobalt using dithizone,[1] 4-(2-pyridylazo)resorcinol (PAR),[2] zincon,[3] 6-amino-4-hydroxy-5-(2-hydroxy-4-nitrobenzeneazo)naphthalene sulfoacid,[4] 5-(2-amino-4-hydroxybenzeneazo)-*o*-benzenebromethyl hydrazide,[5] *etc.*, have already been reported. However, most methods are relatively complicated and organic solvent extraction is necessary, usually using a toxic organic solvent such as chloroform. In addition, many of the current reagents for the spectrophotometric determination of cobalt lack high sensitivity.

A highly sensitive chromogenic agent, 4,4′-diazobenzenediazoaminoazobenzene (BBDAB), has been synthesized and used to determine trace nickel and cadmium by spectrophotometry.[6,7] In this paper, a simple, sensitive, spectrophotometric determination of cobalt(II) using BBDAB in water-soluble surfactant micellar media is proposed. In the presence of the non-ionic surfactant Triton X-100, BBDAB reacted instantaneously with cobalt to form a red 1 : 3 (cobalt–reagent) complex in sodium tetraborate buffer solution of pH 10.2. The calibration graphs were rectilinear in the range 0–7 μg per 25 cm³ cobalt(II) and the colour system is stable for at least 24 h. The apparent molar absorptivity is 1.72×10^5 dm³ mol^{-1} cm^{-1}. The Sandell's sensitivity is 0.00035 μg cm^{-2}. The method has been applied to the determination of cobalt in soil and vitamin B_{12} without further extraction or separation.

Experimental

Apparatus

The spectrophotometers used were a UV-240 (dual-wavelength double-beam recording spectrophotometer) (Shimadzu, Tokyo, Japan) and a Model 721 spectrophotometer from Shanghai, China. A pHS-3C pH meter (Shanghai, China) was used.

Reagents

All reagents and solvents were of analytical-reagent grade except where indicated. Distilled water was used throughout.

Cobalt(II) stock standard solution, 5.0 μg ml^{-1}, was prepared by dissolving 0.1000 g of pure cobalt in 10 ml of 9 mol l^{-1} nitric acid and diluting to 100 ml with distilled water in a calibrated flask. A 5.00 μg ml^{-1} working standard solution was prepared by dilution with distilled water.

BBDAB solution, 0.05% m/v in *N*,*N*-dimethylformamide (DMF), was prepared by dissolving 0.125 g of BBDAB in 250 ml of DMF. Triton X-100, 2% v/v aqueous solution, was prepared by dissolving 4.0 ml of Triton X-100 in 200 ml of water. $Na_2B_4O_7 \cdot 10H_2O$ buffer solution was prepared by dissolving 20 g of sodium tetraborate in 500 ml of distilled water and adjusting the pH with 1 mol l^{-1} sodium hydroxide. Mixed masking agent was prepared by dissolving 0.2 g of KCN and 5.0 g of NaF in 100 ml of 0.1 mol l^{-1} sodium tartrate and mixing thoroughly.

Recommended Procedure

General procedure

Transfer 5 μg of cobalt(II) into a 25 ml calibrated flask and add 3.0 ml of buffer solution (pH 10.2), 1.0 ml of 2% v/v Triton X-100 solution and 2.5 ml of 0.05% BBDAB solution. Dilute to the mark with distilled water and mix well. Measure the absorbance of the coloured solution at 540 nm in a 1 cm cell against a reagent blank.

Procedure for the determination of cobalt(II) in samples

Place a suitable volume of a sample containing not more than 7 μg of cobalt(II) in a 25 ml calibrated flask. Add 3 ml of buffer solution (pH 10.2), 1.0 ml of 2% v/v Triton X-100 solution, 3.0 ml of 0.05% BBDAB solution and 1 ml of mixed masking reagent and mix well. Dilute to the mark with deionized water and mix well. Measure the absorbance at 530 nm in a 1 cm cell against a reagent blank. Prepare a calibration graph for the standard cobalt(II) solution in the same way.

Results and Discussion

Absorption Spectra

The absorption spectra of the ligand BBDAB and of its complex with cobalt(II) are shown in Fig. 1. It is evident that the maximum absorption of the free ligand is at 428 nm and that of the complex is at 540 nm, a difference of 112 nm.

Choice of Surfactant and Effect of Triton X-100 Concentration

The reaction systems between cobalt(II) and BBDAB in the presence or absence of different kinds of surfactants, such as

cetyltrimethylammonium bromide, sodium dodecyl sulfate, sodium *N*-lauroylsarcosine, Tween-60, Triton X-100 and Tween-80, were studied. The reaction system in the absence of a surfactant is unstable, inconvenient and insensitive in comparison with the reaction system in the presence of a surfactant, but a non-ionic surfactant is most effective, and Triton X-100 was the best regarding sensitivity and stability. A maximum and constant absorbance could be obtained by the addition of 0.5–2.0 ml of 2% Triton X-100 solution.

Effect of pH *and Sodium Tetraborate Concentration*

A maximum and constant absorbance was obtained in the pH range of 10.0–10.5 using 2.0 ml of sodium tetraborate buffer solution. Therefore, all subsequent studies were carried out at pH 1.2.

Effect of BBDAB Concentration

The effect of the amount of BBDAB on the procedure was studied while keeping the amount of cobalt(II) constant at pH 10.20. A maximum and almost constant difference of the absorbance was obtained by using 2.0–3.0 ml of 0.05% BBDAB solution. Hence 2.5 ml of the reagent were used in subsequent studies.

Rate of Reaction and Stability of the Complex

In the presence of Triton X-100, the formation of the coloured complex of cobalt(II) with BBDAB is instantaneous and the absorbance of the complex remains virtually constant for at least 24 h at room temperature or by heating below 40 °C.

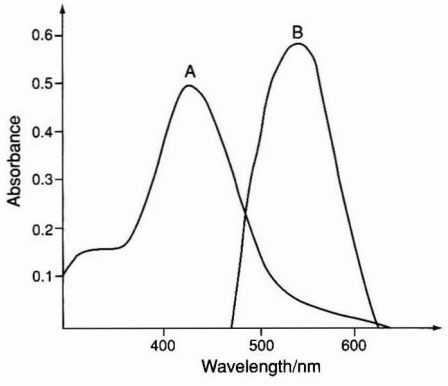

Fig. 1 Absorption spectra of BBDAB and its cobalt complex at pH 10.2, using a 1 cm cell. A, 1.2×10^{-5} M BBDAB against water; B, 5 μg cobalt and 1.2×10^{-4} M BBDAB against reagent blank.

Adherence to Beer's Law and Sensitivity

A calibration graph for the determination of cobalt(II) was obtained using the proposed procedure. Beer's law was followed in the range 0–7 μg of cobalt(II) per 25 ml. The Sandell's sensitivity was 3.5×10^{-4} μg cm^{-2}. BBDAB is one of the most sensitive reagents for cobalt(II) and the proposed method compares favourably with existing methods. The sensitivities of various reagents are compared in Table 1.

Composition of the Complex

The composition of the complex was determined by the equilibrium shifting method (Fig. 2). A ratio of cobalt to BBDAB of 1:3 in the complex molecule was obtained. The stability constant, calculated by the equilibrium shift method, was $K_{ex} = 3.8 \times 10^{23}$.

Effect of Interfering Ions

A systematic study of interfering ions in the determination of 5 μg of cobalt(II) was made and the stated levels of the following species did not cause an error exceeding 5%: 50 mg of Na^+, K^+, Cl^-, F^-, sodium tartrate and thiourea, 25 mg of Br^-, 10 mg of I^-, SO_3^{2-}, SO_4^{2-}, NO_3^-, NO_2^-, CO_3^{2-}, $S_2O_3^{2-}$, PO_4^{3-} and sodium citrate, 5 mg of Ca^{2+}, SCN^- and CN^-, 2 mg of Sr^{2+}, Ba^{2+} and Mg^{2+}, 1 mg of $C_2O_4^{2-}$, 500 μg of Mn^{2+}, 200 μg of Al^{3+}, 100 μg of Pb^{2+}, Ce^{4+}, Au^{3+} and V^V, 50 μg of Cr^{VI}, Sn^{4+}, Ga^{3+}, La^{3+}, Ag^+, Sb^{3+}, W^{VI} and Mo^{VI}, 10 μg of Pd^{2+}, Zr^{4+} and Be^{2+} and 5 μg of Fe^{3+}, Ti^{4+}, Nb^{5+} and Cr^{3+}. However, Hg^{2+}, Ni^{2+}, Cd^{2+}, Cu^{2+} and Zn^{2+} caused positive interferences at the same concentration level as Co^{II}. The interference of 2.5 mg of Fe^{3+}, 500 μg of Ti^{4+}, Nb^{5+} and Zn^{2+}, 200 μg of Ni^{2+}, Cr^{3+}, V^{5+}, Sb^{3+} and Zr^{4+} and 100 μg of Cu^{2+}, Cd^{2+}, Pd^{2+}, Ce^{2+} and Hg^{2+} can be eliminated by adding 1.0 ml of mixed masking agent. The allowed amounts of interfering ions in a mixture are 2.5 mg of Fe^{3+}, 400 μg of Ti^{4+}, 200 μg of Sb^{3+} and Zr^{4+}, 100 μg of Nb^{5+}, Ce^{3+} and V^{5+}, 50 μg of Cr^{3+}, 20 μg of Zn^{2+}, Cu^{2+} and Ni^{2+} and 10 μg of Cd^{2+} and Hg^{2+}.

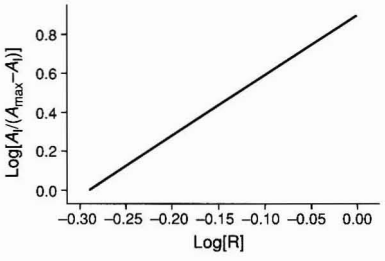

Fig. 2 Determination of the composition of the Co^{II}–BBDAB complex by the equilibrium shift method. $[Co^{II}] = 3.4 \times 10^{-6}$ M; other conditions as Fig. 1.

Table 1 Comparison of reagents for the spectrophotometric determination of cobalt

Reagent	pH	λ_{max}/nm	Range/μg	ε/l mol^{-1} cm^{-1}	Ref.
7-Nitroso-8-hydroxyquinoline-5-sulfonic acid	3.5–8.0	530	250–750	1.21×10^4	6
2-(2-Thiazolylazo)benzoic acid	5.0	655	0–12	1.13×10^5	7
2,2-Dipyridyl-2-benzothiazolyl hydrazone	2.0–9.3	520		3.43×10^4	8
2-(5-Nitro-2-pyridiineazo)-5-dimethylaminobenzoic acid	5.0–7.0	530	0–14	1.30×10^5	9
Cadion 2B	8.8–9.3	550	0–10	1.12×10^5	10
2-(2-Bromobenzothiazolyl)azo-5-dimethylaminobenzoic acid	4.0–4.5	705	0–10	1.18×10^5	11
2-[2-(3,5-Dibromopyridyl)azo]-5-diethylaminobenzoic acid	2.1–5.4	560	0–5	1.52×10^5	12
BBDAB	10.0–10.5	540	0–7	1.72×10^5	This work

Table 2 Results for the determination of cobalt in soil samples from the China National Environmental Monitoring Centre

Sample	Co^{II} (ppm) Added	Measured	Recovery (%)	RSD (%)	Stated value (ppm)
ESS-1 (GSBZ500011-87)	0	15.2		3.8	14.8 ± 0.7
	10.0	25.6	98–104	4.5	
ESS-2 (GBSZ500012-87)	0	26.6		5.1	25.6 ± 1.2
	10.0	36.5	95–101	4.2	

Table 3 Results for the determination of cobalt in vitamin B_{12} (n = 9)

Sample	Co^{II} (ppm) Added	Measured	Recovery (%)	RSD (%)	Certified value (ppm)
Vitamin B_{12} (910701)	0	0.85		2.5	0.85*
	1.00	1.84	98–104	2.2	
Vitamin B_{12} (920709)	0	0.81		3.1	0.82*
	1.00	1.81	98–102	2.8	

* Determined by AAS.

Analysis of Samples

Determination of cobalt(II) in soil

An exact mass of soil (0.100 g), dried at 110 °C, was treated with 3 ml of concentrated nitric acid and 6 ml of concentrated hydrochloric acid at low temperature until the evolution of brown oxides of nitrogen had ceased. The mixture was then evaporated nearly to dryness. The residue was decomposed by heating with 20 ml of 0.1 M sulfuric acid, the insoluble material was then filtered off and washed. The filtrate and washing water were collected in a beaker, then heated to a small volume. The solution was neutralized with 0.1 M sodium hydroxide, then transferred into a 25 ml calibrated flask, following the steps as in Procedure for the determination of cobalt(II) in samples. The results are given in Table 2. The results obtained agreed with the stated values.

Determination of cobalt(II) in vitamin B_{12} injection

Place the hydroxocobalimin (vitamin B_{12}) injection in a 250 ml flask, add 2–3 ml of nitric acid for dissolution transfer into a 100 ml calibrated flask, dilute to the mark with distilled water and mix well, then follow the steps as in General procedure. The results are given in Table 3.

This project was partly supported by the National Natural Science Foundation of China.

References

1 McClellan, B. E., and Sabel, P., *Anal. Chem.*, 1969, **41**, 1077.
2 Maulive, S. G., Pyatnitskii, I. V., and Kolements, L. K., *Chem. Anal. (Warsaw)*, 1981, **35**, 861.
3 Sekheta, M. A., Milovanović, G. A., and Janjić, T. J., *Mikrochim. Acta*, 1978, 297.
4 Dedkora, V. P., Azarashvihi, M. A. A., and Sawin, S. D., *Zh. Anal. Khim.*, 1989, **44**, 2012.
5 Ma, H.-M., and Huang, X.-S., *Hua Xue Xue Bao*, 1994, **52**, 1199.
6 Ozaki, T., *Anal. Lett.*, 1982, **15**, 595.
7 Wada, H., Ishizuki, T., and Nakagawa, G., *Anal. Chim. Acta.*, 1982, **135**, 333.
8 Singh, R. B., Odashima, T., and Ishii, H., *Analyst.*, 1984, **109**, 43.
9 Tong, Y., Liu, Y.-P., and Lou, J.-C., *Fenxi Shiyanshi*, 1993, **12**, 25.
10 Cai, Y.-Z., *Huaxue Shiji*, 1991, **13**, 176.
11 Katami, T., Hayakawa, T., Furukawa, M., and Shibata, S., *Analyst*, 1985, **110**, 399.
12 Sheng, H.-X., and Li, J.-Z., *Fenxi Huaxue*, 1988, **16**, 301.

Paper 6/06804I
Received September 4, 1996
Accepted November 14, 1996

Characterization of Surfactant Selectivity in Micellar Electrokinetic Chromatography

Salwa K. Poole[a] and Colin F. Poole*[ab]

[a] *Zeneca/SmithKline Beecham Centre for Analytical Chemistry, Imperial College of Science, Technology and Medicine, South Kensington, London, UK SW7 2AY*
[b] *Department of Chemistry, Wayne State University, Detroit, MI 48202, USA.*
E-mail: cfp@chem.wayne.edu

The solvation parameter model is used to delineate the contribution of individual intermolecular interactions to the retention properties of seven common surfactants used in micellar electrokinetic chromatography. Buffer composition and concentration, pH, temperature, and voltage had only a small influence on selectivity for sodium cholate micelles in the normal experimental range for separations. Surfactant concentration was found to affect retention by changing the phase ratio without significantly changing selectivity while the addition of organic solvent in low concentration (up to 10% v/v) has an influence on the solvophobic properties of the buffer (lowers cohesion and reduces its capacity as a hydrogen-bond acid) in a manner which seems to depend very little on solvent identity. The bile salt surfactants, sodium cholate, sodium deoxycholate, sodium taurocholate, and sodium deoxytaurocholate, are quite similar as a group, exhibiting modest differences in their cohesion and hydrogen-bond acidity. Sodium dodecyl sulfate has complementary properties to the bile salt surfactants; it is less cohesive and a weaker hydrogen-bond base and a stronger hydrogen-bond acid. The sodium salt of *N*-dodeconyl-*N*-methyltaurine is a stronger hydrogen-bond base than the support buffer and weak hydrogen-bond acid; again properties that set it apart from the bile salts and sodium dodecyl sulfate for the separation of hydrogen-bonding solutes. Hexamethyltrimethylammonium bromide is the least cohesive and the strongest hydrogen-bond base of the surfactants studied but its relatively small migration window may make it less useful in practice for complex separations. Lithium perfluorooctanesulfonate has rather unique selectivity (high cohesion, significant capacity for dipole-type interactions and strong hydrogen-bond acidity) that would make it a good choice with the other surfactants for general selectivity optimization in methods development.

Keywords: *Micellar electrokinetic chromatography; surfactant selectivity; solvation parameter model; experimental parameters that influence selectivity; surfactant selection*

Micellar electrokinetic chromatography (MEKC) is a member of a family of recently introduced separation techniques using electrophoretic or electroosmotic principles as the basis of the differential migration mechanism resulting in separation.[1–4] The distinguishing feature of MEKC is the addition of a surfactant above its critical micelle concentration to the separation buffer such that in an electric field the migration velocity of the micelles and the bulk electrolyte in the direction of general flow are different. Neutral solutes can then be separated if they have different distribution constants between the bulk electrolyte and the micelle phase and will be eluted within the migration window established by the difference in the velocity between the micelle phase and the bulk electrolyte. In the same system ionized solutes can be separated by a combination of differences in their distribution between phases and their effective electrophoretic mobility. The high kinetic efficiency and the possibility of separating both neutral and ionized solutes in the same system are a considerable attraction of MEKC and this combined with the flexibility of adjusting selectivity that can be achieved by adding complexing agents (*e.g.*, cyclodextrins, urea, *etc.*), different surfactants or organic solvents to the separation buffer, has resulted in an extensive number of practical applications. The commonality of the instrumentation for MEKC and capillary electrophoresis has removed any hurdles to the use of micellar-based separation systems in laboratories equipped for capillary electrophoresis.

Although many acceptable separations have been published by MEKC the general approach to methods development is largely based on trial and error experiments assisted by some useful formal general observations.[2,3,5–8] Resolution depends mainly on the choice of the surfactant system, operation under conditions resulting in an acceptable migration window, and maintenance of experimental conditions that provide high kinetic efficiency. These parameters in turn are influenced by the applied field; buffer composition, ionic strength, and pH; capillary surface characteristics; temperature; surfactant type and concentration; and choice of organic modifier and concentration. More often than not these parameters do not vary independently. Some of these aspects will be discussed in the results and discussion section with supporting experimental evidence.

Formal attempts to predict retention in MEKC based on an understanding of the contribution of intermolecular interactions are quite rare. The Kamlet–Taft solvatochromic model, eqn. (1), was applied by Chen *et al.*[9] to estimate the contribution of defined intermolecular interactions to the water–sodium dodecyl sulfate micelle distribution constant of substituted benzene compounds and more extensively by Yang and co-workers[10–13] to characterize the retention properties of aqueous buffer–micelle systems containing the surfactants sodium dodecyl sulfate, sodium cholate, tetradecyltrimethylammonium bromide, and lithium perfluorooctanesulfonate. The product terms ($mV/100$) representing cavity formation, ($s\pi^*$) the

$$\log k = c + mV/100 + s\pi^* + b\beta + a\alpha \quad (1)$$

contribution from dipole-type interactions, and ($b\beta$ and $a\alpha$) the contribution of hydrogen bond acid/base interactions to the retention factor (capacity factor), k. These authors concluded that the type of surfactant has a major influence on selectivity and the size of the migration window but surfactant concentration only influences absolute retention through changes in the phase ratio of the separation system without changing selectivity. For sodium dodecyl sulfate and sodium cholate retention depends mainly on the size of the solute (the micelles are less cohesive than the aqueous buffer) and the basicity of the solute

(water is a strong hydrogen-bond acid favoring retention of hydrogen-bond bases in the buffer). Other factors are of little importance. In the case of lithium perfluorooctanesulfonate the micelles are more cohesive than sodium dodecyl sulfate and sodium cholate, are as strong hydrogen-bond acids as water itself, and weak (by comparison) hydrogen-bond bases. This is a most remarkable result because the perfluorooctanesulfonate group contains no hydrogen-bond acid groups (note proton acidity and hydrogen-bond acidity are unrelated concepts) and the inductive effect of fluorine increases the hydrogen-bond basicity of the perfluorooctanesulfonates, which would be expected to increase their competitive capacity with the aqueous buffer to retain hydrogen-bond acid solutes.[14,15] Tetradecyltrimethylammonium bromide has similar cohesive properties to sodium dodecyl sulfate and sodium cholate but is a significantly stronger hydrogen-bond base than these surfactants and a very weak hydrogen-bond acid, in reasonable agreement with chemical intuition. Thus for all four surfactants differences in their selectivity were assigned to variations in cohesive structure of the micelles and different capacities for hydrogen-bond interactions, with differences in the capacity for dipole-type interactions largely irrelevant.

In many areas of retention modeling in chromatography, for example, stationary phase characterization in gas chromatography[16–19] and retention mapping in column and thin-layer liquid chromatography[20–25] the solvation parameter model has been found preferable to the solvatochromic model. The solute descriptors in the solvation parameter model are clearly free energy related parameters and values for in excess of 2000 solutes are available.[18,22,26–28] The solvation parameter model in a form suitable for characterizing the distribution of solutes between two condensed phases can be set out as indicated by eqn. (2)

$$\log k = c + mV_X/100 + rR_2 + s\pi_2^H + a\alpha_2^H + b\beta_2^H \qquad (2)$$

where V_X is the solute's characteristic volume, R_2 excess molar refraction, π_2^H the ability of the solute to stabilize a neighboring dipole by virtue of its capacity for orientation and induction interactions, and α_2^H and β_2^H are parameters characterizing the solute's effective hydrogen-bond acidity and hydrogen-bond basicity, respectively. The system constants in eqn. (2) are unambiguously defined: the r constant refers to the difference in capacity of the buffer and micellar phase to interact with solute n- or π-electrons; the s constant to the difference in capacity of the buffer and micellar phase to take part in dipole–dipole and dipole-induced dipole interactions; the a constant is a measure of the difference in hydrogen-bond acceptor basicity of the buffer and micellar phase; the b constant is a measure of the difference in hydrogen-bond donor acidity of the buffer and micellar phase; and the m constant is a measure of the relative ease of forming a cavity for the solute in the buffer and micellar phase. For any MEKC system the system constants can be obtained using multiple linear regression analysis. Experimentally data are acquired for the observed parameter, log k, for a group of solutes of known properties sufficiently varied to define all interactions in eqn. (2) and of sufficient number to establish the statistical validity of eqn. (2).

Abraham *et al.* used the solvation parameter model to characterize the distribution constant of solutes between water and sodium dodecyl sulfate micelles[29] and the retention factor for an oil-in-water type emulsion consisting of 1.4% m/m sodium dodecyl sulfate, 6.49% m/m butan-1-ol, and 0.82% m/m heptane in 100 mM borate–500 mM phosphate buffer at pH 7.[30] The system constants along with the statistics for the fit are assembled in Table 1, row A and L, respectively. Adlard *et al.*[31] have provided a collection of retention factor values for substituted benzene compounds in separation systems containing 40 mM potassium deoxycholate (rows G and H) and 40 mM 3β-glucopyranosyl-5β-cholan-12α-hydroxy-24-oic acid potassium salt (row I) and Herbert and Dorsey[32] for 50 mM sodium

Table 1 Application of the solvation parameter model to micellar separation systems. Surfactants: SDS = sodium dodecyl sulfate; SC = sodium cholate; KDOC = potassium deoxycholic acid; KGDC = potassium salt of 3β-glucopyranosyl-5β-cholan-12α-hydroxy-24-oic acid; LPOS = lithium perfluorooctanesulfonate; and TDTMA = tetradecyltrimethylammonium bromide

Row number	Surfactant/ mM	System constants						Statistics*				pH	Reference
		m	r	s	a	b	c	R	SE	F	n		
A	SDS	2.79	0.54	−0.40	−0.13	−1.58	1.20	0.985	0.17	817	187	7	29
		(0.07)	(0.06)	(0.07)	(0.06)	(0.08)	(0.06)						
B	SDS	2.91	0.31	−0.24	−0.44	−1.87	−1.85	0.994	0.11	397	32	7[a]	32
	(50)	(0.17)	(0.08)	(0.08)	(0.08)	(0.15)	(0.15)						
C	SDS	2.81	0.38	−0.28	−0.16	−1.80	−2.18	0.992	0.07	513	47	7[b]	33
	(20)	(0.09)	(0.06)	(0.08)	(0.05)	(0.09)	(0.08)						
D	SDS	2.82	0.37	−0.33	−0.17	−1.82	−1.80	0.991	0.08	457	47	7[b]	33
	(40)	(0.09)	(0.06)	(0.09)	(0.05)	(0.09)	(0.08)						
E	SC	2.41	0.57	−0.55		−2.45	−1.60	0.984	0.10	328	47	7[b]	33
	(60)	(0.12)	(0.09)	(0.11)		(0.13)	(0.12)						
F	SC	2.63	0.40	−0.60		−2.59	−1.47	0.986	0.10	294	47	7[b]	33
	(80)	(0.12)	(0.08)	(0.12)		(0.12)	(0.11)						
G	KDOC	3.12	0.54	−0.97		−2.47	−1.96	0.992	0.10	135	14	8	31
	(40)	(0.18)	(0.16)	(0.20)		(0.27)	(0.15)						
H	KDOC	2.76	0.67	−0.88		−2.42	−1.80	0.992	0.10	140	14	9	31
	(40)	(0.16)	(0.14)	(0.18)		(0.25)	(0.13)						
I	KGDC	2.89	0.24			−2.97	−2.14	0.990	0.10	142	13	9	31
	(40)	(0.21)	(0.12)			(0.21)	(0.19)						
J	LPOS	2.28	−0.54	0.48	−0.89	−0.60	−2.05	0.979	0.10	189	47	7[b]	33
	(40)	(0.12)	(0.08)	(0.11)	(0.07)	(0.12)	(0.11)						
K	TDTMA	2.76	0.28		0.94	−2.62	−2.09	0.989	0.09	422	47	7[b]	33
	(10)	(0.11)	(0.07)		(0.06)	(0.10)	(0.10)						
L	Emulsion	3.05	0.28	−0.69	−0.06	−2.81	−1.13	0.994	0.09	791	53	7[c]	30

* R = correlation coefficient; SE = standard error in the estimate; F = F-statistic; n = number of solutes; and numbers in parentheses indicate the standard deviation in the coefficient. [a] 100 mM borate–60 mM phosphate buffer. [b] 50 mM phosphate buffer. [c] 1.4% m/m sodium dodecyl sulfate, 6.49% m/m butan-1-ol and 0.82% m/m heptane in 100 mM borate–500 mM phosphate buffer.

dodecyl sulfate at pH 7 in 100 mM borate–60 mM phosphate buffer (row B). This data we have fitted to the solvation parameter model summarizing the system constants and the statistics for the fit in Table 1. Finally, we had solute descriptors for 47 of the 60 solutes studied by Yang and co-workers[10–13] and Khaledi,[33] discussed earlier in connection with the solvatochromic model, and have fitted this data to the solvation parameter model, summarizing the results in rows C–F, J, and K in Table 1.

In all cases the statistics for the fit of the model to the data are good with that for lithium perfluorooctanesulfonate being the poorest (Table 1, row J). For sodium dodecyl sulfate and the bile salt surfactants (Table 1, row A to I) the cavity contribution (*m* constant) and lone pair–lone pair electron attraction (*r* constant) favor sorption by the micelle while dipole-type interactions (*s* constant) and hydrogen-bond interactions (*a* and *b* constants) favor retention in the aqueous buffer. Sodium dodecyl sulfate, sodium cholate and potassium deoxycholate differ to a small extent in their cohesive energy (ease of cavity formation) but more significantly in their capacity for dipole-type interactions and hydrogen-bond interactions. Sodium cholate and potassium deoxycholate micelles are significantly weaker hydrogen-bond acids than sodium dodecyl sulfate (*b* constant); stronger hydrogen-bond bases (*a* constant); and show a range of capacity for dipole-type interactions in the order potassium deoxycholate < sodium cholate < sodium dodecyl sulfate. The derivatization of potassium deoxycholate with a sugar group (row I) leads to significant changes in selectivity for polar interactions, particularly for interactions of a dipole-type (*s* constant). Lithium perfluorooctanesulfonate (Table 1, row J) is the most cohesive of the micelles (*m* constant), is the most competitive with the aqueous buffer as a hydrogen-bond acid (*b* constant) and for dipole-type interactions (*s* constant), and is a very weak hydrogen-bond base (*a* constant). The negative *r* constant is characteristic of fluoroalkane compounds, in general, representing their lower polarizability compared to alkane chains. Since the perfluorooctanesulfonate group has no available protons for hydrogen bonding we can only speculate that its hydrogen-bond acidity arises from the inductive effect of fluorine on water molecules selectively solvating the sulfonate group. The characteristic feature of tetradecyltrimethylammonium bromide is its strong hydrogen-bond basicity (*a* constant) compared to the other surfactants. Features to note about the data in Table 1 are that (*a*) the solvation parameter model provides a consistent and chemically sensible interpretation of the data, (*b*) the details of the interpretation are different to those of the solvatochromic model used by Yang and co-workers[10–13] (particularly with respect to the relative importance of polar interactions), and (*c*) the identity of the surfactant is the most important factor in controlling selectivity. Differences in the results between the solvation parameter model and solvatochromic model certainly arise because of numerical differences in the solute descriptors (which are derived from different measurement techniques) and also because Yang and co-workers[10–13] used estimates for many descriptors unavailable by experiment.

The results in Table 1 cannot indicate how the selectivity of a surfactant depends on the full range of experimental variables in MEKC nor provide information about the selectivity of other common surfactants for which there is insufficient experimental data available to satisfy the requirements of the solvation parameter model. We will address both of these points in this paper.

Experimental

Sodium tetraborate, sodium phosphate, sodium dodecyl sulfate, cholic acid sodium salt, taurocholic acid sodium salt, taurodeoxycholic acid sodium salt monohydrate, *N*-dodecanoyl-*N*-methyltaurine sodium salt, hexadecyltrimethylammonium bromide, and 0.1 and 1.0 M sodium hydroxide were obtained from Fluka (Gillingham, Dorset, UK). 1-Phenyloctane and the solutes used for retention measurements (Table 2) were obtained from Aldrich (Gillingham, Dorset, UK). Fused silica capillary tubing of 0.05 mm id was obtained from Composite Metal Services (The Chase, Harlow, Worcestershire, UK) and cut to the required length. Windows for on-column detection were prepared by using an electrical ring heater (built in-house) to burn off a small segment of the protective polyimide coating from the fused silica capillary column. All solvents and water were HPLC grade from J. T. Baker (Milton Keynes, Buckinghamshire, UK).

All separations were performed with a Hewlett-Packard ^{3D}CE system (Stockport, Cheshire, UK) with a UV diode array detector and laser jet printer. The fused-silica capillaries were 48.5 cm long (effective length 40 cm) for the determination of system constants and 80.5 cm (effective length 72 cm) for the separations used in the figures. Prior to each separation the capillaries were flushed with 0.1 M sodium hydroxide for 2 min followed by the separation buffer for 5 min. For hexadecyltrimethylammonium bromide additional conditioning was required to obtain stable results. The capillary was flushed with 1.0 M sodium hydroxide for 2 min followed by water for 5 min, and then the normal conditioning cycle was commenced. Each surfactant was studied using a fresh capillary for the determina-

Table 2 Solute descriptors used in the solvation parameter model

	Descriptors				
Solute	$V_x/100$	R_2	π_2^H	α_2^H	β_2^H
Benzene	0.7164	0.610	0.52		0.14
Toluene	0.8573	0.601	0.52		0.14
Ethylbenzene	0.9982	0.613	0.51		0.15
Naphthalene	1.0854	1.340	0.92		0.20
Fluorene	1.3565	1.588	1.03		0.20
Chlorobenzene	0.8388	0.718	0.65		0.07
Iodobenzene	0.9746	1.188	0.82		0.12
Anisole	0.9160	0.708	0.75		0.29
Acetophenone	1.0139	0.818	1.01		0.48
Benzonitrile	0.8711	0.742	1.11		0.33
Nitrobenzene	0.8910	0.871	1.11		0.28
Benzaldehyde	0.8730	0.820	1.00		0.39
Phenyl acetate	1.0730	0.661	1.13		0.54
Methyl benzoate	1.0726	0.733	0.85		0.46
Propyl benzoate	1.3544	0.675	0.80		0.46
Butyl benzoate	1.4953	0.668	0.80		0.46
1,4-Dichlorobenzene	0.9612	0.825	0.75		0.02
3-Nitrotoluene	1.0320	0.874	1.10		0.25
4-Chloroacetophenone	1.1360	0.955	1.09		0.44
1-Nitrobutane	0.8464	0.227	0.95		0.29
1-Nitrohexane	1.1282	0.203	0.95		0.29
Benzyl alcohol	0.9160	0.803	0.87	0.33	0.56
2-Phenylethanol	1.0569	0.811	0.91	0.30	0.64
4-Phenylbutanol	1.3387	0.811	0.90	0.33	0.70
4-Nitrobenzyl alcohol	1.0902	1.064	1.39	0.44	0.62
Acetanilide	1.1133	0.870	1.40	0.50	0.67
Benzenesulfonamide	1.0971	1.130	1.55	0.55	0.80
4-Nitroaniline	0.9910	1.220	1.91	0.42	0.38
N-Methylbenzamide	1.1137	0.950	1.44	0.35	0.73
Phenol	0.7751	0.805	0.89	0.60	0.30
3-Methylphenol	0.9160	0.822	0.88	0.57	0.34
4-*tert*-Butylphenol	1.3387	0.810	0.89	0.56	0.39
4-Phenylphenol	1.3829	1.560	1.41	0.59	0.45
3,5-Dimethylphenol	1.0569	0.820	0.84	0.57	0.36
4-Chloro-3-methylphenol	1.0384	0.920	1.02	0.65	0.23
Methyl 3-hydroxybenzoate	1.1313	0.905	1.40	0.66	0.45
Propyl 4-hydroxybenzoate	1.4131	0.840	1.35	0.69	0.45
2-Naphthol	1.1440	1.520	1.08	0.61	0.40

tion of system constants. Except as stated otherwise measurements were made at 25 °C, +20 kV, and 210 nm. Standard solutions were made up in methanol (1–2 mg ml^{-1}) to which 1-phenyloctane in acetone was added to indicate the micelle migration time. All sample solutions and buffers were filtered through 0.2 μm poly(propylene) syringe filters (Gelman Sciences, Ann Arbor, MI, USA) prior to use. Samples were introduced into the capillary by applying a pressure of 50 mbar for 1–2 s (1 bar = 10^5 Pa).

The retention factor was calculated using eqn. (3) with the migration time of methanol used to determine the electroosmotic flow (t_{eo}) and 1-phenyloctane the migration time of the micelles (t_{mc}) with t_R as the solute migration time

$$k = (t_R - t_{eo})/(1 - t_R/t_{mc})\, t_{eo} \quad (3)$$

The retention factors used with the solvation parameter model to determine the nature of the selectivity of the different micellar systems are summarized in Table 3. The solute descriptors were taken from several sources and are summarized in Table 2 for the reader's convenience.[18,22,26] Multiple linear regression analysis and statistical tests were performed on a Vectra computer (Hewlett- Packard) using the program SPSS/PC+ V3.1 (SPSS, Chicago, IL, USA).

Results and Discussion

A series of experiments were performed with the surfactant sodium cholate to establish the influence of experimental parameters on selectivity. These results are summarized in Table 4 with the boundary conditions based on previous experiences[34] and the necessity to maintain an acceptable separation time and efficiency, and a useful migration window. It is immediately obvious that experimental parameters have only a small influence on selectivity as indicated by the narrow range of system constant values throughout the table. Selectivity, therefore, is controlled primarily by the choice of surfactant. Varying the concentration of the surfactant primarily causes change in the model constant term (*c* constant). Increasing the surfactant concentration results in a general increase in retention due to changes in the phase ratio for the separation system,[2–5,11] but only minor changes in selectivity. Changing the pH (for non-ionized solutes) has a significant effect on the electroosmotic flow, and therefore, the migration time, but over a useful pH range (8, 8.5, 9) little influence on selectivity. The choice of buffer, in this case, sodium phosphate, sodium tetraborate, or a mixture of the two; or buffer concentration (10, 20, 30 mM) has little influence on selectivity. Changes in selectivity accompanying variations in temperature (15, 25,

Table 3 Retention factors used to characterize surfactant selectivity. Sodium phosphate–sodium tetraborate buffer (20 mM), temperature 25 °C, field strength 20 kV, and other conditions indicted in Table 5

	Logarithm of the retention factor (log *k*)						
Solute	Sodium dodecyl sulfate	*N*-Dodecanoyl-*N*-methyl-taurine	Sodium cholate	Sodium deoxycholate	Sodium taurocholate	Sodium tauro-deoxycholate	Hexadecyl-trimethyl ammonium bromide
Benzene	0.044	0.110	−0.210	−0.040	−0.487	−0.294	0.531
Toluene	0.553	0.611	0.387	0.491	−0.033	0.148	0.834
Ethylbenzene	0.997	0.971	0.701	0.845	0.333	0.619	1.221
Naphthalene	1.185	1.014	0.961	1.244	0.588	0.940	1.778
Fluorene	2.136		1.446	2.117	1.205	1.686	
Chlorobenzene	0.618	0.597	0.402	0.595	0.103	0.311	1.023
Iodobenzene	1.036	1.216	0.762	1.085	0.547	0.820	1.545
Anisole	0.260	0.344	−0.037	0.142	−0.386	−0.176	0.436
Acetophenone	0.275	0.056	−0.411	−0.163	−0.569	−0.336	0.105
Benzonitrile	0.032	−0.016	−0.487	−0.160	−0.617	−0.444	0.107
Nitrobenzene	0.143	0.264	−0.262	0.285	−0.408	−0.225	0.396
Benzaldehyde	−0.017	−0.061	−0.500	−0.314	−0.726	−0.490	0.029
Phenyl acetate	0.169	0.022	−0.561	−0.327	−0.696	−0.478	0.181
Methyl benzoate	0.536	0.288	−0.028	0.124	−0.246	−0.012	0.530
Propyl benzoate	1.316	1.046	0.563	0.866	0.385	0.703	1.638
Butyl benzoate	1.801	1.129	0.867	1.298	0.740	1.136	
1,4-Dichlorobenzene	1.076	1.119	0.885	1.138	0.437	0.818	1.628
3-Nitrotoluene	0.637	0.660	0.150	0.368	−0.056	0.160	0.982
4-Chloroacetophenone	0.794	0.667	0.145	0.373	−0.071	0.177	0.803
1-Nitrobutane	−0.180	−0.250	−0.756	−0.520	−0.932	−0.748	−0.017
1-Nitrohexane	0.733	0.658	0.040	0.323	−0.195	0.008	0.961
Benzyl alcohol	−0.268	−0.294	−0.690	−0.517	−0.906	−0.685	−0.131
2-Phenylethanol	0.025	0.038	−0.539	−0.345	−0.723	−0.529	0.138
4-Phenylbutanol	0.752	0.767	0.110	0.278	−0.120	0.080	0.867
4-Nitrobenzyl alcohol	−0.052	0.066	−0.387	−0.233	−0.561	−0.403	0.263
Acetanilide	−0.083	−0.105	−0.458	−0.288	−0.644	−0.489	0.032
Benzenesulfonamide	−0.381	−0.345	−0.808	−0.583	−0.806	−0.690	−0.088
4-Nitroaniline	0.059	0.232	−0.191	−0.191	−0.332	−0.204	0.445
N-Methylbenzamide	−0.191	−0.378	−0.631	−0.360	−0.738	−0.530	0.242
Phenol	−0.306	0.221	−0.257	−0.370	−0.691	−0.552	0.402
3-Methylphenol	0.144	0.370	−0.193	−0.082	−0.398	−0.206	0.790
4-*tert*-Butylphenol	1.082	1.417	0.989	0.999	0.638	0.757	1.935
4-Phenylphenol	1.412	1.505	1.016	1.207	0.789	0.996	
3,5-Dimethylphenol	0.504	0.769	0.130	0.234	−0.091	0.057	1.224
4-Chloro-3-methylphenol	0.803	1.221	0.596	0.646	0.354	0.475	
Methyl 3-hydroxybenzoate	0.324	0.453	−0.028	0.163	−0.274	−0.088	0.799
Propyl 4-hydroxybenzoate	1.021	1.213	0.659	0.743	0.391	0.528	1.913
2-Naphthol	0.914	1.345	0.567	0.650	0.355	0.542	1.636

35 °C) are again small indicating that, at least for sodium cholate, this is not a particularly useful parameter for selectivity optimization. Adding methanol to the buffer in amounts from 1 to 10% (v/v) has a small influence on the ease of cavity formation (m constant) but more significantly results in a reduction of the hydrogen-bond acidity of the aqueous buffer (either due to alterations of the capacity of the micellar phase or buffer solution for hydrogen-bond interactions). The presence of organic solvent will also affect the critical micelle concentration of the surfactant with a possible change in the phase ratio[35,36] but this must be small for the systems studied here, given the narrow range of values for the model constant. Surprisingly, the choice of organic solvent (5% v/v), whether methanol, acetonitrile, tetrahydrofuran, or propan-2-ol, seems to be virtually without influence on the selectivity, in complete contrast to reversed-phase liquid chromatography, often used as an analogous system to explain separation characteristics in MEKC. It is possible that low-molecular-mass solvents are poorly taken up by the micelles and function primarily as a diluent of the buffer, where within the concentration range studied, they moderate the characteristic solvophobic properties of water more so than modify the selectivity of the micellar phase. Solubility limitations and the unfavorable influence of organic solvents on the electroosmotic flow prevent exploring the mechanism of this observation at significantly higher concentrations of organic solvent. The latter conclusions are roughly corroborated by the studies of Garcia *et al.*[37] on the solute–micelle association constants for a group of benzene derivatives and polycyclic aromatic hydrocarbons using sodium dodecyl sulfate as surfactant. They concluded that the association constants were not significantly influenced by the concentration [5 or 10 mM] or type of organic buffer [2-(*N*-cyclohexylamino)ethanesulfonic acid or sodium acetate], or by different concentrations of propan-1-ol (3% v/v) and butan-1-ol (1, 3, 5% v/v). These studies were performed at pH 9 and 10, at which many of the phenols in their data set would be significantly ionized, leaving too few solutes for a robust fit of the solvation parameter model to their data.

Table 4 Influence of experimental variables on the selectivity of the surfactant sodium cholate in MEKC. Field strength kV. Solutes (n = 40) are indicated in Table 2*

	System constants						Statistics		
Range	m	r	s	a	b	c	R	SE	F
(1) *Sodium phosphate–sodium tetraborate buffer (20 mM); pH 8; temperature 25 °C; vary concentration of surfactant—*									
50 mM	2.59	0.65	−0.47		−2.27	−2.11	0.985	0.11	275
	(0.13)	(0.09)	(0.10)		(0.13)	(0.13)			
75 mM	2.45	0.63	−0.47		−2.29	−1.71	0.983	0.11	241
	(0.12)	(0.08)	(0.09)		(0.13)	(0.12)			
125 mM	2.39	0.48	−0.46		−2.14	−1.34	0.986	0.10	281
	(0.10)	(0.07)	(0.08)		(0.12)	(0.10)			
(2) *Sodium phosphate–sodium tetraborate buffer (20 mM); surfactant concentration (75 mM); temperature 25 °C; vary pH—*									
pH 8.5	2.59	0.61	−0.47		−2.31	−1.90	0.987	0.10	308
	(0.11)	(0.07)	(0.08)		(0.12)	(0.11)			
pH 9.0	2.45	0.57	−0.41		−2.26	−1.77	0.982	0.11	229
	(0.12)	(0.08)	(0.09)		(0.13)	(0.12)			
(3) *Buffer concentration (20 mM); surfactant concentration (75 mM); pH 8; temperature 25 °C; vary buffer type—*									
Sodium phosphate	2.52	0.59	−0.48		−2.26	−1.79	0.988	0.10	343
	(0.10)	(0.06)	(0.07)		(0.11)	(0.10)			
Sodium tetraborate	2.58	0.63	−0.46		−2.30	−1.93	0.982	0.11	229
	(0.11)	(0.07)	(0.08)		(0.13)	(0.11)			
(4) *Sodium phosphate–sodium tetraborate buffer; surfactant concentration (75 mM); pH 8; temperature 25 °C; vary buffer concentration—*									
10 mM	2.43	0.60	−0.50		−2.23	−1.63	0.984	0.11	251
	(0.11)	(0.07)	(0.08)		(0.13)	(0.11)			
30 mM	2.49	0.60	−0.50		−2.29	−1.65	0.986	0.10	289
	(0.11)	(0.07)	(0.08)		(0.12)	(0.11)			
(5) *Sodium phosphate–sodium tetraborate buffer (20 mM); surfactant concentration (75 mM); pH 8; vary temperature—*									
15 °C	2.63	0.61	−0.41		−2.49	−1.87	0.982	0.13	220
	(0.13)	(0.08)	(0.10)		(0.15)	(0.13)			
35 °C	2.38	0.58	−0.49		−2.05	−1.75	0.985	0.10	278
	(0.10)	(0.07)	(0.08)		(0.12)	(0.10)			
(6) *Sodium phosphate–sodium tetraborate buffer (20 mM); surfactant concentration (75 mM); pH 8; temperature 25 °C; vary volume of methanol (v/v)—*									
1%	2.50	0.60	−0.48		−2.26	−1.71	0.985	0.11	261
	(0.11)	(0.07)	(0.08)		(0.13)	(0.11)			
5%	2.34	0.57	−0.41		−2.07	−1.74	0.987	0.09	309
	(0.09)	(0.06)	(0.07)		(0.11)	(0.10)			
10%	2.23	0.56	−0.36		−1.95	−1.79	0.986	0.09	280
	(0.09)	(0.06)	(0.07)		(0.11)	(0.09)			
(7) *Sodium phosphate–sodium tetraborate buffer (20 mM); surfactant concentration (75 mM); pH 8; temperature 25 °C; vary organic solvent identity at 5% (v/v)—*									
Acetonitrile	2.30	0.52	−0.36		−2.08	−1.72	0.987	0.09	315
	(0.09)	(0.06)	(0.07)		(0.11)	(0.09)			
Tetrahydrofuran	2.08	0.49	−0.39		−2.00	−1.52	0.986	0.09	230
	(0.09)	(0.06)	(0.07)		(0.11)	(0.09)			
Propan-2-ol	2.27	0.56	−0.40		−2.03	−1.68	0.986	0.09	299
	(0.09)	(0.06)	(0.07)		(0.11)	0.09)			

* Definition of statistics as in Table 1. Numbers in parentheses indicate to standard deviation in the coefficient.

In terms of selectivity optimization the above experiments indicate that varying the choice of surfactant is more likely to result in significant changes in selectivity for neutral solutes than fine tuning the operational parameters suitable for the separation. Table 5 summarizes the system constants for seven commonly used surfactants in MEKC. The group of bile salt surfactants, sodium cholate, sodium deoxycholate, sodium taurocholate, and sodium taurodeoxycholate, are most similar to each other, while as a group different to the other surfactants in Table 5. Notably, solute hydrogen-bond acid interactions do not contribute to retention (*a* constant is statistically insignificant). Choosing surfactants from within this group can only be expected to provide small changes in selectivity, most notably for solutes with a significant capacity as hydrogen-bond bases. The migration order for the test mixture benzenesulfonamide, 2-phenylethanol, 3-methylphenol, anisole, methyl 3-hydroxybenzoate, 3-nitrotoluene, ethylbenzene, propyl benzoate, and naphthalene is the same for all four bile salts. Separation is complete using sodium taurodeoxycholate, Fig. 1; while anisole and methyl 3-hydroxybenzoate comigrate using sodium cholate, Fig. 2; ethylbenzene and propyl benzoate are incompletely separated using sodium deoxycholate, Fig. 3; and anisole and

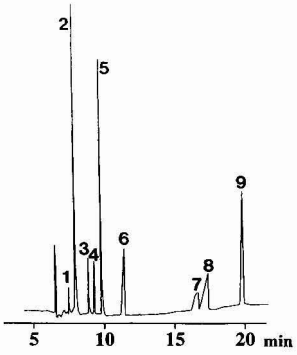

Fig. 1 Separation of a test mixture by MEKC using 50 mM sodium taurodeoxycholate in a 20 mM sodium phosphate–sodium borate buffer, pH 8, 35 °C, 30 kV, and 80.5 cm capillary (effective length = 72 cm). Peak identification: 1, benzenesulfonamide; 2, 2-phenylethanol; 3, 3-methylphenol; 4, anisole; 5, methyl 3-hydroxybenzoate; 6, 3-nitrotoluene; 7, ethylbenzene; 8, propyl benzoate; and 9, naphthalene.

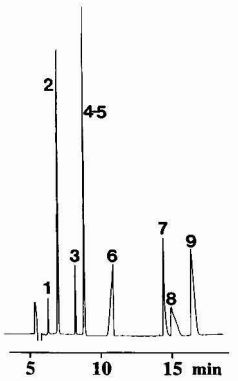

Fig. 2 Separation of a test mixture by MEKC using 75 mM sodium cholate. Other conditions and peak identifications as for Fig. 1.

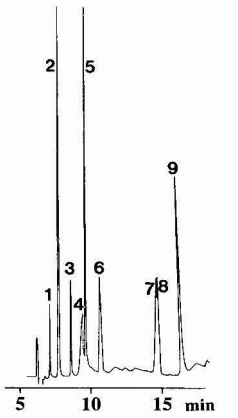

Fig. 3 Separation of a test mixture by MEKC using 75 mM sodium deoxycholate. Other conditions and peak identifications as for Fig. 1.

Table 5 Selectivity of different surfactants at 25 °C in a 20 mM sodium phosphate–sodium tetraborate buffer and field strength 20 kV. The retention factors used to fit the model are given in Table 3

Surfactant	Concentration/ mM	pH	System constants						Statistics*			
			m	*r*	*s*	*a*	*b*	*c*	*R*	*SE*	*F*	*n*
Sodium dodecyl sulfate	50	8	2.99 (0.07)	0.46 (0.05)	−0.44 (0.05)	−0.30 (0.05)	−1.88 (0.08)	−1.82 (0.07)	0.994	0.07	569	40
N-Dodecanoyl-*N*-methyltaurine	50	8	3.07 (0.09)	0.72 (0.06)	−0.50 (0.07)	0.22 (0.06)	−2.58 (0.10)	−2.01 (0.09)	0.992	0.08	338	39
Sodium cholate	75	8	2.45 (0.12)	0.63 (0.08)	−0.47 (0.09)		−2.29 (0.13)	−1.71 (0.12)	0.983	0.11	241	40
Sodium deoxycholate	75	8	2.67 (0.11)	0.66 (0.08)	−0.47 (0.09)		−2.47 (0.13)	−1.69 (0.12)	0.986	0.11	286	40
Sodium taurocholate	50	8	2.43 (0.09)	0.60 (0.07)	−0.34 (0.07)		−2.06 (0.10)	−2.10 (0.09)	0.989	0.09	377	40
Sodium taurodeoxycholate	50	8	2.62 (0.09)	0.67 (0.06)	−0.45 (0.07)		−2.17 (0.10)	−1.99 (0.09)	0.991	0.09	430	40
Hexadecyltrimethylammonium bromide	50	7	3.40 (0.10)	0.61 (0.06)	−0.55 (0.07)	0.58 (0.06)	−3.08 (0.10)	−1.67 (0.11)	0.993	0.08	436	36

* Definition of statistics as in Table 1.

3-methylphenol comigrate using sodium taurocholate, Fig. 4. Peak position in the chromatogram is the result of a balance of intermolecular interactions combined with size differences. For example, the comigration of anisole and methyl 3-hydroxybenzoate using sodium cholate results largely from the fact that the larger contribution to retention from the cavity term ($mV_X/100$) for methyl 3-hydroxybenzoate is compensated by its stronger interactions of a dipole-type ($s\pi_2^H$) and hydrogen-bonding ($b\beta_2^H$) with the aqueous electrolyte compared to anisole resulting in coincidental retention factors. Separation using the other bile salt surfactants results from the fact that the compensating balance of interactions is lost to the extent that separation is now possible. A powerful feature of the solvation parameter model is its usefulness in dissecting retention information into intermolecular interactions that provides a fundamental insight into retention mechanisms that is absent from simply noting peak positions in a series of chromatograms. The latter approach, which is common practice in chromatography, presupposes that dominant intermolecular interactions can be associated with individual compounds, which is not a tenable case as indicated by the varied compounds in Table 2.

Sodium dodecyl sulfate has different selectivity to the bile salt surfactants, Table 5. It is slightly less cohesive (larger m constant) but more importantly, it is a significantly weaker hydrogen-bond base (negative a constant) and stronger hydrogen-bond acid (more competitive with water for hydrogen-bond acid interactions; smaller negative b constant). Compared to the bile salt surfactants solutes with a significant capacity for hydrogen-bond interactions will be most affected in their migration order. This is notable in the relative retention for the test mixture, Fig. 5, where peak reversal for naphthalene and propyl benzoate also occurs compared with the bile salt surfactants. The greater hydrogen-bond acidity of sodium dodecyl sulfate competing more effectively with water for the retention of the hydrogen-bond base propyl benzoate combined with a more favorable cavity term largely explains the change in peak order observed.

Sodium *N*-dodecanoyl-*N*-methyltaurine is a significantly stronger hydrogen-bond base (positive a constant) and weaker hydrogen-bond acid (large negative b constant) than sodium dodecyl sulfate. The most notable difference in separation properties between the sodium salt of *N*-dodecanoyl-*N*-methyltaurine and the bile salts and sodium dodecyl sulfate is again for those solutes with a significant capacity for hydrogen-bond interactions. These differences are reflected in the peak reversal of 3-methylphenol and anisole for the test mixture compared to the bile salts and sodium dodecyl sulfate, Fig. 6.

The selectivity of hexadecyltrimethylammonium bromide is most like the sodium salt of *N*-dodecanoyl-*N*-methyltaurine, except that it is considerably less cohesive (largest m constant of the surfactants in Table 5), it has the lowest capacity for dipole-

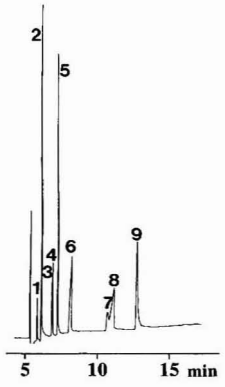

Fig. 4 Separation of a test mixture by MEKC using 50 mM sodium taurocholate. Other conditions and peak identifications as for Fig. 1.

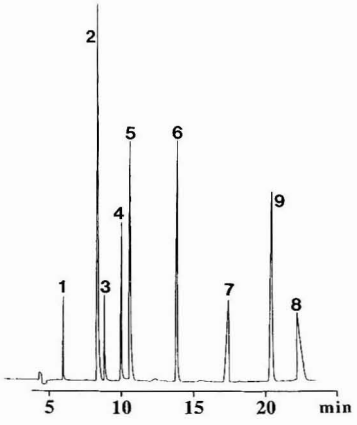

Fig. 5 Separation of a test mixture by MEKC using 50 mM sodium dodecyl sulfate. Other conditions and peak identifications as for Fig. 1.

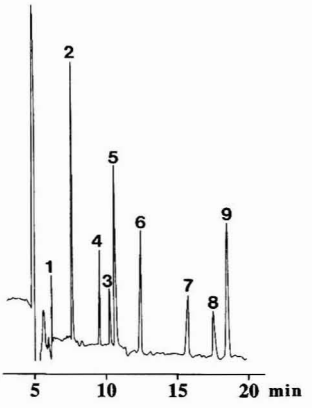

Fig. 6 Separation of a test mixture by MEKC using 50 mM sodium *N*-dodeconyl-*N*-methyltaurine. Other conditions and peak identifications as for Fig. 1.

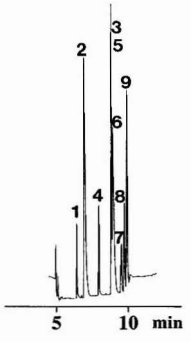

Fig. 7 Separation of a test mixture by MEKC using 50 mM hexadecyltrimethylammonium bromide. Other conditions and peak identifications as for Fig. 1 except that the potential was reversed.

type interactions (largest negative *s* constant), it is the strongest hydrogen-bond base (largest *a* constant), and the weakest hydrogen-bond acid (largest negative *b* constant). As well as a higher general retention of solutes of low polarity, the greatest difference in migration order compared to the other surfactants in Table 5, is expected for hydrogen-bond forming solutes. The separation of the test mixture is shown in Fig. 7.

From Table 5 a choice of one of the bile salts and the three remaining surfactants provides a reasonable range of micellar phases for selectivity optimization with a much greater variation of system constants than was observed for the optimization of experimental conditions in Table 4. To this list should be added lithium perfluorooctanesulfonate from Table 1, whose properties are quite different to those of the surfactants in Table 5. It is noteworthy that the selectivity range for dipole-type interactions is the least satisfactory (*s* constant) and that differences in cohesive properties are quite shallow.

Conclusions

The system constants in Tables 1 and 5 can act as a guide to the selection of surfactants for selectivity optimization in MEKC. Hexadecyltrimethylammonium bromide has complementary selectivity to the other surfactants in Table 5 but provides only a small migration window, which would limit its use for separating complex mixtures. The surfactants exhibit a reasonable range of selectivity but by no means a comprehensive range, such that the introduction of novel surfactants with complementary properties would be welcome. The solvation parameter model provides a basis for characterizing the selectivity of surfactants for MEKC and can be used to identify new surfactants with properties that differ from those indicated here.

The authors thank Professor M. G. Khaledi for providing the retention factor data from references 10–13 used to obtain some of the solvation parameter models in Table 1.

References

1 Poole, C. F., and Poole, S. K., *Chromatography Today*, Elsevier, Amsterdam, 1991, pp. 510–522.
2 Sandra, P., and Vindevogel, J., *Introduction to Micellar Electrokinetic Chromatography*, Huthig, Heidelberg, 1992.
3 Corstjens, H. A. H., Frank, J., and Luyben, K. Ch. A. M., *J. Chromatogr. A*, 1995, **715**, 1.
4 Nishi, H., and Terabe, S., *J. Chromatogr. A*, 1996, **735**, 3.
5 Muijselaar, P. G. H. M., Claessens, H. A., and Cramers, C. A., *J. Chromatogr. A*, 1995, **696**, 273.
6 Ahuja, E. S., and Foley, J. P., *Anal. Chem.*, 1995, **67**, 2315.
7 Pyell, U., and Butehorn, U., *Chromatographia*, 1995, **40**, 175.
8 Terabe, S., *J. Pharm. Biomed. Anal.*, 1992, **10**, 705.
9 Chen, N., Zhang, Y., Terabe, S., and Nakagawa, T., *J. Chromatogr. A*, 1994, **678**, 327.
10 Yang, S., and Khaledi, M. G., *J. Chromatogr. A*, 1995, **692**, 301.
11 Yang, S., and Khaledi, M. G., *Anal. Chem.*, 1995, **67**, 499.
12 Yang, S., Bumgarner, J. G., Kruk, L. F. R., and Khaledi, M. G., *J. Chromatogr. A*, 1996, **721**, 323.
13 Yang, S., Bumgarner, J. G., and Khaledi, M. G., *J. Chromatogr. A*, 1996, **738**, 265.
14 Kollie, T. O., and Poole, C. F., *Chromatographia*, 1992, **33**, 551.
15 Poole, S. K., and Poole, C. F., *Analyst*, 1995, **120**, 289.
16 Poole, C. F., Kollie, T. O., and Poole, S. K., *Chromatographia*, 1992, **34**, 281.
17 Poole, S. K., and Poole, C. F., *J. Chromatogr. A*, 1995, **697**,415.
18 Abraham, M. H., *Chem. Soc. Rev.*, 1993, **22**, 73.
19 Carr, P. W., *Microchem. J.*, 1993, **48**, 4.
20 Seibert, D. S., Poole, C. F., and Abraham, M. H., *Analyst*, 1996, **121**, 511.
21 Seibert, D. S., and Poole, C. F., *Chromatographia*, 1995, **41**, 51.
22 Abraham, M. H., and Roses, M., *J. Phys. Org. Chem.*, 1994, **7**, 672.
23 Abraham, M. H., Roses, M., Poole, C. F., and Poole, S. K., *J. Phys. Org. Chem.*, in the press.
24 Poole, C. F., Poole, S. K., Seibert, D. S., and Chapman, C. M., *J. Chromatogr. B, Biomed. Appl.*, 1997, **689**, in the press.
25 Abraham, M. H., Poole, C. F., and Poole, S. K., *J. Chromatogr. A*, 1996, **749**, 201.
26 Abraham, M. H., Andovian-Haftvan, J., Whitting, G. S., Leo, A., and Taft, R. S., *J. Chem. Soc., Perkin Trans. 2*, 1994, 1777.
27 Abraham, M. H., *J. Phys. Org. Chem.*, 1993, **6**, 660.
28 Abraham, M. H., and Chada, H. S., in *Lipophilicity in Drug Action and Toxicology*, ed. Pliska, V., Testa, B., and van de Waterbeemed, H., VCH, Weinheim, Germany, 1996, p. 311.
29 Abraham, M. H., Chadha, H. S., Dixon, J. P., Rofols, C., and Treiner, C., *J. Chem. Soc., Perkin Trans. 2*, 1995, 887.
30 Abraham, M. H., Treiner, C., Roses, M., Rafols, C., and Ishihama, Y., *J. Chromatogr. A*, 1996, **752**, 243.
31 Adlard, M., Okafo, G., Meenan, E., and Camilleri, P., *J. Chem. Soc. Chem. Commun.*, 1995, 2241.
32 Herbert, B. J., and Dorsey, J. G., *Anal. Chem.*, 1995, **67**, 744.
33 Khaledi, M. G., 1996, personal communication.
34 Poole, S. K., and Poole, C. F., *J. Chromatogr. A*, 1996, **749**, 247.
35 Khaledi, M. G., Peuler, E., and Ngeh-Nguainhi, J., *Anal. Chem.*, 1987, **59**, 2738.
36 Khaledi, M. G., *Trends Anal. Chem.*, 1988, **7**, 293.
37 Garcia, M. A., Marina, M. L., and Diez-Masa, J. C., *J. Chromatogr. A*, 1996, **732**, 345.

Paper 6/05799C
Received August 20, 1996
Accepted November 13, 1996

The Analyst

Determination of Complex Mixtures of Airborne Isocyanates and Amines.

Part 3†. Methylenediphenyl Diisocyanate, Methylenediphenylamino Isocyanate and Methylenediphenyldiamine and Structural Analogues after Thermal Degradation of Polyurethane

Håkan Tinnerberg[a,b], Mårten Spanne[a,b], Marianne Dalene[a] and Gunnar Skarping*[a]

[a] *Department of Occupational and Environmental Medicine, University Hospital, S-221 85 Lund, Sweden*

[b] *Department of Working Environment, Lund Institute of Technology, S-221 00 Lund, Sweden*

A method is presented for the determination of isocyanates in polymeric methylenediphenyl diisocyanate (MDI) and related compounds formed during the thermal decomposition of polyurethane (PUR). Derivatization of isocyanates was performed in impinger flasks containing dibutylamine (DBA) with the formation of urea derivatives. Compounds containing amine groups were then derivatized with ethyl chloroformate (ET) to give urethane derivatives. Reversed-phase liquid chromatography, with a gradient flow rate of 40 μl min^{-1} and mass spectrometry in the electrospray mode monitoring positive ions was studied. Injection volumes of up to 10 μl of the sample were made possible by using column focusing. 1,5-Naphthyldiisocyanate–DBA and 1,5-naphthyldiamine–ET derivatives were used as internal standards. Virtually linear calibration curves were obtained for 4,4′-MDI–DBA and 4,4′-methylenediphenyldiamine–ET (MDA–ET) and the correlation coefficients were 0.9952–0.9964 (n = 14). The precision for five injections of samples spiked with 4,4′-MDA–ET, and 4,4′-MDI–DBA at concentrations of 50 nmol ml^{-1} was 2.76 and 2.55%, respectively. The instrumental detection limit, defined as three times the noise, was 4 fmol of MDI–DBA and 50 fmol of MDA–ET injected. In chromatograms of polymeric MDI derivatized with diethylamine, dipropylamine and DBA, the presence of several structural isomers and analogues in polymeric MDI was demonstrated. In the chromatograms of thermal decomposition products of MDI–PUR, in addition to isocyanates, related amino isocyanates and amines were also observed.

Keywords: *Liquid chromatography–electrospray mass spectrometry; methylenediphenyl diisocyanate, methylene diphenylamino isocyanate; methylenediphenyldiamine; polyurethane; thermal decomposition*

The exposure assessment of isocyanates is important owing to the potential respiratory hazards among exposed workers.[1] Recently we reported a study,[2] in which several workers had experienced work related symptoms after exposure to thermal degradation products of a methylenediphenyl diisocyanate (MDI)-based glue. Even though air measurements performed with impingers containing 9-(*N*-methylaminomethyl)anthracene (MAMA) reagent[3] showed low concentrations of MDI, considerable amounts of methylenediphenyldiamine (MDA) were found in hydrolysed urine and plasma. When monitoring isocyanates at the workplace using a filter tape instrument, indications of considerable exposure were seen.

The complexity of polymeric MDA, the precursor in the manufacture of polymeric MDI, has been described in recent years. In addition to 4,4′-MDA, 2,4′- and 2,2′-MDA and methyl-MDA and MDA structural analogues with up to six rings were also found.[4] Furthermore, in hydrolysed urine and plasma from workers exposed to thermal degradation products of MDI-based polyurethane (MDI-PUR), not only 4,4′-MDA was found but also 2,4′- and 2,2′-MDA, methyl-MDA and MDA with three, four and five rings.[5] Products formed during the thermal degradation of PUR have been studied previously for MDI-PUR in foundries.[6] Trace amounts of phenyl isocyanate (PhNCO) and MDI were found but aniline and methylaniline dominated.

In Parts 1 and 2 of this series,[7,8] sampling in impinger flasks containing dibutylamine (DBA) as the derivatization reagent and further derivatization of amines with ethyl chloroformate (ET) with the use of LC–UV/LC–MS was demonstrated as a useful tool for determination of complex mixtures of isocyanates and amines formed during the thermal decomposition of toluene diisocyanate (TDI)-based PUR. Fast reaction rates were observed for the isocyanate–DBA reaction and it was found to be resistant to interferences. The derivatization of 4,4′-MDA with chloroformates has been reported previously using LC–UV determinations.[9]

The aim of this study was to develop an LC–MS method for the selective determination of isocyanates in polymeric grade MDI (Fig. 1) and the complex isocyanates, amino isocyanates and amines formed during the thermal degradation of MDI-based PUR.

Experimental

Apparatus

A Quattro quadrupole mass spectrometer (VG-Organic, Altrincham, Cheshire, UK) was used in the electrospray ionization (ESI) mode, monitoring positive ions. For ESI the cone voltage was 30 V and the temperature of the ion source was 120 °C. The mass spectrometer was connected to a Rheos 4000 HPLC solvent delivery system (Flux Instruments, Karlskoga, Sweden). A Kontron Model 433 capillary UV detector with a 5 μl cell volume (Kontron, Basle, Switzerland) was connected in series with the LC–MS system and the UV signal (λ = 240 nm) was recorded for each chromatographic run. Loop injections of 1–10 μl of sample in acetonitrile (partially filled loop) were

† For Parts 1 and 2, see refs. 7 and 8.

made using a CMA/200 refrigerated autosampler (Carnegie, Stockholm, Sweden). The loop volume was 10–20 μl and the wash liquid was acetonitrile–water (30 + 70). Different gradients were used consisting of solution A [methanol–acetonitrile (50 + 50)] and B [water–acetonitrile (95 + 5)] with 0.05% formic acid in both solutions. The flow rate of the pump was 400 μl min^{-1}, connected to an Accurate splitter (LC Packings, Amsterdam, The Netherlands) which split the LC flow to 40 μl min^{-1}. The column was Sephasil C_{18} (250 × 1 mm id) with 5 μm particles (LC Packings).

The samples were evaporated at 40 °C in a Speed-Vac 290 centrifuge (Savant, Farmingdale, NY, USA).

Chemicals

Toluene, HPLC grade acetonitrile and methanol were obtained from Lab-Scan (Dublin, Ireland), 4,4′-MDI, polymeric MDI and a mixture of 2,4′- and 4,4′-MDI from ICI Europe (Everberg, Belgium), MDA from Fluka (Buchs, Switzerland), 1,5-NDI from Bayer (Leverkusen, Germany), DBA from Aldrich (Steinham, Germany), ethanol from Kemetyl (Stockholm, Sweden), $NaHCO_3$ and dipropylamine (DPA) from Merck (Darmstadt, Germany), diethylamine (DEA) from Riedel-de Haën (Seelze, Germany) and ethyl chloroformate from Janssen Chimica (Beerse, Belgium). The ethyl chloroformate derivative of 4,4′-MDA was synthesized in our laboratory.[8]

Standard Solutions

Standard solutions of MDI were freshly prepared by dissolving accurately weighed amounts in methylene chloride and further dilutions were made with toluene. Standard solutions of MDA were prepared by dissolving accurately weighed amounts in acetonitrile and further dilutions were made with toluene.

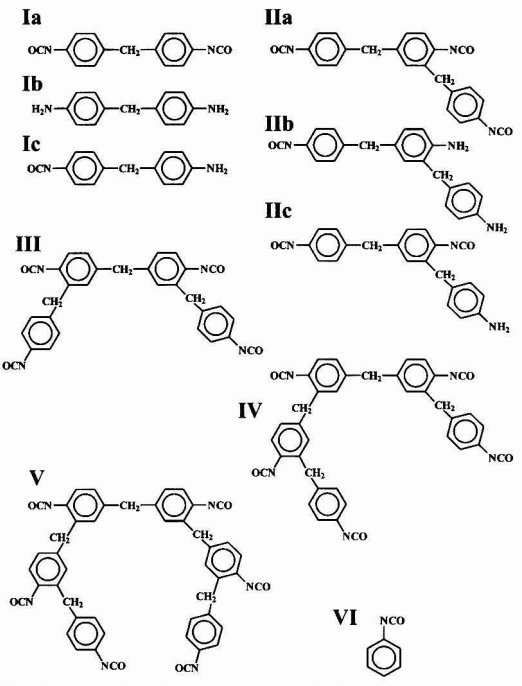

Fig. 1 Schematic molecular structures of MDI analogues in polymeric MDI (**Ia**, **IIa** and **III–V**) and isocyanate, amino isocyanate and amine isomers and analogues in air from thermally decomposed MDI–PUR (**Ia–c**, **IIa–c** and **VI**). **Ia**, MDI; **Ib**, MDA; **Ic**, MAI; **IIa**, three ring isocyanate analogue; **IIb** and **c**, three ring amino isocyanate analogues; **III**, four ring analogue; **IV**, five ring analogue; **V**, six ring analogue; and **VI**, phenyl isocyanate (PhNCO).

Sampling, Work-up Procedure and Derivatization

For the studies of thermal decomposition products in air, sampling was performed using SKC personal air samplers (SKC, Eighty Four, PA, USA) with all-glass midget impinger flasks (30 ml) containing 10 ml of 0.01 mol l^{-1} DBA. Thermal decomposition of MDI–PUR was performed by heating about 10 mg of rigid MDI–PUR foam to about 300 °C. After sampling, the solution, containing isocyanate urea derivatives and aromatic amines, was evaporated to dryness in a vacuum centrifuge. The dry residue was dissolved in 1 ml of toluene. Carbamate esters were formed in a two-phase derivatization procedure by the addition of 1 ml of a 2 mol l^{-1} carbonate buffer (pH 9.5), 50 μl of ethyl chloroformate and 10 μl of pyridine. The mixture was shaken for 5 min and the organic phase was then evaporated to dryness and dissolved in 1 ml of acetonitrile. The solution was then injected into the LC–MS system.

Derivatizations of polymeric MDI were performed with DEA, DPA and DBA by adding 10 μl of the amine to 3 ml of acetonitrile and then adding 10 μg of polymeric MDI dissolved in toluene. The samples were evaporated to dryness and the residues dissolved in 1 ml of acetonitrile prior to the LC–MS analysis.

Quantification

Quantification was performed monitoring the $[M + 1]^+$ ions of 4,4′-MDI–DBA and 4,4′-MDA–ET using NDI derivatized with DBA (NDI–DBA) and ethanol (NDA–ET) as internal standards (IS). Duplicate work-ups with double injections were performed for each concentration and the peak areas were calculated.

Results

Stability and Purity of the MDI–DBA and MDA–ET Derivatives

No degradation, for the derivatives studied, was observed after storage for 3 weeks at room temperature in the light or dark. The purity, checked by LC–UV and elemental analysis, was better than 96%. The compounds studied, together with the methylenediphenylaminoisocyanates (MAI), were further analysed using LC–MS with atmospheric pressure ionization and positive ion ESI, and molecular ions $[M + 1]^+$ were obtained in all cases.

Chromatography

Chromatograms of polymeric MDI derivatized with three different secondary aliphatic amines, DEA, DPA and DBA, were obtained under the same chromatographic conditions (Fig. 2). The derivatives eluted in groups containing derivatives of two rings and later three rings, *etc*. The components (isomers) could not all be baseline separated. The length of the aliphatic chains of the derivatization reagents greatly affects the elution time. MDI–DBA had a retention time about double that of MDI–DEA using the same gradient elution. Using DEA or DPA up to six ring components were seen in the chromatograms, but for DBA only up to four were detected. Further, using DEA as the reagent, the separation of the 2,4′- and 4,4′-MDI–DEA isomers was made possible.

In the chromatograms from air samples containing thermal decomposition products of MDI–PUR numerous components were seen (Fig 3). In the LC–positive ion ESI mass spectra and chromatograms several isocyanates, amino isocyanates and amines were identified. Compounds containing one or more carbamate ester groups eluted much earlier than the corresponding isocyanate–DBA derivatives. Compounds such as

MDA, MDI, PhNCO and three-ring isocyanates and amino isocyantes were clearly seen.

The retention times varied by less than 2%. Injection volumes of up to 10 μl, in a partially filled loop (20 μl loop volume), were made possible using column focusing. The presence of formic acid did not affect the retention times or the peak symmetries.

Mass Spectrometry

ESI monitoring positive ions was studied for the compounds in Fig. 1. The m/z = $[M+1; H]^+$ and $[M + 23; Na]^+$ ions dominated in all spectra. The presence of formic acid in the mobile phase (0.05%) made it possible to reproduce the mass spectra, less fragmentation was seen and the $[M + 1]^+$ ions were the most abundant; without formic acid the $[M + 23]^+$ ions were the most abundant. In the mass spectra of the DBA–isocyanate derivatives also the $[M - 129; DBA]^+$ and the $[M - 173;$ not known$]^+$ ions were typical for all spectra (Fig. 4 A–C). Similar fragmentation patterns were seen for the DEA and DPA derivatives of MDI. In the spectra of the isocyanates the presence of ions at m/z = 157 (DBA spectra), 129 (DPA spectra) and 101 (DEA spectra) indicates DBA–, DPA– and DEA–NCO^+ ions. In the mass spectra of the DBA–isocyanate and ET–amine mixed derivatives, the $[M - 129]^+$, $[M - 46;$ ethanol$]^+$ and the m/z = 157 ions were typical (Fig. 4D and E).

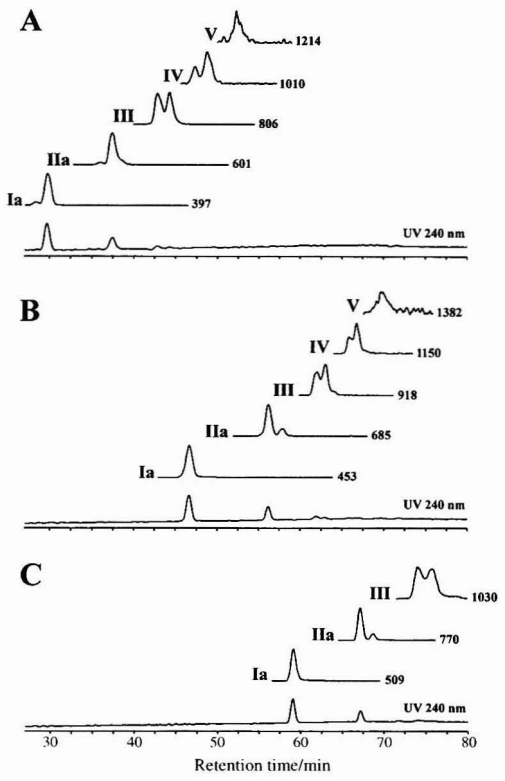

Fig. 2 Polymeric MDI derivatized with secondary aliphatic amines. Positive ion ESI and selected ion monitoring of $[M + 1]^+$ ions of 2–6 ring analogues and LC–UV (λ = 240 nm). A, DEA derivatives; B, DPA derivatives; and C, DBA derivatives. The dwell time for each ion was 0.2 s. The composition of the mobile phase was isocratic solutions A–B (40 + 60) for 1 min, thereafter gradient elution to A–B (95 + 5) during 60 min and then isocratic for 25 min. Compounds as in Fig. 1. The m/z values are given on the lines.

For the ET–amine derivatives, $[M - 46;$ ethanol$]^+$ ions were typical. On studying the spectra and varying the cone voltage between 10 and 80 V (Fig. 5), an optimum for the most abundant ions $[M + 1]^+$ was found at 30–40 V. This was also the optimum for the $[M + 23]^+$ and $[M - 46]^+$ ions in the MDA–ET spectra. For MAI–ET–DBA the optimum cone voltage was about 10 V higher. For the isocyanate–DBA spectra, the $[M + 1]^+$ ions reached a optimum at 40 V but no clear optimum were seen for the $[M + 23]^+$ ions. On increasing the cone voltage the neutral loss of DBA $[(n - 1) \times 129$ u; n = number of DBA in the molecule] became significant.

Micro-LC made it possible to use the instrument without the need to rinse the ESI-interface more than once a month. A high

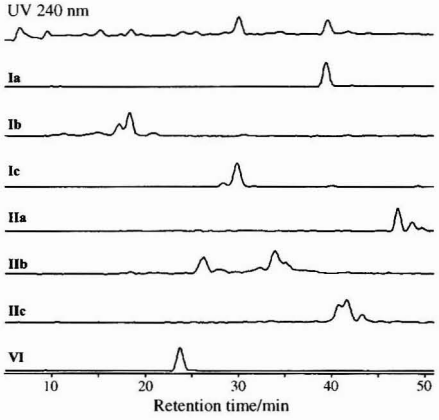

Fig. 3 Thermal decomposition of MDI–PUR. Mass fragmentograms $[M + 1]^+$ of positive ion ESI (continuum mass spectra; scan range, 150–1100 u; scan time, 3 s) and LC–UV (λ = 240 nm) for the isocyanate–DBA, amine–ET and the DBA–ET mixed derivatives are displayed. The composition of the mobile phase was isocratic A–B, (40 + 60) for 1 min, thereafter 60 + 40 and gradient elution to A–B (95 + 5) during 40 min, then isocratic for 30 min. Compounds as in Fig. 1.

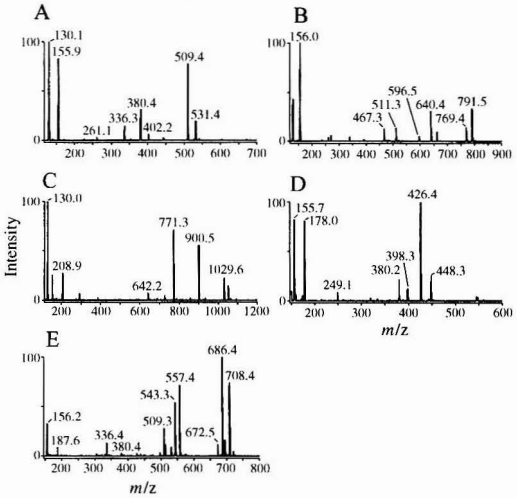

Fig. 4 LC–positive ion ESI mass spectra of: A, MDI–DBA; B, three-ring isocyanate analogue; C, four-ring isocyanate analogue; D, MAI–ET–DBA; and E, three-ring MAI–ET–DBA with one amine group. The isocyanate group was derivatized with DBA and the amine group with ET. Mass spectra were obtained by scanning ions for 3.0 s with an inter-scan delay of 0.15 s.

signal-to-noise ratio was achieved as the sample was less diluted (compared with conventional LC) during the chromatographic run. On injecting the same concentration of MDI–DBA and varying the flow rate, a significantly higher $[M + 1]^+$ peak was obtained for flow rates less than 50 μl min^{-1}.

Quantification

Virtually linear calibration curves were obtained for MDI–DBA and MDA–ET using peak area measurements of seven concentrations in the range 0.02–0.4 nmol ml^{-1}. The correlation coefficients were 0.9952–0.9964 (n = 14) with the IS and 0.9902–0.9876 without the IS for the MDI–DBA and MDA–ET derivatives, respectively. The precision for five injections, performed during approximately 3 h, of samples spiked with 4,4′-MDA–ET and 4,4′-MDI–DBA at concentrations of 50 and 500 nmol ml^{-1} were 2.76, 3.58 and 2.55, 2.55%, respectively. The instrumental detection limit, defined as three times the noise, was 4 fmol of MDI–DBA and 50 fmol of MDA–ET injected.

Discussion

For the determination of monomeric diisocyanates in air, several methods have been used. Most studies were focused on measuring the content of monomers in air and these are normally the only ones that are quantitatively determined. However, in addition to simple monomeric isocyanates, also more complex isocyanates are used in industry. Biuret and allophanate adducts are used to reduce the vapour pressure of the used isocyanates, structural isomers are most often present in technical grade MDI and reaction intermediates are found in prepolymers and are to be expected in air at workplaces once the isocyanate and polyol components have been mixed. In fact, in air the simple monomeric isocyanates may constitute only a minor fraction of the total isocyanate content. This is especially the case during thermal decomposition of PUR. When isocyanates occur in more complex mixtures, a different sampling strategy and improved analytical methods are necessary. This is of great importance since decreasing human exposure is the only available means of reducing isocyanate associated ill-health among workers. A decrease in exposure cannot easily be effected without tools to identify and evaluate the true exposure.

Derivatizing technical grade MDI with DBA makes it possible to determine several kinds of different isomers of isocyanates. In LC–MS they eluted in groups consisting of two, three and four rings. When analysing MDI derivatized with DEA up to six rings were seen. With DEA comparably fast elution and good separation were achieved even between the 2,4′- and 4,4′-MDI isomers. DPA derivatives also eluted faster with better separation than DBA derivatives of the same compounds. For pure chromatographic reasons, derivatization using DEA or DPA would be preferable, as among many reasons the 2,4′- and 4,4′-MDI–DEA isomers are separated, but neither DEA or DPA is suitable for air sampling owing to their high vapour pressures.

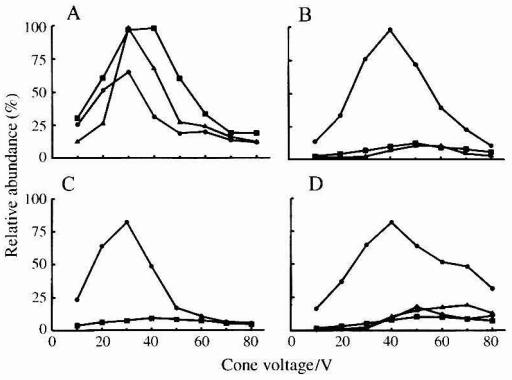

Fig. 5 Influence of cone voltage on the positive ion ESI fragmentation on: A, MDA–ET (●, $[M + 1]^+$; ■, $[M + 23]^+$; ▲, $[M - 46]^+$); B, MAI–DBA–ET (●, $[M + 1]^+$; ■, $[M + 23]^+$; ▲, $[M - 46]^+$); C, PhNCO–DBA (●, $[M + 1]^+$; ■, $[M + 23]^+$; and D, MDI–DBA (●, $[M + 1]^+$; ■, $[M + 23]^+$; ▲, $[M - 129]^+$; ◆, $[M - 173]^+$).

Micro-LC was demonstrated to be a valuable tool in combination with ESI. When comparing LC–UV data obtained with micro-LC and conventional LC, much better signal-to-noise ratios were seen using the micro-LC system as the compounds of interest were much less diluted during the chromatographic run. This is an advantage for ESI as the detector is essentially concentration dependent. Peak broadening was avoided using column focusing and similar injection volumes to those used in Parts 1 and 2 of this series were used in the LC–MS system. It was not possible, however, to maintain a column flow containing more than 95% acetonitrile at a flow rate of 40 μl min^{-1} owing to severe problems with clogging of the PEEK tubing used. This is the main reason why we did not improve the chromatographic system in order to make determinations possible for more lipophilic compounds such as the five- and six-ring DBA derivatives.

Using essentially the same procedure for thermal decomposition of MDI–PUR as described in Part 2 of this series for the thermal decomposition of TDI–PUR, chromatograms containing derivatives of complex isocyanates were observed. The quantification of these derivatives cannot be performed at present as reference compounds are not available. In fact, even the determination of the 4,4′-MDI isomer is a problem as the 2,4′- and 4,4′-MDI isomers co-elute when they are derivatized with DBA, MAMA and most other reagents used for LC determinations.

Conclusion

The presence of structural isomers and analogues in polymeric MDI has been clearly demonstrated in this study. During the thermal decomposition of MDI-PUR many complex isocyanates, amino isocyanates and amines were observed. Since many workers are occupationally exposed to these kinds of compounds, their determination is of great importance.

We gratefully acknowledge the Swedish Work Environment Fund (AMFO) for financial support.

References

1 Kennedy, A. L., and Brown, W. E., *Occup. Med.*, 1992, **7**, 301.
2 Skarping, G., Dalene, M., Svensson, B.-G., Littorin, M., Åkesson, B., Welinder, H., and Skerfving, S., *Occup. Environ. Med.*, 1996, **53**, 180.
3 Sangö, C., and Zimerson, E., *J. Liq. Chromatogr.*, 1980, **3**, 971.
4 Skarping, G., Dalene, M., and Brunmark, P., *Chromatographia*, 1994, **39**, 619.
5 Skarping, G., and Dalene, M., *J. Chromatogr. B*, 1995, **663**, 209.
6 Renman, L., Sangö, C., and Skarping, G., *Am. Ind. Hyg. Assoc. J.*, 1986, **47**, 621.
7 Spanne, M., Tinnerberg, H., Dalene, M., and Skarping, G., *Analyst*, 1996, **121**, 1095.
8 Tinnerberg, H., Spanne, M., Dalene, M., and Skarping, G., *Analyst*, 1996, **121**, 1101.
9 Tiljander, A., Skarping, G., and Dalene, M., *J. Liq. Chromatogr.*, 1990, **13**, 803.

Paper 6/07564I
Received November 6, 1996
Accepted November 26, 1996

Coupling Diffuse Reflectance Fourier Transform Infrared Spectrometry With Gas Chromatography (DRIFT–GC): a High-performance Coupled Technique for Catalyst Characterization

C. Dossi*[a], A. Fusi[a], G. Molteni[a], S. Recchia[a] and R. Psaro[b]

[a] *Dipartimento di Chimica Inorganica, Metallorganica e Analitica, Università di Milano, Via Venezian 21, 20133 Milan, Italy. E-mail: DOSSIC@mail.csmtbo.mi.cnr.it*

[b] *Centro CNR, Università di Milano, Via Venezian 21, 20133 Milan, Italy*

The combination of diffuse reflectance Fourier transform infrared spectrometry and gas chromatography (DRIFT–GC) was applied to the thermal characterization of solid materials. In the instrumental design, particular attention was devoted to minimizing the time delays between the responses of the DRIFT and the GC detectors. It was thus possible to correlate the changes in the IR spectrum with the composition of the gas phase as a function of the linearly increasing temperature. Manganese carbonyl [$Mn_2(CO)_{10}$] dispersed on a porous zeolitic matrix was chosen as reference material to test and validate the analytical methodology, since it combines a simple and predictable decomposition chemistry with a well defined infrared spectrum. Improved insights into the thermal characterization of solid materials and catalysts were achieved with this coupled technique. All gas-phase processes, which are generally hidden to IR investigations, can be revealed and studied. Moreover, the 'fingerprinting' capabilities of IR spectrometry allow the deconvolution of the elementary processes of gas evolution, greatly improving the resolution of temperature programmed techniques.

Keywords: *Diffuse reflectance Fourier transform infrared spectrometry; gas chromatography; thermal techniques; material characterization*

Diffuse reflectance Fourier transform infrared spectrometry (DRIFT) had a significant impact on the *in situ* characterization of solid materials, and catalysts in particular.[1,2] It allows the investigation of chemical transformations of samples in powder form under programmed temperature and flow conditions mimicking those of actual working operations. However, surface and/or bulk reactivity of the sample will also influence the gas phase composition over the surface, which remains hidden to most IR investigations.

Conventional evolved gas analysis (EGA) techniques often show low resolution, irrespective of the type of analyzer being used, for the occurrence under the same temperature regime of different elementary chemical processes. Sophisticated approaches such as constant reaction rate thermal analysis (CRRTA) and stepwise isothermal thermal analysis (SITA)[3] have been proposed to solve the problem. Alternatively, the use of a DRIFT spectrophotometer on-line with an evolved gas analysis apparatus will give a 'chemical' approach to peak resolution, because the fingerprint character of IR spectrometry will allow one to monitor the thermal behavior of single chemical entities in the sample. The information content of the experiment will thus be enhanced, allowing easier discrimination between surface and bulk processes.

In this paper, the coupling of GC with a DRIFT measurement is presented as a coupled analytical technique for catalyst characterization, with a critical discussion of the instrumental design.

Experimental

NaY zeolite (Linde type LZY-52) was purchased from Aldrich (Milwaukee, WI, USA) and used as received. Manganese carbonyl [$Mn_2(CO)_{10}$] was prepared and deposited on NaY by chemical vapor deposition (CVD) as reported in the literature.[4] A conventional Rh–NaY catalyst was prepared by ion exchange of $[Rh(NH_3)_5Cl]^{2+}$ following the methodology of Wong and Sachtler.[5]

A high pressure, high temperature environmental chamber for DRIFT studies (Model HVC-DR3, Harrick Scientific, Ossining, NY, USA) was modified and attached to a vacuum-gas manifold line. All gases (H_2, O_2, CO and N_2) were of ultra-high purity (UHP) grade obtained from SIAD (Milano, Italy). An additional trap filled with activated alumina was fitted in the CO line for removing metal carbonyls formed in the gas cylinder. Flow rates were controlled by a Brooks (Hatfield, PA, USA) Model 5850TR mass flow controller (MFC). The total pressure inside the cell was controlled from 0 to 3 atm by a low dead volume back-pressure controller from Hewlett-Packard (Avondale, PA, USA). A microprocessor-based temperature controller (Eurotherm 808, Reston, VA, USA) was used for heating the cell. The DRIFT cell was then interfaced to an Aerograph Model 1400 (Varian, Walnut Creek, CA, USA) gas chromatograph equipped with a thermostated gas sampling valve and flame ionization detector. Thick-walled, 1/16 in stainless-steel tubing was used in order to minimize time delays between the responses of the DRIFT and the GC detector. A methanizer was installed between the column outlet and the flame ionization detector for converting CO and CO_2 into methane using H_2 as carrier gas. Full details are reported elsewhere.[6] A schematic diagram of the overall instrument is depicted in Fig. 1.

The zeolite powder was introduced into the environmental chamber, which was evacuated in flowing N_2 from 25 to 400 °C in order to remove adsorbed water. According to the thermal treatment required, it was heated from 25 to 400 °C in flowing gas (N_2, H_2; 10 ml min^{-1}). Prior to the DRIFT measurements, the Rh–NaY sample was exposed to a flow (10 ml min^{-1}) of pure CO at room temperature and 1 atm.

Temperature programmed decomposition studies were conducted with a heating ramp of 2 °C min^{-1} by flowing N_2 or H_2 at 5–10 ml min^{-1}. Such conditions were chosen for maximum sensitivity and absence of undesirable time delays between the detectors.

DRIFT spectra were recorded at 4 cm^{-1} by averaging 100 scans with a Digilab (Cambridge, MA, USA) FTS-30 FTIR spectrophotometer, equipped with a DTGS detector and a Harrick Scientific DRA-3CO diffuse reflectance accessory.

It should be pointed out that DRIFT spectra are affected by a significant amount of noise; this is a consequence of the small amount of manganese carbonyl in the samples (1% m/m), together with the need to record spectra at high temperature during the heating ramp. However, we report the original data, avoiding any smoothing procedure.

Results and Discussion

The most critical step in interfacing the DRIFT reaction chamber with an on-line gas chromatograph was to balance the response times of the two techniques. It was essential to parallel the changes in the IR spectrum of the sample with the composition of the gas phase as a function of the increasing temperature. The balance of the response times of the two detectors has to be checked against a suitable reference material in order to calibrate the instrument. Ideally, this reference material should possess a simple one-step decomposition chemistry:

$$A_{(s)} \rightarrow B_{(s)} + C_{(g)} + D_{(g)}$$

to yield a product B with no IR absorption and one or more volatile products (C and D), so the depletion of the IR bands would be directly related to the gas composition.

Metal carbonyls would be convenient reference materials for this purpose; their CO stretching bands in the 2200–1750 cm^{-1} region are generally sharp and well defined with high molar absorptivities making them ideal for such studies. In addition, the decomposition kinetics of metal carbonyls occur in a very clean way at temperatures below 500 °C, resulting in the formation of the metal, or the metal oxide if residual water is present, and in the evolution of CO and occasionally of CO_2:

$$M(CO)_x \rightarrow M + x CO\ (CO_2)$$

However, the pure carbonyl compound cannot be used, for two main reasons; first, saturation of the IR detector is likely to occur with undiluted materials, and second, decomposition kinetics are dependent on the particle size of the material, and often become diffusion-limited as soon as the uppermost layer has reacted.[7] Conversely, simple dilution in an inert matrix in the form of a mechanical mixture is not recommended. In addition, it cannot solve the particle size requirements, with the additional problems of uniformity and reproducibility of the sample. A solution was found in dispersing the carbonyl precursor from the vapor phase inside a porous oxide matrix such as a zeolite. This CVD technology is widely used in the semiconductor industry and recently in the preparation of heterogeneous catalysts, ensuring high dispersion and uniformity of the metal (or metal oxide) phase in the final material.

$Mn_2(CO)_{10}$ deposited on NaY zeolite was shown to have all the desired properties, *viz.*, the easy preparation of the material from commercial precursors [$Mn_2(CO)_{10}$ and NaY zeolite], a simple IR spectrum in the ν_{CO} region and a well known decomposition chemistry, quantitatively yielding MnO around 150 °C with evolution of CO and H_2:[4,8]

$$Mn_2(CO)_{10} \xrightarrow{\Delta} 10\ CO + 2\ Mn^0 \xrightarrow{H_2O} MnO + H_2$$

A series of DRIFT spectra recorded at linearly increasing temperatures showed a progressive decrease in intensity of the carbonyl bands, with the complete removal of all CO IR absorptions around 200 °C (Fig. 2). We can calculate the depletion rate of the IR bands as the first derivative of their integrated intensity. We used the 2050–cm^{-1} band for reporting depletion rates, since this measurement is best done with sharp, intense bands. This parameter can thus be assumed to be a measure of the instantaneous concentration of CO in the gas-phase, making possible the direct comparison of the analytical responses of the two detectors.

In Fig. 3, the depletion rate of the 2050 cm^{-1} band and the CO concentration, measured by GC, are plotted as a function of increasing temperature. The close similarity of the two profiles, showing a maximum at exactly the same temperature, indicates how the time responses of the two detection systems are well balanced. The feasibility of directly comparing surface modifications of the material, as obtained in DRIFT, and, *via* GC, the gas phase reactivity, is thus demonstrated.

DRIFT–GC offers significant advantages over conventional temperature techniques such as EGA, temperature-programmed

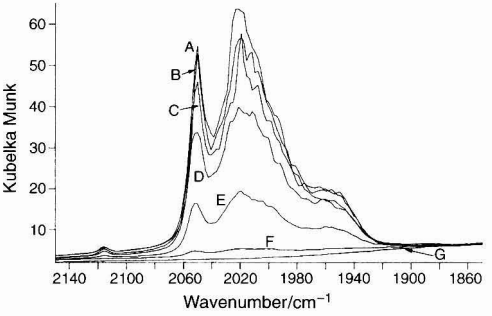

Fig. 2 DRIFT spectra in flowing H_2 of $Mn_2(CO)_{10}$–NaY at increasing temperature: A, 25; B, 100; C, 120; D, 130; E, 140; F, 150 and G, 190 °C.

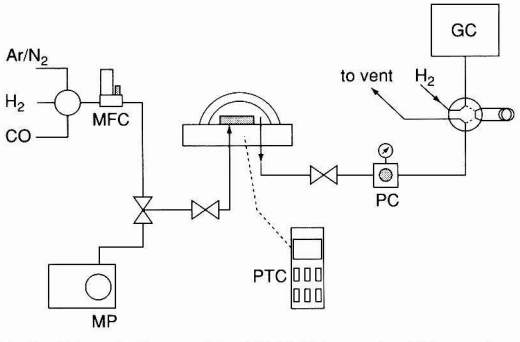

Fig. 1 Schematic diagram of the DRIFT–GC apparatus. MP = mechanical pump; MFC = mass flow controller; PTC = programmable temperature controller; PC = pressure controller; GC = gas chromatograph equipped with methanizer and flame ionization detector. Solid line, gas lines; broken line, electrical wiring (PTC + heater).

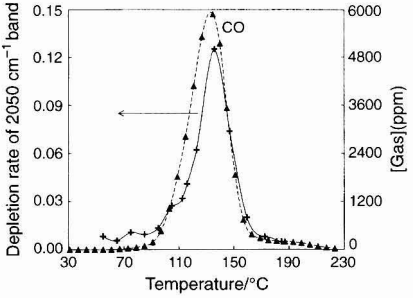

Fig. 3 $Mn_2(CO)_{10}$–NaY: thermal decomposition profiles as a function of temperature. +, Depletion rate, in arbitrary units, of 2050 cm^{-1} band; and ▲, CO evolution.

desorption (TPD)[9] and simple DRIFT studies.[2] These advantages are clearly illustrated when $Mn_2(CO)_{10}$–NaY is decomposed in the presence of a metallic rhodium phase. The presence of this rhodium phase should significantly affect the reactivity of the manganese, as has been well shown in the literature.[10] Instead, the DRIFT spectrum in the ν_{CO} region of $Mn_2(CO)_{10}$ on Rh–NaY closely resembles that of $Mn_2(CO)_{10}$–NaY, although the 2020 cm^{-1} feature is a slightly broader (compare Figs. 4 and 2). Moreover, only a decrease in intensity of the carbonyl absorption is observed on heating, and complete decarbonylation is reached around 200 °C. Finally, the depletion rate of the 2050 cm^{-1} band as a function of increasing temperature still

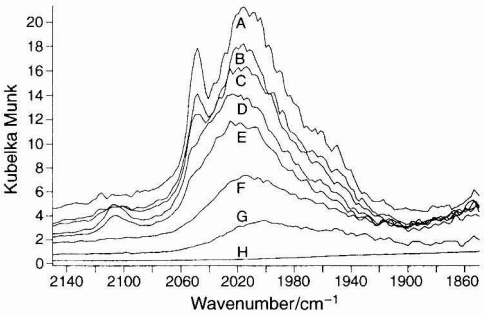

Fig. 4 DRIFT spectra in flowing H_2 of $Mn_2(CO)_{10}$ on Rh–NaY at increasing temperature: A, 50; B, 90; C, 100; D, 130; E, 140; F, 160; G, 200; H, 240 °C.

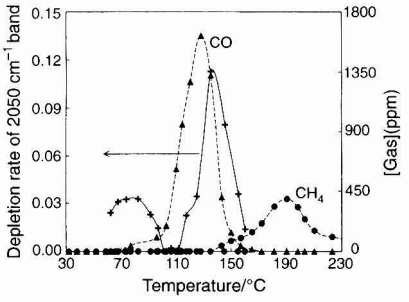

Fig. 5 $Mn_2(CO)_{10}$ on Rh–NaY: thermal decomposition profiles as a function of temperature. +, Depletion rate, in arbitrary units, of 2050 cm^{-1} band; ▲, CO evolution; and ●, CO_2 evolution.

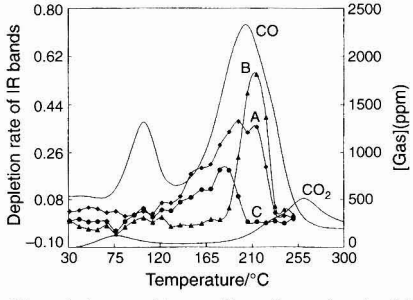

Fig. 6 Thermal decomposition profiles of a carbonylated Rh–NaY catalyst. Depletion rates, in arbitrary units, of different IR bands at A, 2098; B, 2048; and C, 1760 cm^{-1}. Solid lines: upper, CO evolution; and lower, CO_2 evolution.

reveals a maximum centered around 130–140 °C (Fig. 5), although some baseline irregularities may be observed between 60 and 80 °C. The profound effect of rhodium on the surface reactivity of manganese is instead clearly revealed by complementing the DRIFT study with the analysis of the gas composition using the proposed DRIFT–GC technique. Fig. 5 shows clearly how the concentration of CO in the gas phase no longer parallels the depletion rate of the CO IR bands. Instead, the maximum CO concentration in the gas phase is reached at 125 °C and then rapidly decreases in favor of the formation of methane at temperatures higher than 140 °C.

We can also derive useful chemical information from the analysis of the DRIFT–GC data. In particular, it may be speculated that the main effect of rhodium is to activate hydrogen, and to provide a low-temperature pathway for the reduction of desorbing CO to CH_4. The dissociation kinetics of the manganese carbonyl are instead little affected, being primarily dependent on the strength of the metal–carbon bonds.

More significant advantages can be obtained by using DRIFT–GC in the analysis of real materials, such as Rh–zeolite catalyst for CO activation as shown in Fig. 6. At about 100 °C the evolution of CO is revealed by GC without significant changes in the DRIFT spectrum, apart from some noise in the depletion rate of the 2048 and 1760 cm^{-1} bands. This behavior may be related to the interchange of surface species with different CO/Rh ratios, demonstrating the diagnostic power of GC detection for studying surface reactivity. However, temperature-programmed techniques generally show profiles with broad and poorly resolved peaks, as illustrated by the second CO evolution peak in Fig. 6. In order to improve the resolution and provide better conditions for kinetic analysis in temperature-programmed thermal studies, a number of sophisticated techniques, such as CRRTA and SITA,[3] have been proposed. However, all these techniques involve variable heating rates and also require a high time resolution of the analytical methodology, usually much higher than that in GC detection. In our approach, the different elementary processes occurring during the temperature-programmed analysis of the solid sample can be elegantly solved by investigating the changes in the DRIFT spectra. In Fig. 6, the high-temperature CO evolution may be deconvoluted in three elementary processes, as shown by the different profiles in the depletion rates of the 2098, 2048 and 1760 cm^{-1} bands. In particular, the 2098 and 1760 cm^{-1} bands show similar profiles, and are attributed to linear and bridged CO on small Rh clusters, while the 2048 cm^{-1} band shows higher thermal stability of CO-covered large Rh particles.[11]

Conclusions

The combination of DRIFT and GC techniques offers significant advantages in the thermal characterization of solid materials. The use of GC allows the investigation of gas-phase processes occurring over the surface of the sample, which are usually hidden to IR investigation. Also, the limited time resolution of GC detection largely prevents the use of the variable heating methods for improving resolution of temperature-programmed techniques.[3] The coupling of DRIFT with GC detection allows the deconvolution of the elementary process of gas evolution and offers further analytical clues to the understanding of surface chemistry, particularly when reacting gas environments are to be used.

Financial support from the National Research Council (Progetto Strategico Tecnologie Chimiche Innovative) and from the Ministry of Scientific and Technological Research (MURST) is gratefully acknowledged.

References

1 Holmes, P. D., McDougall, G. S., Wilcock, L. C., and Waugh, K. C., *Catal. Today*, 1991, **9**, 15.
2 Sordelli, L., Psaro, R., Dossi, C., and Fusi, A., in *Catalysis and Surface Characterization*, ed. Dines, T. J., Rochester, C. H., and Thomson, J., Royal Society of Chemistry, Cambridge, 1992, pp. 127–135.
3 Barnes, P. A., Parkes, G. M. B., and Charsley, E. L., *Anal. Chem.*, 1994, **66**, 2226.
4 Dossi, C., Fusi, A., Recchia, S., and Psaro, R., *Mater. Eng.*, 1994, **5**, 249; Dossi, C., Psaro, R., Bartsch, A., Brivio, E., Galasco, A., and Losi, P., *Catal. Today*, 1993, **17**, 527.
5 Wong, T. T., and Sachtler, W. M. H., *J. Catal.*, 1993, **141**, 407.
6 Dossi, C., and Fusi, A., *Anal. Chim. Acta*, 1989, **217**, 197.
7 Hurst, N. W., Gentry, S. J., Jones, A., and McNicol, B. D., *Catal. Rev.-Sci. Eng.*, 1982, **24**, 233.
8 Beutel, T., Knözinger, H., Treviño, H., Zhang, Z. C., Sachtler, W. M. H., Dossi, C., Psaro, R., and Ugo, R., *J. Chem. Soc., Faraday Trans.*, 1994, **90**, 1335.
9 Knözinger, H., in *Metal Clusters in Catalysis*, ed. Gates, B. C., Guczi, L., and Knözinger, H., Elsevier, Amsterdam, 1988, p. 259.
10 Treviño, H., Lei, G.-D., and Sachtler, W. M. H., *J. Catal.*, 1995, **154**, 245.
11 Yang, A. C., and Garland, C. W., *J. Phys. Chem.*, 1957, **61**, 1504.

Paper 6/06088I
Received September 4, 1996
Accepted December 2, 1996

Optosensor for Cinchona Alkaloids With C_{18} Silica Gel as a Substrate

Zhilong Gong[a], Zhujun Zhang*[b] and Xiaofeng Yang[b]

[a] *Department of Chemistry, Nanjing University, Nanjing, China 210008*
[b] *Department of Chemistry, Shaanxi Normal University, Xian, China 710072*

A flow-through optosensor for cinchona alkaloids with C_{18} silica gel as a substrate is proposed. The sensor is developed in conjunction with a flow-injection analysis system and is based on the retention of the cinchona alkaloids on a C_{18} column and the enhancement of their fluorescence. The analytical performance characteristics of the proposed sensor for the detection and quantification of these alkaloids were as follows: the detection limits for quinine, cinchonine, quinidine and cinchonidine were 2.3, 31.6, 2.3 and 31.6 ng ml^{-1}, respectively, with relative standard deviations of 0.9% for quinine and quinidine (20 ng ml^{-1}, n = 7) and 1.1% for cinchonine and cinchonidine (4.0 μg ml^{-1}, n = 7), respectively. Most of the common species did not interfere. The recommended method has been successfully tested for determination of quinine in pharmaceutical preparations and soft drinks.

Keywords: *Flow injection; fluorimetry; optosensor; C_{18} column; cinchona alkaloids*

The alkaloids, of which quinine is perhaps the most important, occur in the bark of trees or shrubs of various species of two Rubiaceous genera, Cinchona and Remijia. For the cinchona stereoisomerids, the major alkaloids fall into two configurational and polarimetric groups. The dextrorotatory species constitute cinchonine, quinidine and their dihydroderivatives while cinchonidine and quinine are levorotatory in nature.[1] Therapeutically, the most important are quinine and quinidine, the former having had popular usage in the relief of myalgia, neuralgia, headache and as an antipyretic.[2]

Several methods have been described for the determination of these alkaloids either in crude drug composites, in body fluids or in pharmaceutical formulations. Chromatographic techniques, especially HPLC, have played the most important role in facilitating the detection and quantification of these compounds. Techniques used have included HPLC,[3–7] GC,[8] spectrophotometry,[9–12] fluorimetry,[13,14] immunoassay,[15,16] and chemiluminescence.[17] However, these methods suffer disadvantages, such as poor sensitivity, poor selectivity or a time-consuming procedure.

C_{18} silica gel is the most widely used stationary phase for reversed phase liquid chromatography. For a given mobile system, many substances have their own characteristic retention which can be used for their chromatographic separation. Cinchona alkaloids were well retained on a C_{18} column and showed an approximately seven-fold increase in fluorescence when 0.1 M H_2SO_4 solution was selected as the mobile system with these alkaloids dissolved in it (compared with an aqueous solution). The retained alkaloids were also quickly and completely eluted from the C_{18} column with a mixture of methanol and water (70 + 30, v/v). However, under the same conditions, many other substances were not retained on the C_{18} column or showed no fluorescence on it though they could also be retained. Based on this property, an optosensor for individual cinchona alkaloids was developed using C_{18} silica gel as a substrate. The proposed sensor proved to be simple, rapid and sensitive, and only conventional instrumentation is required.

Experimental

Apparatus

A Perkin-Elmer (Norwalk, CT, USA) LS-50 luminescence spectrometer was used to perform all fluorescence emission measurements. Instrument excitation and emission slits were set at 5 and 15 nm, respectively, throughout this study.

A conventional Perkin-Elmer flow cell (Model L225 1247, 25 μl volume) was used to contain the C_{18} silica gel. At the bottom of the flow cell, some glass wool was placed to prevent particle displacement by the carrier. C_{18} silica gel (15 μl) was loaded with the aid of a syringe and the other end of the flow cell was kept free. The cell was then connected to the flow system, and placed in the spectrometer and the fluorescence was measured directly on the C_{18} beads.

A Model pHs-20 pH meter (Shanghai Rich Instruments Factrory, Shanghai, China) was used to carry out the pH measurements.

A three-channel peristaltic pump (Shanghai Rich Instruments Factory) was used to generate the flowing streams. The flow rate used was 1 ml min^{-1} throughout the experiments. Two six-way valves were used for sample introduction and for the elution of the fixed molecules.

Reagents

All reagents used were of analytical-reagent grade, and distilled, deionized water was used throughout.

Cinchona alkaloids stock standard solution (2.5 mg ml^{-1}) was prepared by dissolving the required amount of cinchona alkaloids (The Second Chemicals Factory of Shanghai, Shanghai, China) in an appropriate amount of 0.1 M H_2SO_4 solution, and diluting to the mark with water, respectively. Working solutions were prepared by appropriate dilution of the stock standard solution with water.

C_{18} silica gel (10 μm particle size, Sigma, St. Louis, MO, USA) was used as the solid support without any pre-treatment.

All commercial soft drinks were purchased from the local market.

The carrier solution used in the FIA experiments was 0.1 M H_2SO_4 solution.

Basic Procedure

Samples or standards (2 ml) were injected and pumped through the flow system. Cinchona alkaloids went through the flow cell and were retained on the C_{18} silica gel. The high fluorescence was measured. Once the fluorescence measurement was taken, 2 ml of the mixture of methanol–water (70 + 30 v/v) was injected to elute the retained alkaloid molecules, then 2 ml of the carrier (0.1 M H_2SO_4 solution) was pumped through the flow cell before proceeding with the next sample or standard injection.

For injection in this flow-through sensor, standards and samples were prepared as follows: an appropriate aliquot of cinchona alkaloids standard (or the sample) was transferred into a 25 ml calibrated flask and 5 ml of 0.5 M H_2SO_4 solution was added before the solution was made up to the mark with water.

Reagent blanks were prepared and measured following the same procedure.

Sample Preparation

Injectio quinini composita (a pharmaceutical preparation) was analyzed without any pretreatment. In order to avoid serious interferences from some other unknown ingredients in soft drinks, a preliminary crystallization of quinine from soft drinks was needed. Soft drink was treated as follows: 5 ml of soft drink solution mixed with 5 ml of 0.1 M NaOH was treated for 1.5 min with 10 ml of $CHCl_3$. After separation, 5 ml of the organic layer was transfered into a small flask and kept at room temperature to wait for $CHCl_3$ to evaporate completely, the resultant quinine crystal was dissolved in an appropriate amount of 0.1 M H_2SO_4 solution and was then analyzed according to the procedure described above.

Results and Discussion

Spectral Characteristics

The fluorescence spectra of quinine both on the C_{18} column and in aqueous solution were obtained. Compared with the spectra in aqueous solution, the spectra on C_{18} silica gel has an 8 nm of blue shift of its emission wavelength. The peak wavelength in the excitation spectrum of quinine on C_{18} silica gel is 346 nm and the emission maximum is located at 430 nm. Fixation on C_{18} silica gel resulted in a stronger fluorescence signal which was about seven times greater than that obtained in aqueous solution in a conventional flow cell and two times greater than that obtained using classical 'batch' fluorescence cells. This should be the result of accumulation of quinine on C_{18} silica gel and changes in the environment of quinine. When quinine solution passed through the flow cell the quinine fixed on the packed C_{18} silica gel, and the effect of water molecules on the fluorescence emission was reduced. Thus, a more favourable environment results in stronger fluorescence. Spectral characteristics for other cinchona alkaloids are listed in Table 1.

Acidity Dependence

The effect of acidity on the fluorescence intensity of these alkaloids was studied using H_2SO_4 solution in the concentration range from 0.02 M to 0.4 M (quinine was selected as an example). The optimum acidity for the fixation of quinine was found to be 0.1 M H_2SO_4. Therefore 5.0 ml of 0.5 M H_2SO_4 solution per 25 ml of the final solution was selected.

Influence of Flow Rate

The dependence of the relative fluorescence intensity of quinine fixed on the gel on the flow rate was studied at different flow rates (0.5, 1.0, 1.5, 2.0 and 2.5 ml min^{-1}) at the same concentration of quinine (1.34 μg ml^{-1}). It was found that the fluorescence signal was affected by the flow rate. The fluorescence maximum increased when the flow rate increased from 0.5 to 2.5 ml min^{-1}, and the time taken to reach the fluorescence maximum reduced and reached a steady value of about only 60 s. As a compromise between sensitivity and throughput, a flow rate of 1.0 ml min^{-1} was selected.

Effect of Eluent Composition

A CH_3OH–H_2O mixture was used to elute the alkaloids fixed on C_{18} silica gel. With an increase of the volume of CH_3OH in the mixture from 10 to 90%, the time taken to elute these alkaloids (fixed on C_{18} silica gel) completely was reduced. The eluting time reaches a steady value when the volume of CH_3OH in the mixture is up to 70% (v/v). Therefore, a CH_3OH volume of 70% (v/v) was selected.

Effect of Sample Volume on Sensitivity

One of the main advantages of the sensor is the potential increase in sensitivity with increase in the sample volume taken for analysis. This effect can be assessed by measuring the fluorescence intensity on C_{18} silica gel with different volumes of solution containing the same concentration of quinine passed through the flow cell.

As shown in Table 2, fluorescence intensity increases with sample volume. Finally, a 2 ml sample volume was selected as a compromise between sensitivity and sample throughput.

Reversibility of the Sensor

It was found that 2 ml of a mixture of methanol–water (70 + 30 v/v) can elute the fixed quinine molecules quickly and completely without damaging the C_{18} silica gel.

Stability of the Sensor

The sensor kept at room temperature was found to be very stable for up to 1 month (no experiments were performed to test the stability after that period of time). This aspect was evaluated by measuring the fluorescence intensity of the solution of quinine at the same concentration every 7 d. It was verified that no C_{18} silica gel was found to be damaged and the fluorescence signal did not decrease.

Effect of Foreign Species

In order to determine the potential effect of foreign species, a study was carried out at a 0.20 μg ml^{-1} level of quinine. A foreign species was considered not to interfere if it produced an error not exceeding +5% in the determination of the analyte. The tolerence ratios were as follows: 500 for Mg^{2+}, 400 for

Table 1 Characteristics of the proposed optosensor

Substance	In solution $\lambda_{ex}/\lambda_{em}$	On C_{18} column $\lambda_{ex}/\lambda_{em}$	LR*/ ng ml^{-1}	DL†/ ng ml^{-1}	r^2
Quinine	346/438	346/430	5.0–20 000	2.3	0.9998
Quinidine	346/438	346/430	5.0–20 000	2.3	0.9998
Cinchonine	350/445	363/436	200–20 000	31.6	0.9989
Cinchonidine	350/445	363/436	200–20 000	31.6	0.9989

* Linear range. † Detection limit.

Table 2 Effect of sample volume on sensitivity

Sample volume/ ml	Concentration of quinine/μg ml^{-1}					Sampling frequency/ h^{-1}
	0.01	0.13	0.64	1.15	5.36	
1	8.4	16.8	37.9	58.9	273.7	12
2	16.8	29.5	63.2	105.3	412.6	10
3	25.3	39.5	84.2	143.2	513.7	8
4	29.5	47.8	101.1	179.4	568.4	7
5	32.0	54.8	113.5	210.1	602.1	6
6	33.7	60.1	122.9	239.1	627.4	6
7	34.9	64.6	130.3	258.4	640.0	5
8	36.0	67.4	134.7	269.5	648.4	5

Ca^{2+}, 150 for Cu^{2+}, 100 for Al^{3+}, 50 for Fe^{3+}, 400 for glucose, 300 for benzoate, 100 for citrate, sucrose and saccharose, 70 for fructose, and 50 for vitamin C. Other cinchona alkaloids caused serious interferences.

Response to Cinchona Alkaloids

The analytical figures of merit for the proposed sensor were evaluated. Calibration graphs were prepared from the results of triplicate 2 ml injections of the corresponding cinchona alkaloids standard solutions. The results are shown in Table 1.

Application of the Method

The method measures all the cinchona alkaloids together because these alkaloids are almost the same in structure and fluorescence characteristics, and so it is applicable only for individual alkaloids. In this paper quinine was selected as an example to evaluate the proposed sensor for its popular usage in clinical chemistry and food chemistry.

Following the procedure detailed under Experimental, the proposed sensor was applied to the determination of quinine in some soft drinks and a pharmaceutical preparation. Soft drinks were pre-treated as described under Sample Preparation and analyzed according to the procedure stated under Experimental. The results were 124.0, 72.2, 64.9, 66.7 and 64.1 μg ml^{-1} (n = 3) which are quite comparable with those obtained by the Food Chemicals Codex recommended method[19] (125.3, 74.0, 65.2, 71.1 and 64.4 μg ml^{-1}). Also, a pharmaceutical preparation (Injectio quinini composita, Shanghai, China) was analyzed without any pre-treatment. The results obtained using the proposed optosensor were 60.9 ± 0.1 mg ml^{-1} (n = 5) which compared favorably with that reported by the manufacturer (61.1 mg ml^{-1}) and that by the Pharmacopoeias[20] (61.4 mg ml^{-1}).

This work was funded by the National Science Foundation of China.

References

1 Manske, R. H. R., and Holmes, H. L., *The Alkaloids Chemistry and Physiology*, Academic Press, New York, 1953, vol. III.
2 John, K. C., and Jelleff, C., *The Pharmacologic Principles of Medical Practice*, Williams and Wilkins, Baltimore, 5th edn., 1961.
3 Valenti, P. L., *J. Assoc. Off. Anal. Chem.*, 1985, **68**, 782.
4 Kral, K., and Sontag, G., *Lebensm Z., Unters. Forsch.*, 1982, **175**, 22.
5 Jeuring, H. J., Van der Hoeven, W., Van Doornick, P., and Ten Broeke, R., *Lebensm, Z., Unters. Forsch.*, 1979, **169**(4), 281.
6 Hoyer, G. L., Clawson, D. C., Brookshier, L. A., Nolan, P. E., and Marcus, F. I., *J. Chromatogr. B., Biomed. Appl.*, 1991, **110**, 159.
7 Brandsteterova, E., Romanova, O., Kralikova, D., Bozekova, L., and Kriska, W., *J. Chromatogr. A*, 1994, **665**(1), 101.
8 Klatsmanyi, J., and Zala, P., *Elelmiszervizsgalati Kozl.*, 1982, **28**(1–2), 49.
9 Beljaars, P. R., and Koken, P. J., *J. Assoc. Off. Anal. Chem.*, 1972, **56**, 1284.
10 Peterdi-Nagy, A., Sperlagh, J., and Vegh, M., *Acta Pharm. Hung.*, 1986, **56**(3), 115.
11 *Spanish Official Method*, Health and Consumption Ministry, Publication services, Madrid, 1985.
12 Zhebentyaev, A. I., and Duksina, S. G., *Farmatsiya (Moscow)*, 1986, **35**(2), 16.
13 Garcia Castro, J. C., Sanchez, M. J., Rodriguez Delgado, M. A., and Diaz Romero, C., *Mikrochim. Acta*, 1993, **110**(4–6), 263.
14 Guilbault, G. G., *Practical Fluorescence: Theory, Methods and Techniques*, Marcel Decker, New York, 1973.
15 O'Reilly, J. E., *J. Chem. Educ.*, 1975, **53**, 610.
16 Morgan, M. R. A., Bramham, S., Webb, A. J., Robins, R. J., and Rhodes, M. J. C., *Planta Med.*, 1985, **3**, 237.
17 Ward, C. W., and Morgan, M. R. A., *Food Addit. Contam.*, 1988, **5**(4), 555.
18 Koukli, I., and Calokerinos, A. C., *Anal. Chim. Acta*, 1990, **236**(2), 463.
19 Health Ministry of the People's Republic of China, *Medical Law of the People's Republic of China*, Chemical Industry Press, Beijing, vol. II, 1995.
20 Fischbach, H., *Food Chemicals Codex*, National Academic Press, London, 3rd edn., 1981.

Paper 6/04450F
Received June 26, 1996
Accepted November 11, 1996

The Analyst

Application of Oscillating Reaction-based Determinations to the Analysis of Real Samples

Rafael Jiménez-Prieto, Manuel Silva and Dolores Pérez-Bendito*

Department of Analytical Chemistry, Faculty of Sciences, University of Córdoba, E-14004 Córdoba, Spain

The application of oscillating reactions to the analysis of real samples by the analyte pulse perturbation technique is reported. The oscillating reaction involving the H_2O_2–NaSCN–$CuSO_4$ system in an alkaline medium was used for the expeditious, convenient, automatic determination of vanillin, paracetamol and ascorbic acid in food and pharmaceutical samples. Six methods (two per analyte) were developed that allow the determination of 1.5–40 μmol of vanillin, 0.5–6 μmol of paracetamol and 0.5–5 μmol of ascorbic acid in real samples. The proposed methods are precise (RSD < 5%) and have a reasonable sample throughput (6–10 h^{-1}) for this type of reaction, which can be implemented with modular equipment available at any laboratory. The effect of influential variables and the selectivity of the determinations was studied in relation to the types of sample used. Determinations are virtually direct and require no removal of interfering species. The results were validated by comparison with standard methods.

Keywords: *Oscillating reaction; analyte pulse perturbation technique; vanillin; paracetamol; ascorbic acid; food samples; pharmaceutical preparations*

Oscillating reactions are complex dynamic systems that involve cyclic or periodic changes in the concentration of some ingredient (whether a reactant, a product or an intermediate) with time.[1] This type of system has been known since early this century, when the first model for an oscillating chemical system was developed.[2,3] Oscillating reactions have so far been analysed mainly in physico–chemical terms in order to elucidate the complex mechanism that they involve. Two of the better known oscillating chemical systems are the Belousov–Zhabotinskii (BZ) reaction[4–10] and the Bray–Liebhafsky reaction.[11–15] From available knowledge on these reactions, it follows that the system must be far from thermodynamic equilibrium (*i.e.*, for ΔG must be large and negative), which entails using a well stirred continuous-flow reactor (CSTR),[16–18] and that one or more autocatalytic or cross-catalytic steps must take place between two steps of the reaction mechanism.[19]

Although some oscillating reactions have been used for analytical purposes, particularly the Ce^{IV}-catalysed reaction between malonic acid and $KBrO_3$ (BZ reaction),[20,21] analytical determinations based on a closed system including the analyte involve labour-intensive procedures that entail re-starting the oscillating system before each new determination. This accounts for the little interest aroused so far by this type of reaction for analytical purposes.

The recent inception of an open system for application of the analyte pulse perturbation (APP) technique by use of a CSTR[22–25] has opened up new avenues for oscillating reactions in routine analyses. As a result, there has been a gradual shift from theoretical to practical interest. The APP technique allows a system to be kept oscillating for a long time (several hours) and thus be employed as an inexhaustible indicator system for successively added samples and/or standards. This technique is a useful analytical tool inasmuch as it uses very simple, modular equipment[22] that can be assembled from parts available in any analytical laboratory. Up to now, the usefulness of the APP technique has been demonstrated only with standards, such as sodium thiosulfate,[22] reduced glutathione[23] and gallic acid,[24] providing different perturbation shapes, and in the resolution of mixtures of gallic acid with resorcinol.[25]

In this work, the application of the oscillating reaction-based determinations to the analysis of real samples was addressed by use of the APP technique. The oscillating reaction of the H_2O_2–NaSCN–$CuSO_4$ system in an alkaline medium was chosen for this purpose.[26–29] The addition of small amounts of vanillin, paracetamol and ascorbic acid to the oscillating system alters some of its properties; this effect can be used to develop methods for the determination of the analytes in real samples.

Experimental

Reagents

All chemicals used were of analytical-reagent grade and supplied by Merck (Darmstadt, Germany), except vanillin and paracetamol (from Sigma–Aldrich Química, Madrid, Spain). Solutions of these two reagents and ascorbic acid, sodium thiocyanate, hydrogen peroxide, copper sulfate pentahydrate, sodium hydroxide and sodium chloride were prepared in doubly distilled water.

Apparatus

The instrumental set-up used to implement the proposed methods consisted of a glass CSTR of 10–50 ml capacity (depending on the particular analyte to be determined) wrapped in a water recirculation jacket fitted to a Selecta (Barcelona, Spain) Model 6000383 thermostat that was furnished with an Eleya (Tokyo, Japan) RC-2 magnetic stirrer. Oscillations were monitored by means of a Model 6-0305.100 Pt electrode and a 6-0733.100 Ag/AgCl indicator electrode, both from Metrohm (Herisau, Switzerland), which were interfaced to a Mitac PC-AT (12 MHz) PC compatible computer equipped with a PC-Multilab PCL-812 PG 12-bit analogue-to-digital converter. Data were acquired and processed by using QuickBasic software specially developed by the authors for the intended purpose. Reactants were added to the CSTR and products withdrawn from it by using a Minipuls-3 peristaltic pump from Gilson (Worthington, OH, USA) furnished with four channels, three of which were used to feed the CSTR with the reactant solutions and the fourth to maintain the reaction volume in the CSTR constant (see Fig. 1). The pump was governed by means of a remote control that allowed the instantaneous selection of different pre-set flow rates. Samples were injected with the aid of Treff Lab (Degersheim, Switzerland) micropipettes.

Procedure for the Determination of Vanillin

The CSTR thermostated at 25 °C was fed with 5 ml of 1 mol l^{-1} H_2O_2, 2.5 ml of 0.25 mol l^{-1} NaSCN, 2.5 ml of 0.50 mol l^{-1}

NaOH, 5 ml of 1 mol l^{-1} NaCl, 5 ml of 1.5×10^{-3} mol l^{-1} $CuSO_4$ and 5 ml of water to a final volume of 25 ml under continuous stirring. Then the indicator and reference electrode were immersed in the reaction mixture and data acquisition by the computer was started. Next, the peristaltic pump was started at an overall reactant feeding flow rate of 1.5 ml min^{-1} (*i.e.*, 0.5 ml min^{-1} through each reactant channel). Reactant solutions were prepared in such a way that the stream fed to the reactor contained 0.4 mol l^{-1} H_2O_2, 0.05 mol l^{-1} NaSCN, 0.1 mol l^{-1} NaOH, 0.2 mol l^{-1} NaCl and 3×10^{-4} mol l^{-1} Cu^{2+}. After the oscillations had reached a steady state, the reaction was perturbed with pulses containing various amounts of vanillin between 1.0 and 40 μmol. The sample must be injected exactly as shown in Fig. 2(A).

Under the flow rate conditions where the system is in oscillation (1.5 ml min^{-1}), the steady state is approached very slowly; the process can be accelerated by having the peristaltic pump provide a high flow rate over a short period in order to replenish most of the CSTR contents. Of the various available options for this purpose, we chose to use a flow rate of 4.5 ml min^{-1} for 1 min immediately after the response cycle was finished [point 1 in Fig. 2(A)], followed by 10 ml min^{-1} for 2 min. Then the initial flow rate (1.5 ml min^{-1}) was re-set [point 2 in Fig. (2A)] and the steady-state oscillating conditions were rapidly restored as a result. At that point, the system was ready for a new determination. This abrupt increase in the flow rate from 1.5 to 10 ml min^{-1} under the special reaction conditions used stopped oscillations and hence allowed one to proceed with the perturbation sequence.

Procedure for the Determination of Paracetamol

For the determination of paracetamol, the CSTR was thermostated at 35 °C and filled with 6 ml of 1 mol l^{-1} H_2O_2, 2 ml of 0.25 mol l^{-1} NaSCN, 2 ml of 0.25 mol l^{-1} NaOH, 4 ml of 1 mol l^{-1} NaCl, 2 ml of 1.5×10^{-3} mol l^{-1} $CuSO_4$ and water to a final volume of 20 ml. As in the previous procedure, the electrodes were immersed in the reaction mixture, data acquisition by the computer was initiated and the pump started. The overall reactant flow rate was 2 ml min^{-1} and the stream fed to the reactor contained 0.6 mol l^{-1} H_2O_2, 0.05 mol l^{-1} NaSCN and NaOH, 0.2 mol l^{-1} NaCl and 1.5×10^{-4} mol l^{-1} Cu^{2+}. Once steady-state oscillating conditions had been reached, the system was perturbed with paracetamol pulses (0.5–6 μmol) as shown in Fig. 2(B). After the system response had been recorded, the flow rate delivered by the pump was raised to 10 ml min^{-1} for 3 min in order to expedite restoration of the steady state [point 1 in Fig. (2B)]. Then the initial flow rate (2 ml min^{-1}) was re-set [point 2 in Fig. 2(B)]; the abrupt rise in the flow-rate was facilitated by the fact that the oscillating state was not lost under the working conditions used. After the steady state had been restored, the system was ready for a new determination.

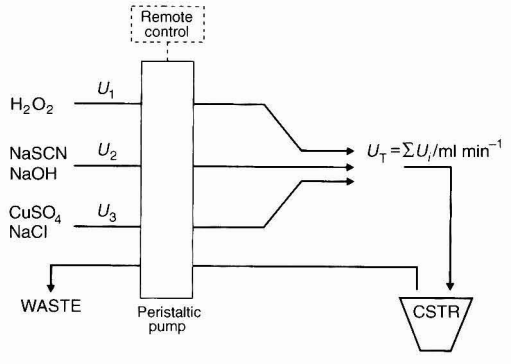

Fig. 1 Reactant and product flow across the peristaltic pump. For details, set text.

Procedure for the Determination of Ascorbic Acid

The determination of ascorbic acid was carried out in a 10 ml reaction tank thermostated at 30 °C and supplied with 1.25 ml of 1 mol l^{-1} H_2O_2, 0.35 ml of 0.5 mol l^{-1} NaSCN, 0.5 ml of 0.5 mol l^{-1} NaOH, 1 ml of 1 mol l^{-1} NaCl, 0.5 ml of 2×10^{-3} mol l^{-1} $CuSO_4$ and water to a final volume of 5 ml. After the electrodes had been immersed in the reaction mixture and data acquisition started, the peristaltic pump was switched to deliver an overall flow rate of 7.5 ml min^{-1} (equivalent to 2.5 ml min^{-1} per individual stream). Once the steady state had been reached, the system was perturbed with pulses containing 0.5–5 μmol of ascorbic acid. For perturbations to have the intended effect, injections must be performed as is shown in Fig. 2(C).

Preparation of Samples

Vanilla sugar samples were prepared by weighing 2–3 g of powdered, homogenized sugar and extraction of the vanillin by using 5 ml of ethanol with stirring for 3 min. The supernatant was filtered in order to clear the solution, a portion of 35–500 μl of which (depending on the amount of each analyte present in the sample) was used for analysis.

Vanilla extract was obtained from vanilla sticks by using the AOAC's recommended procedure.[30] An amount of 1 g of sticks in small pieces was macerated with 2 ml of H_2O in a closed vessel for 12 h, then 4 ml of ethanol were added and the mixture

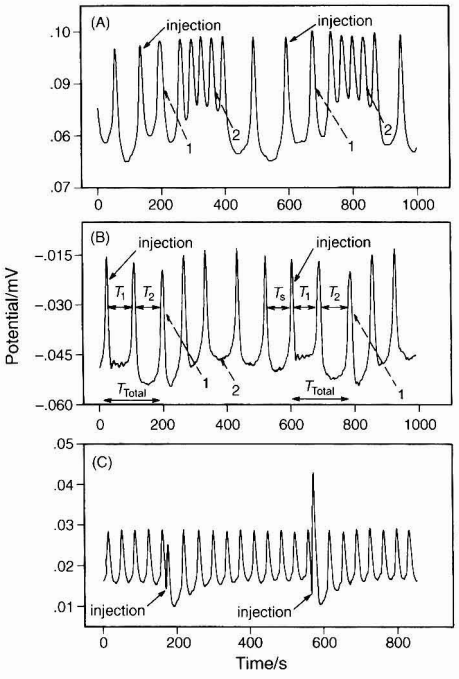

Fig. 2 Typical oscillation sequences and response of the oscillating system to perturbations with (A) 10 and 7.5 μmol of vanillin; (B) 3.0 and 2.0 μmol of paracetamol; and (C) 1.45 and 2.40 μmol of ascorbic acid. For details, see text.

was again macerated for 3 d. The resulting solution was filtered and a portion of 125–150 μl added to the oscillating system to determine vanillin.

About 30–40 ml of fresh orange juice were supplied with an adequate amount of diatomaceous earth; the mixture was made into a fine dough that was rapidly filtered through a Buchner funnel. A portion of 250–400 μl of the filtrate, which should be clear and light orange in colour, was used for the determination.

Pharmaceutical preparations were dissolved or suspended in doubly distilled water. The amount of drug used in each case was dictated by that of analyte present. If the dissolved sample contained any residual solid excipient, the only additional treatment required was filtering or centrifugation, not to remove potential interferents but rather to obtain a clear solution. Aliquots of appropriate volume were used to perturb the oscillating system.

Results and Discussion

As noted earlier, vanillin, paracetamol and ascorbic acid were used as analytes to demonstrate the potential of the APP technique for analytical determinations in real samples of interest. The choice was based on two essential criteria: (*a*) each analyte responded differently to perturbations of the oscillating system, which allowed for different methods to be established and compared, and (*b*) the analytes are present in a variety of drug and food samples (the latter include natural products such as stick vanilla and orange juice and foodstuffs such as vanilla sugar), so they are of great practical interest.

Effect of Reaction Variables

In developing the different determination methods, the effect of the more influential variables on the oscillating system studied was investigated. Such variables included the peroxide concentration, an increase in which decreased the response of vanillin as regards the oscillation amplitude and, especially, the oscillation period [Fig. 3(A)]. Conversely, an increase in the H_2O_2 concentration from 0.2 to 0.36 mol l^{-1} increased both measured parameters (T_2 and T_T) by about 25% in the case of paracetamol. The effect of H_2O_2 on ascorbic acid was the most complex of all [Fig. 3(B)]. The H_2O_2 concentration used for each analyte was selected on the basis not only of its influence on the perturbation (maximum response) but also of the effect of its changes on the oscillating system in the absence of perturbations (more uneven oscillations, exceedingly long periods, drifts in the oscillating system, *etc.*).

The influence of the copper concentration on the determinations was also examined. Specifically, an increase in the concentration of Cu^{2+} from 1×10^{-4} to 4×10^{-4} mol l^{-1} resulted in an increase in the response of vanillin by 20 and 7.5% in terms of oscillation amplitude and period, respectively [Fig. 3(C)]. A copper concentration of 3×10^{-4} mol l^{-1} was selected for the determination of vanillin because increasing the catalyst concentration gave rise to gradually shorter periods that hindered the determination. The copper concentration also significantly affected the determination of ascorbic acid. Thus, an increase in $[Cu^{2+}]$ from 1×10^{-4} to 3×10^{-4} mol l^{-1} decreased the oscillation amplitude by about 25%. On the other hand, this variable did not affect the determination of paracetamol at the above-mentioned concentration levels of copper.

Variations in the sodium thiocyanate concentration had a marked effect on the determination of ascorbic acid. Thus, as shown in Fig. 3(D), the response of the oscillating system to perturbations was nearly doubled on raising the SCN^- concentration from 2.0×10^{-2} to 4.5×10^{-2} mol l^{-1}. A concentration of 3.0×10^{-2} mol l^{-1} was chosen because greater amounts of thiocyanide resulted in considerably extended oscillation periods and in the appearance of induction periods preceding the oscillations.

The presence of sodium chloride in the reaction medium was dictated not only by its ability to act as an electrolyte controlling the ionic strength, but also by its inhibitory effect on the passivation of the Pt electrode by precipitated copper hydroxide on its surface. This shortcoming, previously reported elsewhere,[22] arises in the absence of the electrolyte or at concentrations below 0.2 mol l^{-1}.

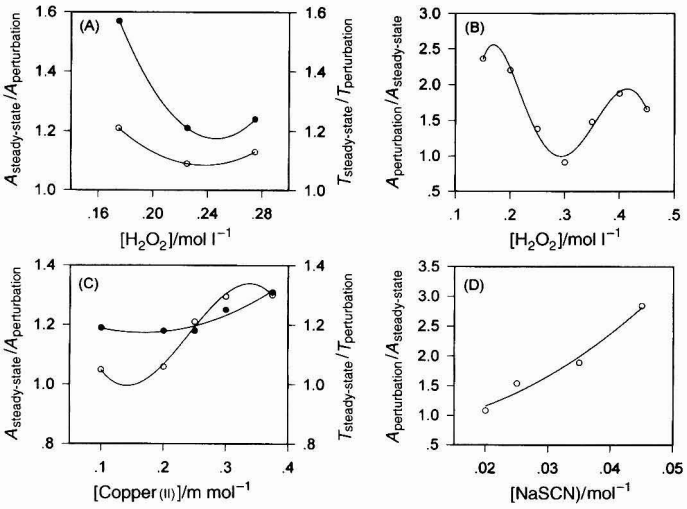

Fig. 3 Influence of the concentration of (A) H_2O_2 and (C) Cu^{II} on the determination of vanillin, and effect of the concentration of (B) H_2O_2 and (D) NaSCN on the determination of ascorbic acid. The white circles in (A) and (C) represent the ratio of the amplitude for the system in its steady state to that of the perturbation response cycle. Black circles have the same meaning for the period. (B) and (C) are plots of the ratio of the amplitude for the cycle following the perturbation to that for the oscillations in the steady state against the concentration of H_2O_2 and NaSCN, respectively.

The flow rate of the peristaltic pump feeding the CSTR was found to affect strongly the determinations of vanillin and paracetamol since both rely on measurements of the oscillation period following the perturbation and the period was directly related to such a flow rate. Thus, an increase in the flow rate caused a decrease in the oscillation period of the steady-state system and *vice versa*. On the other hand, too high a flow rate might sweep part of the analyte before it could exert its effect on the oscillating system and too low a flow rate lengthened the oscillation period to such an extent that the change introduced by the perturbation was negligible. Flow rates of 1.5 and 2.0 ml min^{-1} for volumes of 20 and 25 ml in the CSTR were used in the determinations of vanillin and paracetamol, respectively.

Analytical Figures of Merit

The oscillating system was perturbed with variable amounts of vanillin, paracetamol and ascorbic acid under the above-described optimum conditions and the response obtained in each case was analysed in two different ways for each analyte:

(*a*) For vanillin, changes in the oscillation amplitude and period afforded application of amplitude- and period-based methods, respectively.

(*b*) For paracetamol, T_2 (second-period method) or $T_1 + T_2$ (total-period method) was correlated with the amount of analyte added [see Fig. 2(B)]. It should be noted that the calibration curve provided by the second-period method was linear, whereas that obtained with the total-period method fitted a second-order polynomial.

(*c*) For ascorbic acid, both proposed methods rely on the dependence of the maximum potential (absolute-signal method) or the amplitude of the response cycle (relative-signal method) on the analyte concentration.

Table 1 shows the figures of merits for the calibration graphs and also other parameters of analytical interest. In general, the proposed methods exhibit a wide linear range, excellent precision (the RSD for vanillin and paracetamol is $<2\%$) and acceptable throughput. The method of choice will in some cases (*e.g.*, that for vanillin) be dictated by the precision. However, the actual choice should rely on the results obtained by applying these methods to the determination of the different analytes in real samples.

Applications

The potential of the proposed methods for routine analyses was assessed by applying them to samples of interest containing the analytes studied. Thus, vanillin was determined in vanilla sugar and stick vanilla. Before the determinations proper, particularly that of vanillin in vanilla sugar, the potential interference of sucrose in the samples was examined. Thus, the system was perturbed with a mixture consisting of a fixed amount of vanillin (10 μmol) and various amounts of sucrose between 0.2 and 2.5 mol. The results obtained revealed the absence of interferences with the amplitude method and the presence of random, erratic deviations in the average oscillation period. The solubility of sucrose in ethanol–water mixtures of variable composition was also studied; the sugar was found to be virtually insoluble above 80% ethanol. Finally, the influence of the presence of ethanol on the oscillating system was investigated by perturbing it with various volumes of an ethanol–water solution containing 10 μmol of vanillin. For a volume of reaction mixture of 25 ml in the CSTR, injecting up to 1 ml of ethanol caused no significant changes in the system response to the perturbation. Consequently, vanillin was extracted from the samples with ethanol, which ensured quantitativeness and the absence of sucrose in the extract, and hence of any interfering effects with the period method.

Table 2 shows the results obtained in the determinations, which were validated by contrast with the AOAC's recommended method for the determination of vanillin by UV/VIS spectroscopy.[30] Statistical tests were performed in every case in order to compare the results of the AOAC and the amplitude or period methods. The Student's *t*-values obtained were always smaller than their tabulated counterparts at $P = 0.05$. Note the extremely high error obtained for sample 2 (vanilla sugar) with the amplitude method, probably as a result of the presence of the antibinding agent E-551 in this sample alone; the additive may

Table 1 Characteristic parameters for the calibration plots and analytical figures of merit of the determination of vanillin, paracetamol and ascorbic acid

Compound	Linear range/μmol	Regression equation[a]	r[b]	RSD[c] (%)	Sample throughput/h^{-1}
Vanillin	1–30	$A = 30.45 - 0.283C$	0.9959	0.78[d]	8.5
	1–40	$P = 88.88 - 1.668C$	0.9979	2.04[d]	8.5
Paracetamol	1–6	$T_2 = 80.17 + 5.516C$	0.9959	0.95[e]	6
	0.5–6	$T_T = 168.97 + 1.218C + 1.682C^2$	0.9995	0.61[e]	6
Ascorbic acid	0.5–5	$S_a = 8.69 + 14.091C$	0.9961	4.65[f]	10
	0.5–5	$S_r = 1.07 + 14.328C$	0.9959	7.64[f]	10

[a] A, amplitude; P, period; T_2, second period; T_T, total period; S_a, absolute signal; S_r, relative signal; C, analyte mass (μmol). [b] Correlation coefficient ($n = 9$). [c] From 11 determinations of [d] 10 μmol vanillin, [e] 2 μmol paracetamol and [f] 2 μmol ascorbic acid.

Table 2 Determination of vanillin in food samples by use of the proposed oscillating method

Sample	Found by AOAC method[a]/mg g^{-1}	Amplitude method: Found[a]/mg g^{-1}	Amplitude method: Error (%)	Period method: Found[a]/mg g^{-1}	Period method: Error (%)
Vanilla sugar 1	78.64 ± 5.16	83.70 ± 4.30	6.43	83.83 ± 14.06	6.60
Vanilla sugar 2	3.60 ± 0.26	7.73 ± 0.63	104.7	3.29 ± 0.25	−8.61
Vanilla sugar 3	82.14 ± 2.74	85.76 ± 12.09	4.41	78.36 ± 1.01	−4.60
Stick vanilla 1	15.63 ± 1.15	15.10 ± 0.31	−3.39	14.90 ± 0.99	−4.67
Stick vanilla 2	13.83 ± 2.26	12.51 ± 2.82	−9.54	14.46 ± 2.27	4.56

[a] Average of three individual determinations ± standard deviation.

Table 3 Determination of paracetamol in pharmaceutical preparations

		Second-period method		Total-period method	
Pharmaceutical	Nominal content/ mg per tablet	Found[a]/ mg per tablet	Error (%)	Found[a]/ mg per tablet	Error (%)
Termalgin	500	522.5 ± 57.1	4.50	519.1 ± 92.2	3.82
Efferalgan[b]	500	519.3 ± 35.0	3.86	690.7 ± 62.2	38.1
Saldeva[c]	300	317.0 ± 29.1	5.67	307.3 ± 14.7	2.43
Cortafriol[d]	500	516.5 ± 46.6	3.30	591.4 ± 59.4	18.3
Melabón[e]	350	319.9 ± 16.7	−8.60	364.1 ± 13.7	4.03
Propalgina Plus[f]	500 mg/bag	558.0 ± 29.7	11.6	495.9 ± 24.8	−0.82

[a] Average of three individual determinations ± standard deviation. [b–f] Other ingredients (in mg) include: [b] sodium saccharin (7); [c] caffeine (50), dimenhydrinate (15); [d] chlorphenamine maleate (2), pseudoephedrin sulfate (30); [e] propyphenazone (200), caffeine (8); [f] chlorphenamine maleate (2), phenylephrine hydrochloride (7.5), dextromethorphan hydrobromide (10), ascorbic acid (200), sodium cyclamate (180), sodium saccharin (20) sucrose (3670).

Table 4 Determination of ascorbic acid in orange juice and pharmaceutical preparations

		Absolute-signal method		Relative-signal method	
Sample	Nominal content/ mg per bag	Found[a]/ mg per bag	Error (%)	Found[a]/ mg per bag	Error (%)
Orange juice	0.563 ± 0.002 mg^{-1} g[b]	0.343 ± 0.012	−38.9	0.527 ± 0.007	−6.23
Algidol[c]	500	490.4 ± 7.4	−1.92	485.9 ± 25.7	−2.82
Propalgina Plus[d]	200	229.1 ± 25.1	14.5	225.6 ± 21.6	12.8
Frenadol[e]	250	318.1 ± 18.9	27.2	279.4 ± 4.21	11.8

[a] Average of three individual determinations ± standard deviation. [b] Determined by the NBS method. [c–e] Other ingredients (in mg) include: [c] paracetamol (650), codeine phosphate (10), sodium saccharin (2.5), sucrose (3714); [d] paracetamol (500), chlorphenamine maleate (2), phenylephrine hydrochloride (7.5), dextromethorphan hydrobromide (10), sodium cyclamate (180), sodium saccharin (20) sucrose (3670); [e] paracetamol (650), dextromethorphan hydrochloride (20), caffeine citrate (30), chlorphenamine maleate (4), sucrose (8200).

inhibit the effect of vanillin in the sample on the perturbation amplitude.

The proposed method for the determination of paracetamol was used to analyse for this compound in various pharmaceutical preparations. As in the previous case, potential interferences from other active principles usually accompanying paracetamol in its formulations were investigated. Many paracetamol preparations contain caffeine and ephedrine (also added as pseudoephedrine). Their potential effects on the determination were examined by injecting various samples containing a fixed amount of paracetamol (2 μmol) and variable amounts of caffeine (100–1500 μg) and ephedrine (30–900 μg) into the oscillating system. No significant difference (errors less than ±2%) from the previous results was observed.

Table 3 gives the results obtained in the determinations. The relative error was calculated in terms of the deviation of the results from the nominal paracetamol contents in the different pharmaceutical preparations. While such contents may be subject to inherent errors arising in the manufacturing process, they were used as reference values because they allowed the potential of oscillating reactions for this type of analytical determination to be demonstrated. As can be seen in Table 3, both methods tested provided acceptable results. However, the second-period method was the more appropriate, probably as a result of the preparations containing some interferent that might interact briefly with the oscillating system in such a way that its effect is felt in the first oscillation cycle following the perturbation but not in the second; as a result, the total period, $T_1 + T_2$, is obviously altered.

Finally, ascorbic acid was determined in orange juice and various pharmaceutical preparations. Table 4 shows the results obtained in the determinations. Those for ascorbic acid in orange juice were validated by contrast with the NBS standard method; the significance tests provided experimental Student's *t*-values smaller than their tabulated counterparts. The results for the pharmaceutical preparations were compared with the manufacturer's nominal contents as references. As can be seen from the table, in general the relative-signal method provided better results than the absolute-signal method. This may have been the consequence of a potential interferent in the matrix displacing the oscillation cycle to more positive or negative potentials, thereby altering the deviation in the absolute-signal method but not the signal increment for the perturbation response in the relative-signal method.

The authors gratefully acknowledge financial support from Spain's Dirección General Interministerial de Ciencia y Tecnología (DGICyT) for the realization of this work as part of Project PB91-0840.

References

1 Field, R., and Schneider, F., *J. Chem. Educ.*, 1989, **66**, 195.
2 Lotka, A., *J. Phys. Chem.*, 1910, **14**, 271.
3 Noyes, R., *J. Chem. Educ.*, 1989, **66**, 190.
4 Karavaev, A., and Kazakov, V., *React. Kinet. Catal. Lett.*, 1987, **34**, 15.
5 Saigusa, K., *Chem. Phys. Lett.*, 1989, **157**, 251.
6 Kazakov, V., Karavayev, A., and Vakhidova, S., *React. Kinet. Catal. Lett.*, 1991, **45**, 199.
7 Weight, H., *Angew. Chem., Int. Ed. Engl.*, 1992, **31**, 355.
8 Zhuravlev, A., and Trainin, V., *J. Biolumin. Chemilumin.*, 1990, **5**, 227.
9 Yatsimirrskii, K., Strizhak, P., and Ivaschenko, T., *Talanta*, 1993, **40**, 1227.
10 Echols, T., Caroll, M., and Tyson, J., *Anal. Proc.*, 1995, **32**, 3.
11 Kolar-Anic, L., and Schmitz, G., *J. Chem. Soc., Faraday. Trans.*, 1992, **88**, 2343.
12 Anic, S., and Kolar-Anic, L., *J. Chem. Soc., Faraday Trans.*, 1988, **84**, 3413.
13 Anic, S., Kolar-Anic, L., Stanisavljev, D., Begovic, N., and Mitic, D., *React. Kinet. Catal. Lett.*, 1991, **43**, 155.
14 Anic, S., Mitic, D., and Curcija, M., *J. Serb. Chem. Soc.*, 1987, **52**, 575.
15 Schmitz, G., *J. Chim. Phys. Phys.-Chim. Biol.*, 1987, **84**, 957.

16 Nagy, A., and Treindl, L., *Chem. Listy*, 1988, **82**, 1097.
17 Yoshimoto, M., Yoshikawa, K., Mori, Y., and Hanazaki, I., *Chem. Phys. Lett.*, 1992, **189**, 18.
18 Epstein, I., *J. Chem. Educ.*, 1989, **66**, 191.
19 Melka, R., Olsen, B., Beavers, L., and Draeger, J., *J. Chem. Educ.*, 1992, **69**, 596.
20 Qingyuan, Z., and Jie, C., *Fenxi Shiyanshi*, 1988, **7**, 4.
21 Jiang, M., Li, Y., Zhou, X., Zhao, Z., Wang, H., and Mo, J., *Anal. Chim. Acta*, 1990, **236**, 411.
22 Jiménez-Prieto, R., Silva, M., and Pérez-Bendito, D., *Anal. Chem.*, 1995, **67**, 729.
23 Jiménez-Prieto, R., Silva, M., and Pérez-Bendito, D., *Analyst*, 1996, **121**, 563.
24 Jiménez-Prieto, R., Silva, M., and Pérez-Bendito, D., *Anal. Chim. Acta*, 1996, **321**, 53.
25 Jiménez-Prieto, R., Silva, M., and Pérez-Bendito, D., *Anal. Chim. Acta*, 1996, **334**, 323.
26 Orbán, M., *J. Am. Chem. Soc.*, 1986, **108**, 6893.
27 Orbán, M., *React. Kinet. Catal. Lett.*, 1990, **42**, 343.
28 Amrehn, J., Resch, P., and Schneider, F., *J. Phys. Chem.*, 1988, **92**, 3318.
29 Luo, Y., Orbán, M., Kustin, K., and Epstein, I., *J. Am. Chem. Soc.*, 1989, **111**, 4541.
30 *Official Methods of Analysis of the Association of Official Analytical Chemists*, AOAC, Arlington, VA, 15th edn., 1990.

Paper 6/06506F
Received September 23, 1996
Accepted December 12, 1996

Hydrolysis of 4-Nitrophenyl Diphenyl Phosphate Assisted by Tetraminecobalt(III) in Microemulsion Media

Fikru Tafesse†

Chemistry Department, University of Botswana, Private Bag 0022, Gaborone, Botswana

Reactions of hydroxoaquatetraminecobalt(III) in microemulsion media towards hydrolysis of 4-nitrophenyl diphenyl phosphate (NPDPP) were investigated at 10^{-4} M concentration in several oil-in-water microemulsions. The reactions were monitored by measuring the absorbance of the nitrophenolate ion produced in the reaction aliquots with time. The amount of nitrophenolate ion was then determined from a calibration curve and the percentage hydrolysis calculated. The order of effectiveness of the N_4 ligand in Co(III)(N_4)(aq) complexes at pH 6.5 towards hydrolysis of NPDPP was found to be trpn > $(tn)_2$ > $(en)_2$ (where trpn is tris(3-aminopropyl)amine, tn is trimethylenediamine, and en is ethylenediamine). The possible application of the above systems to environmental clean-up problems is discussed.

Keywords: *Environmental clean-up; microemulsion media; hydrolysis of phosphate esters; tetraminecobalt(III); 4-nitrophenyl diphenyl phosphate;* p-*nitrophenol*

Much consideration is given to reducing pollution caused by organic phosphate esters that are resistant to biological degradation and can potentially accumulate in the biosphere and biological organisms. To achieve this requires: (a) destruction of the bulk material and (b) rapid deactivation in cases of contamination of the surrounding area.

Alkyl diesters of phosphoric acid are normally highly resistant to hydrolysis in neutral aqueous solutions. For example the estimated half life for hydrolysis of phosphate ester linkages in DNA at physiological pH is of the order of millions of years.[1] This high kinetic barrier exists despite a thermodynamic situation which favours hydrolysis. Thus where catalytic pathways are available, rates of hydrolysis can increase markedly. The primary mechanism leading to increased hydrolysis involves nucleophilic participation at the phosphorous center by coordinated hydroxides of metal ions forming reactive chelate intermediates.[2–4] The main focus of this investigation is to develop artificial hydrolytic metalloenzymes that hydrolyze the unactivated phosphate esters intermolecularly. The ultimate challenge is to hydrolyze phosphate diesters under environmental conditions.

Metal ion catalysis has been the subject of numerous reports in both chemical and biological group transfer reactions and much effort has been directed on the mechanism of catalysis of phosphoryl transfer.[5,6] In the present study a system consisting of tetraminecobalt(III) in microemulsion media has been chosen as a decontaminant. The microemulsion based method is simple, inexpensive, mild and relatively rapid. These features arise from the fact that microemulsions represent a community of molecules that function only by virtue of cooperative action.[7] Each of the initial components (water, hydrocarbon, surfactant, cosurfactant, nerve agent simulant (4-nitrophenyl diphenyl phosphate, NPDPP), and the tetraminecobalt(III) ion has its own residence site and its own role in the reaction. This kind of self assembly, inherent to microemulsions, results in the formation of an organized system that helps in assisting the reaction.

† Present address: National University of Lesotho, P.O. Roma 180, Lesotho.

Experimental

All reagents used were either analytical-reagent grade or the purest grade available commercially and were used without further purification. Measurement of pH was made with a Philip Harris (London, UK) pH meter Model w87063, using a combination electrode. A Shimadzu (Kyoto, Japan) uv-2101pc UV/VIS spectrometer was used to obtain spectra and collect rate data. The pH of the reaction mixture was maintained by adding drops of NaOH or $HClO_4$ from a glass rod. The diaqua complexes $[CoN_4(H_2O)_2]^{3+}$, where N_4 = $(en)_2$, $(tn)_2$ or trpn [en = ethylenediamine; tn = trimethylenediamine; trpn = tris(3-aminopropyl)amine], were prepared in solution from the carbonato complexes $[CoCO_3N_4]$ as described previously.[2,3,8,9] Microemulsions were prepared by mixing hexane, sodium dodecylsulfate (SDS) and butan-1-ol and titrating the slurry with water, agitating mildly to give a clear solution. The following compositions (by mass) were used: ME1, H_2O (90%)–hexane (2%)–SDS (2%)–butan-1-ol (6%); ME2, H_2O (82%)–hexane (3%)–SDS (5%)–butan-1-ol (10%); ME3, H_2O (60%)–hexane (4%)–SDS (18%)–butan-1-ol (18%); ME4, H_2O (43.2%)–hexane (10.4%)–SDS (14.8%)–butan-1-ol (31.6%). Synthesis of NPDPP was achieved by using previously published methods.[10]

The protocol for the study consists of mixing 8 ml of a 5×10^{-4} M solution of DPNPP in ethanol in a thermostated reaction vessel with 4 ml of $NaClO_4$ (1 M) and 20 ml of the solvent. The solvent was either ethanol or one of the microemulsions. The pH of the solution was adjusted to 6.5. An 8 ml volume of temperature equilibrated diaquatetraminecobalt(III) in ethanol (5×10^{-4} M), pH 6.5, hydroxoaqua form predominant was then added, making the total volume to 40 ml. Aliquots (2 ml) were withdrawn from the reaction vessel at 0, 1, 3, 5, 10, 15, 30, and 60 min, respectively, and mixed with 1 ml of TRIS buffer (pH 7.2). The buffer system was prepared by mixing 25 ml of TRIS (0.2 M) and 44.7 ml of HCl (0.1 M) and making up to 100 ml with carbon dioxide free, distilled water. The absorbance of the reaction solution was then measured at 400 nm after mixing. The amount of nitrophenolate produced was determined from the calibration curve and the percentage hydrolysis calculated, assuming 100% nitrophenolate production for complete hydrolysis. In an unbuffered solution the acid–base reaction of *p*-nitrophenol changes in concentration resulting in a shift in the equilibrium position and a consequent deviation from Beer's law. In buffer solution, the pH would be fixed and the ratio of the concentration of *p*-nitrophenolate to the *p*-nitrophenol would be constant thereby obeying Beer's law. The advantages of this technique over direct spectrophotometric determination of phosphates on the basis of the reaction of Heteropoly Yellow, Heteropoly Blue and their ion associates with cationic dyes is that its analysis time is short and the sensitivity is high. Above all the method did not require addition of extra quenching reagents to release the bound species as has been reported previously.[2,3,5] All absorbances were taken against a water blank. Interference from other compounds in the analyte was

not detected. The molar absorption coefficient was determined from caliberation curve studies with standard *p*-nitrophenol solutions as 1.118×10^4 M^{-1} and the system confirmed to Beer's law over the concentration range 0–20 μg l^{-1} of nitrophenol when measured at 400 nm in a 1 cm cell.

Results and Discussion

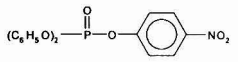

NPDPP

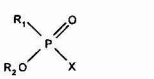

General formula for nerve agents

x = CN, R_1 = $N(CH_3)_2$, R_2 = C_2H_5 .....Tabun (GA)

x = F, R_1 = CH_3, R_2 = $CH(CH_3)_2$ .....Sarin (GB)

x = F, R_1 = CH_3, R_2 = $CHCH_3C(CH_3)_3$ .....Soman (GD)

x = F, R_1 = CH_3, R_2 = cyclo C_6H_{11} .....(GF)

x = $SCH_2CH_2N[CH(CH_3)_2]_2$, R_1 = CH_3, R_2 = C_2H_5 ...(VX)

NPDPP was utilized as a simulant for nerve agents since direct study of the nerve agents was difficult for safety and licensing reasons.

Although NPDPP is expected to be less reactive towards hydrolysis than the nerve agents, the hydrolytic scheme developed for NPDPP is likely to be useful for the 'real thing'.[11]

Hydrolysis of NPDPP was followed by monitoring the amount of *p*-nitrophenolate ion produced under the experimental condition. The use of buffer for the analysis was required since the pH of the analyte would affect changes in the concentration of the *p*-nitrophenolate ion. The N_4Co^{III} moiety where N_4 = en_2, tn_2 or trpn is advantageous as a model system because in the pH 6–7 region $[CoN_4(OH)(H_2O)]^{2+}$ predominates with rapid *cis*/*trans* isomerization and water substitution.[12] The reactivity of the hydroxoaqua complex has been attributed to the electron freed from the diaqua complex by loss of a proton labilizing the coordinated water molecule by increasing the electron density on the cobalt center.[13] The results of the investigations are given in Table 1. The values given in the table are average values of triplicate experiments. As is evident from the data, enhanced reactivity was noted in the oil-in-water type microemulsions (O/W), *i.e.*, hydrocarbon droplets suspended in water. Maximum hydrolysis was achieved in ME2 reaction solutions. The bicontinuous type microemulsions, *i.e.*, comparable amounts of hydrocarbon and water, did not show considerable hydrolysis. No appreciable hydrolysis of DPNPP was evident for all of the $Co^{III}(N_4)(aq)$ complexes in W/O (water-in-oil) microemulsions, *i.e.*, water droplets suspended in hydrocarbon.

Each of the microemulsion components has its own function that makes the system useful. Water acts as the solvent and hexane suspended as microdroplets serves as a residence for the water insoluble reactants. The surfactant (SDS) adsorbs to the hexane/water interface and stabilizes the droplets. The presence of the co-surfactant is critical in reducing the interfacial tension between the droplets and the continuous phase to near zero.[7,14]

Enhanced reactivity for the $[Co(trpn)(OH)(H_2O)]^{2+}$ complex is attributed to the trpn ligand being able to stabilize four membered rings.[15] Crystallographic studies revealed that the N–CO–N bond angle opposite to the O–Co–O bond in $[Co(CO_3)(trpn)]^+$ can expand to 100 degrees thereby stabilizing the four membered ring. It appears that increasing the bond angle opposite the four membered Co^{III} complex has a marked stabilizing effect.[15] The high rate of hydrolysis by $[Co(trpn)(OH)(H_2O)]^{2+}$ can therefore be attributed to the 100% *cis* geometry of the complex and the flexible six membered ring chelate of the ligand that enjoys different conformations. The hydrolysis rate was found to be moderate for the reaction solutions that utilized $Co^{III}(tn)_2$ complexes when compared to the extraordinary reactivity of $Co^{III}(trpn)$. The results for the $Co^{III}(en)_2$ promoted hydrolysis of NPDPP showed even a lower rate compared to those of $Co^{III}(tn)_2$. The marked influence of the $Co^{III}(N_4)$ ligands on substitution reaction in such complexes as *cis*-$[Co(Cl)_2(N_4)]^+$ have long been recognized.[12,16] Similar influences of N_4 on substitution of water in $[Co(N_4)(OH)(H_2O)]^{2+}$ ions were also reported.[17] The order of effectiveness of the N_4 ligands in $Co^{III}(N_4)(aq)$ complexes at pH 6.5 [trpn > $(tn)_2$ > $(en)_2$] towards hydrolysis of NPDPP parallels the water substitution rates in the complexes. Compar-

Table 1 $Co^{III}(N_4)(aq)$ promoted hydrolysis of DPNPP in microemulsion media at 25 °C and pH 6.5 [N_4 = trpn, $(tn)_2$, $(en)_2$]

		Nitrophenol produced (%)*							
Reaction	Media	0	1	3	5	10	15	30	60
DPNPP	Ethanol	2.5	2.5	2.5	2.5	2.5	2.5	2.5	2.5
	ME1	3.5	3.5	3.6	3.6	3.7	3.7	3.8	3.8
	ME2	3.5	3.7	3.7	3.7	3.8	3.8	3.9	4.0
	ME3	3.5	4.4	4.5	4.5	4.4	4.5	4.5	4.5
	ME4	3.5	3.6	3.7	3.7	3.7	3.9	3.9	3.9
DPNPP + $Co^{III}(en)_2(aq)$	Ethanol	3.5	3.5	3.5	3.5	3.5	3.5	3.5	3.5
	ME1	3.5	4.6	5.9	7.4	8.1	8.1	8.8	9.6
	ME2	3.5	10.0	12.0	12.7	13.5	14.0	14.5	15.3
	ME3	3.5	4.5	4.6	4.7	5.8	6.4	8.3	9.2
	ME4	3.5	3.7	4.4	4.8	4.9	4.9	4.9	5.0
DPNP + $Co^{III}(tn)_2(aq)$	Ethanol	2.5	2.5	2.6	2.6	2.8	2.9	2.9	3.1
	ME1	3.5	6.3	7.4	8.7	9.3	9.7	10.2	10.3
	ME2	3.5	12.7	15.3	15.9	16.9	17.2	17.5	17.9
	ME3	3.5	7.8	8.3	8.5	9.0	9.4	9.6	9.8
	ME4	3.5	4.4	4.8	4.9	5.0	5.2	5.5	6.1
DPNPP + $Co^{III}(trpn)(aq)$	Ethanol	7.8	7.8	8.1	8.2	8.7	8.9	9.1	9.8
	ME1	10.9	19.7	23.1	27.2	29.1	30.3	31.9	32.2
	ME2	10.9	28.8	30.0	30.9	31.6	47.4	48.4	52.2
	ME3	10.8	24.4	26.1	26.6	28.1	29.4	30.1	30.5
	ME4	10.9	13.8	14.9	15.3	15.6	16.2	17.2	19.1

* For the times given in minutes. (aq) in $Co^{III}(N_4)(aq)$ refers to hydroxoaqua, *i.e.*, $(OH)(H_2O)$. The standard deviation for the three assays ranged from 0.01 to 0.02 in each case.

ison of substitution and dephosphorylation rates have been undertaken for the $Co^{III}(N_4)(aq)$ complexes in previous studies.[18] It can therefore be deduced that for $Co^{III}(N_4)(aq)$ promoted hydrolysis, significant reorganization of the cobalt coordination sphere is required to achieve the transition state, and it seems likely that there would be closely related influences of the N_4 ligands on rates of both $Co^{III}N_4$ substitution and $Co^{III}N_4$ promoted hydrolysis reactions.

Manipulation of the location of the reagents and the simulant by partitioning in microemulsions has helped in promoting hydrolytic cleavage of the DPNPP. Owing to the huge interface between the hexane and aqueous phases, the reaction between the water soluble $Co^{III}(N_4)(aq)$ and the organic soluble simulant proceeded at a fast rate. Synergistic effects of the tetraminecobalt(III) and the microemulsion media are important in bringing about effective hydrolysis of DPNPP. An attempt was made to conduct the reaction in water solutions of the reactants. But, the insolubility of DPNPP in water hampered the study. The experimental findings of this investigation establish that the tetraminecobalt(III) ions in O/W microemulsions are a potent means for destroying NPDPP. Hence it is presumed that the model can be used as a decontamination system for environmental clean-up. The reactions are rapid under mild conditions and no specialized equipment is needed for the procedure. Hence it might be adapted to field situations where decontamination is anticipated.

References

1 Westheimer, F. H., *Science*, 1987, **235**, 1173.
2 Tafesse, F., *Transition Met. Chem. (London)*, 1991, **16**, 114.
3 Tafesse, F., Massoud, S. S., and Milburn, R. M., *Inorg. Chem.*, 1985, **24**, 2591.
4 Creaser, I. I., Haight G. P., Peachy, R., Robinson, W. T., and Sargeson, A. M., *J. Chem. Soc., Chem. Commun.*, 1984, 1568.
5 Tafesse, F., and Milburn, R. M., *Inorg. Chim. Acta*, 1987, **135**, 119.
6 Siegel, H., and Hofsteter, F., *Eur. J. Biochem.*, 1983, **132**, 569.
7 Menger, F. M., *Angew. Chem., Int. Ed. Engl.*, 1991, **30**, 1086.
8 Hubner, P. W. A., and Milburn, R. M., *Inorg. Chem.*, 1980, **19**, 1267.
9 Springborg, J., and Schaffer, C. E., *Acta Chem. Scand.*, 1973, **27**, 223.
10 Gulik, W. M., and Geske, D. H., *J. Am. Chem. Soc.*, 1966, **88**, 2928.
11 Katritzky, A. R., Duell, B. L., Hurst, H. D., and Knier, B. L., *J. Org. Chem.*, 1988, **53**, 3972.
12 Jonasson, I. R., Lincolin, S. F., and Stranks, D. R., *Aust. J. Chem.*, 1970, **23**, 2267.
13 Kruse, W., and Taube, H., *J. Am. Chem. Soc.*, 1961, **83**, 1280.
14 Menger, F. M., and Erlington, A. R., *J. Am. Chem. Soc.*, 1991, **113**, 9621.
15 Chin, J., Drouin, M., and Michel, A., *Acta Crystallogr. C: Cryst. Struct. Commun.*, 1990, **46**, 1022.
16 Pearson, R. G., Boston, C. R., and Basolo, F., *J. Am. Chem. Soc.*, 1952, **74**, 2943.
17 Massoud, S. S., and Milburn R. M., *Inorg. Chim. Acta*, 1989, **163**, 87.
18 Tafesse, F., Massoud, S. S., and Milburn, R. M., *Inorg. Chem.*, 1993, **32**, 1865.

Paper 6/05876K
Received August 27, 1996
Accepted November 12, 1996

Quality Issues

Quality and Accreditation in Clinical Chemistry Laboratories Analysis in the National Health Service

Keith Davies*[a] and David Burnett[b]

[a]*Department of Medical Biochemistry, University Hospital of Wales, Heath Park, Cardiff, UK CF4 4XW*

[b] *24 Bowers Way, Harpenden, Hertfordshire, UK AL5 4EW*

There are around 350 clinical chemistry laboratories attached to National Health Service (NHS) Trust hospitals in the UK. A typical trust hospital laboratory will analyse 400 samples each day, each sample requiring on average six tests. Together with calibration, quality control and proficiency testing samples, this equates to around 3000 tests a day, or 750 000 per year per lab, 262 500 000 each year in the UK.

Pathology laboratories (mainly morbid anatomy and post mortem) were developed in the early part of this century and remained virtually unchanged until the Second World War when they differentiated into the four main sections we know today: histopathology, microbiology, haematology and clinical chemistry. The major increase in workload in clinical chemistry came in the 1960s and 1970s due mainly to changing technology. The use of flame emission spectrometry for the estimation of serum sodium and potassium in the 1950s, and the sequential automated analysers which automated tests by using dialysis to get rid of laborious protein precipitation procedures in test analyses in the 1960s, considerably reduced the analytical bottleneck in the laboratories.

Clinical chemistry is concerned with the diagnosis and prognosis of disease and with patient management through the analyses of body fluids and tissues for specific constituents. Specimens of blood, serum, plasma, urine, cerebrospinal fluids, faeces and other bodily fluids from patients provide the samples which are analysed to diagnose illness or to monitor the progress of disease.

The practice of clinical chemistry requires a knowledge of chemistry, biochemistry, physiology and molecular biology. Consultants in chemical pathology are also frequently involved in direct patient care and together with clinical biochemists in the investigation of disease processes. The present day laboratory is characterised by the utilisation of a wide variety of techniques and equipment. More than 60% of the work is processed by automated analysers which, although very sophisticated, require constant maintenance, internal quality control and external quality assessment. Such analysers are expensive to purchase and are increasingly installed using an operational leasing arrangement as an alternative to capital outlay. The majority of laboratories have a high level of computerisation both as an integral part of analysis to manage the test results and to provide both paper based and/or electronic reporting systems.

Two reports from the Audit Commission,[1,2] and the NHS Executive's 'Strategic Review of Pathology Services' (1995) investigated the efficiency, cost and future of pathology services in the NHS. The second report brings together the results of audits done in many Health Authorities following the first document's publication. Pathology services in the UK cost over 400 million pounds per annum, or 3% of the hospital and community service budget, with clinical chemistry accounting for about a third.

The service is changing, patient expectations are increasing, whereas financial restraints are more imposing now than ever before. Advances in technology, which reduce the need to increase the workforce as the workload increases, are nevertheless expensive. The spectrum of tests offered increases year by year, whilst departmental budgets often do not. Cost improvement programmes of between 1.5 and 3.0% are demanded per annum in an attempt to pare the 'fat' from the system. This fat is not always present and real cuts have to be made to stay within budget. In most clinical chemistry laboratories the staff : non-staff cost ratio is 50 : 50. Thus reductions in budget often mean lost jobs.

The spectre of privatisation by companies either taking over laboratory services or having a large interest through the Private Finance Initiative, also concerns staff, who until recently might have thought that they were in a secure vocational job. Competition between neighbouring laboratories by the Government imposed internal competitive market has often damaged fruitful co-operation between them.

Against these pressures, the clinical chemistry service is continually improving the quality of its services. Test methods are being fine tuned to produce values which are nearer to the clinician's requirements using biological variation as a target for results, rather than just an adequate analytical result.

The six Valid Analytical Measurement (VAM) principles as outlined in the DTI initiative, are not well known in NHS laboratories, but all are applied to some extent.

1 Analytical measurements should be made to satisfy an agreed requirement

The demands of doctors to provide quality services for their patients, together with the 'Patient's Charter' obligations which are being instigated in NHS Trust Hospitals, are the driving force for laboratories to produce a high quality service. The concept of Continuing Quality Improvement is increasingly used in laboratories and there is pressure to achieve a form of accreditation to provide evidence to clinicians and managers that laboratory processes provide quality outcomes. Service level agreements are made between purchasers (clinicians) and providers (laboratories) which include quality items such as turn-round times of patient results, quality of staff, statements on training and accreditation of laboratory procedures.

2 Analytical measurements should be made using methods and equipment which have been tested to ensure they are fit for their purpose

Competition between equipment manufacturers in clinical chemistry is fierce. Most of the major manufacturers are international companies, complying with one of the BS EN ISO9000 series of standards and Good Manufacturing Practice. Often they make and sell customised reagents for their analysers and validate their homogeneous systems against certified reference materials or methods. Reference methods are agreed by international acclaim and where possible are traceable to a definitive method. Thus for example for serum cholesterol, the definitive method is a gas chromatographic/isotope dilution method which is used to establish a cholesterol value in a serum reference material (SRM911b). This in turn is used to calibrate a reference method, the Abell–Kendall chemical method which is used to provide secondary reference values for calibrators used in clinical chemistry. Most of the routine analysers use an enzymatic reaction using cholesterol oxidase to estimate cholesterol. More and more methods are being validated in this manner.

3 Staff making analytical measurements should be both qualified and competent to undertake the task

The sectors' needs differ from that of the the general chemical sector in that the vocational educational requirements needed are special and specific to the job. Medical Laboratory Scientific Officers (MLSO) are state registered under the Council of Professions Supplementary to Medicine Board; Biochemsits and medical staff train for the membership of the Royal College of Pathologists (MRCPath). There are programmes of Continuing Medical Education (CME) for senior Biochemists and medical staff and Continuing Professional Development (CPD) for State Registered MLSOs.

The use of qualified and competent staff in NHS clinical chemistry laboratories has been well structured and established since the 1950s. There are around 250 medical staff (Chemical Pathologists and junior medical staff), 1300 biochemists and 5000 Medical Laboratory Scientific Officers in UK clinical chemistry laboratories. Medical Laboratory Assistants appointed without the need for formal qualifications are increasingly used to perform specific tasks under the supervision of qualified staff.

4 There should be a regular independent assessment of the technical performance of a laboratory

From the inception of the NHS in 1948 and as the technology improved and became available, the laboratory came to be used more frequently by physicians, the workload increased and the requirement to test the quality of the results became paramount. Laboratories employed internal quality control procedures to assess their own reproducibility but it was not until the mid 1960s that proficiency testing was introduced.

Early proficiency testing (or external quality control as it was better known in the NHS laboratories) later changed to the more correct term 'external quality assessment' (EQA) showed large differences in performance from laboratory to laboratory based on comparative accuracy. Continuous proficiency testing has led to a dramatic improvement of performance in both precision and accuracy, and today it is an essential part of laboratory testing. It is a compulsory 'standard' in CPA accreditation procedures, where inspected laboratories have to show participation in 'recognised EQA schemes'.

5 Analytical measurements made in one location should be consistent with those elsewhere

The homeostatic mechanisms in the body mean that analytes in the healthy individual are held within precise 'normal' ranges, pathological conditions will alter these and measuring the differences from normal will aid in diagnosis or monitoring of diseases. It is essential therefore to be able to determine these differences with accurate, precise and reproducible analytical methods.

When patients are transferred from one hospital to another it is not unusual for more than one laboratory to monitor test results. External quality assessment is one way to ensure that results from both hospitals are consistent.

It was in the 1960s that the 'consensus mean value' was agreed for comparative accuracy, and interlaboratory performance improved. Today, external quality assessment is an essential part of clinical chemistry laboratory practice. 'Consensus mean values' for test analytes are now being replaced wherever possible by 'true values'. True values are those values which are traceable to definitive values established in acceptable circumstances, and assigned to certified 'reference material' which can be used as a standard in the analysis.

Instrument manufacturers have played a major role in the increasing reliability of performance of clinical chemistry assays. Automated procedures in particular have lead to a dramatic improvement in the precision of assays, and in reducing operator bias in their estimation. Most problems are now caused by the calibration procedures adopted by different manufacturers not always providing comparable results.

Certified reference materials are being used, mainly through manufacturers' homogeneous assay/analyser systems to achieve comparability and traceability of measurements. Networking of reference laboratories, *e.g.*, the lipid and steroid analyses, is also influencing the traceability of assays. With regards to 'Measurement Uncertainty', the concept is not new to clinical chemists but not one which is expanded on beyond total imprecision measurement such as 'standard deviation' or 'coefficient of variation'. However, notice has always been taken about which part of an assay contributes most to the imprecision, and then measures have been taken to improve it.

6 Organisations making analytical measurements should have well defined quality control and quality assurance procedures

The development of quality and accreditation systems for clinical pathology laboratories is a relatively recent development in the NHS. Prior to April 1992 there was no system that was suitable for use by a clinical laboratory. Laboratories undertaking work on specimens from pre-clinical studies could apply to the Department of Health's Good Laboratory Practice (GLP) Monitoring Unit for recognition under the United Kingdom Compliance Programme, or to NAMAS (now part of the United Kingdom Accreditation Service, UKAS) for accreditation according to EN45001: 1989 General criteria for the operation of testing laboratories, or to a number of certifying bodies for certification to one of the ISO 9000 series of quality system standards.

In 1988, an *ad hoc* committee of The Royal College of Pathologists (RCPath) was formed to explore the feasibility and desirability of establishing a laboratory accreditation scheme. After an initial pilot study, a steering committee was formed with representatives from the College, the Association of Clinical Pathologists, the Association of Clinical Biochemists, the Institute of Medical Laboratory Sciences, the Institute of Health Service Managers and the Independent Health Care Association, together with observers from government health departments, the Advisory Committee on the Assessment of Laboratory Standards and the King's Fund.

Following a project development programme spanning three years, Clinical Pathology Accreditation (UK) Ltd. (CPA), was incorporated on 6 January 1992. This non-profit making enterprise is owned by the share holders represented on the original steering committee. The main documentation consists

of a guideline handbook and an application form. Forty-four 'standards' were adopted, forty-one of which apply to clinical chemistry. They are divided into six groupings covering organisation and administration, staffing and direction, facilities and equipment, policies and procedures, staff development, education, evaluation and appraisal. Figures provided by CPA show that between April 1992 and October 1996 there have been overall 1361 enquiries, 909 registrations and 820 inspection visits in Pathology, of which 256 enquiries, 186 registrations and 170 inspection visits were for clinical chemistry.

An inspection visit to clinical chemistry will involve two inspectors, one covering a medical or scientific background and one covering a technical background. Inspections normally last one day and the inspectors can recommend full or conditional accreditation. Those laboratories given conditional accreditation are given a schedule of items which have to be corrected in a given time span. The emphasis of the inspection is not only on the technical aspects of the laboratory function but also on qualification of the staff, pre- and post-analytical functions such as interpretation of results and performance in external quality assessment schemes. Accreditation will increasingly be demanded by purhcasers of pathology services to satisfy them of the competency of staff and approval of technical and administration procedures which prove the quality of the laboratory.

More recently (1996), the Department of Health asked the CPA to develop proposals for EQA oversight and the CPA is now responsible for the recognition of EQA schemes in Clinical Biochemistry, Haematology, Immunology and Microbiology. Inspections for CPA (EQA) recognition started in January 1997. Sixty-two 'standards' have to be complied with before recognition can be achieved.

The six VAM principles set out in very general terms the broad principles which should be followed in the pursuit of quality. For specific sectors, they require further discussion and interpretation to ensure that they adequately address all the sector specific issues. In the clinical chemistry sector, as this article shows, many aspects of VAM are currently receiving attention and good progress is being made with implementation of VAM across a broad front. There remain many opportunities for NHS laboratories to strengthen their response to the VAM principles, and there are also many ways in which the particular experiences of NHS laboratories may help other laboratories to implement the VAM principles and achieve quality improvements.

This article was solicited on behalf of The Royal Society of Chemistry by Dr. John Flemming at the Laboratory of the Government Chemist, Teddington, Middlesex.

References

1 *The Pathology Services, A Management Review*, Report, Audit Commission, 1991.
2 *Critical Path, An Analysis of the Pathology Services*, Report, Audit Commission, 1993.

Paper 7/00508C

AUTHOR INDEX

Where on the paper an asterisk appears against the name of one or more authors, it indicates the author(s) to whom correspondence should be addressed.

INTERNATIONAL UNION OF PURE AND APPLIED CHEMISTRY

ROYAL AUSTRALIAN CHEMICAL INSTITUTE

AUSTRALIAN ACADEMY OF SCIENCES

XXX COLLOQUIUM SPECTROSCOPICUM INTERNATIONALE

World Congress Centre, Melbourne, Australia, September 21st - 26th, 1997

This traditional biennial conference provides a forum for the international community of analytical spectroscopists to meet and exchange ideas. Participants are invited to submit contributions for presentation in English, French or German (there will be no translation facilities) on the following topics:

Theory, Techniques and Instrumentation of;

Atomic Spectroscopy (Emission, Absorption, Fluorescence)
Computer Applications and Chemometrics
Electron Spectroscopy
Gamma Spectroscopy
IR Spectroscopy
Laser Spectroscopy
Luminescence Spectroscopy
Mass Spectrometry (Inorganic and Organic)
Methods of Surface Analysis and Depth Profiling
UV/Visible Spectroscopy
NIR Spectroscopy
Mössbauer Spectroscopy
Nuclear Magnetic Resonance Spectrometry
Photoacoustic and Photothermal Spectroscopy
Raman Spectroscopy
X-Ray Spectroscopy

Applications of Spectroscopy in the Analysis of:

Biological and Environmental Samples
Food and Agricultural Products
Metals, Alloys and Geological Materials
Industrial Processes and Products

Plenary and Invited Speakers

The following eminent spectroscopists have accepted invitations to present plenary lectures;

Freddy Adams *Microscopical X-ray Fluorescence and Related Methods with Laboratory and Synchrotron Radiation Sources*

Bruce Chase *Raman Spectroscopy: A Laboratory Tool in an Industrial Environment.*

Michael Gross *Mass Spectrometry in Biomedicine: Applications in Cancer and Protein Research*

Hiroshi Masuhara *Time-resolved Microspectroscopy and Interferometry of Organic Molecular Materials.*

Nicolo Omenetto *The Role of Lasers in Analytical Atomic Spectroscopy: Where, When and Why.*

Barry Sharp *The ICP - Provider, Scrambler and Destroyer of Information.*

In addition the following scientists have accepted invitations to speak at XXX CSI;

Mike Adams	UK	Gary Hieftje	USA	Douglas Rutledge	France
Arne Bengtson	Sweden	Joachim Heckel	Germany	Alfredo Sanz Medel	Spain
Mike Blades	Canada	Kazuhiro Imai	Japan	Heinz Siesler	Germany
Marcela Burguera	Venezuela	Qinhan Jin	China	Margaret Sheil	Australia
John Chalmers	UK	Robert Kellner	Austria	Richard Snook	UK
Gerry Downey	Ireland	Russell MacLean	Australia	Ralph Sturgeon	Canada
Peter Fredericks	Australia	Jean-Michel Mermet	France	Anne Thorne	UK
Manfred Grasserbauer	Austria	Carolyn Mountford	Australia	Yngvar Thomassen	Norway
Mike Guilhaus	Australia	Reinhard Niessner	Germany	Bernhard Welz	Germany
Peter Hannaford	Australia	Mike Ramsey	USA	John Williams	UK
		Andrew Zander	USA		

Sponsors

The following companies are proud to be major sponsors of XXX CSI;
GBC, Hewlett Packard, Perkin Elmer, Thermo Instruments and Varian
Labnews has been appointed the official colloquium newspaper

For further information contact;

Secretary
Mr Peter Larkins
CSIRO Division of Materials Science & Technology,
Private Bag 33, Rosebank MDC, Clayton,
VIC 3169
AUSTRALIA
Tel: +61 3 95422003
Fax: +61 3 95441128
E-mail: larkins@rivett.mst.csiro.au

Conference Secretariat
The Meeting Planners,
108 Church Street,
Hawthorn, VIC 3122,
AUSTRALIA
Tel: +61 3 98193700
Fax: +61 3 98195978

Updated information may be obtained from the XXX CSI homepage on the World Wide Web at: http://www.latrobe.edu.au/www/xxxcsi

QANTAS has been appointed the sole official carrier to the XXX CSI.

When making QANTAS reservations quote JIF 73Q

Book Reviews

Accreditation and Quality Assurance in Analytical Chemistry

Edited by Helmut Günzler. Translated by Gaida Lapitajs. Pp. xvi + 266. Springer-Verlag. 1996. Price (Hardcover) DM148.00; öS1080.40; sFr130.50. ISBN 3-540-60103-1.

This book is a collection of papers giving an overview of accreditation and quality assurance in analytical chemistry. It has been written to predominantly reflect the European dimension. The book attempts to cover a large number of topic areas within the general subject; in particular, the significance of certification and accreditation within the European Market, brief descriptions of the procedures for accreditation in chemical analysis laboratories and the systems used in a large number of different countries, other aspects of quality assurance in the analytical laboratory (most notably the stragegy, use of statistics and traceability of measurements to SI Units) and differences in the available accreditation and certification systems. Some particular practical aspects of interest to the bench analyst are outlined, notably the validation of analytical methods and the use of reference materials. It completes the picture by describing the setting up of the EURACHEM organisation.

Each chapter is prepared by a different author and inevitably there is some element of duplication. The book tends to skim too many subjects and so does not present a very in-depth view of any one particular subject. In particular, a considerable amount of the book is devoted to a brief outline of the accreditation systems in different countries which is interesting but not very helpful to an individual laboratory.

I found the book to be unstructured without logical flow and organisation between the various chapters. Similar topics were considered at different unconnected places throughout the book, thereby giving a disjointed impression to the reader. The book is not an easy read.

This book would be of use to a legislator or manager but it will not help the bench analyst to achieve accreditation without a considerable amount of supplementary material.

Roger Wood
6/90048H *Ministry of Agriculture, Fisheries and Food*
Norwich

Photothermal Spectroscopy Methods for Chemical Analysis

By Stephen E. Bialkowski, *Volume 134 in Chemical Analysis: A Series of Monographs in Analytical Chemistry and Its Applications.* Series Editor: J. D. Winefordner. Pp. xxix + 584. Wiley. 1996. Price £70.00. ISBN 0-471-57467-8.

This book is part of the comprehensive and well respected series of monographs on *Analytical Chemistry and Its Applications.* As Volume 134 in *Chemical Analysis* it lives up to the standard of this excellent series being comprehensive in its approach yet accessible to those with limited knowledge of the more physical and theoretical aspects of the subject.

After an introduction to the different types of photothermal techniques and a very brief sketch of the basic optical and thermal phenomena involved the author takes some time in Chapters 2–5 to explore in detail the physical processes underlying these phenomena. Quite logically these processes are divided into: absorption, energy transfer and excited state relaxation (Chapter 2); hydrodynamic relaxation, heat transfer and acoustics (Chapter 3); optical principles from photothermal spectroscopy (Chapter 4); and temperature change and optical elements in homogeneous samples (Chapter 5). Thus in 350 pages the reader is fully equipped to understand the detailed physical processes and theory behind photothermal phenomena described in subsequent chapters perhaps to a depth which is not required for application of these techniques to chemical analysis. It is here that my only criticism of the book can be made. The balance between the physics presented and the chemical analysis aspects is tipped too firmly towards the former. For example it is not until page 421 that analytical applications are considered and even then most chemical applications are consigned to a table with very little description of analytical figures of merit, comparisons with other techniques or discussion of the relevance of these to the practising analyst. One exception is the treatment of photothermal spectroscopy for chromatographic detection and flow analysis where more detailed comments are made. The book is not recommended, therefore, for general readership in the analytical community.

Nevertheless there is a wealth of information in this book for the specialist concerned with photothermal phenomena and spectroscopy or even in the wider field of the interaction of laser radiation with homogeneous media. For the first time the whole process from optical absorption to thermal transport and detection has been described in a complete and readable fashion with detailed analysis of the theoretical and practical constraints of the techniques described with respect to their use. Extension of this approach to the design and description of instrumental systems offers the specialist an important text bringing these areas together. It is therefore a valuable addition to the collection of researchers and graduate students working in photothermal spectroscopy providing a single source of information normally only found in a diverse range of texts in different disciplines.

As a source book I suspect it will not be surpassed for a good few years. It is in this respect that the book should be judged as an excellent text. I am sure it will find its way into many a research laboratory and University library. I had bought a copy before receiving the review copy. I am also sure that parts of it, with due reference of course, will crop up in many a PhD thesis and this in itself is recognition enough for an academic book.

R. D. Snook
6/90021F *UMIST*
Manchester

Protein and Peptide Analysis by Mass Spectrometry

Edited by John R. Chapman. *Methods in Molecular Biology, Volume 61.* Pp. x + 350. Humana Press. 1996. Price US$69.00. ISBN 0-896-03345-7.

The book begins with an informative chapter by P. Roepstorff outlining the history of MS methods, particularly with respect to the pioneering work of the late Michael Barber in the development of FAB MS/LSIMS. This is followed by a very readable step-by-step guide to the ionisation methods by the editor, J. R. Chapman. Armed with this information one is then catapulted into the world of MS analysis for peptide fingerprinting, sequencing, location of disulfide bonds, detection of variants, *etc.* These areas are familiar to many, but also dealt

with are conformational analysis using hydrogen exchange (C. V. Robinson) and tertiary structure determination in detergents (Ogorzalek Loo, *et al.*), which are exciting new areas. In the latter chapter we are refreshingly told that 'It is naive to believe that all biochemical problems can be solved without detergents'. Besides information at the level of protein chemistry and fragmentation there is also advice on how to set up and run the instruments. For example B. Spengler discusses post source decay MALDI where it is suggested that 'a skilful home-built modification of a MALDI instrument' might be a reasonable alternative to buying commercially.

The choice of methodology for your own particular application is made obvious from the comprehensive examples given in the chapters described in detail. One can readily obtain an overview of the best use of ESI versus MALDI, for example, and decide on the choice of matrix for MALDI and FAB or LSIMS (PD is not mentioned after the introduction). A list of MALDI matrices in an appendix is useful, but a more comprehensive view of the rationale of when to use each type of matrix would have been helpful. There is also a helpful appendix on the concentration of sample contaminants tolerated in MALDI operation. The use of ESI for disulfide loop characterisation and peptide mapping is well covered here and also the use of MALDI together with comparison of peptide fragments with PIR/SWISSPROT as a screening tool (J. S. Cottrell and C. W. Sutton).

Chapters 7, 17, 18 and 19 deal directly with glycoproteins. D. J. Harvey describes MALDI for analysis of released *N*-linked oligosaccharides including information on the matrices used. One interesting demonstration of the technique is the identification of at least eleven glycoforms of ovalbumin together with six contaminants of hydrazinolysis. There is a useful chapter by G. J. Rademaker and J. Thomas-Oates describing the methodology for a general strategy of glycoprotein and glycopeptide analysis by FAB. Methods covered include reduction and carboxymethylation and β-elimination of *O*-linked oligosaccharides together with PNG-ase for release of *N*-linked chains. A detailed definitive overview of oligosaccharide MS is given by C. A. Settineri and A. L. Burlingame including LC–ES methods of analysis. In the penultimate chapter the analysis is described of mixtures of proteins and glycoproteins to a mass accuracy of 0.01% by ESI with maximum entropy processing (B. N. Green *et al.*). Finally there is a chapter by R. W. A. Oliver and M. P. Carrier on databases for searching the rapidly burgeoning literature on biological mass spectrometry, which perhaps could have been complemented by a review of spectral databases themselves.

Overall this is a very good book for the beginner and also for those who want to be reminded of the diversity, applicability and success stories of presently popular MS techniques. The book is a necessity to have lying beside the mass spectrometer and I therefore suggest that the comb bound format of the previous books in the *Methods in Molecular Biology Series*, is purchased if this is available. Also, less abundant are the 'Notes' that are a selling point of other books in the series, but useful hints abound in the present volume if you look for them.

E. F. Hounsell
6/90096H *University College London*

Advances in Liquid Chromatography. 35 Years of Liquid Chromatography in Japan
Edited by T. Hanai and H. Hatano. *Methods in Chromatography Volume 1.* Pp. xviii + 338. World Scientific. 1996. Price US$119.00. ISBN 9-810-21906-7.

This book was produced to celebrate the 35th Anniversary of the founding of The Research Group on Liquid Chromatography in Japan. Apart from the first chapters it does not provide a historical review but is a series of descriptions of recent work from Japanese academic and industrial laboratories. Together these cover changes in instrumentation, columns and sample handling that emphasise the breadth and depth of the development in liquid chromatography in Japan.

A principal bias is towards instrumental developments, particularly detectors, and after a brief introductory chapter, Yamamoto and Ganno describe the historical development of the amino acid analyser. The next chapter continues the biochemical theme with a short description of the glycated albumin analyser, using affinity and ion-exchange columns. The next group of chapters covers detectors starting with a review by Takata of coulometric detection. Moriya and Makino then describe the detection of free-radicals using a novel coupling of HPLC and electron spin resonance spectroscopy (HPLC–ESR). The radicals must first be stabilised using a spin-trap technique but the method demonstrates the ability of LC to provide useful information even on quite unstable species.

The following chapter by Nakashim and Imai reviews the reactions and methods of chemiluminescence detection coupled to LC. It is followed appropriately by a chapter on the development of laser fluorimetric instrumentation for LC and CE by Imasaka. Miniaturisation of LC has been a major development from Japan and the background is described in a chapter by Takeuchi and Ishii. This is followed by a description of coupling microcolumn LC to FTIR by Jinno and Fujimoto. There is also a chapter describing on-line degassing.

The remaining part of the book covers column materials and again emphasises one of the areas where Japan has led the world. The first chapter by Oi reviews recent progress in chiral stationary phases. This is followed by a description of chiral synthetic polymer phases by Yashima and Okamoto and of protein bonded chiral packings by Oda and Miwa. The final two chapters by Hanai describe organic polymer columns for different types of LC and then recent developments in stable bonded silica gel-based column materials.

Overall most readers will pick a section of interest as the diverse nature of the topics prevents the establishment of a unifying theme. The chapters vary greatly from scholarly reviews to being close to descriptions of commercial equipment. This problem possibly emphasises the close connections between the advances made by the academic and the instrumental manufacturer. Unfortunately by concentrating on recent advances, the book tends to emphasis often obscure or little-used areas at the expense of developments, such as microcolumns or chiral chromatography, where the impact of the Japanese chromatographer over the last 35 years has been internationally the most significant.

R. M. Smith
6/90071B *Loughborough University*

Biochemical and Biotechnological Applications of Electrospray Ionization Mass Spectrometry
Edited by A. Peter Snyder. *ACS Symposium Series 619.* Pp. xii + 602. American Chemical Society. 1996. Price £99.00. ISBN 0-8412-3378-0.

Mass spectrometry has changed dramatically over the last decade from a technique which was mainly concerned with measurement of molecular weights of relatively small organic molecules to one in which most advances are in the areas of biopolymers, some of which have molecular weights in excess of 10^6 Da. The change was mainly brought about by the advent of the ionization techniques of matrix-assisted laser desorption/ionisation (MALDI) and electrospray. So popular has electro-

spray become that, in 1994 and 1995, it exceeded all other forms of ionization for mass spectrometry as illustrated by abstracts from the annual conferences of the American Mass Spectrometry Society, a publication regarded as an accurate reflection of current trends. The current widespread application of the technique to different areas of research is well reflected in this book which is based on a symposium sponsored by the American Chemical Society in April 1995 and devoted mainly to applications of the technique. The ability of electrospray to handle low concentrations of sample in aqueous solutions combined with easy coupling to liquid chromatographic systems, makes it an ideal ionization method for biopolymer analysis. Latest developments are discussed in detail, and enable molecules to be detected and fragmented in the sub-picomole range with flow rates of a few tens of nl min^{-1}.

'a source of much valuable information'

Of its 26 chapters, only two are devoted to the theory of the technique itself. The first of these deals with the ion source construction and characteristics and the second with the fundamentals of the ionization process. The remainder of the book is devoted to applications, with chapters on protein analysis forming a significant section. Probably the most exciting development in this area is the combination of electrospray with 2-dimensional gel separation of proteins where it can rapidly provide sequence information that can be used directly for database searching. The mildness of the ionization procedure has also enabled it to be used for the study of non-covalent interactions such as those involved in protein binding to carbohydrates, drugs and other ligands. Another major protein-related topic that is covered in detail is the detection and identification of the major forms of posttranslational modification such as phosphorylation and glycosylation. Carbohydrate analysis, in fact, occupies a substantial section of the book as electrospray has proved invaluable for identification of monosaccharides from polysaccharide-containing polymers and for direct analysis of complex molecules such as lipid-A derivatives found in the glycolipid fraction of pathogenic bacteria. Because of the ease of coupling of electrospray with liquid chromatography, it has become the preferred method for LC–MS coupling, another topic that is well covered in several chapters. A natural application of this combined technique is for the identification of drug metabolites separated by liquid chromatography and for measuring drug pharmacokinetics. Examples include the drugs timolol and simvastatin. Other types of compound successfully analysed by electrospray and included in this book are glycolipids, phospholipids, hydroxy fatty acids, nucleotides, shellfish toxins and environmental pollutants. Finally, there is an author index and a comprehensive subject index.

The book is well produced and is a source of much valuable information for anyone wishing to apply electrospray to biological problems.

David J. Harvey
University of Oxford

6/90089E

Atomic Absorption Spectrometry in Occupational and Environmental Health Practice
By D. L. Tsalev. *Progress in Analytical Methodology. Volume 3.* Pp. 349. CRC Press. 1995. Price £120.00. ISBN 0-8493-4999-0.

This volume by Dmiter Tsalev from the University of Sofia, Bulgaria, is an update of two previous comprehensive volumes, published in 1983 and 1984, on the determination of trace elements in biological and related materials by atomic absorption spectrometry (AAS). Of the 3223 references listed in the book, occupying 64 pages, more than 2100 have been selected from literature published between 1982 and mid-1993.

This is truly a reference book, one intended for consultation as the need arises to determine a particular element in a particular matrix. There are 42 chapters, one per selected element except for that on lanthanum and lanthanoids. The lengthiest chapters, as one might expect, are on lead, arsenic, selenium, cadmium, tin, aluminium, chromium and mercury. The elements sodium, potassium, calcium and magnesium are not included.

Each chapter is typically divided into four sections, namely (i) a brief review of different analytical techniques (including those not based on AAS) for the determination of the element in biological samples, (ii) AAS of the element, (iii) AAS methods for analysis of biological samples, and (iv) a brief conclusion. Accompanying these are summary tables, typically (i) element concentrations in human body fluids and tissues, (ii) AAS techniques (*e.g.*, flame, electrothermal) for determination of the element in biological and related samples, (iii) selected AAS procedures for element determination, where brief procedural outlines are given for specific designated materials such as blood, brain, urine, *etc.*, and sometimes, (iv) procedures for chelation/solvent extraction of some elements (*e.g.*, lead, cadmium) from biological fluids and digests, and (v) AAS speciation studies (*e.g.*, for arsenic, selenium).

'as a work of reference, this book would be a very worthwhile addition in any analytical laboratory'

Compilation of this work must have been a daunting task for the author. At first glance, it is almost equally daunting for the reader, with reference numbers scattered like confetti throughout the text and tables. The author, however, has clearly worked very hard to write a terse and authoritative narrative, full of preparative and instrumental analytical recommendations (and the underlying rationale) and, reassuring to see, safety precautions. The tables are also extremely useful. Thus, if one is interested in the determination of lead in teeth, Table 3 on page 132 gives 'Wet digestion with HNO_3; final digests in 5% v/v HNO_3; ETAAS with a fast program: 130 (1 + 20 s), 750 (5 + 15), 2300 (2 + 5), and 2700 °C (1 + 2 s); acid-matched calibration' and cites ref. 1409. On page 292, one finds that this is Keating, A. D., Keating, J. L., Halls, D. J. and Fell, G. S., *Analyst*, 1987, **112**, 1381–1385.

Books of this sort are inevitably out-of-date by the time they are published. In this respect, the regular review articles and similar reference lists which appear in the *Journal of Analytical Atomic Spectrometry* perhaps have the edge. But, as a work of reference, this book would be a very worthwhile addition in any analytical laboratory. Incidentally, the most prolific first-named authors in the 3223 references are B. Welz (32), K. S. Subramanian (27) and J. R. Castillo (20)!

J. G. Farmer
University of Edinburgh

6/90093C

Chromatographic Detectors. Design, Function, and Operation
By R. P. W. Scott. *Chromatographic Science Series. Volume 73.* Pp. xi + 514. Marcel Dekker. 1996. Price US$150.00. ISBN 0-8247-9779-5.

The book under review is *Volume 73* in the *Chromatographic Science Series* published by Marcel Dekker. Scott's stated aim is to write the book in a straightforward style devoid of unnecessary jargon and acronyms. Only essential references are

included to acknowledge those responsible for a particular invention or significant development in detector technology. The author has achieved these aims, for the book is comprehensive and up to date, yet is easy to read; equations and formulae are clearly explained and the ideas and themes easy to follow. All the diagrams are very clear and uncluttered.

The book is organised into four parts. The first comprises three introductory chapters presenting a concise general introduction to the terminology, characteristics and classification of detectors, chromatographic data and nomenclature. Detector characteristics and sensitivity and data acquisition and processing are also discussed, particularly with reference to the overall chromatography system and quantitative analyses. This forms a sound basis for looking at detectors used in chromatography instruments, hence, Part 2 covers GC detectors, Part 3 detectors for LC, HPLC and TLC, and Part 4 is on spectroscopic detectors and quantitative techniques.

'a straightforward style devoid of unnecessary jargon and acronyms'

The group of chapters on GC detectors has an interesting introduction on their development, from the early detectors developed by James and Martin to the present day. All of the frequently used families of detectors (FIDs, other ionisation detectors and katherometers) are then discussed in subsequent chapters each starting with the invention and development of that detector followed by an explanation of the principles of operation, construction and specific characteristics. Chromatograms of typical applications are included to demonstrate specific features of the detectors. The explanations are very readable, supported by many figures and diagrams, equations being included only where essential, for example, to show the relationship between detector signal output and concentration of the analyte vapour.

Liquid chromatography (HPLC, TLC) detectors are presented and discussed in a similar manner to the GC chapters with UV, fluorescence, refractive index, chiral, conductivity and electrochemical detectors and their variants covered. The final part includes a mixture of topics, including spectroscopic detectors and tandem systems, quantitative analysis and derivatisation.

Should you buy the book? Probably yes if you are looking for a none-too academic up to date account of chromatography detectors. I would certainly recommend that readers should have a look at the book; the almost unique style for scientific texts is refreshing. The book gives an excellent account of the principles and practice of detectors without all the maths and a myriad of equations. It should be useful as a general text for laboratory staff and as a no-nonsense book for undergraduates and postgraduates who do not need to know the theoretical principles of detectors in detail.

Alan Braithwaite
Nottingham Trent University

6/90080A

Chemometrics in Analytical Spectroscopy
By Mike J. Adams. Pp. viii + 216. *RSC Analytical Spectroscopy Monographs.* Series Editor Neil W. Barnett. Royal Society of Chemistry. 1995. Price £39.50. ISBN 0-85404-555-4.

This is a very neat little introduction to some of the chemometric techniques commonly applied to analytical problems. It takes a 'nuts and bolts' approach, giving a good feel for how to implement, not just apply, a technique. The book starts with a reminder of some basic statistics, covering the normal distribution, significance testing, ANOVA and outliers, then extending to the concept of multivariate data to develop the concepts of covariance and correlation and describing some useful multivariate data display methods. There is a brief chapter on acquisition and pre-processing of data, covering required sampling rate and data smoothing. Fourier transforms are described briefly, though only as a means of data preprocessing, with FT spectroscopy barely mentioned. That seemed odd, when time domain acquisition is so prevalent in NMR, heavily used in IR and sometimes used in MS. However, the book is not about spectroscopy, and the short introductory chapters make for a commendably compact volume.

The remainder of the book is divided into four main chapters covering feature selection and extraction, supervised and unsupervised pattern recognition, and calibration and regression. The first deals with the problems of finding real information in raw data. Derivative methods for finding and quantifying a peak in a spectrum are covered, as is basic integration. I was impressed by the clear descriptions and illustrations here and elsewhere in the book; sticking to a simple description of selected methods has paid dividends in a very readable and understandable text.

That becomes particularly evident as the author develops principal components analysis (PCA) as a subset of feature extraction. It is possible to follow the simple two-variable PCA example manually, giving a good feel for the principles. I was a little disappointed to find factor analysis rotation methods left entirely to other texts; a visual example would have been good. References to other texts on eigenvector extraction would also have been welcome here. Nonetheless, a very good introduction to both PCA and the use of factor analysis. The next chapter, on unsupervised pattern recognition, actually covers cluster analysis in surprising detail, with different distance metrics and algorithms covered individually. K-means clustering properly receives most attention. There is also a description of one fuzzy clustering algorithm. I felt that a reader could make a very good attempt at implementing any of these methods after reading the chapter.

'a very good introductory text for those wishing to understand the workings of chemometrics techniques'

The following chapter covers supervised discrimination, starting with discriminant functions, touching on k-nearest neighbour classification and discussing perceptron and basic neural network approaches, though the latter are described very briefly and without considering problems in training time and validation (for example, over-training is not discussed). The final topic, calibration, covers univariate regression for linear and polynomial cases in the usual way, though the illustration uses the normal form, which would not usually be recommended in practice for higher order polynomials due to the sensitivity to numerical errors. It was, however, interesting to see the orthogonal polynomial forms covered in an introductory text. Also welcome is the emphasis on significance testing for higher order coefficients. Most of the chapter, however, describes various multivariate regression methods; multiple least squares, principal components regression and partial least squares, again showing simple implementations. A final appendix details the matrix algebra used in the book.

Overall, the book forms a very good introductory text for those wishing to understand the workings of chemometrics techniques. With the increasing application of these techniques both in exploratory data analysis and interpretation and quantitation, this book will be valuable to those studying chemometrics at early graduate level and for many general users of chemometrics.

S. Ellison
Laboratory of the Government Chemist
London

5/90032H

Conference Diary

1997

213th American Chemical Society National Meeting

April 13-17

San Francisco, CA, USA

For further details contact: Department of Meetings, American Chemical Society, 1155-16th St. NW, Washington, DC 20036, USA. Telephone: +1 202 872 4396; Fax: +1 202 872 6128; E-mail: natlmtgs@acs.org

Chemistry Forum '97

April 14-16

Warsaw, Poland

For further details contact: 'Forum Chemiczne '97', Wydzial Chemiczny, Politechnika Warszawska, ul. Noakowskiego 3, 00-664 Warszawa, Poland. Telephone: (48-22) 660 54 27 (Dr. Wojciech Wroblewski); Fax: (48-22) 660 74 08; E-mail: forum@ch.pw.edu.pl; Internet: http://www.ch.pw.edu.pl

Chemistry in the Oil Industry Sixth International Symposium

April 14-17

Cumbria, UK

For further details contact: M. Fielder, BP, Fax: +44(0) 1224 833444 or T. Schmidt, Statoil, Fax: 47 51 80 70 42

Genes and Gene Families in Medical, Agricultural and Biological Research: 9th International Congress on Isozymics

April 14-19

Texas, USA

For further details contact: Mrs. Janet Cunningham, Barr Enterprises, 10120 Kelly Road, P.O. Box 279, Walkersville, MD 21793, USA. Telephone: +1 301 898 3772; Fax: +1 301 898 5596

Computer and Process Validation in the Pharmaceutical and Fine Chemical Industries

April 15-16

Manchester, UK

For further details contact: Spring Innovations Ltd., 185A Moss Lane, Bramhall, Stockport, Cheshire SK7 1BA, UK. Telephone: +44 (0) 161440 0082; Fax: +44 (0)161 440 9127; E-mail: spring.innovations@dial.pipex.com

Scanning 97

April 19-22

Monterey, CA, USA

For further details contact: Mary K. Sullivan, FAMS Inc., SCANNING 97 Program Committee, Box 832, Mahwah, NJ 07430-0832, USA. Telephone: +1 201 818 1010; Fax: +1 201 818 0086; E-mail: fams@holonet.net; Internet: http://www.scanning-fams.org

Seventh International Symposium on Biological and Environmental Reference Materials (BERM-7)

April 21-25

Antwerp, Belgium

For further details contact: J. Pauwels, Institute for Reference Materials and Measurements, Retieseweg, B-2440 Geel, Belgium. Telephone: +32 14 571 722; or Wayne Wolk, US Department of Agriculture, 10300 Baltimore Blvd, Beltsville, MD 20705, USA. Telephone: +1 301 504 8927

Elements of Industrial Analysis

April 23

Manchester, UK

For further details contact: Dr. Sharon C Stephen, Zeneca Specialties, Specialties Research Centre, P.O. Box 42, Blackley, Manchester, M9 8ZS, UK. Telephone: +44 (0) 161 721 1976; Fax: +44 (0) 161 721 1654

Flavours and Fragrances

April 30-May 2

Warwick, UK

For further details contact: Elaine Wellingham, Conference Secretariat, Field End House, Bude Close, Nailsea, Bristol BS19 2FQ, UK. Telephone and Fax: +44 1275 853311; E-mail: confsec@dial.pipex.com

PBA 97, 8th International Symposium on Pharmaceutical and Biomedical Analysis

May 4-8

Orlando, FL, USA

For further details contact: Shirley E. Schlessinger (Symposium Manager), Suite 1015, 400 East Randolph Drive, Chicago, IL 60601, USA

NATO Advanced Research Workshop on Biosensors for Direct Monitoring of Environmental Pollutants in the Field

May 4-8

Smolenice, Slovakia

For further details contact: Dr. D. P. Nikolelis (Director NATO ARW), Laboratory of Analytical Chemistry, Chemistry Department, Athens University, Panepistimiopolis-Kouponia, 15771 Athens, Greece. Fax: +30 301 7231608; E-mail: nikolelis@nestor.dc.uoa.gr

Chiral USA 97

May 12-13

Boston, USA

For further details contact: Spring Innovations Ltd., 185A Moss Lane, Bramhall, Stockport, Cheshire SK7 1BA, UK. Telephone: +44 (0)161 440 0082; Fax: +44 (0)161 440 9127 or Brandon Associates, P.O. Box 1244, Merrimack, NH 03054, USA. Telephone and Fax: +1 630 424 2035

Fifth International Conference on Progress in Analytical Chemistry in the Steel and Metals Industries

May 12-14

Luxembourg

For further details contact: Mr. Sven Sundberg or Ms. Kajsa Lindblom, Jernkontoret, Box 1721, SE-111 87 Stockholm, Sweden. Telephone: +46 8 679 17 00; Fax: +46 8 611 20 89

European Symposium on Photonics in Manufacturing III

May 12-16

Paris, France

For further details contact: Françoise Chavel, Executive Secretary, European Optical Society, B.P. 147-91403 Orsay Cedex, France. Telephone: +33 1 69 85 35 92; Fax: +33 1 69 85 35 65; E-mail: francoise.chavel@iota.u-psud.fr

19th International Symposium on Capillary Chromatography and Electrophoresis

May 18-22

Wintergreen, VA, USA

For further details contact: Joy Wise, P.O. Box 4153, Frederick, MD 21705-4153, USA. Telephone: +1 301 473 8311; Fax: +1 301 473 8312; E-mail: Wisejoy@aol.com

IInd Miniaturisation in Liquid Chromatography *versus* Capillary Electrophoresis Conference

May 27-28

Ghent, Belgium

For further details contact: Professor Dr Willy R G Baeyens, Chairman MINI-LC II, University of Ghent, Faculty of Pharmaceutical Sciences, Department of Pharmaceutical Analysis, Laboratory of Drug Quality Control, Harelbekestraat 72, B-9000 Ghent, Belgium. Telephone: +32 9 264 80 97; Fax: +32 9 264 81 96; E-mail: willybaeyens@rug.ac.be

1997 International Symposium, Exhibit and Workshops on Preparative Chromatography, Ion Exchange, and Adsorption/Desorption Processes and Related Techniques

June 1-4

Washington, DC, USA

For further details contact: Janet Cunningham, Barr Enterprises, P.O. Box 279, Walkersville, MD 21793, USA. Telephone: +1 301 898 3772; Fax: +1 301 898 5596; E-mail: Janetbarr@aol.com

45th ASMS Conference on Mass Spectrometry and Allied Topics

June 1-5

Palm Springs, CA, USA

For further details contact: American Society for Mass Spectrometry, 1201 Don Diego Avenue, Santa Fe, NM 87505, USA. Telephone: +1 505 989 4517; Fax: +1 505 989 1073

Geoanalysis '97, 3rd International Conference on the Analysis of Geological and Environmental Materials

June 1-5

Vail, CO, USA

For further details contact: Belinda Arbogast, USGS, Denver Federal Center, Box 25046, MS 973, Denver, CO 80225, USA. Telephone: +1 303 236 2495; Fax: +1 303 236 3200; E-mail: plamothe@helios.cr.usgs.gov

5th Symposium on Analytical Sciences

June 2-4

Nice, France

For further details contact: Deauville Conference 97, SAS 5th Symposium on Analytical Sciences, Nicko & Cri Associes, 7 rue d'Argout, F-75002 Paris, France. Telephone: +33 1 42334766; Fax: +33 1 40419241; E-mail: dc_jc@compuserve.com

LIMS '97, 11th International LIMS Conference and Exhibition

June 3-5

The Hague, Netherlands

For further details contact: Conference Secretariat, LIMS 97, 45 Hilltop Avenue, Hullbridge, Hockley, Essex, UK SS5 6BL. Telephone: +44 (0)1702 231268; Fax: +44 (0)1702 230580; E-mail: 1013201617@compuserve.com

Seventh International Hans Wolfang Nuernberg Memorial Symposium on Metal Compounds in Environment and Life

June 4-7

Modena, Italy

For further details contact: Marianne Frei, IAEAC Secretariat, P.O. Box 46, CH-4123 Allschwil 2, Switzerland. Fax: ++41 61 482 08 05; Telephone: ++41 61 481 27 89; E-mail: iaeacmfrei@access.ch

6th Symposium on Chemistry and Fate of Modern Pesticides

June 4-6

Amsterdam, The Netherlands

For further details contact: Mrs. Marianne Frei-Haeusler, IAEAC Office, P. O. Box 46, CH-4123 Allschwil-2, Switzerland. Fax: 41 61 4820805; E-mail: iaeacmfrei@access.ch

5th European Meeting on Mass Spectrometry in Occupational and Environmental Health

June 9-11

Nijmegen, The Netherlands

For further details contact: Dr. P. Scheepers, Department of Toxicology, Faculty of Medical Sciences, University of Nijmegen, P. O. Box 9101, NL-6500 HB Nijmegen, The Netherlands. Telephone: (+31-243) 616 878; Fax: (+31-243) 541 802; E-mail: p.scheeper-s@toxi.kun.nl

27th International Symposium on Environmental Analytical Chemistry

June 15-19

Jekyll Island, GA, USA

For further details contact: J. A. de Haseth, Department of Chemistry, University of Georgia, Athens, GA 30602-2556, USA. Telephone: +1 706 542 1968; Fax: +1 706 542 9454; E-mail: jekyllsymp@sunchem.chem.uga.edu

International Conference on Analytical Chemistry

June 15-21

Moscow, Russia

For further details contact: Dr. L. N. Kolomiets, Scientific Council on Chromatography of the Russian Academy of Sciences Leninsky Prospect 31, 117915 Moscow, Russia. Telephone: +7 95 952 0065; Fax: +7 095 952 0065; E-mail: larionov@lmm.phyche.muk.su

ChemiChromics '97 — "Color Change and Functional Dye's"

June 16-17

Manchester, UK

For further details contact: Spring Innovations Ltd., 185A Moss Lane, Bramhall, Stockport, Cheshire SK7 1BA, UK. Telephone: +44 (0)161 440 0082; Fax: +44 (0)161 440 9127; E-mail: spring.innovations@dial.pipex.com

European Symposium on Environmental Sensing III

June 16-20

Munich, Germany

For further details contact: Françoise Chavel, Executive Secretary, European Optical Society, B.P. 147-91403 Orsay Cedex, France. Telephone: +33 1 69 85 92; Fax: +33 1 69 85 33 65; E-mail: francoisechavel@iota.u-psud.fr

European Symposium on Environmental and Public Safety II

June 16-20

Munich, Germany

For further details contact: Françoise Chavel, Executive Secretary, European Optical Society, B.P. 147-91403 Orsay Cedex, France. Telephone: +33 1 69 85 35 92; Fax: +33 1 69 85 35 65; E-mail: francoisechavel@iota.u-psud.fr

HPLC 97, 21st International Symposium on High Performance Liquid Phase Separations and Related Techniques

June 22-27

Birmingham, UK

For further details contact: HPLC 97 Symposium Secretariat, ICC, Broad Street, Birmingham B1 2EA, UK . Telephone: +44 121 200 2000; Fax: +44 121 643 0388

EUROTOX '97

June 25-28

Aarhus, Denmark

For further details contact: Scientific Secretariat, University of Aarhus, Universitetsparken, Bldg. 180, DK-8000 Aarhus C, Denmark. Telephone: +45 8942 2943; Fax: +45 8942 2970; E-mail: HA@mil.aau.dk

Analytical Science and the Environment

June 30-July 3

Newcastle, Northumbria, UK

For further details contact: The Secretary, Analytical Division, The Royal Society of Chemistry, Burlington House, Piccadilly, London W1V 0BN, UK. Telephone: +44 (0)171 437 8656; Fax: +44 (0)171 734 1227

6th European ISSX Meeting

June 30-July 3

Gothenburg, Sweden

For further details contact: Meeting Secretariat, 6th European ISSX Meeting, c/o The Swedish Academy of Pharmaceutical Sciences, P.O. Box 1136, S-111 81 Stockholm, Sweden. Telephone: +46 8 723 5000; Fax: +46 8 20 551 1

Recent Developments in Affinity Chromatography, Affinity Bioprocessing and Molecular Imprints

July 1-3

Cambridge, UK

For further details contact: The Chromatographic Society, Suite 4, Clarendon Chambers, 22 Clarendon Street, Nottingham, NG1 5JD, UK

10th International Symposium on High Performance Capillary Electrophoresis and Related Microscale Techniques

July 9-11

Kyoto, Japan

For further details contact: Prof. Shigeru Terabe (Chairman) or Prof. Koji Otsuka (Secretary General), Faculty of Science, Himeji Institute of Technology, Kamigori, Hyogo 678-12, Japan. Telephone: +81 7915 8 0172 (Terabe) or +81 7915 8 0171 (Otsuka); Fax: +81 7915 8 0132; E-mail: hpcekyt@sci.himeji-tech.ac.jp

International Symposium on Optical Science, Engineering, Instrumentation

July 18-23

San Diego, CA, USA

For further details contact: SPIE, P.O. Box 10, Bellingham, WA 98227-0010, USA. Telephone: +1 360 676 3290; Fax: +1 360 647 1445; E-mail: spie@spie.org

4th International Conference on Laser Ablation

July 21-25

Monterey, CA, USA

For further details contact: Richard E. Russo, Lawrence Berkeley Laboratory, MS 90-2024, Berkeley, CA 94720, USA. Telephone: +1 510 486 4258; Fax: +1 510 486 4260; E-mail: rerusso@lbl.gov; http://cola97.ornl.gov

4th International Conference on the Biogeochemistry of Trace Elements

July 23-26

Berkeley, CA, USA

For further details contact: I. K. Iskandar, US Army Cold Regions Research and Engineering Laboratory, 72 Lyme Rd, Hanover, NH 03755, USA. Telephone: +1 603 646 4198; Fax: +1 603 646 4561; E-mail: iskandar@crrel.usace.army.mil

43rd International Conference on Analytical Sciences and Sprectroscopy

August 10-13

Montreal, Quebec, Canada

For further details contact: Ian Butler, Department of Chemistry, McGill University, 801 Sherbrooke St. West, Montreal, PQ K1S 5B6, Canada. Telephone: (514) 398-6910; Fax:(514) 398-3797; E-mail: butler@omc.Ian.mcgill.ca

11th International Conference on Fourier Transform Spectroscopy

August 10-15

Athens, GA, USA

For further details contact: James A. de Haseth, Department of Chemistry, University of Georgia, Athens, GA 30602-2556, USA. Telephone: +1 706 542 1968; Fax: +1 706 542 9454; E-mail: dehaseth@dehrsv.chem.uga.edu

The 10th International Symposium on Polymer Analysis and Characterization (ISPAC-10)

August 11-13

Toronto, Ontario, Canada

For further details contact: Professor Stephen T. Balke, Dept. of Chemical Engineering and Applied Chemistry, University of Toronto, Toronto, Ontario, M5S 1A4, Canada. Telephone/Fax: +1 416 978 7495; E-mail: balke@ecf.toronto.edu

Capillary Electrophoresis

August 18-21

Heslington, York, UK

Details from: Dr. Terry Threlfall, Department of Chemistry, University of York Heslington, York, YO1 5DD, UK. Telephone: +44 (0)1904 432576/434079; Fax: +44 (0)1904 432516; E-mail: js20@york.ac.uk

13th International Symposium on Plasma Chemistry

August 18-22

Beijing, China

For further details contact: Lin He, Secretary ISPC-13, The Chinese Society of Theoretical and Applied Mechanics, 15 Zhing Guan Cun Road, Beijing 1000080, China. Fax: +86 10 62559588; E-mail: cstam@sun.ihep.ac.cn

VII Flow Conference

August 25-28

Aguas de Sao Pedro-Piracicaba, Brazil

For further details contact: Henrique Bergamin Filho, CENA-USP, Caixa Postal 96, 13400-970 Piracicaba, SP, Brazil. Telephone: +55 194 335122; Fax: +55 194 228339; E-mail: flow97@aguia.cena.usp.br

IMSC '97 - 14th International Mass Spectrometry Conference

August 25-29

Tampere, Finland

For further details contact: 14th IMSC Congress Secretariat, c/o Congress Management Systems, P.O. Box 151, SF-00141, Helsinki, Finland

111th AOAC International Annual Meeting and Exposition

September 7-11

San Diego, CA, USA

For further details contact: Margreet Lauwaars, P.O. Box 153, 6720 AD Bennekom, The Netherlands. Telephone: +31 318 418725; Fax: +31 318 418359; or Derek Abbott, 80 Chaffers Mead, Ashtead, Surrey, UK KT2 1NH. Telephone: +44 372 274856; Fax: +44 372 274856

214th American Chemical Society National Meeting

September 7-11

Las Vegas, NE, USA

For further details contact: Department of Meetings, American Chemical Society, 1155-16th St. NW, Washington, DC 20036, USA Telephone: +1 202 872 4396; Fax: +1 202 872 6128; E-mail: natlmtgs@acs.org

11th International Conference on Secondary Ion Mass Spectrometry (SIMS XI)

September 7-12

Orlando, FL, USA

For further details contact: SIMS XI, 1201 Don Diego Ave., Santa Fe, NM 87505, USA. Telephone: +1 505 989 4735; Fax: +1 505 989 1073

4th International Conference on Nanometer Scale Science and Technology

September 8-12

Beijing, China

Shijin Pang, Beijing Laboratory of Vacuum Physics, Chinese Academy of Sciences, P.O. Box 2724, Beijing 100080, China. Telephone: +86 10 256 8306; Fax: +86 10 255 6598; E-mail: pang@irnage.blem.ac.en

Biomedical Optics V

September 9-12

Poland

For further details contact: Françoise Chavel, Executive Secretary, European Optical Society, B.P. 147-91403 Orsay Cedex, France. Telephone: +33 1 69 95 35 92; Fax: +33 1 69 95 35 65; E-mail: francoise.chavel@iota.u-psud.fr

IICS '97

September 14-17

Santa Clara, CA, USA

For further details contact: Century International, P. O. Box 493, Medfield, MA 02052-0493, USA. Telephone: +1 508 359 8777; Fax: +1 508 359 8778; E-mail: century@ixl.net

The 134th British Pharmaceutical Conference

September 15-18

Scarborough, UK

For further details contact: BPC Secretariat, Royal Pharmaceutical Society of Great Britain, 1 Lambeth High Street, London SE1 7JN, UK. Telephone: +44 (0)171 820 3275; Fax: +44 (0)171 582 4985

3rd International Symposium on Speciation of Elements in Biological, Environmental and Toxicological Sciences

September 15-19

Port Douglas, Queensland, Australia

For further details contact: Dr. J. P. Matousek, Department of Analytical Chemistry, University of New South Wales, Sydney, NSW 2052, Australia. Telephone: +61 2 3854713; Fax: +61 2 3856141; E-mail: j.matousek@unsw.edu.au

XXX Colloquium Spectroscopicum Internationale

September 21-26

Melbourne, Australia

For further details contact: The Meeting Planners, 108 Church Street, Hawthorn, Victoria 3122, Australia. Telephone: +61 3 9819 3700; Fax: +61 3 9819 5978

4th International Symposium on Environmental Geochemistry

October 5-10

Vail, CO, USA

For further details contact: R. C. Severson, U.S. Geological Survey, Federal Center, Box 25046, MS 973, Denver, CO 80225, USA. Telephone: +1 303 236 5514; Fax: +1 303 236 3200; E-mail: iseg@helios.cr.usgs.gov

1st Euroconference on Environmental Analytical Chemistry

October 11-17

Neusiedl, Austria

For further details contact: Dr. Erwin Rosenberg, Institute of Analytical Chemistry, TU Wien, Getreidemarkt 9, A-1060 Wien, Austria. Fax: +43 1 5867813; E-mail: erosen@fbch.tuwien.ac.at; WWW-page: http://www.iac.tuwien.ac.at/~euconeac/welcome.html

BCEIA '97, The 7th International Beijing Conference and Exhibition on Instrumental Analysis

October 14-18

Shanghai, China

For further details contact: BCEIA '97 General Service Office, Room 585, Chinese Academy of Sciences Building, San Li He, Xi Jiao, PO Box 2143, Beijing 100045, China. Telephone: +86 10 8511133 Ext. 1585, +86 10 8511814; Fax: +86 10 8511814; E-mail: bceia@aphy01.iphy.ac.cn

35th International Exhibition of Chemistry, Analysis, Research, Test Equipment and Biotechnology

October 21-24

Milan, Italy

For further details contact: General Secretariat, 20149 Milano, Italy - Via Domenichino, 11 (C.P. 15117 - 20150 Milano, Italy). Telephone: +39 2 4815541; Fax: +39 2 4980330; E-mail: assoexpo@assoexpo.com; http://www.assoexpo.com

24th Annual Meeting of the Federation of Analytical Chemistry and Spectroscopy Societies

October 26-30

Providence, RI, USA

For further details contact: Jo Ann Brown, Federation of Analytical Chemistry and Spectroscopy Societies, 210B Broadway Street, Frederick, MD 21701, USA. Telephone: +1 301 694 8122; Fax: +1 301 694 6890; E-mail: jbrownsas@aol.com

8th Symposium on Handling of Environmental and Biological Samples in Chromatography 26th Scientific Meeting of the Group of Chromatography and Related Techniques of the Spanish Royal Society of Chemistry

October 26-29

Almeria, Spain

For further details contact: M. Frei-Häusler, IAEAC Secretariat, Postfach 46, CH-4123 Allschwil 2, Switzerland. Fax: +41 61 482 08 05

ISPPP '97: 17th International Symposium on the Separation of Proteins, Peptides and Polynucleotides

October 26-29

Washington, DC, USA

For further details contact: Janet Cunningham, Barr Enterprises, P.O. Box 279, Walkerville, MD 21793, USA. Telephone: +1 301 898 3772; Fax: +1 301 898 5596; E-mail: Janetbarr@aol.com

1997 Eastern Analytical Symposium

Somerset, NJ, USA

November 16-21

For further details contact: EAS, P.O. Box 633, Montchanin, DE 19710-0633, USA. Telephone: (302) 738-6218; Fax: (302) 738-5275; E-mail easinfo@aol.com; Internet: http://www.eas.org/-easweb/

The 2nd Mediterranean Basin Conference on Analytical Chemistry

23-28 November

Rabat, Morocco

For further details contact: Professor Abderrahmane Laachach, Laboratoire de Chimie Analytique, Ecole Nationale de l'Industrie Minerale, Av. Hadj Ahmed Cherkaoui, B.P. 753 Agdal Rabat, Morroco. Telephone: +212 (7) 77 13 60 and 77 16 67; Fax: +212 (7) 77 45 37 and 77 10 55

3rd BMSS LC/MS Symposium

December 17-18

Cambridge, UK

For further details contact: Dr. J. Oxford, BMSS, P.O. Box 38, Royston, Herts, SG8 5BX, UK

1998

1998 Winter Conference on Plasma Spectrochemistry

January 5-10

Scottsdale, AZ, USA

For further details contact: Ramon Barnes, Department of Chemistry, Lederle GRC Towers, University of Massachusetts, Box 34510, Amherst, MA 01003-4510. Telephone:+1 413 545 2294; Fax: +1 413 545 3757; E-mail: winterconf@chem.umass.edu

Fifth International Symposium on Hyphenated Techniques in Chromatography and Hyphenated Chromatographic Analyzers

February 11-13

Bruges, Belgium

For further details contact: Ordibo bvba, Lucas Henninckstraat 18, B-2610 Wilrijk Antwerp, Belgium. Telephone: +32 3 561 2831 or +32 3 217 2905; Fax: +32 3 827 8439; E-mail: smitsr@innet.be

28th Annual International Symposium on Environmental Analytical Chemistry

March 2-5

Geneva, Switzerland

For further details contact: Mrs. M. Frei-Haeusler, IAEAC Secretariat, P. O. Box 46, CH-4123 Allschwil 2, Switzerland. Fax: ++41 61 482 0805; E-mail: iaeacmfrei@access.ch

4th International Symposium on Hygiene and Health Management in the Working Environment

April 27-29

Ostend, Belgium

For further details contact: Technologisch Instituut vzw, Desguinlei 214, B-2018 Antwerpen, Belgium. Telephone: +32 3 216 09 96; Fax: +32 3 216 06 89; E-mail: hygiene@ti.kviv.be

The First International Conference on Trace Element Speciation in Biomedical, Nutritional and Environmental Sciences

May 4-7

Neuherbert/Munchen, Germany

For further details contact: First Speciation Conference, c/o Ulla Schrodel, GSF - Forschungszentrum, Congress Service, Postfach 1129, D-85758 Oberschleissheim, Germany. Telephone: +89 3187 3030 (2669); Fax: +89 3187 3362

HPLC '98—22nd International Symposium on High Performance Liquid Phase Separations & Related Techniques

St. Louis, MO, USA

May 3-8

For further details contact: American Society for Mass Spectrometry, 1201 Don Diego Avenue, Sante Fe, NM 87505, USA. Telephone: +1 505 989 4517; Fax: +1 505 989 1073

The Scientific Instrument Association Conference 1998

11-14 May

London, UK

For further details contact: David Lofty/Rosemary Gregory, SIA '98 Conference Office. Telephone: +44 (0)1280 822873

VIIIth International Symposium on Luminescence Spectrometry in Biomedical and Environmental Analysis-Detection Techniques and Applications in Chromatography and Capillary Electrophoresis

May 26-29

Las Palmas de G.C., Spain

For further details contact: Dr. Jose Juan Santana Rodriguez, Department of Chemistry, Faculty of Marine Sciences, University of Las Palmas de G.C., 35017 Las Palmas de G.C., Spain. Telephone: +34 28 452915; Fax: +34 28 452922; E-mail: josejuan.santana@quimica.ulpgc.es

22nd World Congress and Exhibition of the International Society for Fat Research (ISF)

September 8-12

Kuala Lumpur, Malaysia

For further details contact: Mary Belding, Meetings & Exhibits Department, ISF Secretariat, P.O. Box 3489, Champaign, IL 61826 3489, USA. Telephone: +1 217 359 2344; Fax: +1 217 351 8091; E-mail: meetings@aocs.org

112th AOAC International Annual Meeting and Exposition

September 13-17

Montreal, Ontario, Canada

For further details contact: Carolyn Dell, Meetings and Education Department, AOAC International, 481 North Frederick Ave., Suite 500, Gaithersburg, MD 20877, USA. Telephone: +1 301 924 7077; E-mail: cdell@aoac.org

XIVth Conference on Analytical Chemistry

September 24-26

Piatra Neamt, Romania

For further details contact: Dr. G. L. Radu, Romanian Society of Analytical Chemistry, 13 Bvd, Republicii, 70346 Bucharest III, Romania. Telephone and Fax: +40 1 410 2279

2000

HPLC '2000: 24th International Symposium on High Performance Liquid Phase Separations and Related Techniques

June 25-30

Seattle, WA, USA

For further details contact: Janet Cunningham, Barr Enterprises, PO Box 279, Walkerville, MD 21793, USA. Telephone: +1 301 898 3772; Fax: +1 301 898 5596; E-mail: Janetbarr@aol.com

Courses

1997

Crystal CE Series European Seminar Tour

April 8-18

Various venues throughout Europe

For further details contact: Mebs Surve,.Thermo CE, PO Box 205, York Street, Cambridge, CB1 2SS. Telephone: +44 (0) 1223 374524; Fax: +44 (0) 1223 374338; E-mail: mebs.surve@unicam.co.uk

Analysis and Examination of Foods and Other Materials

April 8-11

Reading, UK

For further details contact: Brian Taylor, The A.P.A. Educational Trust, 5 Thornton Close, Little Lever, Bolton, BL3 1NZ, UK. Telephone and Fax: +44 (0) 1204 575095

Rational Tools in Research and Development - Multivariate Data Analysis in Bristol

April 9-11

Bristol, UK

For further details contact: Bristol Chemometrics, School of Chemistry, University of Bristol, Cantock's Close, Bristol, BS8 1TS, UK. Telephone: +44 (0)117 9287658; Fax: +44 (0)117 9251295; E-mail: R.G.Brereton@UK.AC.BRISTOL

Chemistry of Waste Minimisation

April 14-16

Heslington, York, UK

For further details contact: Dr. Terry Threlfall, Department of Chemistry, University of York, Heslington, York YO1 5DD, UK. Telephone: +44 (0)1904 432576/434079; Fax: +44 (0)1904 432516; E-mail: js20@york.ac.uk

Laboratory Health and Safety

April 28-May 1

Loughborough, Leicestershire, UK

For further details contact: Joyce Bostock, Centre for Hazard & Risk Management (CHaRM), Loughborough University, Loughborough, Leics, LE11 3TU, UK. Telephone: +44 (0) 1509 222175; Fax: +44 (0) 1509 223991

Modern Practice of Gas Chromatography

May 5-7

West Chester, PA, USA

For further details contact: Bruce Strasser, Union Camp, P. O. Box 3301, Princeton, NJ 08543, USA. Telephone: +1 609-844-7206

5th European Workshop on Modern Developments and Applications in Microbeam Analysis

May 11-15

Torquay, UK

For further details contact: EMAS Secretariat, University of Antwerp, Department of Chemistry, Universiteitsplein 1, G-2610 Antwerp-Wilrijk, Belgium. Fax: +32 3 820 2376; E-mail: vantdack@uia.ua.ac.be

Eighteenth Annual Introductory HPLC Short Course

May 12-14

West Chester, PA, USA

For further details contact: Bill Champion, DuPont Merck Pharmaceutical Co., PRF Building, Chambers Works, Deepwater, NJ 08023, USA. Telephone: +1 609 540 4826; E-mail: champiwl@al.lldmpc.umc.dupont.com

ASMS Short Course-Interpretation of Mass Spectra

May 31-June 1

Palm Springs, CA, USA

For further details contact: American Society for Mass Spectrometry, 1201 Don Diego Avenue, Santa Fe, NM 87505, USA. Telephone: +1 505 989 4517; Fax: +1 505 989 1073

ASMS Short Course-Principles and Practice of Quantitative Mass Spectrometry

May 31-June 1

Palm Springs, CA, USA

For further details contact: American Society for Mass Spectrometry, 1201 Don Diego Avenue, Santa Fe, NM 87505, USA. Telephone: +1 505 989 4517; Fax: +1 505 989 1073

ASMS Short Course-LC-MS: The Techniques of Electrospray and API

May 31-June 1

Palm Springs, CA, USA

For further details contact: American Society for Mass Spectrometry, 1201 Don Diego Avenue, Santa Fe, NM 87505, USA. Telephone: +1 505 989 4517; Fax: +1 505 989 1073

ASMS Short Course-Proteins and Peptides

May 31-June 1

Palm Springs, CA, USA

For further details contact: American Society for Mass Spectrometry, 1201 Don Diego Avenue, Santa Fe, NM 87505, USA. Telephone: +1 505 989 4517; Fax: +1 505 989 1073

ASMS Short Course-Principles of Ion Mass Spectrometry

May 31-June 1

Palm Springs, CA, USA

For further details contact: American Society for Mass Spectrometry, 1201 Don Diego Avenue, Santa Fe, NM 87505, USA. Telephone: +1 505 989 4517; Fax: +1 505 989 1073

ASMS Short Course-Fundamentals of MALDI

May 31-June 1

Palm Springs, CA, USA

For further details contact: American Society for Mass Spectrometry, 1201 Don Diego Avenue, Santa Fe, NM 87505, USA. Telephone: +1 505 989 4517; Fax: +1 505 989 1073

6th Annual Course on Practical Methods of Digestion for Trace Analysis

June 2-5

Amherst, MA, USA

For further details contact: Beverly Lissner, Questron Corporation, 4044 Quakerbridge Rd, Mercerville, NJ 08619, USA. Telephone: +1 609 587 6898; Fax: +1 609 587 0513

Design of Mixture Experiments

July 2-4

Bristol, UK

For further details contact: Bristol Chemometrics, School of Chemistry, University of Bristol, Cantock's Close, Bristol, BS8 1TS, UK. Telephone: +44 (0) 117 9287658; Fax: +44 (0) 117 9251295; E-mail: R.G.Brereton@bris.ac.uk

Problem Solving for Analytical Leaders

July 16-18

Heslington, York, UK

Details from: Dr. Terry Threlfall, Department of Chemistry, University of York Heslington, York YO1 5DD, UK. Telephone: +44 (0)1904 432576/434079; Fax: +44 (0)1904 432516; E-mail: js20@york.ac.uk

NMR Spectroscopy

September 17-19

Heslington, York, UK

For further details contact: Dr. Terry Threlfall, Department of Chemistry, University of York Heslington, York, YO1 5DD, UK. Telephone: +44 (0)1904 432576/434079; Fax: +44 (0)1904 432516; E-mail: js20@york.ac.uk

Interpretation of Infrared Spectra

September 30-October 2

Heslington, York, UK

For further details contact: Dr. Terry Threlfall, Department of Chemistry, University of York, Heslington, York YO1 5DD, UK. Telephone: +44 (0)1904 432576/434079; Fax: +44 (0)1904 432516; E-mail: js20@york.ac.uk

Entries in the above listing are included at the discretion of the Editor and are free of charge. If you wish to publicize a forthcoming meeting please send full details to: *The Analyst* Editorial Office, Thomas Graham House, Science Park, Milton Road, Cambridge, UK CB4 4WF. Tel: +44 (0)1223 420066. Fax: +44 (0)1223 420247. E-mail:Analyst@RSC.ORG

Interesting Applications of Elemental Analysis

May 21, 1997, Sheffield Hallam University, UK

A one day meeting featuring younger scientists. Techniques covered will include AA, ICP(MS), XRF and EM-EDX, with samples ranging from medieval dust to modern materials. Invited speakers will provide short lectures while other participants are encouraged to present posters describing their work. Organised by the Royal Society of Chemistry Analytical Division North East Region and the Atomic Spectroscopy Group.

LECTURES

Antimony, Cot Deaths and Atomic Fluorescence
Fergus Keenan and Michael Cooke (Sheffield Hallam University)

Ultra-trace Analysis and Trace Element Speciation via ICP-MS
Petra Krause (University of Sheffield)

Speciation of Antimony (III) and (V) Compounds by Ion Chromatography Coupled to ICP-OES and ICP-MS
Alen Guy, Philip Jones, Steven J. Hill (University of Plymouth) and **John Marshall** (ICI Wilton)

Array Detector Technology in Atomic Spectroscopy
Daran Sadler (University of Strathclyde)

Organo-mercurials in Environmental Samples; Extraction and Sample Preparation
Claire T. Costley, John R Dean (University of Northumbria) and **Louise M. Garden** (ICI Wilton)

Hazardous Liquid Wastes; Analysis using Energy-dispersive X-ray Fluorescence
Philip A. Russell and Andrew Ellis (Oxford Analytical)

Elemental Analysis with Electron Microscopes - Small Particles and Defects in Layered Structures
Ian Wadsworth (Sheffield Hallam University)

Send applications or requests for further details to Dr David Crowther, Chemistry Division, Sheffield Hallam University, Pond Street, Sheffield S1 1WB; Tel 0114 253 3016; Fax 0114 253 3085; E-mail d.crowther@shu.ac.uk

Conference Report

$EuAsC_2S$-5, Guangzhou, China, December 10–14, 1996

The Eurasia Conference on Chemical Science ($EuAsC_2S$) was initiated in Bangkok ($EuAsC_2S$-1, 1988) and held every other year in East Asia to provide a forum for the chemists of Asian countries to meet with their colleagues from Europe and other parts of the world. About 400 participants from 40 different countries gathered for the Fifth Eurasia Conference ($EuAsC_2S$-5) in Guangzhou. The conference covered various branches of chemistry with analytical chemistry very well represented.

The conference was divided into 12 sections and minisymposiums, and the distribution of the papers was as follows: bioremediation, 12; environmental and analytical chemistry, 127; chemical solution to problems in life science, 75; organic synthesis and chiral catalysis, 71; natural products and biopolymers, 34; nano-materials with special attention to coordination materials, 64; theoretical, computational and modeling chemistry, 63; solution coordination chemistry and transfer of chemicals between solvents, 77; molecular structure under extreme conditions in solution, 19; traditional drugs, 13; chemometrics, 13; bioinorganic catalysis, 29.

The conference opened with the welcome addresses by J. Reedijk (Leiden University, Leiden, The Netherlands), one of the founders of $EuAsC_2S$, and Kui Wang (Beijing Medical University, Beijing).

There were many interesting analytical papers presented in the appropriate sections. The analysis of surface water by laser dual-photon ionization with a detection limit of 9 ppt for pyrene was reported by T. Ogawa (Kyushu University, Fukuoka, Japan). The role of chemisorption in the establishment of the potentiometric response of ion-sensitive electrodes was discussed by E. Pungor (Technical University of Budapest, Hungary). An interesting new pH sensor was prepared by Daming Feng *et al.* (Guangzhou Research Institute of Nonferrous Metals, Guangzhou) using Ti strips or wires bombarded by nitrogen ions at 750–950 °C. Some nanoheterogeneous metal–polymer composites have been used by G. N. Gerasimov *et al.* (Karpov Institute of Physical Chemistry, Moscow, Russia) as materials for chemical sensors. The photolithography technique has beeen used by Ui-Rak Kim (Keimyung University, Daegu, Korea) to prepare ion-sensitive field-effect transistors as urea and glucose sensors by immobilizing urease and glucose oxidase using polyurethane and poly(vinyl alcohol), respectively. Benli Huang (Xiamen University, Xiamen) described high current, microsecond pulsed, hollow cathode lamp excited, ICP–ionic fluorescence spectrometry. The surface adsorbate analysis using low energy Cs^+ reactive scattering (Heon Kang *et al.*, Pohang University of Science and Technology, Gyeong-Buk, Korea) seems useful for the identification of chemical states of these absorbates. The DNA analysis for breast tumour cells was undertaken by Hong-Wu Tang *et al.* (Wuhan University, Wuhan) using Hadamard transform image microscopy. The characterization of solid surfaces using time-of-flight secondary ion mass spectrometry (TOF-SIMS) was discussed by Yeonhee Lee (Korea Institute of Science and Technology, Seoul) who showed the advantage of the non-resonant multiphoton ionization over conventional SIMS for quantitative depth profiling. The fast atom bombardment MS of polynuclear metal clusters involving mixed thiolate and phosphine ligands was reported by Yuan-Ba Cai *et al.* (Zhongshan University). Nuclear analytical techniques were used by Chifang Chai (Institute of High Energy Physics, Beijing), including neutron activation analysis (NAA) of methylmercury in infant scalp hair, molecular activation analysis and Mossbauer spectrometry for chemical speciation of selenium in corn samples taken from a high-Se region and the mechanism study for Se-deficiency in soil and plant from a low-Se region, NAA and dual-photon absorption spectrometry for studying the bioavailability and pharmacodynamics of calcium in rabbits, synchronous radiation-based X-ray fluorescence spectrometry for *in vivo* Fe determination, epithermal NAA for certification of iodine values in environmental samples, *etc.* M. A. Bolshov (Institute of Spectroscopy, Troitzk, Russia) reported very interesting results for the determination of toxic metals at the fg level in ice layers in the central regions of large Antarctic and Greenland ice caps. As the estimation of the difference between the natural (pre-industrial) and modern toxic metal content (including Pb, Cd, Bi, *etc.*) of the environment is of great scientific interest, the Russian scientists tried to reconstruct the past natural tropospheric cycles of these metals in the investigation of toxic metal occurrences in the well preserved dated snow and ice layers deposited in the aforementioned regions. Laser excited atomic fluorescence spectrometry turned out to be a very useful method for this purpose.

The author of present report had the honour, together with R. Tauler (University of Barcelona, Barcelona, Spain) to organize the chemometric minisymposium, which is very closely related to analytical chemistry. R. Tauler discussed the use of multivariate resolution in chemistry with the conformational changes of macromolecules in solutions as examples. M. Maeder (University of Newcastle, Callaghan, Australia) compared model-based least-square fitting and model-free chemometric treatment of chemical data. The author of this report discussed some new robust chemometric methods for multivariate calibration proposed by the chemometrics group of Hunan University. Besides robust Kalman filtering, the maximum sum of binary-coded residuals (MASBR) regression and robust principal component analysis, the introduction of the concept of morphological analysis into chemistry seems a very promising approach for solving some chemical problems. The use of some nonparametric regression methods was reported by Nguyen-Cong Vu (University of Hochiminh City, Vietnam). Lun-Jun Bao *et al.* (Zhongshan University) compared the wavelet transform and fast Fourier transform in analytical signal processing. Nianyi Chen (Shanghai Institute of Metallurgy, Shanghai) gave a comprehensive review of the practical application of his expert system KDPAG consisting knowledge base, database, pattern recognition, artificial neural networks and genetic algorithm modules. Chen's group worked with about 100 different factories and got very exciting results in solving industrial optimization and related problems.

A multidisciplinary conference like $EuAsC_2S$-5 is very beneficial for the participants from different branches of chemistry, in particular for the analytical chemists. Well organized lectures in various research fields were quite inspiring. Each day a plenary lecture was delivered. After the plenary lecture, during the coffee break, the convention center was quickly divided into three rooms for minisymposia and keynote lectures. Jean-Marie Lehn (College de France, Paris and University Louis Pasteur, Strasbourg, France), the 1987 Nobel prize winner, gave a very interesting plenary lecture with the title 'Supramolecular chemistry: from molecular recogni-

tion towards self-organization'. He discussed the design of systems undergoing molecular self-organization, *i.e.*, systems capable of spontaneously generating a well-defined supramolecular architecture by self-assembling from their components in a given set of conditions. The molecular information necessary for the process to take place must be stored in the components and act through selective molecular interactions. The design of molecular information controlled 'programmed' and functional self-organizing systems represents new horizons in supramolecular chemistry towards 'intelligent', functional supramolecular materials. Lehn's concept seems very attractive for chemists from many branches, including the analysts. Some examples of the possible analytical application of such a concept were found in the keynote lecture given by U. Mayer (Technical University of Vienna, Austria).

Yu Ru-Qin
Hunan University, Changsha
China

Future Issues Will Include

Simultaneous Determination of the Colourants Sunset Yellow FCF and Quinoline Yellow by Solid-phase Spectrophotometry by Using Partial Least Squares Multivariate Calibration—**L. F. Capitan-Vallvey, Maria D. Fernandez, Ignacio de Orbe, J. L. Vilchez, Ramiro Avidad**

Speciation of Primary Expolosives in Environmental Samples by Sequential Injection Amperometry—**Roger T. Echols, Ryan R. James, Joseph H. Aldstadt**

Microwave-Assisted Extraction of Monoterpenols in Musts Samples—**N. Carro, C. M. Garcia, R. Cela**

Applicability of a Sol–Gel Derived CeO_2–TiO_2 Thin Film Electrode as Amperometric Sensor in Flow Injection Analysis—**Bozidar Ororevc, Gabrijela Tavcar, K. Kalcher**

Intrinsic Molecular Fluorescence of Lactate Dehydrogenase: an Analytical Alternative for Enzymatic Determination of Pyruvate—**Susana de Marcos, Javier Galban, Cristina Alonso, Juan R. Castillo**

Study on a Novel System of Lanthanide Fluorescence with Coupled Reaction Based on Hemin Catalysis—**Jin-Gou Xi, Xue-Ying Zheng, Jian-Zhong Lu, Qing-Zhi Zhu, Qing-Ge Li**

Determination of Cadmium in Environmental Samples by Hydride Generation With *In Situ* Concentration and Atomic Absorption Detection—**Henryk Matusiewicz, Mariusz Kopras, Ralph E. Sturgeon**

Lactate Amperometric Biosensor Based on an Electrosynthesized Bilayer Film With Covalently Immobilized Enzyme—**F. Palmisano, G. E. de Benedetto, P. G. Zambonin**

Flow Injection Spectrophotometric Determination of L-Dopa and Carbidopa in Pharmaceutical Formulations Using a Crude Extract of Sweet Potato Root [*Ipomoea batatas* (L) Lam] as Enzymatic Source—**Orlando Fatibello-Filho, Iolanda Da Cruz Vieira**

Sampling Intercomparisons for Aldehydes in Simulated Workplace Air—**E. Goelen, M. Lambrechts, F. Geyskens**

Enhancement of Rayleigh Light Scattering of Acid Chrome Blue K by Proteins and Proteins Assay by Scattering Technique—**Ke An Li, Chun Qi Ma, Shen Yang Tong**

Multiple Complex Formation of Unstable Compounds With Cyclodextrins: Efficient Determination and Evaluation of the Binding Constant With Improved Kinetic Studies—**Yannis L. Loukas**

Evaluation of Hydromatrix and Magnesium Sulfate Drying Agents for Supercritical Fluid Extraction of Multiple Pesticides in Produce—**Steven J. Lehotay, Konstantin I. Eller**

Amperometric Bienzymatic Sensor for Aspartame—**George G. Guilbault, D. Compagnone, D. O'Sullivan**

Integrated Automatic Determination of Nitrate, Ammonium and Organic Carbon in Soil Samples—**Miguel Valcarcel, Evaristo Ballesteros, Angel Rios**

Electrothermal Atomic Absorption Spectrometry Determination of Pb and Sn in Slurries Optimization Study—**Vera I. Slaveykova, Michel Hoenig**

Identification of Endogenous 19-Nortestosterone in Pregnant Ewes by Gas Chromatography–Mass Spectrometry—**A.-S. Clouet, B. Le Bizec, Marie-Pierre Montrade, F. Monteau, F. Andre**

Role of Quenching on Alpha–Beta Separation in Liquid Scintillation Counting for Several High Capacity Cocktails—**Lluis Pujol, J. A. Sanchez-Cabeza**

Crown Ether Coated Piezoelectric Crystal Sensor Array for Detection of Organic Vapor Mixtures Using Several Chemometric Methods—**Wan-Li Xing, Xi-Wen He**

Approaches to Predicting Stability Constants. A Critical Review—**Robert D. Hancock**

Five-way ANOVA Interaction Analysis of the Selective Extraction of Carbaryl, Pirimicarb and Aldicarb from Soils by Supercritical Fluid Extraction—**I. Stuart, John MacLachlan, Peter A. Bather, W. P. Gardiner**

4-(5′6′-Dimethoxybenzothiazolyl)benzoyl Fluoride and 2-(5′6′-Dimethoxybenzothiazolyl)benzenesulfonyl Chloride as Sensitive Fluorescence Derivatization Reagents for Amines to High-performance Liquid Chromatography—**Shuuji Hara, Junichi Aoki, Ker-Ichiro Yoshikuni, Yasuhumi Tatsuguchi, Masatoshi Yamaguchi**

Potentiometric and Coulometric Titration of 6-Propyl-2-thiouracil—**Witold Ciesielski, Robert Zakrzewski**

Selective Precipitation Separation and Inductively Coupled Plasma Mass Spectrometry Determination of Trace Metal Impurities in High Purity Silver—**Mo-Hsiung Yang, Yuh-Chang Sun, Jerzy Mierzwa, Chien-Feng Lin, T. I. Yeh**

Technical Abbreviations and Acronyms

The presence of an abbreviation or acronym in this list should NOT be read as a recommendation for its use. However, those defined here need not be defined in the text of your manuscript. Abbreviations also cover the plural form.

AAS	atomic absorption spectrometry
ac	alternating current
A/D	analogue-to-digital
ADC	analogue-to-digital converter
ANOVA	analysis of variance
AOAC	Association of Official Analytical Chemists
ASTM	American Society for Testing and Materials
bp	boiling point
BSA	bovine serum albumin
BSI	British Standards Institution
CEN	European Committee for Standardization
cpm	counts per minute
CMOS	complementary metal oxide silicon
c.m.c.	critical micellization concentration
CRM	certified reference material
CVAAS	cold vapour atomic absorption spectrometry
CW	continuous wave
CZE	capillary zone electrophoresis
dc	direct current
dpm	disintegrations per minute
DRIFT	diffuse reflectance infrared Fourier transform spectroscopy
DELFIA	dissociation enhanced lanthanide fluorescence immunoassay
DNA	deoxyribonucleic acid
EDTA	ethylenediaminetetraacetic acid
ELISA	enzyme linked immunosorbent assay
emf	electromotive force
ETAAS	electrothermal atomic absorption spectrometry
EXAFS	extended X-ray absorption fine structure spectroscopy
EPA	Environmental Protection Agency
FAAS	flame atomic absorption spectrometry
FAB	fast atom bombardment
FAO-WHO	Food and Agriculture Organization, World Health Organization
FIR	far-infrared
FT	Fourier transform
FPLC	fast protein liquid chromatography
FPD	flame photometric detector
GC	gas chromatography
GLC	gas-liquid chromatography
HGAAS	hydride generation atomic absorption spectroscopy
HPLC	high-performance liquid chromatography
ICP	inductively coupled plasma
id	internal diameter
INAA	instrumental neutron activation analysis
IR	infrared
ISFET	ion-selective effect transistor
iv	intravenous
im	intramuscular
IGFET	insulated gate field effect transistor
ISE	ion-selective electrode
LC	liquid chromatography
LED	light emitting diode
LOD	limit of detection
LOQ	limit of quantification
mp	melting point
MRL	maximum residue limit
mRNA	messenger ribonucleic acid
MS	mass spectrometry
NIR	near-infrared
NMR	nuclear magnetic resonance
NIST	National Institute of Standards and Technology
od	outer diameter
OES	optical emission spectrometry
PBS	phosphate buffered saline
PCB	polychlorinated biphenyl
PAH	polycyclic aromatic hydrocarbon
PGE	platinum group element
PIXE	particle/proton-induced X-ray emission
ppt	parts per trillion (10^{12}; pg g^{-1})
ppb	parts per billion (10^{9}; ng g^{-1})
ppm	parts per million (10^{6}; μg g^{-1})
PTFE	poly(tetrafluoroethylene)
PVC	poly(vinyl chloride)
PDVB	poly(divinyl benzene)
QC	quality control
QA	quality assurance
REE	rare earth element
rf	radiofrequency
RIMS	resonance ionization mass spectrometry
rms	root mean square
rpm	revolutions per minute
RNA	ribonucleic acid
RSD	relative standard deviation
SCE	saturated calomel (reference) electrode
SE	standard error
SEM	scanning/surface (reflection) electron microscopy
SIMS	secondary-ion mass spectrometry
SIMCA	soft independent modelling of class analogy
S/N	signal-to-noise ratio
SRM	Standard Reference Material
STM	scanning tunnelling (electron) microscopy
STP	standard temperature and pressure
TIMS	thermal ionization mass spectrometry
TLC	thin-layer chromatography
TOF	time-of-flight
TGA	thermogravimetric analysis
TMS	trimethylsilane
TRIS	2-amino-2-(hydroxymethyl)-propane-1,3-diol (reagent)
UV	ultraviolet
UV/VIS	ultraviolet–visible
VDU	visual display unit
XRD	X-ray diffraction
XRF	X-ray fluorescence
YAG	yttrium aluminium garnet

Commonly Used Symbols

M	molecular mass
M_r	relative molecular mass
r	correlation coefficient
s	standard deviation of sample
σ	population standard deviation
u	atomic mass

6TH NORDIC SYMPOSIUM ON

TRACE ELEMENTS IN HUMAN HEALTH AND DISEASE

JUNE 29--JULY 3, 1997, ROSKILDE UNIVERSITY, DENMARK

SCIENTIFIC PROGRAMME

*Dietary exposures and requirements
*Trace element imbalances in human disease
*Molecular mechanisms of metal toxicity
*Chelation in metal intoxication
*Occupational and environmental exposures
*Metabolism of trace elements
*Reproductive and developmental effects
*Analytical and clinical chemistry
*Mutagenic and carcinogenic metal compounds
*Risk assessment of metal exposures

ORGANISING COMMITTEE

A. Aito
P. Grandjean
Y. Thomassen
G.F. Nordberg
O. Andersen (Chair)
J. Clausen
B. Sandstrom

SPECIAL ISSUE

Oral or poster presentations, once written up as full papers will be peer reviewed for publication in *The Analyst*. Authors are encouraged to submit their manuscripts to the attending editor during the course of the symposium.

FURTHER INFORMATION

Ole Anderson
Fax: + 45 46 75 77 21
E-mail: Andersen@virgil.RUC.DK

REGISTRATION AND SUBMISSION OF ABSTRACTS

SYMPOSIUM SECRETARIAT, 6th Nordic Symposium on
TRACE ELEMENTS IN HUMAN HEALTH AND DISEASE,
Department of Life Sciences and Chemistry
House 16.1, Roskilde University
Post Box 260, DK-4000 Roskilde, Denmark

CSI XXX PRE-SYMPOSIUM

The Third International Conference on

SPECIATION OF ELEMENTS IN BIOLOGICAL, ENVIRONMENTAL AND TOXICOLOGICAL SCIENCES

The Torresian Resort Port Douglas, Queensland, Australia, September 15-19, 1997

INVITATION AND CALL FOR PAPERS

The Organising Committee extends an invitation to all individuals involved in element research or its applications. A major goal of the symposium is to facilitate interdisciplinary and inter-sector discussion about all aspects of elements requiring an understanding of speciation, the five main themes of this symposium being :

A, *Speciation of Elements in Biology, Toxicology and Medicine*;
B, *Speciation of Elements in Nutrition*;
C, *Speciation of Elements in Environmental Toxicology*;
D, *Surface and Particle Characterisation*; and
E, *New Developments in Methods/Techniques of Species Determination.*

A small number of travel scholarships will be provided to encourage overseas graduate students to attend and participate.

THE SCIENTIFIC PROGRAMME

The symposium programme will comprise four days of oral presentations, posters and discussion. All presenters will be asked to focus on new developments in research. Oral presentations (invited or submitted) will be 20 or 30 mins in duration. As at previous symposia (Loen, Norway, 1991 and 1994) posters will play a central role, after formal viewing each poster presenter will be given five minutes to present the salient features of their work to a discussion group to encourage in-depth feedback.

SYMPOSIUM LOCATION AND DETAILS

The venue for the symposium, is The Torresian Resort of Port Douglas, Australia. This tropical Queensland location is situated near Cairns, between the Great Barrier Reef and the Daintree Rainforest. A Symposium Package rate has been arranged: AUD $155(per person, per night, twin share) and AUD $225 (single occupancy) and includes accommodation (Garden View Room) all meals and morning and afternoon teas. A limited amount of less expensive accommodation (room and board) will be available. This conference (as a pre-symposium to CSI XXX) is scheduled to allow the participants to join the **XXX Colloquium Spectroscopicum Internationale (21-26 September) in Melbourne.**

CONFERENCE PROCEEDINGS

As with previous Speciation Symposia (see ***The Analyst*** 117; 549-691 and 120; 29-30N and 583-763) all papers presented as posters or lectures may be submitted as full papers for publication in a special issue of ***The Analyst***, subject to the normal review procedure of this journal.

SOCIAL PROGRAMME

All participants and accompanying persons are invited to the symposium reception on Monday evening, September 15, and the dinner on Friday evening, September 19. Because of the numerous attractions available (e.g., swimming, all other watersports, cruises, canoeing, hiking, horse riding etc.) no other formal social events are planned. However, please note that for each full day of scientific sessions, the period 15.30 onwards will be set aside for the enjoyment of the mentioned activities by all. Port Douglas has a comfortable, year round, tropical climate. Day tours to the outer Barrier Reef are available.

REGISTRATION FEE

The registration fee per delegate is AUD $480 (AUD $150 for students)and includes the cost of the symposium dinner.

SECRETARIAT

Local (Registration)

Third Speciation Symposium
c/o Dr J. P. Matousek,
Department of Analytical Chemistry, The University of New South Wales, Sydney, NSW 2052, Australia
Tel : + 61 2 3854713 **or** + 61 2 4512322 (home)
Fax : + 61 2 3856141
E-mail : Matousek@unsw.edu.au

THE SYMPOSIUM IS ORGANISED BY :

The University of New South Wales (*Sydney, Australia*)
The National Institute Of Occupational Health (*Oslo, Norway*)
The Institute of Environment and Health (*Universities of Toronto and McMaster, Canada*)
MAFF CSL Food Science Laboratory (*Norwich, UK*)

ORGANIZING COMMITTEES

Local	Programme
Graeme Batley (*CSIRO, Lucas Heights*)	Helen Crews (*MAFF CSL, UK*)
R. (Dick) Finlayson (*Sydney, NSW*)	Jarda P. Matousek (*Sydney, NSW*)
D. Brynn Hibbert (*Sydney, NSW*)	Evert Nieboer (*Hamilton, Canada*)
Jarda P. Matousek (*Sydney, NSW*)	Yngvar Thomassen (*Oslo, Norway*)

Cover picture: Measuring hydrogen in a jet engine turbine blade by prompt gamma-ray activation analysis. Illustration kindly supplied by Rick L. Paul and Heather Chen-Mayer, National Institute of Standards and Technology, Gaithersburg, MD 20899-0001, USA (see p. 35R).

Initiative for Emerging Young Professionals 1997: Advancement and Recognition

A follow-up to the successful Buxton meeting in April 1996 will be held at Wood Norton Hall and Conference Centre, Evesham, Worcestershire on April 25–27, 1997.

The meeting will consider the following points:

- Enhancement of the professional status of analytical scientists
- Ongoing training needs
- Continuing professional development

The meeting is designed to encourage lively debate and provide networking opportunities with other young professionals. It is aimed at young analytical scientists in the age range 25–35. The total cost will be £60, inclusive of meals and accommodation.

Those wishing to be considered should send a 1-page résumé of their career to date to the address below by March 14, 1997.

For information contact Diana Hort, Analytical Division, The Royal Society of Chemistry, Burlington House, Piccadilly, London W1V 0BN. Tel: +44 (0)171 734 8656. FAX: +44 (0)171 734 1226. E-mail: hortd@rsc.org

ANALAO 122(3) 35R–42R, 209–302, 33N–48N (1997) MARCH 1997

The Analyst

The analytical journal of The Royal Society of Chemistry

CONTENTS

Continued on inside back cover

THE ROYAL SOCIETY OF CHEMISTRY Information Services

Typeset and printed by Black Bear Press Limited, Cambridge, England

0003-2654(1997)122:3;1-S